

Investigation of Avian defensins

Sherko Nariman Subhan Niranji

Thesis submitted for the degree of Doctor of Philosophy
Institute for Cell and Molecular Biosciences Newcastle
University

September 2015

Abstract

Banning the use of antibiotic growth promoters in animal feed has forced poultry breeding companies to select birds with improved disease resistance. One area of focus is the chicken innate immune system, which includes a family of avian β -defensins (AvBDs) that are synthesised by epithelia in response to microbial challenge. The aim of this thesis was to investigate the *in vivo* gene expression, antimicrobial activity (AMA) and mechanisms of action of AvBDs 6 and 9.

Endpoint and qPCR were used to investigate AvBD6 and 9 gene expression in an array of epithelial tissues taken from day 7 and 35 broiler chickens reared in low and high hygiene conditions. The expression profiles of pro (interleukin-6: IL-6) and anti (Transforming Growth Factor β 4:TGF β 4) inflammatory cytokine genes, and the chicken galectin-3 gene (CG3) were also examined. To explore AMA recombinant (r)AvBD peptides and their variants, including rAvBD9 3CA (lacking 3 of the 6 conserved cysteine (C) amino acids), rAvBD9 6CAG (lacking all the conserved C amino acids) and rAvBD9 W38G were synthesised, and their AMAs against *E. coli* and *E. faecalis* tested *in vitro* using time-kill assays. The structural properties and membrane interactions of the rAvBDs and custom synthesized linear (s) AvBD6 and 9 peptides were also investigated using circular dichroism (CD), liposome entrapped calcein leakage assays and peptide modelling.

The *in vivo* gene expression analyses revealed that AvBD6 and 9, IL-6, TGF β 4 and CG3 were expressed in all the broiler chicken tissues examined. However, the data were compromised by the small bird numbers, and the variability in the tissue expression data between individual birds within a group resulted in no statistically significant trends associated with rearing environment being detected.

The AMA data showed that the rAvBD6 and 9 peptides were antimicrobial against both Gram negative and positive microbes with rAvBD6 > rAvBD9 (using 100 μ g/ml peptide, 76.4% (23.6 \pm 2.3 % survival) of *E. coli* were killed by rAvBD6 compared to 64.3% (35.7 \pm 7.2% survival) for rAvBD9). These data were potentially related to the physical properties of the peptide with AvBD6 being more cationic (+6.8) and hydrophobic than AvBD9 (+3.8), although modelling data also suggested that AvBD6 contained a hook-like foramen structure.

The AMAs of the rAvBD9 and AvBD9 3CA peptides were not significantly different. Using 50 μ g/ml peptide 49% (51 \pm 12% survival) and 60% (40 \pm 8% survival) of *E. coli* were killed compared to 53% (47 \pm 20% survival) and 69% (31 \pm 13% survival) killing for *E. faecalis*. Nu-PAGE data suggested the AMA potency of AvBD9 3CA was associated with dimer formation. At 50 μ g/ml neither the rAvBD9 6CAG nor the synthetic linear AvBD9 peptides were active against the *E. coli* isolate. However, in the presence of proteinase inhibitor (Roche-1:1000 dilution), 45% *E. coli* BL21 killing (55 \pm 1% survival) was observed, which strongly supported the roles of the di-sulphide bonds in protecting the AvBD peptides against proteolysis. Substituting the C-terminal tryptophan (W) of rAvBD9 for a glycine (G) also resulted in a loss of AMA against bacteria (at 50 μ g/ml 0% killing of *E. coli* and 15% (85.5 \pm 20.5% survival) killing of *E. faecalis* was detected). These data indicated that the C terminal W amino acid is also important for AvBD9 AMA.

In the presence of SDS micelles mimicking the bacterial membrane synthetic AvBD1, 6 and 9 peptides showed increased α -helicity. Membrane leakage experiments using calcein-entrapped liposomes and synthetic peptides (1.5 μ g/ml) showed sAvBD6 induced more leakage at 4 minutes than sAvBD9 (60.3 \pm 6.3% (n=4) versus 11.5% (n=1)). Although compromised by the lack of replicates these data suggested that AvBD9 may not function through membrane disruption suggesting other mechanisms including inhibition of nucleic acid synthesis and/or cell division. Membrane leakage experiments using sAvBD1 peptides modelling an AvBD1 SNP found in poultry showed NYH >SSY > NYY.

Overall these data show AvBD6 and 9 are expressed in bird tissues and have AMA against gram negative and positive bacteria. The studies supported different mechanisms of action of the two defensins with AvBD6 causing membrane damage compared to AvBD9, which probably functions through disrupting intracellular systems. These data suggest that the AvBD peptides work in synergy in defending the epithelia and warn against poultry geneticists selecting individual AvBD genes for breeding purposes.

Acknowledgements

I would like to thank my supervisor Dr. Judith Hall, for her great support and patience during my PhD study. I would like also to acknowledge my second supervisor, Dr. Catherine Mowbray for her collaboration as she helped me performing expression and immunohistochemical experiments.

I would like to acknowledge the following people in my group:

- Kevin Cadwell (former PhD student and my colleague for his help during AM assays)
- Vanessa Butler (her advice and support in cloning and hyperexpression)
- Claire Townes (her advice and help in PCR and basic molecular techniques).
- Marcello Lanz and Anna Stanton, who were part of J hall group as we always helped each other shared materials.

I am grateful to Professor Jeremy Lakey (Newcastle University) who collaborated with me in performing CD spectra and calcein leakage assays.

I would like to thank both Professor Harry Gilbert and Dr. David Bolam (Newcastle University), and their groups for using their lab utensils.

Thanks to Mr. Carl Morland (lab technician, Newcastle University) for his advices during protein purifications.

A special thanks to Dr. Git Chung (PhD Newcastle University) for his inspiration and support during my PhD study.

Thank you to my uncle Abdullah Sulaiman and my brother Ako Niranji for their support when I was away from Kurdistan. I would like also to thank my family who always supported me.

Finally I would like to thank to:

- Newcastle University
- Kurdistan Regional Government (KRG scholarship financial sponsor)
- University of Sulaimani- College of Veterinary Medicine as they gave me this opportunity to grant the KRG scholarship.

Table of Contents

Contents

Abstract	ii
Acknowledgements	iii
List of Figures	viii
List of Tables	xiv
List of Abbreviations	xv
Chapter 1	1
1. Introduction	1
1.1. Background	1
1.2. Host- microbial interactions	2
1.3. Host defence proteins	3
1.4. Defensins	4
1.5. Evolution of defensins	8
1.6. AvBD sequence homology	9
1.7. Avian β -defensin	10
1.7.1. AvBD expression	13
1.7.2. Localisation of AvBD peptides in tissues	17
1.7.3. Structure of AvBDs	18
1.7.4. Anti-microbial activity of AvBDs	19
1.8. Mechanism action of defensin	21
1.9. Resistance of the microbes to AMPs:	24
1.10. Chicken cytokines	26
1.10.1. Interleukin-2	26
1.10.2. Interleukin-6	27
1.10.3. Transforming growth factor β 4 (TGF β 4)	27
1.11. Chicken galectin-3	28
Chapter 2	31
2. Materials and Methods	31
2.1. Chemicals and consumables	31
2.2. Bacterial culture:	31
2.2.1. Growth medium broth	31
2.2.2. LB agar plates	31
2.2.3. Blood agar based plates	31
2.3. Bacterial strains	32
2.4. Buffers	32
2.4.1. Phosphate buffered saline (PBS)	32
2.4.2. Sodium phosphate buffer	32
2.4.3. GST 'cleaving' buffer	32
2.4.4. Sample loading buffers	33
2.4.5. Gel running buffers	33
2.4.6. Tris glutathione elution buffer (TGE)	33
2.4.7. Neutral buffered formalin	33
2.5. Tissue sample collection	33
2.6. RNA extraction	34

2.7.	RNA quantification	35
2.8.	DNase treatment.....	35
2.9.	Reverse transcription.....	35
2.10.	Endpoint PCR primers.....	36
2.11.	End point polymerase chain reaction (PCR)	38
2.12.	Real time (Quantitative- Q) PCR.....	38
2.12.1.	Real time PCR primers:	38
2.12.2.	Standard curves:.....	40
2.12.3.	Real time PCR reaction.....	40
2.13.	Production of recombinant plasmids	40
2.13.1.	cDNA PCR product purifications	40
2.13.2.	pGEX-6p-1 vector system and cDNA cloning	41
2.13.3.	pGEM T Easy vector system and cDNA cloning	41
2.13.4.	Competent cell preparation	42
2.13.5.	Bacterial cell transformation.....	42
2.13.6.	Blue-white colony screening method.....	42
2.13.7.	PCR screening for gene inserts	43
2.13.8.	Recombinant plasmid extraction from the competent cells.....	43
2.14.	DNA gel electrophoresis	43
2.15.	DNA sequencing.....	44
2.16.	AvBD9 site directed mutagenesis.....	44
2.16.1.	Mutagenesis primers	45
2.16.2.	Mutagenesis reaction	47
2.16.3.	Transformation of mutagenised plasmids.....	47
2.17.	Hyper expression of AvBD6 and AvBD9	47
2.18.	Purification of AvBD peptides	48
2.18.1.	Column chromatography using glutathione sepharose resin	48
2.18.2.	Desalting by gel infiltration	48
2.18.3.	Hyperexpression and purification of GST-tagged 3C PreScission protease enzyme	48
2.18.4.	Cleaving the peptide from GST by PreScission protease enzyme (cutting off the columns)	49
2.18.5.	Cleaving the peptide from GST by PreScission protease enzyme (Cutting on the columns)	49
2.18.6.	Protein separation by concentrator columns	49
2.18.7.	Freeze drying of the peptide	49
2.19.	Synthetic peptides.....	50
2.20.	Peptide quantification	50
2.21.	Identification of the peptide.....	50
2.21.1.	SDS PAGE.....	50
2.21.2.	NUPAGE	51
2.21.3.	MALDI TOF mass spectrometry	51
2.22.	Anti-microbial activity assays	51
2.22.1.	Radial immuno-diffusion Assay	52
2.22.2.	Time-kill colony counting Assay.....	52
2.23.	Calcein leakage assay	52

2.24.	Circular dichroism (CD)	53
2.25.	Immuno-histochemistry (IHC)	54
2.25.1.	Antibodies for IHC	54
2.25.2.	Tissue processing	54
2.25.3.	IHC staining and antibody procedure	54
2.26.	Statistical analysis.....	55
Chapter 3.....		56
3.	<i>In vivo</i> expression analyses of chicken genes associated with gut innate immunity..	56
3.1.	Introduction	56
3.2.	Endpoint PCR analyses of AvBDs 6 and 9, chicken galectin-3, IL-2, IL-6 and TGFβ-4 gene expression	57
3.2.1.	Tissue panels investigating AvBD6 and 9 gene expression in birds raised in Low and High hygiene conditions	57
3.2.2.	Sequencing results for AvBD6 and 9 cDNA:	59
3.2.3.	Tissue panels investigating IL-2, IL-6, TGFβ4 and chicken galectin-3 gene expression	60
3.2.4.	Sequence results of IL-2, IL-6, TGFβ4 and CG 3 cDNAs	62
3.3.	Real time PCR analyses of AvBD6, AvBD9, chicken galectin-3, IL-6 and TGFβ-4 expression in line X bird tissues	70
3.3.1.	qPCR assay development.....	70
3.3.2.	Real time PCR.....	73
3.3.2.1.	AvBD6 mRNA expression by real time PCR	73
3.3.2.2.	AvBD9 mRNA expression by real time PCR	76
3.3.2.3.	Chicken galectin-3 mRNA expression by real time PCR	78
3.3.2.4.	IL-6 mRNA expression by Real time PCR	80
3.3.2.5.	TGFβ4 mRNA expression by real time PCR.....	82
3.4.	Immuno-histochemical examination of gut tissues:.....	84
3.4.1.	Localisation of AvBD9 by immunohistochemistry	84
3.4.2.	Immuno-localisation of chicken IL-6 in gut tissues	85
3.5.	Discussion	87
3.6.	Conclusions	92
Chapter 4.....		93
4.	<i>In vitro</i> synthesis and analyses of the anti-microbial properties of AvBD6 and AvBD9 peptides.....	93
4.1.	Introduction	93
4.2.	Recombinant AvBD synthesis	94
4.2.1.	AvBD6 and AvBD9 cloning.....	94
4.2.2.	Hyper expression of AvBD6 and AvBD9 peptide variants	97
4.2.3.	Purification of AvBD6 and AvBD9 peptides	99
4.2.3.1.	Purification: cleaving off the column.....	99
4.2.3.2.	Purification: cleaving on the column	101
4.2.4.	MALDI TOF mass spectrometry.....	104
4.3.	AvBD9 site directed mutagenesis	106
4.3.1.	Mutagenesis of cysteine residues.....	108
4.3.2.	Site directed mutagenesis of C- terminal tryptophan residue	108
4.4.	Antimicrobial activities of the AvBD peptides	113

4.4.1.	Radial immuno-diffusion assay (RIDA) for AvBD6 and AvBD9 peptides against <i>E. coli</i>	113
4.4.2.	Time kill-colony counting assay.....	117
4.4.2.1.	rAvBD6 peptide AMA against <i>E. coli</i>	117
4.4.2.2.	AvBD6 AMA against <i>E. faecalis</i>	118
4.4.2.3.	AvBD9 AMA against <i>E. coli</i>	119
4.4.2.4.	Dimerization of AvBD9 C3A.....	122
4.4.2.5.	AvBD9 AMA against <i>E. faecalis</i>	124
4.4.3.	Recombinant AvBD10 production and AMA.....	126
4.4.3.1.	AvBD10 site directed mutagenesis:.....	126
4.4.3.2.	AvBD10 AMA against <i>E. coli</i>	128
4.4.3.3.	AvBD10 AMA against <i>E. faecalis</i>	130
4.5.	Time-kill assays using synthetic AvBD peptides.....	131
4.5.1.	Comparison of synthetic and recombinant AvBD6 mature, AvBD9 mature and AvBD9 W38G peptide AMAs against <i>E. coli</i>	133
4.5.2.	Comparison of synthetic and recombinant AvBD6 mature, AvBD9 mature and AvBD9 W38G peptide AMAs against <i>E. faecalis</i>	135
4.5.3.	Effect of proteases and buffer ionic strength on sAvBD6/9 and rAvBD6/9 AMAs against <i>E. coli</i>	136
4.6.	Discussion.....	140
4.7.	Conclusions.....	144
	Chapter 5.....	145
5.	AvBD structure-membrane interactions (Part I).....	145
5.1.	Introduction.....	145
5.2.	Secondary structure-membrane interaction activities of recombinant AvBD9 peptides.....	146
5.2.1.	CD spectra of recombinant AvBD9 peptides.....	146
5.2.2.	Investigations of rAvBD9 peptide/ bacterial membrane interactions using calcein leakage assays.....	153
5.3.	Secondary structure-membrane interaction activity of synthetic AvBDs.....	155
5.3.1.	Circular dichroism of the synthetic peptides.....	156
5.3.1.1.	CD spectra for synthetic AvBD6 peptide.....	156
5.3.1.2.	CD spectra for synthetic AvBD9 variants.....	158
5.3.2.	Calcein leakage assay: sAvBD6 and sAvBD9.....	161
5.3.2.1.	Leakage assay and AvBD6.....	161
5.3.2.2.	Leakage assay and AvBD9 peptides.....	163
5.4.	AvBD6 and 9 structure modelling.....	167
5.5.	Discussion.....	172
5.6.	Conclusions.....	175
	Chapter 5 (Part II).....	176
	AvBD1 structure-membrane interactions.....	176
5.7.	Introduction.....	176
5.8.	CD analyses of synthetic AvBD1 Peptides.....	178
5.9.	Leakage assay and sAvBD1 Peptides.....	185
5.10.	AvBD1 modelling.....	188
5.11.	Discussion.....	191

5.12. Conclusions	193
Chapter 6.....	194
Final Discussion.....	194
References:.....	200

List of Figures

Figure 1.1 Structures of host defence peptides	4
Figure 1.2 Sequences and 3D structures of selected defensins.....	6
Figure 1.3 Organization of β -defensin gene clusters.	11
Figure 1.4: Genomic organisation of gallin gene clusters in relation to the last cluster of AvBDs (AvBD 13)	11
Figure 1.5 Genomic organization of avian and mammalian.....	12
Figure 1.6 AvBD amino acid sequences.....	13
Figure 1.7 Global fold and lipophilic and electrostatic potentials of Sphe-2 (AvBD103b)..	18
Figure 1.8 Global fold and lipophilic and electrostatic potentials of (AvBD2).....	19
Figure 1.9 Sequences and charges of chicken AvBD8 and its modified versions.....	20
Figure 1.10 Mechanisms of action of antibacterial peptides.	22
Figure 1.11 Schematic of the overall structures of galectin-1, -2, -3, and 4.....	29
Figure 2.1 pGEX-6P-1 plasmid map.	41
Figure 2.2 Basic steps of PCR based site directed mutagenesis.....	45
Figure 3.1 AvBD6/ 9 and 18S cDNA expression panels.....	58
Figure 3.2 Sequencing results for AvBD6 (A) and AvBD9 (B) DNA products..	60
Figure 3.3 IL-2 (A), IL-6 (B), TGF β 4 (C), CG3 (D) and 18S (E) expression panels.....	61
Figure 3.4 A: Sequencing and BLAST results of an IL-2 PCR product amplified from D7 caecum Line X bird.....	62
Figure 3.5 A: Sequencing and BLAST results of a TGF β 4 PCR product amplified from D7 Line X bird (caecum).....	64
Figure 3.6 A: Sequencing and BLAST results of a CG3 PCR product amplified from caecal tissue..	66
Figure 3.7 Sequencing and BLAST results of a putative IL-6 PCR product D7 Line X bird	68

Figure 3.8 Panel (A): End point PCR for IL-6. kidney (Kd), Spleen (Sp), Liver (Lv), Bursa (Bu), Thymus (T) Duodenum (Du), Jejunum (Je), Ileum (Il), Caecum (Ca), and Caecal tonsils (CT) of LH, Day 7 birds..	69
Figure 3.9 GeNorm analysis showing the most appropriate genes for real-time qPCR in avian tissues.	70
Figure 3.10 Amplification curves of diluted chicken galectin-3 plasmids.	71
Figure 3.11 Melting curves for diluted chicken galectin-3 plasmids.....	71
Figure 3.12 Standard curve of diluted chicken galectin-3 plasmids.....	72
Figure 3.13 Melting curves of diluted TGF β 4 plasmids.....	72
Figure 3.14 Amplification curves of diluted TGF β 4 plasmids.	72
Figure 3.15 Standard curve of diluted TGF β 4 plasmids.....	72
Figure 3.16 Dot plots showing AvBD6 expression in chicken tissues as measured by qPCR. Gut (A), kidney (B), Liver (C) and Lung (D). LH= low hygiene, HH=high hygiene.	75
Figure 3.17 Dot plots showing AvBD9 expression in chicken tissues as measured by qPCR. Gut (A), kidney (B), Liver (C) and Lung (D). LH= low hygiene, HH=high hygiene.	77
Figure 3.18 Dot plots showing CG3 expression in chicken tissues as measured by qPCR. Gut (A), kidney (B), Liver (C) and Lung (D). LH= low hygiene, HH=high hygiene.	79
Figure 3.19 Dot plots showing IL-6 expression in chicken tissues as measured by qPCR. Gut (A), kidney (B), Liver (C) and Lung (D). LH= low hygiene, HH=high hygiene.	81
Figure 3.20 Dot plots showing TGF β 4 expression in chicken tissues as measured by qPCR. Gut (A), kidney (B), Liver (C) and Lung (D). LH= low hygiene, HH=high hygiene.	83
Figure 3.21 Immuno-localisation of AvBD9 in duodenal tissues from D7, Line X birds..	85
Figure 3.22 Immuno-localisation of IL-6 (dilution 1:120 in EDTA) in duodenal tissues from D7, Line X birds.	86
Figure 4.1 Amino acid composition of AvBD6 and 9 including pro and mature sequences..	93
Figure 4.2[A]: BamH1 and EcoR1 restricted cDNAs encoding: AvBD6 mature (1), AvBD6 promature (2), AvBD9 mature (3), AvBD9 promature (4), restricted pGEX-6P-1 plasmid (5), uncut pGEX-6P-1 plasmid (6).....	95
Figure 4.3 Sequencing results of recombinant pGEX-6P-1 plasmid. It contains inserts of AvBD6 mature peptide (A), AvBD6 promature peptide (B), AvBD9 mature peptide (C), and AvBD9 promature peptide (D).....	96

Figure 4.4 SDS PAGE (A) and NUPAGE (B) gels of recombinant pGEX-6P-1/AvBD6..	97
.....	
Figure 4.5 SDS PAGE gels of hyperexpressed pGEX-6P-1 BL21/AvBD9.....	98
Figure 4.6 NUPAGE gel stained with Instant Blue showing AvBD9 purification (cleaving off the column).....	100
Figure 4.7 NUPAGE gel stained with Instant Blue showing AvBD6 purification (cleaving off the column).....	100
Figure 4.8 NUPAGE gel stained with Instant Blue showing AvBD9 purification (cleavage on the column).	101
Figure 4.9 NUPAGE gel stained with Instant Blue showing AvBD6 purification (cleaving on the column).	102
Figure 4.10 NUPAGE gel stained with Instant Blue showing AvBD6 purification (cleaving on the column eluting with PBS).	103
Figure 4.11 A sample of purified AvBD9 promature peptide analysed by MALDI-MS/MS using CHCA (A), DHB (B) and DAN matrices (C).	105
Figure 4.12 AvBDs 1 – 14 primary amino acid sequences.....	107
Figure 4.13: Suggested disulphide bond arrangement of AvBD9 between each three pairs of cysteines (C1-C5), (C2-C4) and (C3-C6).....	108
Figure 4.14 A-H: DNA sequencing results of mutagenised plasmids.	110
Figure 4.15 NUPAGE gel stained with Instant Blue showing AvBD9 3CA purifications..	111
.....	
Figure 4.16 NUPAGE gel stained with Instant Blue showing AvBD9 6CA/G (Lanes 1-4) and AvBD9W38G (Lanes 5-8) purifications.....	112
Figure 4.17 Radial immuno-diffusion assay results following incubation of 0.5, 1 and 4 µg/µl recombinant AvBD6 mature peptide (A).	114
Figure 4.18 Radial immuno-diffusion assay of recombinant AvBD9 peptides using lawn of <i>E. coli</i> grown on TSB agar.....	115
Figure 4.19 Percentage inhibition zone created using 3 µg/µl of AvBD9 promature and 3CA peptides compared to AvBD9 mature.....	115
Figure 4.20 Radial immune-diffusion assay of rAvBD9 peptides in different concentrations against <i>E. coli</i> grown on TSB agar.	116
Figure 4.21 Percentage inhibition zone created by 3 µg/µl of AvBD9 6CA/G and W38G peptides compared to AvBD9 mature against <i>E. coli</i>	117

Figure 4.22 Time–kill assay data comparing <i>E. coli</i> killing by rAvBD6 mature and promature peptides.....	118
Figure 4.23 Time–kill assay data comparing <i>E. faecalis</i> killing by rAvBD6 mature peptides.	119
Figure 4.24 A: Time–kill assay data comparing <i>E. coli</i> killing by rAvBD9 peptides. .	120
Figure 4.25 Time–kill assay data comparing <i>E. coli</i> killing by rAvBD9 mature, rAvBD9 W38G; GST-3C and BSA.....	122
Figure 4.26 NUPAGE gel stained with Instant Blue and comparing AvBD9 mature and AvBD9 3CA in both reducing (1 and 2) and non-reducing (3 and 4) conditions.....	123
Figure 4.27 Time–kill assay data comparing <i>E. faecalis</i> killing by rAvBD9 peptides. ..	125
Figure 4.28 AvBD10 DNA sequences of the mature (A) and mutagenized plasmids (B). Restriction sites (BamH1) and (EcoR1) are highlighted in grey.	127
Figure 4.29 NUPAGE stained by Instant Blue showing purification of AvBD10 recombinant peptides.	128
Figure 4.30 Radial immuno-diffusion assay comparing the AMAs of AvBD10 mature and AvBD10 A45W (A) using <i>E. coli</i> grown on TSB (C).....	129
Figure 4.31 Time–kill assay data comparing <i>E. coli</i> killing by rAvBD10 mature and AvBD10 A45W peptides.	130
Figure 4.32 Time–kill assay data comparing <i>E. faecalis</i> killing by AvBD10 mature and AvBD10 A45W peptides.	131
Figure 4.33 HPLC analysis of mature sAvBD9.....	132
Figure 4.34 HPLC analysis of mature sAvBD6.....	132
Figure 4.35 HPLC analysis of AvBD9 W38G.....	133
Figure 4.36 Time–kill assay data comparing <i>E. coli</i> killing by synthetic and recombinant peptides.....	134
Figure 4.37 Time–kill assay data comparing <i>E. faecalis</i> killing by synthetic and recombinant peptides.	135
Figure 4.38 Time-kill assay data using 100 µg/ml of synthetic and recombinant AvBD6 peptides against <i>E. coli</i> clinical isolate (A, C and E) and BL21 (B, D and F) in PBS (A and B), protease inhibitors (C and D), and sodium phosphate (NaP) buffer 10 mM (E and F).	137
Figure 4.39 Time-kill assay comparing synthetic AvBD9 peptides against <i>E. coli</i> clinical isolate (A, C and E) and BL21 strain (B, D and F) in PBS (A and B), protease inhibitors (C and D), and sodium phosphate (NaP) buffer 10 mM (E and F).....	139

Figure 5.1 CD spectra of standard peptide conformations A-helix (A), β -sheet (B), type I β -turn (C), Unordered (D).....	147
Figure 5.2 CD spectra of recombinant AvBD9 variants in 50 mM Na P buffer	148
Figure 5.3 A: CD spectra of recombinant AvBD9 variants in 1% SDS micelles.....	150
Figure 5.4 Calcein leakage recorded using entrapped liposomes incubated for 60 minutes at room temperature in 50 mM NaP buffer (A); following the addition of 10 % Triton X 100 (1% final concentration) (B).	154
Figure 5.5 Calcein leakage assay following addition of rAvBD9 and variants to dye-entrapped liposomes.....	155
Figure 5.6: A: CD spectra of sAvBD6 in NaP buffer (Blue) and 1% SDS micelle solution (Red).	157
Figure 5.7 A: CD spectra of sAvBD9 in NaP buffer (Blue) and 1% SDS micelle solution (Red).	159
Figure 5.8 A: CD spectra of sAvBD9 W38G in NaP buffer (Blue) and 1% SDS micelle solution (Red).....	160
Figure 5.9 A: CD spectra of sAvBD9 W38G in NaP buffer (Blue) and 1% SDS micelle solution (Red).....	
Figure 5.10 Calcein leakage recorded using entrapped liposomes incubated for up to 1 minute (A) and 4 minutes (B) at room temperature in 50 mM NaP buffer and either 1.5 μ g/ml sAvBD6 (red line) or melittin (blue line).	162
Figure 5.11 Calcein leakage recorded using entrapped liposomes incubated for up to 1 minute (A) and 4 minutes (B) at room temperature in 50 mM NaP buffer and either 1.5 μ g/ml sAvBD9 (blue) or sAvBD9 W38G (green).	163
Figure 5.12 Calcein leakage recorded using entrapped liposomes incubated for up to 1 minute (A & C) and 4 minutes (B & D) at room temperature in 50 mM NaP buffer and either 3 (A & B) or 10 μ g/ml (C & D) sAvBD9 (blue) or sAvBD9 W38G (green).	165
Figure 5.13 Calcein leakage assay of sAvBD9 and sAvBD9 W38G at 2.5, 5 and 10 μ g/ml incubated with the vesicles for 1 hour.	166
Figure 5.14 Predicted structure of AvBD6.	167
Figure 5.15 Predicted structures of AvBD9 (A) and AvBD9 W38G (B).	168
Figure 5.16 Simulated 3D structure of AvBD6.	169
Figure 5.17 Simulated 3D structures of AvBD9 (A) and AvBD9 W38G (B).	171
Figure 5.18 Amino acid sequences of synthetic AvBD1 SNP peptides..	176

Figure 5.19 A: Radial diffusion assay showing the inhibitory effect of AvBD1 variants ‘NYH’, ‘SSY’ and ‘NYY’ at 4, 2 and 1µg. B: Time-kill assay showing percentage bacterial (<i>E. coli</i>) growth following 2 h incubation of <i>E.coli</i> (1/1000 dilution) with NYH, SSY and NYY AvBD1 peptides.	177
Figure 5.20 A: CD spectra of sAvBD1, NYH (Blue), NYY (Red) and SSY (Green).....	179
Figure 5.21 A: CD spectra of sAvBD1, NYH (Blue), NYY (Red) and SSY (Green).....	181
Figure 5.22 A: CD spectra of sAvBD1 NYH in NaP buffer (Blue) and 1% SDS micelle solution (Red).....	182
Figure 5.23 A: CD spectra of sAvBD1 SSY in NaP buffer (Blue) and 1% SDS micelle solution (Red).....	183
Figure 5.24 A: CD spectra of sAvBD1 NYY in NaP buffer (Blue) and 1% SDS micelle solution (Red).....	184
Figure 5.25 Calcein leakage recorded using entrapped liposomes incubated for up to 1 minute (A) and 3 minutes (B) at room temperature in 50 mM NaP buffer and 1.5 µg/ml sAvBD1 NYH (blue), SSY (green), NYY (red) and melittin (purple).....	186
Figure 5.26 Calcein leakage recorded using entrapped liposomes incubated for up to 1 minute (A) and 3 minutes (B) at room temperature in 50 mM NaP buffer and 2.5 µg/ml sAvBD1 NYH (blue) SSY (green) NYY (red) and melittin (purple).....	187
Figure 5.27 Predicted secondary structures (β -sheet and α -helix) of AvBD1 variants NYH (A), SSY (B) and NYY (C).....	189
Figure 5.28 Simulated 3D structures of AvBD1 NYH (A), SSY (B) and NYY (C) variants.	190

List of Tables

Table 2.1 Genotypes of competent cells used for cloning and hyperexpression	32
Table 2.2 Primers designed for AvBDs, cytokines, and Chicken Galectin-3 genes.....	37
Table 2.3 Real-time PCR primers.....	39
Table 2.4 Primers (forward and reverse) designed for site directed mutagenesis.	46
Table 3.1 List of 5 SNPs in an Illumina study that were identified in Aviagen Line X birds.....	57
Table 4.1 Primers used to mutagenise cysteines, C3, C4 and C5 of AvBD9 to Alanines.	111
Table 4.2 Yields of AvBD9 recombinant peptides (mg/L bacterial growth media).....	112
Table 4.3 Final yields of AvBD10 and AvBD10 A45W (mg/L BL21) purification.	128
Table 5.1 Dichroweb quantification of CD secondary structures (%) including α -helices, β -strands, β -turns and unordered structure following exposure of rAvBD9 variants to 50 mM NaP buffer.	149
Table 5.2 Quantification of CD secondary structures (%) including α -helices, β -strands, β -turns and unordered structure following exposure of rAvBD9 variants to 1% SDS micelle solution.....	152

List of Abbreviations

ACTB	β -actin
AMA	anti-microbial activity
AMP	anti-microbial peptide
AvBD	avian β -defensin
AvBD9 3CA	avian β -defensin three cysteines mutagenised to alanines
AvBD9 6CA/G	avian β -defensin six cysteines mutagenised to alanines/glycines
AvBD9 W38G	avian β -defensin c-terminal tryptophan mutagenised to glycine
A.U.	arbitrary unit
bp	base pairs
BD	big defensin
BCA	bicinchoninic acid
BSA	bovine serum albumin
C	cytosine
calcein	carboxyfluorescein
CD	Circular dichroism
cDNA	complementary DNA
CCA	colony counting assays
CG3	chicken galectin-3
CFE	cell free extract
CHCA	4-hydroxy--cyano-cinnamic acid
cLEAP-2	chicken liver expressed anti-microbial peptide 2
CP	crossing point
Cys	cysteine
D7	day 7
D35	day 35
Da	Dalton
DAB	3,3-diaminobenzidine tetrahydrochloride
DAN	1,5-diaminonaphthalene
degP	Periplasmic serine endoprotease
Defr1	Defensin-related peptide 1
DHB	2,5-dihydroxybenzoic acid
di-S	di-sulphide

diS-C3-5	diisopropylthiadicarbocyanine Iodide
DNA	deoxyribose nucleic acid
dNTP	deoxyribonucleotide triphosphate
ds	double stranded
DTT	dithiothreitol
EDTA	ethylenediaminetetraacetate
F	forward
E.U.	European Union
g	grams
G	guanine
GAPDH	glyceraldehydes-3-phosphate dehydrogenase
GM-CSF	Granulocyte macrophage colony-stimulating factor
GST	glutathioneS-transferase
h	hour
HBD	human β -defensin
HD-5	human defensin-5
HDP	host defense peptide
HH	high hygiene
HNP	human neutrophil peptide
HKG	house keeping gene
HPLC	high pressure liquid chromatography
HRV	human rhinovirus
IPTG	isopropyl β -D-1-thiogalactopyranoside
IL-2	interleukin-2
IL-6	interleukin-6
IHC	immunohistochemistry
ISD	In-Source Decay
Kb	kilobase
kDa	kilodalton
L	liter
LB	Luria Bertani
LC-MS	liquid chromatography mass spectrometry
LH	low hygiene
lon	lon protease

LPS	lipopolysaccharide
M	moles
mA	milliamp
MALDI-TOF	matrix-assisted laser desorption/ionization time of flight
MCS	multiple cloning site
mg	milligram
min	minute
ml	milliliter
mM	milimolar
MLV	multilamellar vesicle
mRNA	messenger RNA
m/z	mass-to-charge ratio
NaP	sodium phosphate buffer
NCBI	National Centre for Biotechnology Information
NFκB	nuclear factor kappa-light-chain-enhancer of activated B cells
nM	nanometers
NMR	Nuclear magnetic resonance
NPN	N-phenylnaphthylamine
OD	optical density
OmpT	outer membrane protease
PAMP	pathogen associated molecular pattern
PBS	phosphate buffer saline
PG	peptidoglycan
PCR	polymerase chain reaction
POPE	Palmitoyl oleoyl phosphatidyl ethanolamine
POPG	Palmitoyl oleoyl phosphatidyl glycerol
POPC	Palmitoyl oleoyl phosphotidyl choline
DPX	p-xylene-bispyridinium bromide
qRT-PCR	quantitative real-time PCR
R	reverse
rec	recombinant
RNA	ribonucleic acid
RNAasin	RNAase inhibitor
RIDA	radial immuno-diffusion assay

rpm	revolutions per minute
RT	reverse transcription
SD	site directed
SDHA	Succinate dehydrogenase complex, subunit A
SDS PAGE	sodium dodecyl sulphate polyacrylamide gel electrophoresis
SDS	sodium dodecyl sulphate
SF3A1	Splicing factor 3 subunit 1
sec	seconds
SEM	standard error of the mean
SNP	single nucleotide polymorphism
Sphe-2	spheniscin-2
T	thymine
TBE	Tris-borate-EDTA
TBS	tris base saline
TEMED	<i>N,N,N,N</i> '-tetramethylethylenediamide
TFE	Trifluoroethanol
TGFβ4	transforming growth factor β-4
TLRs	toll like receptors
Tm	annealing temperature
Tris	tris (hydroxymethyl)methylamine
TSB	Tryptic soy broth
UBC	ubiquitin
UK	United Kingdom
ULV	unilamellar vesicle
UV	ultra violet
UTR	untranslated region
Y	tyrosine
YWHAZ	Tyrosine 3-Monooxygenase/Tryptophan 5-Monooxygenase Activation Protein Zeta
v/v	volume to volume
W	tryptophan
w/v	weight for volume

Chapter 1

1. Introduction

1.1. Background

Poultry, particularly chicken, meat is a major source of protein worldwide and its commercial value has, for decades, underpinned research into maximising meat production per bird. However, more recent research has focussed on rearing ‘robust’ birds that not only show optimal feed to gain ratios, but that can also resist infectious and/or zoonotic diseases (Lowenthal *et al.*, 2013). In fact, breeding disease resistant birds is a major research objective of poultry breeders supplying birds for the poultry industry with the research driven, primarily, by EU legislation banning the use of antibiotics in poultry feeds (Huyghebaert *et al.*, 2011). The research aims are directed, primarily, towards genetically selecting birds with ‘improved’ innate immunity and therefore enhanced resistance to disease.

One particular focus of poultry breeders is the bird gut and the selection of commercial chicken lines with improved gut innate immunity. The challenge is to breed chicks that are especially resistant to infection during the first week after hatch, when they are particularly susceptible to disease. A particular area of interest is the expression and synthesis of avian antimicrobial peptides (AMPs), which are antimicrobial agents produced by epithelia and antigen presenting cells, and hence an important part of the bird innate immune defences.

An understanding of the involvement and roles of the host innate defences, specifically Avian β -defensins (AvBDs) that exhibit potent antimicrobial properties, in protecting birds (young and growing) against disease is lacking. Commercially such information on the roles of AvBDs in bird gut health may be used to improve disease resistance in commercial lines and exploited through selective breeding programmes.

1.2. Host- microbial interactions

The avian gut is particularly susceptible to infection as birds feed from the environment immediately from hatch. While transfer of maternal antibody via the egg yolk does help chick survival antibody titres suggest the antibodies have disappeared by day 10 and thus no longer afford the bird protection against disease (Gharaibeh and Mahmoud, 2013).

Innate factors participating in the vertebrate gut host response that help protect against microbial damage include gastric acid and mucus production, the epithelial barrier and the presence of pathogen recognition receptors (PRRs) such as Toll-like receptors (TLRs) on the epithelium. The latter detect microbial components including lipopolysaccharides (LPS), peptidoglycan (PG) and flagellin leading to AMP and /or cytokine production resulting in microbial death directly and/or the attraction of phagocytes including heterophils and macrophages (Wigley, 2013) that precipitate microbial death. However, in contrast to their mammalian counterpart, avian heterophils depend on AMP synthesis rather than oxidative myeloperoxidase activity for bacterial killing (Cuperus *et al.*, 2013).

The gut however, is a unique organ in that it is colonised naturally by microbes. The gut commensal microbiota contains bacteria that survive naturally and colonize the host gastrointestinal tract without causing disease. Identification of microbiota colonizing the gut mucosal surfaces by molecular analysis of 16S rRNA sequences using pyrosequencing and/or metagenomics analysis of whole extracted microbial DNA, allows the type and composition of the microbes living mutually within the host intestine to be defined (Sergeant *et al.*, 2014). In health this gut colonization is balanced, but it can change in response to nutrition, drug administration, disease and environment resulting in gut problems. Interestingly one of the most important factors affecting gut microbial colonization, although not normally negatively, is genetic variation between animal species and individuals within the same species (Bevins and Salzman, 2011).

Many genera of bacteria have been identified in the chicken gut, including bacteria from the family *Enterobacteriaceae* in the small intestine, and *Bacteroides*, *Bifidobacterium*, *Clostridium*, *Enterococcus*, *Escherichia*, *Fusobacterium*, *Lactobacillus*, *Streptococcus* and *Campylobacter* within the cecum (Brisbin *et al.*, 2008). Host-microbial interactions, particularly those of gut commensals, play significant roles in gut immunity that is indicated by vulnerability of germ free animals to infections and the impact of the microflora on T cell populations and cytokine profiles (Brisbin *et al.*, 2008). Antibiotic usage as a growth promoter is probably linked to the reduction of gut microbial loads and

the increased absorption of nutrients by the intestinal epithelia (Brisbin *et al.*, 2008). However, gut bacterial populations have been shown in poultry to be changed by antibiotic use (Brisbin *et al.*, 2008), with low dose antibiotic added as a feed additive decreasing gut colonisation by some species of *Lactobacillus*, eg *Lactobacillus salivarius*. These data suggest that the long term use of antibiotics can have negative effects, for example by reducing *Lactobacilli* lactic acid production which is involved in inhibiting the growth of pathogens via a reduction of the gut niche pH (Brisbin *et al.*, 2008).

Colonisation of the gut with microbes is also proposed to play a role in the development and maturation of the gut immune system and vice versa, i.e., the microbiota and host immune system function to maintain a symbiosis. For example, bacteria are detected by PRRs located on the gut epithelia and their numbers are controlled by the secretion of cytokines and/or antimicrobial peptides, often referred to as physiological inflammation (Crhanova *et al.*, 2011). The system breaks down due to gut pathogens, including *Salmonella enterica*, being able to avoid the gut innate immune defences, resulting in an increase in the pathogen and dysbiosis (Salzman *et al.*, 2010). Moreover, this disruption of the microbiota and induction of pathological inflammation enhances pathogen colonisation, and persistence, resulting in poor gut health, and in extreme cases the potential death of the host. Thus potentially AMPs are important in controlling the natural gut microbiota and maintaining optimal gut health.

1.3. Host defence proteins

The term host defence proteins (HDPs) encompasses groups of gene encoded innate immune peptides and proteins including the AMPs as well as other molecules such as lactoferrin and lysozyme (Hancock and Scott, 2000). The focus of this thesis is primarily the AMPs which are 12-50 amino acids in size, cationic (net charge +2 to +11) and generally rich in histidine, lysine and arginine amino acids, with the presence of hydrophobic and hydrophilic amino acids providing their amphipathic characteristics (Sugiarto and Yu, 2004). The peptides show broad spectrum anti-microbial activity (AMA) against various microbes including bacteria, fungi, enveloped viruses and some protozoa, and in mammals immuno-modulatory activities including cytokine induction and immune cell recruitment to the site of infection (Wilmes *et al.*, 2011).

There are four classes of these host defence AMPs as defined by their amino acid composition, secondary structure and number of disulphide bonds (Figure 1.1). The first

group includes the linear α -helical peptides such as magainin 2 (synthesised by frog skin), the second contains cysteine free extended helical peptides with repeated amino acids such as the tryptophan rich indolicidin (synthesised by bovine neutrophils), the third, which includes Thanatin (an insect peptide), is defined by a loop structure and a disulphide bond while the final group is characterised by β -(β) sheet structures and three disulphide bonds. The latter group includes the defensins, which are secreted by vertebrates, invertebrates, fungi and plants (reviewed by Wilmes (2012)).

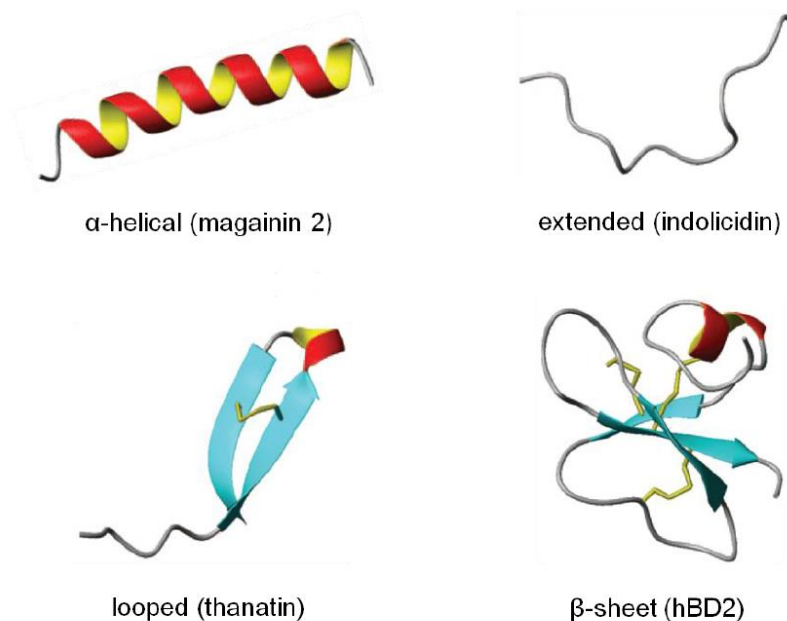


Figure 1.1 Structures of host defence peptides (Wilmes, 2012)

1.4. Defensins

Depending on their cysteine disulphide bonding patterns, there are three groups of defensins found in vertebrates, invertebrates, fungi and/or plants (Figure 1.2) (reviewed by Wilmes (2012)). In vertebrates, three classes have been described including α -(α), β -(β)

and theta (θ) defensins. The first two groups are present in humans while the latter group, the θ -defensins, has been found only in the Rhesus monkey (Semple *et al.*, 2003). Furthermore, only β -defensins have been identified in birds (van Dijk *et al.*, 2008). The observation that α - and θ -defensins have not been found in phylogenetically older vertebrates, such as birds and fish, suggests that all the defensin subfamilies evolved from an ancestral β -defensin gene, presumably by duplication and diversification (Zhao *et al.*, 2001; Semple *et al.*, 2003; van Dijk *et al.*, 2008). While β -defensins are expressed and synthesised by epithelia, α -defensins are localised to bone marrow cells, neutrophils (Linde *et al.*, 2009) and in humans the gut Paneth cells (Salzman, 2010).

Both α - and β -defensins differ according to the location and connection of their disulphide bridges (Selsted and Ouellette, 2005; van Dijk *et al.*, 2008). These bridges are arranged as Cys1–Cys6, Cys2–Cys4, Cys3–Cys5 for α -defensins versus Cys1–Cys5, Cys2–Cys4, Cys3–Cys6 for β -defensins.

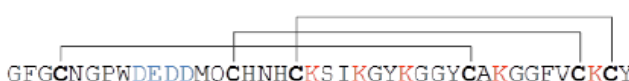



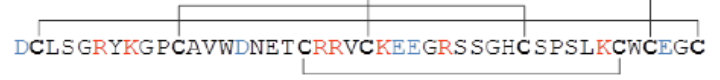

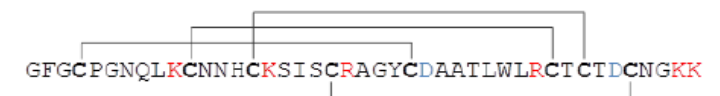

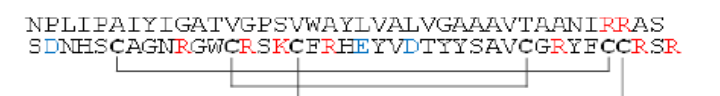

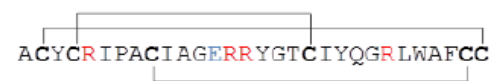




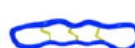
	Sequence	3D structure	Defensin	Activity spectrum
Fungi	 <p>GFGCNGPWNDEDDMQCHNHCKSIKGYKGGYCAKGGFVCKCY</p>		plectasin	Gram ⁺ bacteria
Plant	 <p>QKLCQRPSGTWSGVCGNNACKNQCIRLEKARHGSCNYVFPAHKCICYFFC</p>		Rs-AFP2	fungi
Invertebrate	 <p>DCLSGRYKGPCAVWDNETCRRVCKEEGRSSGHCSPSLKCWCEGC</p>		drosomycin	fungi
	 <p>GFGCPGNQLKCNNHCSISCRAGYCDAATLWLRCTCTDCNGKK</p>		Cg-Defm	Gram ⁺ bacteria
	 <p>NELIPAIYIGATVGPSVWAYLVALVGAAVTAANIRRAS SDNHSCAGNRGWCRSKCFRHEYVDTYSAVCGRYFCCRSR</p>		big defensin BDEF_TACTR	Gram ⁺ and Gram ⁻ bacteria, fungi
Vertebrate	 <p>ACYCRIPACIAGERRYGTCIYQRLWAFCC</p>		α-defensin HNP-1	
	 <p>GIINTLQKYYCRVRGGRCAVLSCLPKEQIGKCSTRGRKCCRRKK</p>		β-defensin hBD3	Gram ⁺ and Gram ⁻ bacteria, fungi, viruses
	 <p>GFCRCLCRRGVCRCICTR</p>		θ-defensin RTD-1	

Figure 1.2 Sequences and 3D structures of selected defensins. Residues with a positive charge are marked in red, negatively charged residues are marked in blue (Wilmes, 2012)

Defensins are broad spectrum antimicrobials active against a wide variety of pathogens, including both Gram positive and negative bacteria, in addition to yeast, fungi and viruses (Sugiarto and Yu, 2004; Soman *et al.*, 2009). The molecules serve as a first line of defence against invading pathogens (Soman *et al.*, 2009) and show immuno-regulatory characteristics boosting the acquired immune defences through attraction of monocytes, T cells, juvenile dendritic cells and mast cells to areas of inflammation (van Dijk *et al.* 2008; Soman *et al.* 2009). In addition they can stimulate histamine liberation from mast cells as well as macrophage phagocytosis (Soman *et al.*, 2009). Thus in mammals they serve as key factors in connecting the innate and adaptive immune responses (Soman *et al.*, 2009).

Bacterial killing is proposed to occur through mechanisms including membrane disruption and pore formation leading to cell lysis and irregular septum formation in dividing cells (Ganz 2003; van Dijk *et al.* 2008). It is proposed that the anti-microbial mechanisms of defensins involving pore formation depend on the two characteristics of antimicrobial peptides ie their cationic charge and amphipathicity. Basically, β -defensins bind to bacterial membranes as a result of interactions between the anionic (negatively charged) bacterial membrane and the exposed cationic (positively charged) amino acid side chains of the peptide. One killing mechanism suggests a peptide dimer forms that initiates a channel between the amino-end of the β -strands of the two β -defensin monomers; the channel is created such that the hydrophobic sites of the peptides are facing the inner bacterial membrane and the hydrophilic sites are facing each of the β -defensin monomers (Sugiarto and Yu, 2004). The dimer effects transmembrane potential, membrane permeability and resulting in cell death (Sugiarto and Yu 2004; Higgs, *et al.* 2005). Defensin antibacterial activity can also reflect the environmental availability of positively charged divalent cations. For example, magnesium cations (Mg^{2+}), found free in serum, are able to compete with the positively charged defensins for binding to the negatively charged microbial membranes. Thus microorganisms are more susceptible to defensins in areas of low cation concentration, which include the vacuoles of phagocytes and on the surfaces of the skin, and epithelia (Sugiarto and Yu, 2007a).

1.5. Evolution of defensins

AMPs are secreted by all organisms including prokaryotes and eukaryotes, and an evolutionary relationship between the two has recently been hypothesised, focused on the bacteriosin laterosporulin synthesised by *Brevibacillus* sp. strain GI-9. This bacterial molecule exhibits β -strands and its six cysteines form three disulphide bonds [Cys1-Cys5, Cys2-Cys4, and Cys3-Cys6] like that of β -defensins, lending support to it being a link between the bacterial bacteriocins and mammalian defensins (Singh *et al.*, 2015). Additionally, the amino acid sequence homology of the fungal defensin, plectacin, to dragonfly and mussel defensins also indicates the fungal defensin being an ancestor to vertebrate defensins (Lehrer *et al.*, 2012). However, the evolutionary links remain controversial as the C-terminal part of 'big defensin' (BD) from horseshoe crab has also been hypothesised to be the ancestor of vertebrate β -defensins, as argued through comparisons of amino acid sequences, conserved defensin motifs (CXXXXGXCRXXCFXXE), net charges, disulphide bond arrangements and functions of invertebrate and vertebrate defensins including the human β -defensin 125, chicken AvBD13, Anole (reptile) β D, Tetraodon (teleost) β D, Amphioxus (cephalo-chordate invertebrate) β D, Crassostrea (oyster) β D and Tachyplesus (horseshoe crab) β D (Lehrer and Lu, 2012). Furthermore, bioinformatics analyses suggest that exon reshuffling and intronisation has underpinned the emergence of the vertebrate β -defensins from its ancestral 'big defensin' origin (Zhu and Gao, 2013). Further factors supporting a common ancestry among the β -defensins are the conservation of cationic, hydrophobic and hydrophilic amino acid sequence patterns in the plant, insect and human defensins, the similar defensin mechanisms of action and the sharing of functional features in the different kingdoms eg treating mouse fungal infections with plant defensins (reviewed by Wilmes *et al.* (2011)).

Evidence for the divergence of the β -defensins to both α - and θ -defensins is that α -defensins are synthesised only in mammals and marsupials with the θ -defensin synthesised only by some species of rhesus monkey (Lehrer and Lu, 2012). Interestingly, the θ -defensin gene is present in humans, but a premature stop codon in its signal peptide sequence inhibits its synthesis (Lehrer and Lu, 2012). It has been proposed that the θ -defensin gene evolved from the α -defensin gene with the causative mutations resulting in the synthesis of a heterodimeric θ -defensin composed of two monomers each containing nine residues and linked by three intra disulphide bonds forming a cyclic peptide (Lehrer *et al.*, 2012;

Kudryashova *et al.*, 2015). In addition, the θ -defensin genes reside within the α -defensin genes that in turn cluster within the β -defensin gene cluster suggesting that the β -defensins evolved to α -defensins, which further evolved to theta defensins (Cuperus *et al.*, 2013). It has been suggested that in mammals, apart from New World Monkeys, the θ -defensins, known to have anti-viral and anti-toxic activities, were 'lost' due to the high production of α -defensins in neutrophils. Although the α -defensin peptides appear *in vitro* to show reduced antimicrobial potency compared to the θ -defensins their increased synthesis presumably provided far greater protection against microbial assault and supported their evolutionary selection (Lehrer *et al.*, 2012).

Comparison of defensin gene clusters among vertebrates including human, mouse and chicken suggest that gene duplications, fusions, diversifications and translocations also played significant roles in the evolution of the defensin genes (Xiao *et al.*, 2004). Exon fusion is also another feature predicted to have occurred during defensin evolution as typified by the fusion of the last two exons of AvBD12, which has three exons, compared to the four of other AvBDs (Cuperus *et al.*, 2013).

1.6. AvBD sequence homology

The Avian β -defensins (AvBDs) in particular show a close evolutionary relationship. For example, AvBD6 and AvBD7 are located in the middle of the chicken defensin family gene cluster, and their DNA sequences suggest gene duplication (Meade *et al.*, 2009a). This is further illustrated by AvBD3, AvBD4, AvBD5 and AvBD14, which share similar promotor elements. In fact, bioinformatic analyses of a number of bird genomes reveals the depth of AvBD conservation. For example Duck AvBD1 shares 78% and 68% amino acid homology with the turkey and chicken AvBD1 sequences, with geese AvBD1 having amino acid similarities of 88%, 71%, 68%, and 66% with duck, ostrich, turkey and chicken, respectively (Ma *et al.*, 2013). Ostrich AvBD2 has 86%, 83%, 83% and 82% nucleotide sequence similarities with those of geese, chicken, duck and turkey respectively (Lu *et al.*, 2014). Duck AvBD3 and 6 peptides reveal 100% similarity to the comparable chicken sequences (Peng *et al.*, 2013). AvBD4 and AvBD9 show identical amino acid sequences among the majority of passerine species (Cuperus *et al.*, 2013). Duck AvBD5 displays 97% and 88% homology to the comparable chicken and geese peptide sequences (Ma *et al.*, 2012a). Moreover, ostrich AvBD7 shows 81% homology to AvBD7 of chicken and duck and 75% similarity with AvBD6 of chicken, duck and geese, which strongly supports the

suggestion that AvBD6 evolved from AvBD7 by gene duplication (Hellgren and Ekblom, 2010; Lu *et al.*, 2014).

1.7. Avian β -defensin

To date 40 AvBD genes have been identified in birds and these include the 14 chicken β -defensin genes which are localised to a 129 kb single β -defensin cluster on chromosome 3 (Lan *et al.*, 2014) as well as those genes identified in other avian genomes including the duck, zebra finch and crested ibis (Figure 1.3). Gallins or ovodefensins are also viewed as AvBDs based on their disulphide bond arrangement and 3D β -sheet structures (Herve *et al.*, 2014). Additionally, the gallin gene cluster is located on chromosome 3 and close to the AvBDs gene cluster; the AvBD13 gene is positioned at 107,019.512K, gallin-3 is positioned at 106,750.937K, gallin-2 at 106,747.961K, and gallin-1 at 106,740.473 K (NCBI gene map viewer):

(http://www.ncbi.nlm.nih.gov/gene?cmd=retrieve&dopt=full_report&list_uids=422030).

Thus the gap between the AvBD and gallin clusters is 268.575K (Figure 1.4), which suggests and supports close genomic relations.

As stated previously chicken β -defensin genes consist of four exons, with the exception being the AvBD12 gene where the last two exons have fused (Figure 1.5). The genes each encode a signal sequence that directs the peptide through the endoplasmic reticulum for secretion, a pro-region, although this is absent in AvBDs 3, 12, 14, and a mature antimicrobial peptide (Figure 1.6).

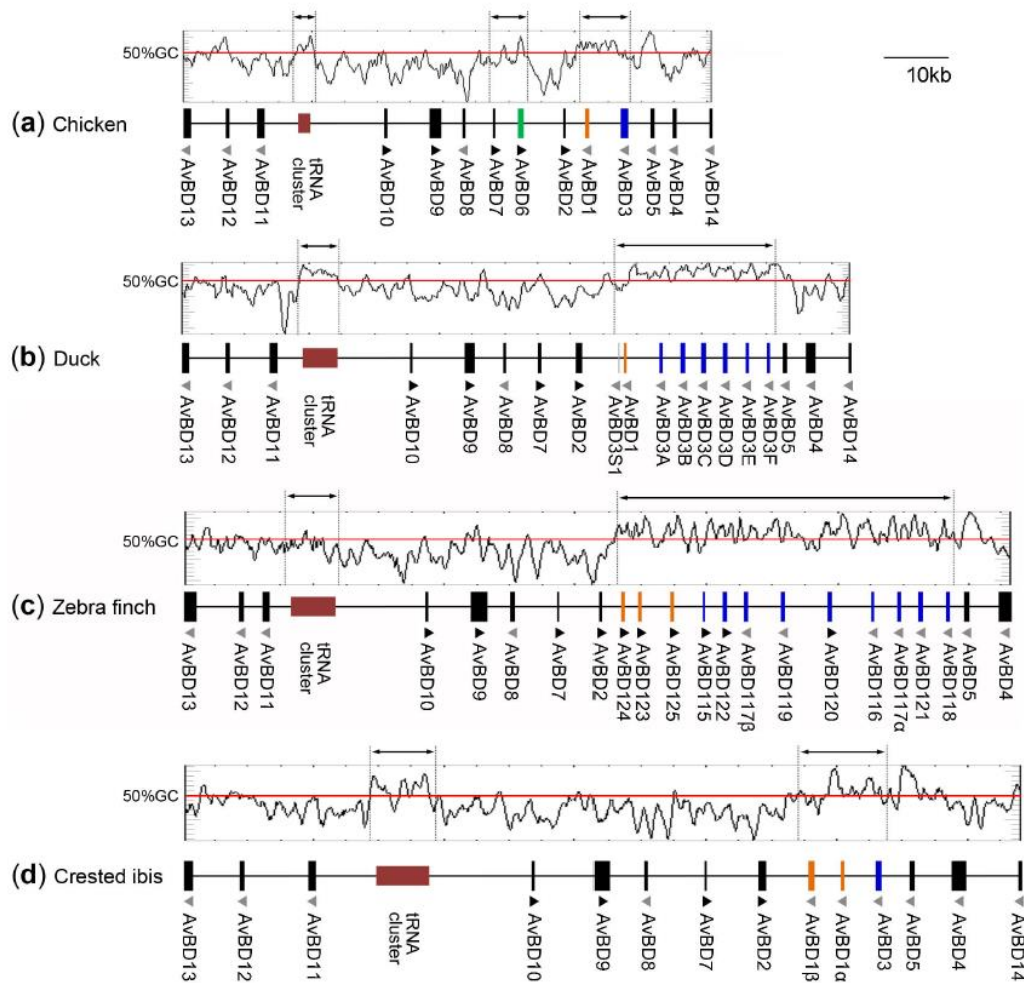


Figure 1.3 Organization of β -defensin gene clusters. Avian β -defensin clusters from (a) chicken, (b) duck, (c) zebra finch, and (d) crested ibis. Vertical bars: gene locations; lengths drawn to scale (upper right corner). Paralogous genes for AvBD1 (orange) and AvBD3 (blue) and chicken-specific AvBD6 (green) are shown. Red: tRNA clusters. Small triangles: transcriptional orientations of defensin gens. Duplicated regions are bracketed by double-sided arrows and dotted lines (Lan *et al.*, 2014).

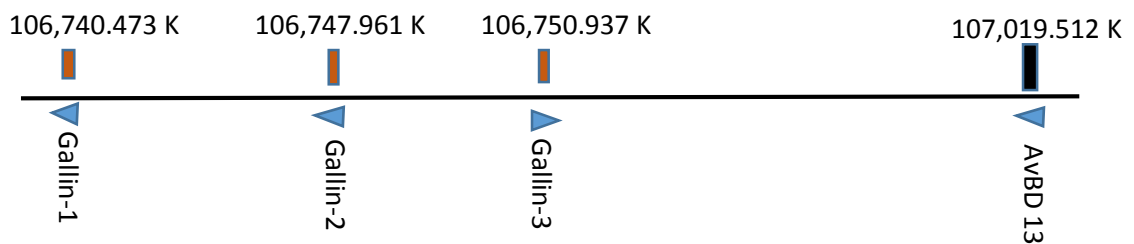


Figure 1.4: Genomic organisation of gallin gene clusters in relation to the last cluster of AvBDs (AvBD 13)

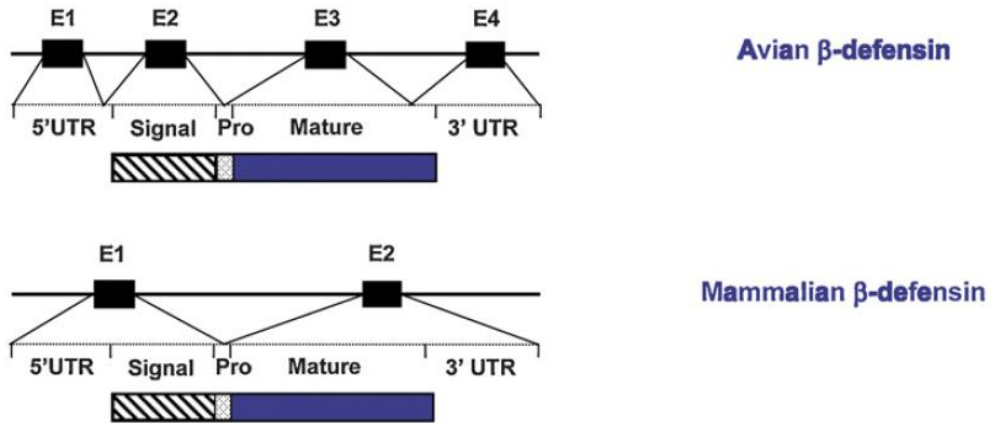


Figure 1.5 Genomic organization of avian and mammalian. Differential transcription and subsequent translation of exons (E1–4) into the 5' and 3' untranslated regions (UTR) and peptide encoding regions for: signal peptide (diagonal striped bars), propeptide (dotted bars) and mature peptide (solid blue bars) (van Dijk *et al.*, 2008).

The mature AvBD peptide sequences contain the six cysteines (C), which are essential for disulphide bond folding, cationic residues such as histidine (H), lysine (K) and arginine (R), which are important for electrostatic interaction between the peptide and microbial lipid membrane, and hydrophobic aromatic amino acids including tryptophan, tyrosine, and phenylalanine that are proposed to play a role in the insertion of the peptide into the microbial membrane (Figure 1.6). Interestingly ten of the AvBDs display a C-terminal tryptophan amino acid in their mature peptide sequence (Figure 1.6).

AvBD 1: GRKSDCFRKS^YSGFC^YAF^YLK^YPSLTLISGK^YCSR^YF^YL^YCCK^YR^YI^YW^YG

AvBD 2: RDM^YLF^YCK^YGG^YSC^YH^YFGG^YCP^YSH^YL^YIK^YVGS^YCF^YGR^YSC^YCK^YW^YP^YW^YNA

AvBD 3: GTATQ^YCR^YIR^YGG^YFC^YR^YVGS^YCR^YF^YPH^YIAI^YGK^YCAT^YIS^YCC^YGR^YAY^YEV^YD^YALNSV^YRTSP^YW^YLLAPGNNPH

AvBD 4: RY^YH^YM^YQC^YGY^YR^YGT^YFC^YTPG^YK^YCP^YHGNA^YYLGL^YCR^YPK^YYS^YCCR^YWL

AvBD 5: GLPQ^YDC^YERR^YGG^YFC^YSH^YRS^YCPPGIG^YRIGL^YCK^YED^YF^YCCR^YSR^YW^YYS

AvBD 6: SPI^YH^YAC^YRY^YQR^YGV^YCIPGP^YCR^YWP^YY^YRVGS^YCGSGL^YK^YSC^YV^YRNR^YWA

AvBD 7: R^YPI^YDC^YRL^YR^YNGI^YCF^YPGI^YCRR^YPY^YW^YIGT^YCNNGIG^YSC^YARG^YW^YRS

AvBD 8: NNE^YAQ^YCE^YQAGG^YISK^YD^YH^YCF^YHL^YH^YTRAF^YH^YC^YQR^YGV^YPCR^YTV^YY^YD

AvBD 9: AD^YTLA^YCR^YQ^YSH^YGS^YCF^YV^YA^YCR^YAPSV^YD^YIGT^YCR^YGG^YKL^YCK^YW^YAPSS

AvBD 10: DTVA^YCR^YTQGN^YFC^YRAG^YAC^YPPTFTISGQ^YCH^YGLLN^YCCA^YKIP^YAQ

AvBD 11: R^YDT^YSR^YCVG^YY^YH^YGY^YCR^YSK^YV^YCP^YKP^YFAAF^YGT^YCS^YWR^YQKT^YCC^YV^YDTT^YDF^YHT^YC^YQ^YDK^YGG^YH^YCVSP^YK^YIR^YCL^YEE^YQLGL^YC^YPL^YKR^YWT^YCCK^YE^YI

AvBD 12: H^YGP^YDS^YCN^YH^YDR^YG^YLC^YRVGN^YCN^YPG^YE^YYLA^YKY^YCF^YEPVIL^YCK^YPLSPTPT^YKT

AvBD 13: SDS^YQL^YCR^YNNH^YH^YCR^YRL^YCF^YH^YME^YSWAGS^YCMN^YGR^YLR^YCCR^YFST^YKQ^YPSN^YPK^YH^YSVL^YHTA^YE^YQ^YD^YPSPSLGGT

AvBD 14: SD^YTVT^YCR^YKMK^YGK^YCS^YELL^YCP^YFF^YK^YR^YSSGT^YCY^YNGLAK^YCCR^YPF^YW

Figure 1.6 AvBD amino acid sequences.

Yellow: cysteine; red: anionic; blue: cationic; green: and aromatic hydrophobic

1.7.1. AvBD expression

Investigation of AvBD expression in response to microbial challenges helps to explain the roles of the peptides in the protection of the host against potential pathogens. Experiments have been performed *in vitro* and *in vivo* and overall the results often appear confusing and contradictory, which probably reflects the different cell lines used, bird genetics, rearing environment, bird age and/or the microbes used in the challenges.

The expression of several AvBDs have been identified in healthy gut tissues. AvBD1, 2, 4, 6, 9, and 13 expression were detected in the small intestinal tissues of avian species (reviewed by van Dijk *et al.* (2008)). AvBD3 was detected in small intestine, large intestine and caecal tonsils of 15 day old geese (Ma *et al.*, 2013). AvBD2, but not AvBD7, was expressed in gut tissues of 90 day old ostriches (Lu *et al.*, 2014). Duck AvBD6 expression was reported in the intestinal tissues of 5 month old Chaohu ducks (Peng *et al.*, 2013).

A study of AvBD expression in Cobb strain birds, performed by Meade *et al.*, (2009), indicated that AvBD expression varied with bird age and tissue analysed. For example, all AvBDs, except AvBD11, were expressed in day 3 embryos with high expression reported for AvBD5, AvBD7, AvBD9 and AvBD10. At 6 days post hatch, the expression of all AvBDs, except AvBD8 and 13, were elevated compared to day 3, with the highest gene expression recorded for AvBD5, AvBD9 and AvBD10. Moreover, AvBD8, AvBD9 and AvBD10 gene expression were confined to the abdomen, while the other genes were expressed in both the head and abdomen (Meade *et al.*, 2009a). In another study performed by Wang *et al.*, (2010), quail AvBD9 expression was detected in most tissues analysed, including caecal tonsils, small intestine and caecum at day 14. However, in 80 day old birds, the expression levels were lower indicating lesser roles for the AvBDs in fighting infection in older birds (Wang *et al.*, 2010a).

AvBD mRNA expression is generally enhanced in response to bacterial challenges and this has been reported to occur either directly in response to bacterial components (reviewed by Cuperus *et al.* (2013)) or via the pro-inflammatory cytokines. For instance, using an ovarian theca cell culture AvBD12 expression was stimulated by recombinant IL-1 β , which was induced by *Salmonella* lipopolysaccharide (Abdelsalam *et al.*, 2012). These data suggested that LPS can trigger IL-1 β -which in turn can regulate the AvBD12 expression. Furthermore, AvBD1, 7 and 12 expression were enhanced in thecal cells of hen ovarian follicles by injection of 1 mg of bacterial LPS/Kg body weight (Subedi *et al.*, 2007). LPS also induced AvBD5, 9, 10 and 12 expression in sperm (Das *et al.*, 2011). An *in vitro* study showed that AvBD1 and 3 were upregulated by CpG oligodeoxynucleotides and pro-inflammatory cytokines in hen vaginal cells (Sonoda *et al.*, 2013). A recent *in vivo* study also showed that LPS injection in 1-day-old Taihe silky chicks enhanced the intestinal expression of AvBD6, 7 and 9 after 4, 24 and 48 hours (Lu *et al.*, 2015).

To help explain the variability in AvBD expression it has been suggested that expression is related to the breed/strain of bird being used. For example, AvBD1 and 2 were more highly expressed in a line of chickens (known as Line 6) resistant to *Salmonella* infection, than the comparable bird line (known as Line 151) showing increased susceptibility (Derache *et al.*, 2009a). Interestingly challenge with live *Salmonella enteritidis* was shown to suppress the expression of AvBD2 in 151 intestinal cells, while inactivated bacteria resulted in enhanced expression. The authors linked the suppression mechanism to the switching off or evasion of the host defences by bacterial mechanisms that were inactivated

or lost during the bacterial inactivation process (Derache *et al.*, 2009a). Therefore, the authors suggested that AvBD expression supports protection of the gut epithelium against *Salmonella* infection (Derache *et al.*, 2009a). Furthermore, Hong *et al.*, (2012) reported that the AvBD expression patterns in two bird lines, Cobb and Ross, were different following infection with the same microbes (*E. maxima* and *C. perfringens*), with the Ross line showing increased levels of expression. These data probably reflect the genetics of the lines of birds employed in the different studies and presumably impacts on their susceptibilities to infection (Hong *et al.*, 2012).

The expression of AvBDs also varies according to the types of microbial challenges. For instance, using Ross 308 birds most of AvBDs were upregulated including AvBD3, 10 and 12 mRNA expression following an *in vivo* *Salmonella* infection, but AvBD gene, particularly AvBD3, 4, 8, 13 and 14, downregulation was observed in response to *Campylobacter* challenge (Meade *et al.*, 2009b). Moreover, chickens infected with the respiratory associated microbe *Haemophilus paragallinarum*, showed increased tracheal AvBD3 expression compared to healthy control birds (Zhao *et al.*, 2001). AvBDs are also upregulated in response to viral infections such as duck hepatitis virus, which were shown to induce liver mRNA expression of AvBDs1, 3, 5 and 6 (Ma *et al.*, 2012a).

Reports indicate that the AvBD expression levels varies in response to different kinds of infections. For example, AvBD1 and 2 were not significantly changed in response to a salmonella infection (Derache *et al.*, 2009a), but AvBD1 and 7 were increased in birds suffering from with necrotic enteritis which is a disease caused by coccidian and clostridia.

The mRNA expression of the AvBDs in response to the bacterial challenges also varies markedly between genes. For example, all AvBDs were expressed in normal gut tissues including duodenum, jejunum, ileum and caecum of 3 day old Punjabi broiler-1 chicks (Ramasamy *et al.*, 2012). Twenty four hours post infection with *Salmonella enterica pullorum*, AvBD 3, 4, 5, 6 and 12 mRNA expression were upregulated while AvBD10, 11, 13 and 14 were downregulated, with no significant differences in AvBD1, 2, 7, 8 and 9 gene expression (Ramasamy *et al.*, 2012). Moreover, Ma *et al.*, (2013) have also explored the impact of *in vivo* bacterial challenging on AvBD1, 3 and 6 mRNA expression in different gut tissues of geese in response to *Salmonella* infection. The authors only reported upregulation of AvBD3 expression after *Salmonella* infection, indicating the variable responses of the genes to microbial challenge (Ma *et al.*, 2013).

Despite the wide range of AvBD expression in various organs, Cuperus *et al.*, (2013) argued that the variability in AvBD expression between different studies was due to the different environments, ages, breeds and technical issues eg design of PCR primers (Cuperus *et al.*, 2013). Dietary factors also seem to have impact on AvBD expression. For instance, AvBD9 expression was enhanced in jejunal cells in response to short chain fatty acid-like butyrate molecules (Sunkara *et al.*, 2014). Moreover, vitamin D₃ treatment also increased the upregulation of AvBD4, 5, 6 and 10 expression following LPS treatment (Lu *et al.*, 2015).

It has been proposed that single nucleotide polymorphisms (SNPs) impact on AvBD gene expression and resultant functions of the encoded proteins (Hasenstein and Lamont, 2007). Hasenstein and Lamont (2007), analysed genetic variations in the AvBD1-13 genomic cluster of two bird lines within eight generations, in relation to *Salmonella* loads. The authors identified 109 intronic SNPs and studied one SNP for each of the 13 AvBDs. They reported that an AvBD5 SNP was related to an increase in splenic colonisation by *Salmonella* while AvBD3, AvBD11, AvBD12 and AvBD13 SNPS were correlated with the *Salmonella* colonisation of the caeca of Leghorn birds. The authors argued that the intronic AvBD SNP genetic variations, allowed the AvBDs to be used as genetic markers for monitoring bird susceptibility to bacterial infections (Hasenstein and Lamont, 2007). Similarly Yacoub *et al.*, (2011), claimed that AvBD genes can be used as candidate gene markers for the genetic selection of disease resistant birds since all AvBDs are located on the same chromosome and assembled in one location (Yacoub *et al.*, 2011). It is probable that SNPs, intronic and within non-coding regions, affect the expression of AvBDs, resulting in variability within individual birds especially in response to different environments and microbial loads.

Twenty seven SNPs in the AvBD9 gene have been recorded on the NCBI website (on 20.10.2014). However, no SNP has been found in the mature peptide coding sequence which would affect, potentially, the functionality of AvBD9. One of the SNPs is located at the C-terminus of AvBD9 pro-peptide, but the change GAC to GAT is synonymous as both encode an aspartic acid (D). Also 17 AvBD6 SNPs were recorded in NCBI (20.10.2014) with all located either in 5' non-coding or intron sites. Several intronic AvBD6 and 9 SNPs have been reported in Aviagen birds (Butler, 2010).

1.7.2. Localisation of AvBD peptides in tissues

Immuno-histochemistry can be considered a useful method to identify sites of protein and peptide synthesis. Mammalian defensin synthesis has been identified in gut tissues with α -defensin peptides localised to Paneth cells (Ouellette *et al.*, 1999; Salzman and Bevins, 2013), but studies within the avian have been compromised by a lack of commercial antibodies. Previous immunohistochemical analyses were reported for AvBD 3, 11 and 12 but focussed in the avian reproductive tract (Shimizu *et al.*, 2008; Watanabe *et al.*, 2011), and gallin in chicken egg (Gong *et al.*, 2010).

AvBD3 peptides have been identified as being secreted in the male reproductive organs, with the anatomical locations including the spermatids and seminiferous tubules, suggesting that the AvBDs are produced during the final phase of spermatogenesis and remain in the sperm until ejaculation. This observation supports the potential importance of AvBD3 in the protection of sperm against infection before and after ejaculation (Shimizu *et al.*, 2008). Immunoreactive staining for AvBD11 and AvBD12 were also found in the epididymis and testis, suggesting that these AvBDs are synthesised in both organs and like AvBD3 probably function in innate protection of the reproductive tissues (Watanabe *et al.*, 2011).

Staining for gallin, an egg defensin, was identified in the tubular glands and ciliated cells of magnum and shell glands of the hen oviduct. These data suggest that gallin functions in the egg white and shell to help protect the embryo against potential pathogens (Gong *et al.*, 2010). Proteomics has also been utilised to identify the presence of peptides in avian tissues. Using mass spectrometry, AvBD11 and AvBD10 (gallinacin-8) have also been identified in the chicken egg shell (Mann *et al.*, 2006), and AvBD11 in both egg white (Mann, 2007) and vitelline membranes (Mann, 2008).

1.7.3. Structure of AvBDs

Structural studies of the AvBDs supports understanding of the functionality of the peptides, particularly antibacterial activity. To date, the 3D structures of Penguin AvBD103 (Figure 1.7), AvBD2 (Figure 1.8) and gallin have been solved and shown to contain β -sheets linked by three disulphide bonds (Landon *et al.*, 2004; Derache *et al.*, 2012; Herve *et al.*, 2014). The AvBD103b backbone structure bears an N-terminal α -helix, which is proposed to facilitate bacterial membrane permeation, and the surface of the peptide shows a ‘hydrophobic patch’, which is proposed to be responsible for antimicrobial action, and is preserved in avian species (Landon *et al.*, 2004). In contrast to AvBD103b, AvBD2 does not appear to contain a N-terminal α -helix and three of the cysteine residues participating in disulphide bond formation are fully buried in the AvBD2 structure (Derache *et al.*, 2012). Interestingly, the even distribution of cationic and hydrophobic residues on the surface of AvBD2 may reflect the peptide AMA characteristics via bacterial membrane interaction (Figure 1.8) (Derache *et al.*, 2012).

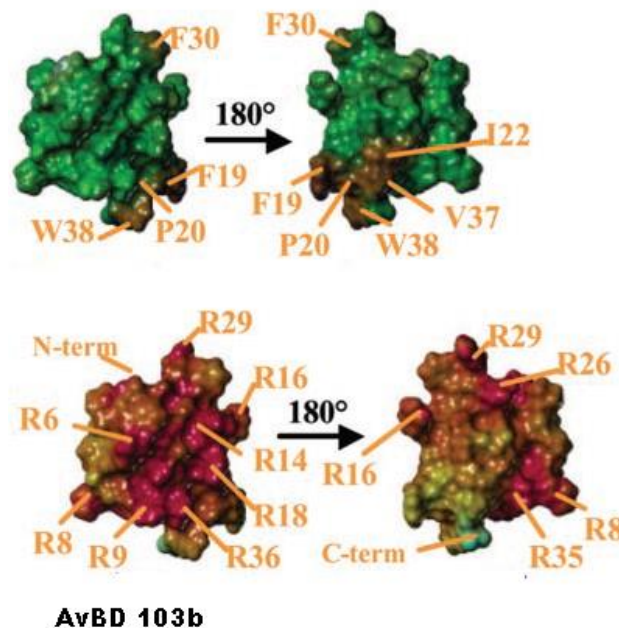


Figure 1.7 Global fold and lipophilic and electrostatic potentials of Sphe-2 (AvBD103b). Two above pictures showed hydrophobic (brown) and hydrophilic (blue) potential areas. The two bottom pictures showed electrostatic positive (red) and negative (blue) areas. Intermediate areas are in green in both cases (Landon *et al.*, 2004).

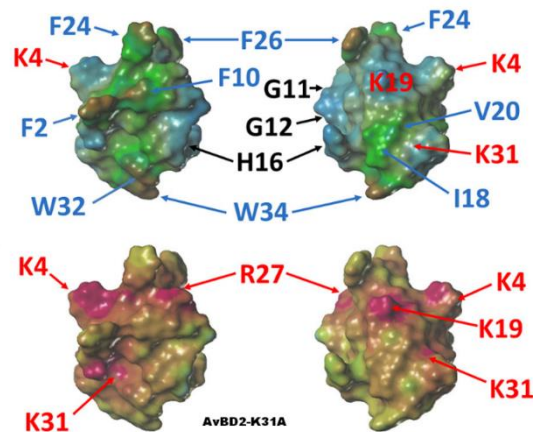


Figure 1.8 Global fold and lipophilic and electrostatic potentials of (AvBD2). Two above pictures showed hydrophobic (brown) and hydrophilic (blue) potential areas. The two bottom pictures showed electrostatic positive (red) and negative (blue) areas. Intermediate areas are in green in both cases (Derache, *et al.*, 2012).

1.7.4. Anti-microbial activity of AvBDs

The mammalian defensins are multi-functional and properties include anti-microbial activity (AMA) against microbes including bacteria, viruses, yeast and fungi; chemoattractant capacity for monocytes and immature dendritic cell; anti-oncogenic ability against cancer cells and wound healing (Taylor *et al.*, 2008; Semple and Dorin, 2012). Classically however, anti-microbial activity (AMA) is considered the most important function of the defensin family.

There are several reports exploring the AMAs of the AvBDs and while the majority of studies have used either synthetic (linear) or GST-tagged peptides all support AvBDs having AMA. For example synthetic linear and recombinant GST tagged geese AvBD1, 3 and 6 peptides at 50 and 100 ug/mL peptide concentrations were highly antimicrobial against *Pseudomonas aeruginosa*, *Pasturella multocida* and *Proteus mirabilis* but only moderately antimicrobial against *E. coli* and *Salmonella* species (Ma *et al.*, 2013). In comparison quail AvBD9, both synthetic linear and GST tagged forms, displayed the same AMA against both Gram positive and negative bacteria (Wang *et al.*, 2010b). Synthetic linear ostrich AvBD2 and AvBD7 were reported to be highly active against *E. coli*, *P. multocida*, *Salmonella choleraesuis* and *Streptococcus agalactiae* (Lu *et al.*, 2014), while synthetic linear and GST-AvBD6 both similarly inhibited the growth of Gram positive and negative bacteria including *E. coli* and *E. faecalis* (Peng *et al.*, 2013). Synthetic, but

refolded Penguin spheniscin 2 also showed AMA against both Gram positive and negative bacteria (Thouzeau *et al.*, 2003).

Higgs *et al.* (2007), investigated the effects of amino acid substitution on AvBD8 killing activities against *Escherichia coli*, *Listeria monocytogenes*, *Salmonella typhimurium*, and *Streptococcus pyogenes* (Higgs *et al.*, 2007). In this study the authors changed Valine (V), Isoleucine (I), or Threonine (T) amino acids to either Arginine (R), which bears a positive charge or to Aspartic acid (D), which carries a negative charge (Figure 1.9), and these changes increased or decreased the overall charge of AvBD8. The authors concluded that an increased charge enhanced the antibacterial activity of AvBD8. For example, using wild type AvBD8 a peptide concentration of 27 μ M was needed to kill 50% of viable cells of *E. coli*, but modifying the peptide to include Arginine resulted in a concentration of only 2-3 μ M required to kill 50% of the *E. coli* cells. In contrast, modifying the peptide to include Aspartic acid required a concentration of 27 μ M, comparable to the wild type, to kill the 50% of the *E. coli* sample.

Peptide	Modification	Sequence	Charge
AvBD8		NNEAQCEQAGGICSKDHC <u>F</u> HLHTRAFGHCQRGVPCCRTVYD	0.7
AvBD8ps+	V33R,V39R	NNEAQCEQAGGICSKDHC <u>F</u> HLHTRAFGHCQ <u>R</u> GR <u>P</u> CCRT <u>R</u> YD	2.7
AvBD8ns+	I12R,T38R	NNEAQCEQAGG <u>R</u> C <u>S</u> KDHC <u>F</u> HLHTRAFGHCQRGVPCC <u>R</u> <u>R</u> VYD	2.7
AvBD8ps-	V33D,V39D	NNEAQCEQAGGICSKDHC <u>F</u> HLHTRAFGHCQ <u>R</u> GD <u>P</u> CCRT <u>D</u> YD	-1.3
AvBD8ns-	I12D,T38D	NNEAQCEQAGG <u>D</u> C <u>S</u> KDHC <u>F</u> HLHTRAFGHCQ <u>R</u> GVPC <u>D</u> <u>R</u> <u>D</u> VYD	-1.3

Figure 1.9 Sequences and charges of chicken AvBD8 and its modified versions. Substituted amino acids are underlined (Higgs *et al.* 2007)

The susceptibility of bacteria to the AvBDs is variable according to the actual strain. For example AvBD2 was reported to be less active against *Salmonella enteric* serovar *Enteritidis* LA5 strain which is a field isolate strain, than against *Salmonella enterica* serovar *Enteritidis* ATCC, a laboratory strain (Derache *et al.*, 2009b).

1.8. Mechanism action of defensin

Generally, AMPs kill bacteria either through microbial membrane permeabilisation or inhibition of intra-cellular molecular synthesis mechanisms. The former mechanism can be described by four models: aggregate, toroidal pore, barrel stave and carpet models. These models vary according to the size and structure of the peptides and are mostly based on pore forming α -helical peptides (Jenssen *et al.*, 2006). In the aggregate model, shown here using the horseshoe crab peptide polyphemusin I, the peptides do not form organised structures, but through translocation, create informal channels in the membrane (Figure 1.10 A). In the toroidal model, the peptides, for example the bee peptide Melittin, are perpendicularly embedded into the microbial membrane, forming distinct pores into which the phospholipid head groups are directed (Figure 1.10 B). In the barrel stave model the peptides form a membrane channel lined with perpendicularly organised peptides with their hydrophobic tails directed into the lumen of the pore (Figure 1.10 C). Finally in the carpet model, peptides such as sheep cathelicidin Smap29 cause a ‘membrane flip flop’ in which a piece of the membrane is detached from the whole lipid bilayer resulting in the formation of a large pore sealed by the aggregation of the peptides (Figure 1.10 D). Other models that do not rely on membrane disruption involve peptides that inhibit intracellular DNA, RNA, protein, enzyme and cell wall syntheses (Figure 1.10 E to I). These inhibitory activities are initiated by the peptides binding to the outer membrane of bacteria followed by peptide translocation and blocking of molecular synthetic pathways. This mechanism has been observed for both α -helical and disulphide bond containing peptides (Wilmes *et al.*, 2011).

It has been reported that fungal, invertebrate and human defensins can inhibit the molecules responsible for cell wall biosynthesis. For example, the fungal defensins plectasin, oryzeasin and eurocin, the invertebrate oyster defensins lucifensin and gallicin and the human defensins HNP1 (α) and HBD3 (β) can bind to lipid II and consequently interfere with peptidoglycan formation (Wilmes *et al.*, 2011). The lipid II binding ability of defensin has been confirmed by crystallisation of both peptide and lipid together, and the finding that Isoleucine 20 and Leucine 25 residues of the HNP-1 monomer bind to Lysine 3 and D-alanine 4 of lipid II pentapeptide while Isoleucine 20, Leucine 25 and Arginine 15 amino acids bind to γ D-Glu-2 and the phosphate/N-acetyl muramic acid moiety of Lipid II (Varney *et al.*, 2013).

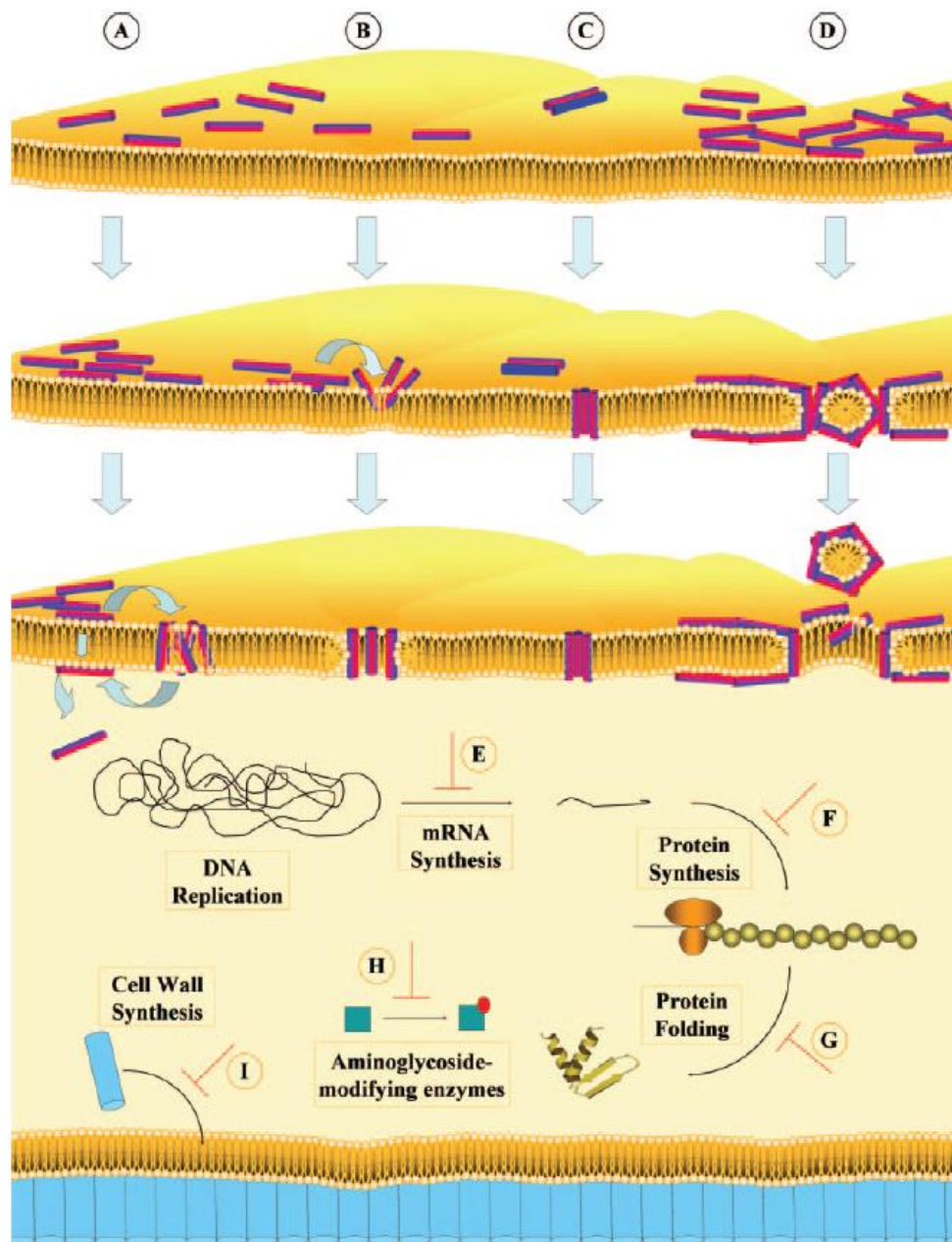


Figure 1.10 Mechanisms of action of antibacterial peptides. The bacterial membrane= yellow lipid bilayer. Peptides= cylinders, the hydrophilic regions are colored red and the hydrophobic regions are blue. Cell wall-associated peptidoglycan molecules are depicted as purple cylinders. Models to explain mechanisms of membrane permeabilisation are indicated (A to D). The “aggregate” model (A), the “toroidal pore” model (B), the “barrel-stave” model (C) and the “carpet” model (D) causing formation of micelles and membrane pores. The mechanisms of action of peptides which do not act by permeabilising the bacterial membrane are depicted in E to I. Inhibition of DNA and RNA synthesis (E). Decrease in the rate of protein synthesis (F). Targeting an enzyme involved in chaperone-assisted protein folding (G). Inhibition of enzymes involved in the modification of aminoglycosides (H). Targeting the formation of the cell wall (I); such as the transglycosylation of lipid II, which is necessary for the synthesis of peptidoglycan (Jenssen et al., 2006).

Investigation of specific residues of antimicrobial peptides are important to reveal their potential roles in the antimicrobial mechanism of action. The cationic amino acids Arginine (R), Lysine (K), and Histidine (H) are important in membrane-defensin interactions. The mammalian α -defensin has more conserved arginines than lysine, but in contrast β -defensin has more selected lysines (Zou *et al.*, 2007). To explore the importance of R and K residues, research was performed by Zou *et al.* (2007), in which all the lysine amino acids of human β -defensin 1 were mutagenised to arginine (RHBD1), and all the arginine residues of human neutrophil peptide 1 were modified to non-coded α -amino acids (aacHNP-1). The results, which supported increased AMA associated with charged amino acids and suggested key roles of the arginine and lysine positive amino acids in the antimicrobial specificities of each type of defensin (Zou *et al.*, 2007). In HBD3 the positively charged amino acids are located in the C-terminal region of the peptide. This region of the peptide is proposed to interact with the anionic part of the bacterial membrane lipid bilayer thus facilitating the embedding of the hydrophobic residues into the membrane (Sudheendra *et al.*, 2015).

There are relatively few reports investigating the mechanisms by which the AvBDs interact with bacterial membranes. Ovotransferrin, a chicken cationic AMP, caused leakage of a NPN fluorescent dye and β -galactosidase from *E. coli*, and released K^+ ions from liposomes created by *E. coli* phospholipids. These data suggested that the peptide can kill the bacteria through membrane permeabilisation and consequent leakage of the cytoplasmic content (Ibrahim *et al.*, 2000).

In a study performed by Sugiarto and Yu (2004), both ostrich AvBDs, ostracin 1 and ostracin 2 were able to bind *E. coli* lipopolysaccharide, and induce leakage of fluorescent dyes taken up by the model bacterial membranes. However, the binding and leakage abilities were remarkably weaker than that of a membrane lytic AMP, sheep myeloid antimicrobial peptide-29 (SMAP-29), suggesting a different mechanism of action associated potentially with DNA binding rather than membrane lysis (Sugiarto and Yu, 2007b). Furthermore, a recent study has shown that the Penguin defensin, AvBD103b has both bacterial DNA binding capabilities and membrane lytic activities (Teng *et al.*, 2014). These authors found that the peptide attaches to the bacterial (*Salmonella enteritidis*) surface via increasing cell surface hydrophobicity. They also identified using NPN dye methodology, atomic absorption and electron microscopy that the peptide causes membrane leakage. The DNA binding capacity of the peptide was also investigated using

gel retardation assays and its cell cycle arrest properties identified using flow cytometry (Teng *et al.*, 2014).

Electron microscopy has also been employed as a tool to investigate the anti-microbial mechanism action of defensins. For example, AvBD9 peptides have been shown to cause morphological changes such as granulation of intracellular materials, irregular septum formation in a dividing cell, cytoplasmic retraction, lysis at the cell septa, cytoplasmic membrane degranulation and complete bacterial cell lysis (van Dijk *et al.*, 2007). Electron microscopy showed that GST tagged AvBD6 cause lysis and shrinkage of *Aeromonas veronii* (Peng *et al.*, 2013), while bovine neutrophil defensins killed *E. coli* and *Staphylococcus aureus* by inducing bacterial cell content release (Wu *et al.*, 2011).

1.9. Resistance of the microbes to AMPs

Alongside the evolution of AMPs, microbes have also evolved to resist the activity of AMPs. There are several mechanisms through which microbes have acquired resistance against antimicrobial peptides including the secretion of proteolytic enzymes to destroy the peptides, active efflux of the peptides, down regulation of host AMP expression and modification of their bacterial cell membrane to reduce the negative charge (Nizet, 2006). For example, *Salmonella typhimurium* has replaced LPS with L-arabinose thus decreasing the net anionic charge of its outer membrane (Yeaman and Yount, 2003). Some gram negative strains of bacteria acquire resistance by the translocation of the AMP into the their membrane via acylation of the lipid A (Yeaman and Yount, 2003). Other examples include the Phop/PhoQ system of *Salmonella typhimurium*, the energy dependent efflux system of *Neisseria gonorrhoea* and the Dlt operon functioning in the *Staphylococcus aureus* cell wall (Ganz, 2003).

Protease enzymes are used by bacteria as a defence mechanism for both survival and growth. Common examples of proteases in the field of antimicrobial research are the *E. coli* outer membrane protease (OmpT) and the *Salmonella* PgtE protease, which play important roles in the survival resistance mechanism against host AMPs (Yeaman and Yount, 2003). Their importance is shown by experiments using mutant strains with the OmpT mutant strain, showing increased sensitivity to AMPs. Interestingly the PgtE mutant *Salmonella* strain showed no resistance against protamine that is folded and contains disulphide bonds (Yeaman and Yount, 2003). These data suggest that folded peptides such as the defensins are more resistant to proteolysis. This characteristic has been explored by

researchers using cysteine mutant AMPs, e.g., mouse α -defensin cryptidin-4 which is sensitive to proteolysis when lacking di-S bonds (Maemoto *et al.*, 2004). Other proteases include the heat shock serine protease DegP, which increases the survival rate of *E. coli* against Lactoferricin B, and proteases secreted by pathogenic bacteria including *Streptococcus*, *Staphylococcus*, and *Yersinia*, are proposed to have a major role in pathogenesis of host diseases and antimicrobial resistance (Yeaman and Yount, 2003).

In addition to proteolysis, ionic buffer strength plays a role in the inactivation of AMPs. For instance, folded AvBD9 AMA is inactive when tested in high salt (150 mM) against both Gram positive and Gram negative bacteria including *E. coli*. However, this inactivity can be rescued by using sodium phosphate buffer (10 mM) or low salt concentrations (20 mM) (van Dijk *et al.*, 2007). Using 150 mM NaCl also reduced the AMA of duck AvBD1, 3, 5, 6, and 16 against *Micrococcus tetragenus* and *Pasturella multocida*, and geese AvBD1, 3 and 6 against *S. aureus* and *P. mirabilis* (Ma *et al.*, 2012a; Ma *et al.*, 2013). Similarly the AMA of synthetic linear ostrich AvBD2 and 7 against both *E. coli* and *S. aureus* was decreased at 150 mM compared to 100mM, suggesting the ions prevent the binding of the peptide to the bacterial membrane (Lu *et al.*, 2014). Moreover, the cysteine-mutant HNP-1 was more active than wild type HNP-1 against *E. coli*, *S. aureus* and *Pseudomonas aeruginosa* although the latter was highly resistant to the cysteine-mutant HNP-1 in high salt concentrations, indicating that ionic buffer strength also has a negative impact on the AMA of linear peptides (Varkey and Nagaraj, 2005)

Furthermore, the increasing salt concentration of the airways of cystic fibrotic patients has been linked to the decreased AMA of HBD1 (Goldman *et al.*, 1997). The synergetic effects of several AMPs were also reported to be reduced in the salt concentration of the airway fluid of cystic fibrotic patients (Singh *et al.*, 2000). However, Ratussin, a five cysteine peptide expressed in rat gut, which has a potent AMA against both *E. coli* and *S. aureus* linked to homo-dimerisation, retains its AMA regardless of the salt concentration and presence of divalent ions (Patil *et al.*, 2013). Interestingly the peptide folding state seems to play a role in the stability of AMPs in marine organisms, for example, the presence of four disulphide bonds in oyster defensins is proposed to make the peptide more resistant to the high salt concentration of the sea water (Wilmes *et al.*, 2011).

1.10. Chicken cytokines

The avian β -defensins are antimicrobial agents and have been reported to kill bacteria and fungi (Milona *et al.*, 2007; Ma *et al.*, 2008; van Dijk *et al.*, 2008). Although research has focussed mainly on the mammalian defensins the peptides have also been shown to interact with other innate immune defences, including cytokines (Soman *et al.* 2009).

Cytokines are small (less than 30 kDa in size) soluble peptides that have either pro or anti-inflammatory functions resulting in either stimulatory or inhibitory effects on cell immunity, development and inflammation. In this way, they help modulate the types of immune response to an infection (Davison *et al.*, 2008).

The cytokine structure is comparable to that of the defensins as it includes 4-6 cysteine residues, 2-3 disulphide bonds and hydrophobic residues, and is generally conserved between animal species. Many chicken cytokines have been identified including IL-3, IL-4, IL-13, GM-CSF (Avery *et al.*, 2004), IL-18 (Schneider *et al.*, 2000), IL-17 (Min and Lillehoj, 2002), IL-16 (Min and Lillehoj, 2004), IL-10 (Rothwell *et al.*, 2004). Kaiser *et al.* (2005), have in their review listed the genes encoding 23 ILs including IL-1 β , IL-2, IL-6 and TGF β 4 (Kaiser *et al.*, 2005). Like the defensins, cytokines are activated early in infection (Kaiser *et al.*, 2006), supporting potential relationships between the two groups of peptides.

1.10.1. Interleukin-2

The chicken IL-2 gene, located on chromosome 4, consists of 4 exons and 3 introns and is similar to that identified in mammals although exon 2, and introns 2 and 3, are shorter (Kaiser and Mariani, 1999). It encodes a signal peptide of 22 amino acids and a mature protein of 143 amino acids (Wigley and Kaiser, 2003) and is known to activate both T-cells and heterophils (Kaiser *et al.*, 2006) although the mechanism by which avian IL-2 functions is not well-understood. In mammals, IL-2 is known to bind to a cytokine receptor on immune cells, including T cells, leading to receptor phosphorylation, signal transduction and transcriptional activation of signal transducer and activator of transcription (STAT) proteins involved in the further functioning of the immune system (Wigley and Kaiser, 2003).

Limited studies have been performed investigating IL-2 gene expression in gut tissues. Choi and Lillehoj (2000), showed that following *Eimeria* (parasite) infection of poultry gut

IL-2 gene expression was increased and associated with an increase in gamma delta cells in the gut mucosa. Gamma delta cells are proposed to function as a link between the innate and adaptive immune systems and these data suggest that IL-2 may function to activate that link (Choi and Lillehoj, 2000). Interestingly, the gut expression of IL-2 appears to vary according to the infectious agents. For example, in chickens IL-2 mRNA expression increased during a primary infection of *Eimeria acervulina*, but decreased in response to *E. tunella*. However, expression remained unchanged in response to secondary infections of both *Eimeria* strains (Hong *et al.*, 2006).

1.10.2. Interleukin-6

Interleukin-6 (IL-6) is a pro-inflammatory cytokine that can modulate the innate response by activating a number of immune cells including macrophages and lymphocytes (Wigley and Kaiser, 2003). The chicken IL-6 gene is located on chromosome 2 (2p21–p13), identified by fluorescent and *in situ* hybridization, and is comprised of 4 exons and 3 introns. Interestingly the mammalian IL-6 gene has 5 exons and 4 introns and in the chicken it appears that the first two exons are fused together, forming one exon. The chicken IL-6 promoter region resembles that of the human gene in the regulatory sequences identified (Kaiser *et al.*, 2004) The mechanism by which avian IL-6 functions is not well understood, but in mammals, it is known to bind to cytokine receptors which like IL-2 activates the transcription of STAT proteins (Wigley and Kaiser, 2003).

1.10.3. Transforming growth factor β 4 (TGF β 4)

Originally TGF β 4 was thought to have a role in tumour development, but it is now accepted that TGF β 4 has anti-inflammatory characteristics (Burt and Jakowlew, 1992; Wigley and Kaiser, 2003; Kaiser *et al.*, 2006) and is important for T-lymphocyte activation (Wigley and Kaiser, 2003). TGF β 4 gene expression has been shown to be increased in the chicken cecal, spleen and duodenal lymphocytes following *E. acervulina* infection (Choi *et al.*, 1999). The expression of TGF β s was investigated in lymphoid tissues, including thymocytes, thymic stromal cells, and splenocytes of chicken as well as embryonic chicken fibroblasts, and the data suggested that TGF β s help modulate the development of the immature cells, particularly thymocytes (Mukamoto and Kodama, 2000).

Jakowlew *et al.* (1997) compared TGF β s 2, 3 and 4 mRNA expression in chicken embryos and adults, and showed that TGF β 2 and 3 spleen expression was increased in embryos, but

decreased in adults. Using immunohistochemistry, the authors showed that TGFβs stained weakly in the intestinal epithelia of young birds (1-2 weeks of age), with staining localised to the tips of intestinal microvilli. These results suggested that TGFβs 2 and 3 isoforms are important for cell growth and development. In contrast TGFβ4 expression increased in the intestine of one month old birds, suggesting that it has additional roles in the defence of the gut against infection (Jakowlew *et al.*, 1997).

To date there is significant interest in exploring potential links between gut cytokine profiles and gut microbial populations, particularly in humans with inflammatory diseases (Sydora *et al.*, 2010). Similarly in birds the effects of age, rearing conditions and microbial challenge on gut development, microbiota and cytokine profiles are of significant interest to commercial breeders selecting for birds with improved innate immunity and good gut health.

1.11. Chicken galectin-3

Galectin, previously known as animal lectin, has been identified in lower and higher vertebrates suggesting a pivotal role in vertebrate physiology and/or immunology. Galectins can be categorised into three groups according to their protein structures: proto, chimera, and tandem-repeat types. While their biological functions are not completely understood they are known to have roles in cell differentiation, morphogenesis and metastasis (Kasai and Hirabayashi, 1996).

In mammals, four types of galectins (Galectin-1, -2, -3, and -4) and their structures have been described (Barondes *et al.*, 1994). As shown in Figure 1.11, Galectin-3 is composed of one carbohydrate binding domain of 130 amino acid residues, an N-terminal domain (which is not present in other galectins) and a link peptide (Barondes *et al.*, 1994).

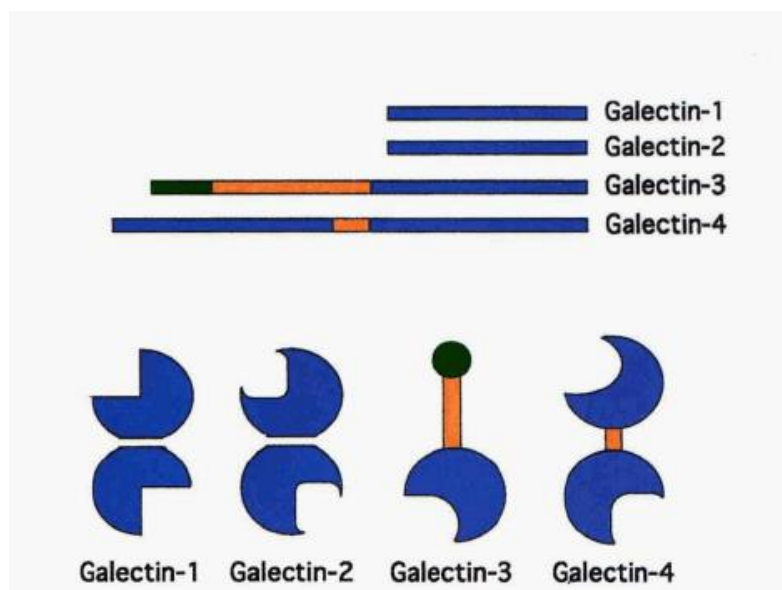


Figure 1.11 Schematic of the overall structures of galectin-1, -2, -3, and 4. The proteins are shown schematically as linear diagrams corresponding to single peptide chains (top) and as assembled proteins (bottom). The carbohydrate-binding domains of about 130 amino acid residues are blue, the proline-, glycine-, and tyrosine-rich repeating domain of galectin-3 (about 100 residues) and link peptide of galectin-4 (about 30 residues) are orange, and the N-terminal domain of galectin-3 (about 30 residues) is green. (Barondes *et al.* 1994).

Chicken galectins (CG) have been reported and include CG1A (liver) CG1B (lung), CG2 (gut), CG3 (gut) and CG8 (jejunum and caecum) (Kaltner *et al.*, 2009). The Chicken Galectin-3 (CG3) gene consists of 6 exons and 5 introns, and is located on chromosome 5 (Kaltner *et al.*, 2011). Chicken galectin-3 is expressed in a number of tissues including thymus, lung, heart, spleen, liver, esophagus, proventriculus, gizzard, jejunum, cecum, kidney, ovary, shell egg, bursa, skin and fibroblasts (Kaltner *et al.*, 2011).

An immunological function of chicken Galectin-3 is not obvious. Galectins can however interact with glycoproteins and glycolipids of the host cell-surface and extracellular matrix, through lectin-carbohydrate bindings (Liu, 2005). They can also enhance cell growth, affect cell survival, regulate cell adhesions and induce cell migration (Liu, 2005). Galectin-3 may also act as an opsonin, forming a link between the carbohydrate components of bacteria cell membranes and the surface glycoproteins of phagocytes (Almkvist and Karlsson, 2004). Moreover, in mammals at high concentrations (1 μ M) it acts as a chemo-attractant to macrophages and stimulates monocyte migration (Sano *et al.*, 2000). In fact in the studies by Sano *et al.* (2000), using an *in vivo* mouse model, Galectin-3 was shown to increase the

number of monocytes in mouse air pouches (Sano *et al.*, 2000). Thus, it is feasible that chicken Galectin-3 expression and synthesis at the avian gut epithelium functions in attracting monocytes and macrophages to a site of inflammation during bacterial infection and helps to increase phagocytosis of the bacteria.

Aims and objectives

In depth knowledge of the involvement and roles of the host innate defences, specifically avian β -defensins (AvBDs) in protecting birds (young and growing) against disease, particularly in commercial environments is lacking. Scientifically and commercially such information is of value as it may be used to improve disease resistance in commercial lines and exploited through selective breeding programmes. This research presented in this thesis aimed to explore the expression and functions of the AvBDs with the objectives of defining their roles in bird health.

1. The first study using qPCR and immunocytochemistry aimed to explore potential relationships between the expression and synthesis of AvBDs and other immuno-regulatory molecules. The focus was on AvBD6 and 9, IL-6, TGF β 4 and CG3 in gut, kidney, liver and lung tissues of birds.
2. The second study using recombinant and synthetic peptides aimed to explore the antimicrobial activity (AMA) of the AvBDs 6 and 9, against bacterial strains isolated from commercially reared birds.
3. The third area of study using synthetic peptides, bacterial membranes, and structure modelling aimed to explore the killing mode of actions of the AvBDs 6 and 9 peptides.

Chapter 2

2. Materials and Methods

2.1. Chemicals and consumables

All chemicals were purchased from Sigma Aldrich (Poole, U.K.) unless otherwise stated. All plastics were purchased from Starlab (Milton Keynes, U.K.).

2.2. Bacterial culture:

2.2.1. *Growth medium broth*

Luria-Bertani (LB) growth media including Bacto-Tryptone and Bacto-Yeast were purchased from BD Biosciences (Oxford, UK). LB broth was prepared by dissolving 10 g Tryptone, 5 g yeast and 10 g sodium chloride in 1L double-distilled (ddH₂O) water. The pH was adjusted to 7.4 using 1 M sodium hydroxide solution (NaOH) and the broth was autoclaved for 20 minutes at 121 °C and 15 PSI pressure.

Tryptic soy broth (TSB) was prepared by dissolving 15 g of Tryptone soya broth (TSB) powder in 500 ml ddH₂O and sterilised as described previously by autoclaving.

NZY broth was prepared by dissolving 10 g NZ amine, 5 g Yeast and 5 g NaCl in 1L H₂O, adjusted to pH 7.5, and sterilised by autoclaving. This broth required the addition of 12.5 ml 1 M MgCl₂, 12.5 ml 1 M MgSO₄, and 10 ml 2 M Glucose before use.

2.2.2. *LB agar plates*

Plates were prepared by dissolving 15 g of agar (BD Biosciences, Oxford, UK) in 1L of the LB broth. After sterilisation, approximately 20 ml of LB agar was poured into each petri dish and left to solidify. The plates were dried at 37 °C before use. Antibiotics including Ampicillin (50 µg/ ml dissolved in ddH₂O) and Chloramphenicol (30 µg/ ml dissolved in ethanol) were added to the cooled agar medium as required.

2.2.3. *Blood agar based plates*

Forty grams of blood agar base (Sigma) was dissolved in 1L ddH₂O. Following autoclaving, the agar (~ 20 ml) was poured into each petri dish, allowed to set and the plates dried at 37 °C.

2.3. Bacterial strains

The bacteria used in the anti-microbial assays included *Escherichia coli* and *Enterococcus faecalis*, which were clinical isolates purified from two birds resident on Aviagen farms and described previously by V. Butler (2010).

The competent cells exploited for cloning and hyperexpression were *E. coli* DH5 α - and *E. coli* BL21 (DE3) pLysS strains (Table 2.1), purchased from Promega, Southampton, U.K.

Strains	Genotype
DH5 α	F ⁻ Φ 80 <i>lacZ</i> Δ M15 Δ (<i>lacZYA-argF</i>) U169 <i>recA1 endA1 hsdR17</i> (rk ⁻ , mk ⁺) <i>phoA supE44 λ thi-1 gyrA96 relA1</i>
BL21 (DE3) pLysS	F ⁻ , <i>ompT</i> , <i>hsdS_B</i> (r _B ⁻ , m _B ⁻), <i>dcm</i> , <i>gal</i> , λ (DE3), pLysS, Cm ^r .

Table 2.1 Genotypes of competent cells used for cloning and hyperexpression

2.4. Buffers

2.4.1. Phosphate buffered saline (PBS)

Phosphate buffered saline (PBS) tablets were purchased from Sigma. To prepare 1 x PBS (8 g of NaCl, 0.2 g of KCl, 1.44 g of Na₂HPO₄, 0.24 g of KH₂PO₄, per 1L of distilled H₂O, pH 7.2), one tablet was dissolved in 200 ml distilled water. All PBS solutions were sterilised by autoclaving.

2.4.2. Sodium phosphate buffer

Monobasic phosphate buffer (200mM), was prepared by dissolving 13.8 g of NaH₂PO₄·H₂O (MW= 137.99) in 500 ml ddH₂O. Dibasic phosphate buffer (200 mM), was prepared by dissolving 17.8 g of Na₂HPO₄·2 H₂O (MW = 177.99) in 500 ml ddH₂O. Sodium Phosphate buffer (100 mM) was prepared by mixing 47.5 ml of monobasic phosphate buffer with 202.5 ml dibasic phosphate buffer. The pH was adjusted to 7.4 if required and the final solution sterilised by autoclaving.

2.4.3. GST 'cleaving' buffer

GST 'cleaving' buffer used to facilitate removal of the GST tag from recombinant peptides was prepared by dissolving 0.88 g NaCl, 0.029 g Na-EDTA and 0.015 g DDT in 100 ml Tris- HCL (50 mM). The pH was adjusted to 7.4 and the solution sterilised by autoclaving.

2.4.4. Sample loading buffers

Protein: SDS sample loading buffer was prepared as follows: 1 g SDS, 5 ml 0.25M Tris pH 6.8, 2.5 ml of 50% Glycerol, 2.5 ml 2- β -Mercaptoethanol and 4 ml 0.1% Bromophenol blue dye.

DNA: DNA loading buffer was prepared by mixing 3 ml glycerol (30%), 25 mg bromophenol blue (0.25%), and sterile distilled water to 10 ml.

2.4.5. Gel running buffers

Protein: SDS PAGE running buffer was prepared by mixing 3% w/v Tris, 14% w/v Glycine and 1% w/v SDS. The pH was adjusted to 8.3 using 1 M NaOH. DNA: The buffer used for DNA agarose gel electrophoresis was 1 X Tris borate EDTA (TBE), which was prepared by dissolving 10.8 g of Tris base, 5.5 g of boric acid and 0.74 g of EDTA in 1L of distilled water, pH 8.3.

2.4.6. Tris glutathione elution buffer (TGE)

TGE buffer was prepared by dissolving 0.06 g reduced L- Glutathione (20 mM), and 0.06 g Tris pH 8 (50 mM) in 10 ml sterile ddH₂O, in a sterile 20ml universal.

2.4.7. Neutral buffered formalin

Neutral buffer formalin (10%) was prepared by mixing 100 ml 37% Formaldehyde, 900 ml deionised water, 4 g Sodium phosphate monobasic buffer and 6.5 g sodium phosphate dibasic buffer, pH 7.

2.5. Tissue sample collection

For the tissue panel expression analyses tissue samples collected previously by V Butler from Day 7 and Day 35 Aviagen Line X birds reared in low and high hygiene conditions, preserved in RNA later solution (Ambion, Applied Biosystems, UK) and stored at -80 °C were utilised.

The tissue samples for immunohistochemistry were fixed in 10% neutral buffered formalin for 48 hours. The fixed samples were transferred to 70% ethanol and stored at room temperature.

2.6.RNA extraction

Endpoint PCR: RNA extractions were performed by homogenising 10-20 mg tissue samples in 1 ml of Trizol (Invitrogen, Paisley, UK), with a rotor-stator style homogenizer (Tissue Rupter, Qiagen, Crawley, UK). Isopropanol 200 µl/ ml was added to each sample, the solutions mixed for 3 minutes at room temperature and centrifuged at 12000 x g, 4 °C for 15 minutes. The clear supernatant layer was removed and mixed with an equal volume of 70 % ethanol. This mixture was loaded onto a purification column (PureLink™RNA mini kit, Invitrogen, Paisley, UK), washed three times with wash buffers and eluted using 30 µl molecular grade water. To aid RNA preservation, 1 µl of RNase inhibitor (RNAsin, Promega, Southampton, UK), was added to all samples before storage at -80 °C.

Real time PCR: RNA extractions of tissues from small intestine, caecum, caecal tonsils, kidney, liver and lung were performed using a SV Total RNA Isolation System (Promega, Southampton, U.K.). Tissue samples stored at -80 °C were cut into small pieces (10-20 mg) using a sterile scalpel, and cells lysed by the addition of 300 µl lysis buffer (5 ml β-mecaptoethanol+ 500 ml RNA lysis buffer). The tissues, in liquid nitrogen, were ground using pestle and mortar, homogenised for one minute and kept at -20 °C overnight. The thawed mixtures were further diluted by adding 350 µl RNA dilution buffer and mixed well by inverting the tubes at least 5 times. This was followed by incubation at 70 °C for 3 minutes and centrifugation twice at 4 °C, 13,000 x g for 10 minutes and the supernatants collected and stored in clean sterile microfuge tubes. The samples were washed by adding 200 µl 95% ethanol, mixed by pipetting, transferred onto the columns and centrifuged at 4 °C, 13,000 X g for 1 minute. The samples were further washed using 600 µl RNA wash solution (350 µl 95% ethanol+206 µl RNA wash solution) and centrifuged at 4 °C, 13,000 x g for 1 minute. The columns were treated with 50 µl DNase I (5 µl MnCl₂+5 µl DNase+40 µl yellow core buffer) and incubated at room temperature for 15 minutes. The DNase treatment was stopped by adding 200 µl DNase stop solution to each column and centrifuging at 4 °C, 13,000 x g for 1 minute. After washing twice with 600 and 250 µl of RNA washing solution, each time centrifuging at 4 °C, 13,000 for 1 minute, the samples were eluted with 100 µl pure molecular grade water, again centrifuging at 4 °C, 13,000 x g for 1 minute, and collected in clean sterilised microfuge tubes. The eluted samples were kept at -80 °C.

2.7.RNA quantification

The RNA concentration of each sample was determined using a NanoDrop (NanoDrop®,ND-1000). The RNA concentration was measured and the purity checked by measuring ODs at (A260/A280) and (A260/A230). Values between (1.8-2.2) were considered as a pure RNA.

2.8.DNAse treatment

Endpoint PCR: Prior to RNA expression analyses DNAase treatment of each RNA sample was performed to remove any potential contaminating genomic DNA (Promega kit, USA). Essentially 4.5 µg RNA was mixed in a microfuge tube with 4.5 µl DNAse enzyme (1 unit/ µl), 2 µl 10 X DNAse buffer and sterile molecular grade water (to final volume of 20 µl). The tube contents were mixed and incubated at 37 °C for 30 minutes. The reaction was stopped by adding 4 µl DNA Stop solution for 10 Minutes at 65 °C.

Real time PCR: The DNAse treatment was performed as described in section 2.6.

2.9.Reverse transcription

Endpoint PCR: Reverse transcription of the RNA to cDNA was performed in a microfuge tube using reagents from a cDNA Reverse Transcription kit (Applied BioSystem, UK). Briefly, 10 µl DNAsed treated RNA sample was mixed with 1.0 µl Mulv Reverse transcriptase enzyme (50 units/ µl), 3.2 µl MgCl₂ 25 mM, 2.0 µl HEX (Hexamer solution), 4 µl of 10 X reverse transcriptase buffer, 16 µl dNTPs 10 mM, and 3.8 µl sterile molecular grade water. The solutions were incubated for 60 minutes at 42 °C, 5 minutes at 95 °C, and finally 5 minutes at 5 °C. Samples were either used in subsequent PCR reactions or stored at -80 °C.

Real time (q) PCR: The RNA was reverse transcribed as for end point PCR but in this case 250 ng RNA was used for each tissue sample. The master mix was prepared by mixing 5 µl Mulv RT buffer, 6.25 µl dNTPs 2 mM, 0.25 µl RNAsin, and 0.5 µl Mulv RT enzyme. The reaction was set up by adding 1 µl of Hexamer 0.5 mg/ ml to 250 ng RNA/10 µl H₂O and the PCR tubes incubated in the light cycler at 60 °C for 5 minutes. Twelve (12 µl) of the master mix was added to each sample, the samples incubated at 42 °C for 2 hours and kept at -20 °C. Each RT was diluted 1:4 before qPCR.

2.10. Endpoint PCR primers

Endpoint PCR primers are shown in Table 2.2. BamH1 and EcoR1 restriction sites were incorporated into the Avian β -defensin 6 and 9 primers to allow cloning into the expression vector pGEX6p-1 (GE Healthcare Life Sciences, Buckinghamshire, U.K.). Primers encoding chicken cytokines IL-2, IL-6, TGF β 4 and Galectin-3 were designed, to cross at least two exons. All primers were purchased from Integrated DNA Technologies (UK) in a lyophilized form and diluted with sterilised molecular grade water to give a stock solution of 100 mM. This stock solution was further diluted to a PCR working solution of 10 mM.

Gene	Gene bank accession No.	Forward primer	Reverse primer	Size (bp)	T _m
AvBD6 M	NM_001001193.1	CGCGGATCCAGCCCTATTCATGCTTG	CGAGAATTCTCAGGCCACCTGTTCTC AC	126	61
AvBD6 P+M	NM_001001193.1	CGCGGATCCGGTCAGCCCTACTTTTC	CGAGAATTCTCAGGCCACCTGTTCTC AC	144	61
AvBD9 M	NM_001001611.2	CGCGGATCCGCTGACACCTTAGCATG	CGAGAATTCTCAGGAGCTGGGTGCCCA TTTG	126	63
AvBD9 P+M	NM_001001611.2	CGCGGATCCGCTTACAGCCAAGAAGAC	CGAGAATTCTCAGGAGCTGGGTGCCCA TTTG	144	63
IL-2	AJ224516.1	GATAACTGGGACACTGCCATGATG	GTCTCAGTTGGTGTGTAGAGCTCG	305	56
IL-6	AJ250838.2	GTCCGGAGAGGTTGGGCTGG	GCCGTCCTCCTCCGTCACCTTG	280	60
TGFβ4	M31160.1	GACCTCGACACCGACTACTG	GCAGGCACGGACCACCATATTG	332	58
CG3	EF429082.1	GCCATATCCTGGAGGACCAACTG	GAAGTTGAACTGCAGCAGGTGAG	385	56

Table 2.2 Primers designed for AvBDs, cytokines, and Chicken Galectin-3 genes.

AvBD6 M= Avian β-defensin 6 primer encoded mature peptide, AvBD6 P+M= Avian β-defensin 6 primer encoded promature peptide, AvBD9 M= Avian β-defensin 9 primer encoded mature peptide, AvBD9 P+M= Avian β-defensin 9 primer encoded promature peptide. Underlined nucleotides represent the restriction sites of BamH1 (forward primers) and EcoR1 (reverse primers). IL-2= Interleukin-2 primer, IL-6= Interleukin-6 primer, TGFβ4= Transforming growth factor β4 primer, CG3= Chicken galectin-3 primer. T_m= Melting temperature. Size= product size (bp) amplified by the PCR primers.

2.11. End point polymerase chain reaction (PCR)

PCR was performed in a microfuge tube using reagents from a Bioline kit (Bioline London, UK). RT samples (10.0 μ l) were mixed with 10X PCR buffer (4.0 μ l), MgCl₂ 50 mM (0.8 μ l), sterile molecular grade water (20.7 μ l), BioTaq Polymerase (0.5 μ l), forward primer 10mM (2.0 μ l) and reverse primer 10mM (2.0 μ l). Following mixing the tube contents were incubated at 95 °C for 3 minutes; 35 cycles of (94 °C / 1 minute, Tm/ 1 minute, 72 °C/ 1 minute) using a thermal cycler (Techne, Bibby Scientific Limited, UK); 72 °C / 12 minutes and a hold cycle of 4 °C.

2.12. Real time (Quantitative- Q) PCR

AvBD6, AvBD9, IL-6, TGF β 4 and chicken Galectin-3 QPCR were performed using the Sybr green system, and a Roche Lightcycler 480 (Roche, Basel, Switzerland).

2.12.1. Real time PCR primers:

Primers for the real time PCR analyses are shown in Table 2.3. TGF β 4 and chicken Galectin-3 primers were designed for this project while AvBD6, AvBD9 and IL-6 primers were designed previously by Dr Catherine Mowbray (Newcastle University).

Gene	Gene Bank No.	Forward primers	Reverse primers	Size (bp)	Tm
AvBD6	NM_001001193	TCTTGCTGTGTGAGGAACAGG	TTAGAGTGCCAGAGAGGCCA	95	61
AvBD9	NM_001001611.2	GCAAAGGCTATTCCACAGCAGA	CTTCTTGGCTGTAAGCTGGAGCA	103	62
IL-6	NM_204628.1	CTTCGACGAGGAGAAATGCCT	ACTCGACGTTCTGCTTTTCG	110	58
TGFB4	M31160.1	GTACAACCAACACAACCCG	GCAGGCACGGACCACCATATTG	136	57
CG3	EF429082.1	GCCGCTCCACTGAAAGTC	GTGGAAGGCAATGTCTTGC	143	56

Table 2.3 Real-time PCR primers. AvBD6, AvBD9 and IL-6 primers were designed by Dr.Catherine Mowbray, Newcastle University

2.12.2. Standard curves:

Real time PCR standard curves for TGF β 4 and Chicken Galectin-3 were prepared by serial dilution of the cloned plasmids (pGEM-T[®] easy vector, Promega, Southampton, U.K.). Standard curves for AvBD6, AvBD9 and IL-6 were prepared by Dr Catherine Mowbray (Newcastle University).

Ten (10) microlitres of plasmid standard diluted 10^{-4} , 10^{-5} , and 10^{-6} were added to 90 μ l of pure molecular grade water to make 10^{-5} , 10^{-6} and 10^{-7} dilutions respectively for each gene. Pure molecular grade water was used as a negative control.

2.12.3. Real time PCR reaction

A master mix was prepared as follow: 5 μ l Sybrgreen, 0.5 μ l mixed primers 10 μ M and 2.5 μ l pure molecular grade water. Eight (8) μ l of the master mix was added into each well of a 96 qPCR plate (Roche, Basel, Switzerland), followed by either 2 μ l reverse transcribed cDNA (1:4 diluted), water [negative control] or plasmid standard [positive control]. Each sample was loaded into the wells in duplicate. The plates were sealed by nylon sheets and mixed by spinning (Labnet MPS 1000 mini plate spinner) for one minute. Expression was calculated by normalisation of the crossing point (CP) values with the plasmid standards to acquire arbitrary units (A.U.) of the expressed mRNA. The relative quantification of the expression was performed by dividing the AU value of each sample by the geometric mean of two housekeeping genes, SDHA (Succinate dehydrogenase complex, subunit A, flavoprotein variant) and SF3A1 (Splicing factor 3 subunit 1) (GeNorm kit, Primerdesign Ltd, Southampton, U.K.). The housekeeping genes were cloned into the same plasmid by Dr. Catherine Mowbray (PhD, Newcastle University).

2.13. Production of recombinant plasmids

2.13.1. cDNA PCR product purifications

PCR products were purified using a Qiagen purification kit as recommended by the manufacturer instructions. Essentially 5 volumes (600 μ l) of PB buffer was added to one volume of PCR product (120 μ l). This was pipetted onto a Qiagen column and centrifuged for 1 minute at 4 °C 13,000 g with the flow through being discarded. The column was washed twice, using centrifugation, each time with 750 μ l PE buffer and the flow through discarded. The DNA was eluted from the column using 50 μ l molecular grade water.

2.13.2. pGEX-6p-1 vector system and cDNA cloning

AvBD cDNAs were cloned into pGEX-6P-1 (Figure 2.1) via BamHI (GGATCC) and EcoRI (GAATTC) restriction sites.

The purified PCR products and pGEX-6P-1 were restricted with BamHI and EcoRI, and the enzymes removed using the Qiagen PCR purification kit. Ligations were set up and each ligation included 1 µl of vector DNA (100 ng), 5 µl of the PCR product, 1 µl T4 DNA Ligase (Promega, Southampton, U.K.), 1 µl of ligase buffer, and 2 µl of water. Ligations were incubated for 2 hours at room temperature.

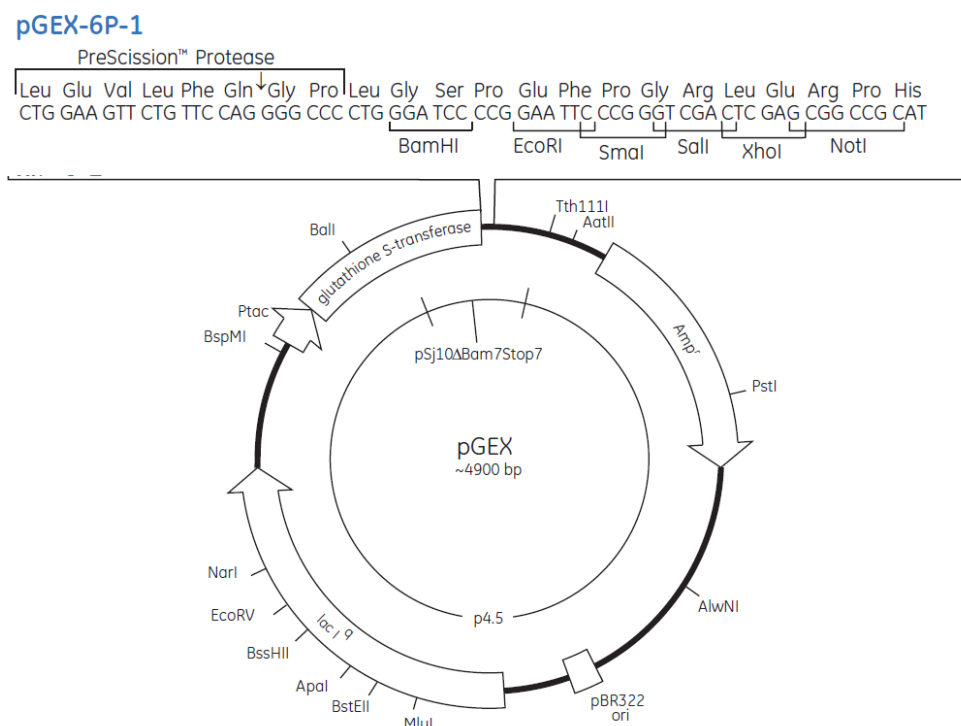


Figure 2.1 pGEX-6P-1 plasmid map.

It contains multiple cloning sites such as BamHI and EcoRI. It also bears Ampicillin resistant gene (Amp), GST tag and PreScission protease sites (GE Healthcare Bio-Sciences AB).

2.13.3. pGEM T Easy vector system and cDNA cloning

TGFβ4 and chicken galectin-3 cDNAs were cloned into pGEM T Easy vector (Promega, Southampton, U.K.). The ligation reaction was as follows: 1 µl of the vector (50 ng), up to 2 µl of the cDNA, 1 µl of T4 DNA ligase, 2 µl of the ligation buffer and 4 µl of molecular grade water. Ligations were incubated at 4 °C overnight.

2.13.4. Competent cell preparation

Bacterial strains of *E. coli*, DH5 α -and BL21 (DE3) pLysS, stored at -80°C were thawed on ice, streaked out on LB agar plates and incubated overnight at 37 °C. A single colony was picked and cultured in 10 ml LB overnight at 37 °C, with gentle shaking (Gallenkamp orbital shaker, Sanyo Gallenkamp Plc, Leicester, UK). For competent cells, 1 ml of overnight culture was added to 100 ml LB broth and shaken vigorously at 37 °C, for approximately 80 minutes or until an optical density [OD_{600nm}] of 0.3-0.4 was reached. The culture was decanted into two Falcon tubes (50 ml for each), the bacterial cells pelleted by 5 minutes centrifugation at 4000 x g and 4 °C (Heraeus Biofuge Stratos centrifuge) and the supernatant decanted off. Four ml of 0.1 M MgCl₂ was added to each pellet, mixed well by vortexing, the solutions transferred to one tube and the cells re-centrifuged. After the supernatant was discarded, 4 ml of 0.1 M CaCl₂ was added to the pellet, the solution vortexed and the cells left on ice for 2 hours before being used in the transformation process.

To prepare glycerol stocks, 0.5 ml of competent cells plus 0.5 ml of 50% glycerol were mixed in a microfuge tube and stored at -80 °C.

2.13.5. Bacterial cell transformation

The ligated vector was transformed into the competent cells by heat shock. To achieve this 100 μ l of competent bacterial cells were added to 5 μ l of the ligation mix in a microfuge, incubated on ice for 10 minutes, incubated at 42 °C for 2 minutes and returned to ice for 3 minutes. Finally, 200 μ l of LB broth was added to the transformation mix and this was gently shaken at 37 °C for at least 1 hour. Increasing amounts of the transformation mix (50 μ l, 100 μ l, and 150 μ l) were spread on LB-Ampicillin or LB-Ampicillin-Chloramphenicol plates for either DH5 α or BL21 competent cells respectively, and the plates incubated at 37 °C overnight.

2.13.6. Blue-white colony screening method

To screen for recombinant pGEM T Easy colonies, LB-Ampicillin agar plates were prepared and spread with 100 μ l of 10 mM isopropyl-1-thio- β -D-galactopyranoside (IPTG) followed by 100 μ l of 50 mM 5-bromo-4-chloro-3-indolyl- β -D-galactopyranoside, (X-gal). As described in section 2.13.5, increasing volumes of the appropriate transformation mix

(25 µl, 50 µl, 75 µl, and 150 µl) were spread on the LB- Ampicillin- IPTG- X gal plates, and the plates incubated at 37 °C overnight.

2.13.7. PCR screening for gene inserts

Using a sterile toothpick single white colonies were picked, spotted onto a LB-Ampicillin agar plate and also mixed into 5 µl of molecular grade water contained in a PCR microfuge tube. To each colony solution, 11.5 µl of molecular grade water, 0.6 µl MgCl₂, 2.0 µl 10X PCR buffer, 0.6 µl forward primer, 0.6 µl of forward and reverse primer (10 mM), 0.5 µl dNTPs, 0.2 µl BioTaq polymerase was added and the contents subjected to PCR at 94 °C for 1 min, 25 cycles of (94 °C for 30 sec, T_m °C for 30 sec, 72 °C for 1 min) 72 °C for 12 minutes and 4 °C hold. Agarose gel electrophoresis was used to identify which colonies contained recombinant plasmid. Positive colonies that contained the required plasmid were cultured overnight in 5 ml LB- broth containing the appropriate antibiotic, subjected to plasmid preparation by QIAprep Spin Miniprep Kit (Qiagen, Crawley, UK) and DNA sequenced.

2.13.8. Recombinant plasmid extraction from the competent cells

Each five ml of overnight culture was pelleted by centrifugation at 8000 g, for 3 minutes at 4 °C (Microcentrifuge Peqlab) and the plasmid prepared using the QIAprep Spin Miniprep Kit protocol. The plasmid DNA was eluted with 30 µl molecular grade water in a sterilized microfuge tube and stored at -20 °C. The purified extracted plasmid were confirmed by PCR using cDNA primers and 1.5 % agarose gel electrophoresis.

2.14. DNA gel electrophoresis

PCR products were analysed using either 1.5 or 2 % agarose gels. To prepare the gels 0.75 (1.5%) or 1 (2%) g agarose was dissolved in 50 ml 1x TBE, the gel was allowed to cool to approximately 60 °C, 5 µl ethidium bromide solution (5 µg/ ml) was added, and the gel poured into electrophoresis apparatus. The gel was allowed to set for 15-30 minutes and then submerged in 1X TBE buffer. Each sample (8 µl) was mixed with 2 µl DNA loading buffer and the samples loaded into the wells; the gel electrophoresed at 50V for 1 hour or as required. DNA markers (Bioline, London, UK) included hyperladder IV (4 µl/well) (10 bands from 100 bp – 1013 bp) and Hyperladder I (14 bands from 200 bp – 10,037 bp).

2.15. DNA sequencing

The cDNA products and recombinant plasmids were sequenced using forward/reverse primers of either the plasmid or gene insert (GeneVision, Newcastle, UK). The sequences were read by chromatograph (Chromas lite, Version 2.0, Technelysium Pty Ltd), (<http://chromas-lite.software.informer.com/2.0/>) and where appropriate blasted against the chicken genome (*Gallus gallus*) (<http://blast.ncbi.nlm.nih.gov/Blast.cgi>).

2.16. AvBD9 site directed mutagenesis

Site directed mutagenesis (Quick-change Lightning Multi Site-Directed Mutagenesis Kit, Agilent Technologies) was used to change the DNA sequence of the AvBD genes. The method is shown in Figure 2.2. This is a PCR-based mutagenesis using double stranded plasmid as template. To mutagenise the targeted sequence, three steps were required. In the first step (A), using thermal cycling, the DNA template was denatured so that the mutagenic primers could be annealed and extended, and the new template ligated using Pfu Fusion-based polymerase enzyme blend. The second step (B) involved Dpn 1 (endonuclease, target sequence: 5'-Gm6ATC-3') digestion of the template to remove the parental non-mutated methylated and hemimethylated DNA. Finally, the newly mutagenised single stranded DNA (C) was transformed into the Gold ultra-competent cells.

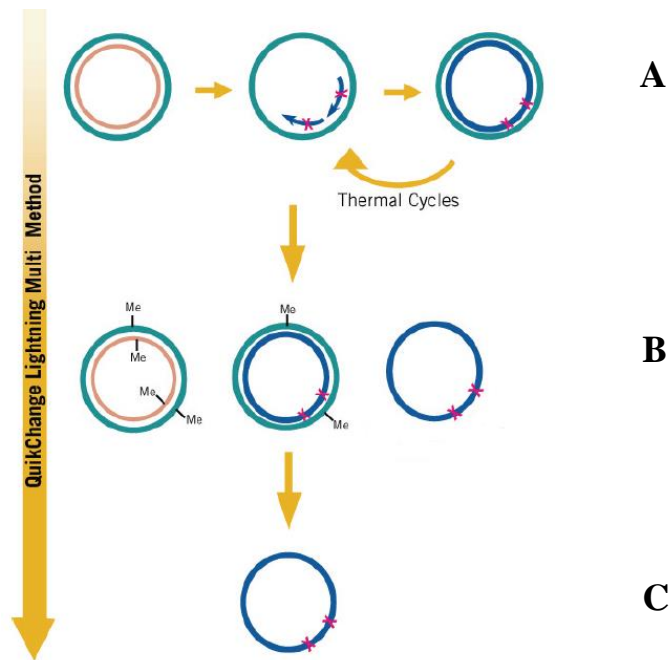


Figure 2.2 Basic steps of PCR based site directed mutagenesis.

A: DNA template denatured, primers with desired mutation annealed and extended through PCR using Pfu DNA polymerase. **B:** Dpn I digestion of the parental DNA (Me groups of parental DNA recognised) resulting in the stable mutagenised SS DNA (**C**), which is transformed into competent cells.

Parental DNA is methylated (Me) and shown as light blue (outer circle) and brown (inner circle). The mutagenised SS DNA is non-methylated and shown as dark blue. Agilent technologies, UK.

2.16.1. Mutagenesis primers

Mutagenesis primers are shown in Table 2.4, and designed using a quick change primer design programme on the Agilent Technologies website:

(<https://www.genomics.agilent.com/primerDesignProgram.jsp>.)

Primer	Forward	Reverse	Mutagenised
AvBD9 C1/A	GCTGACACCTTAGCA <u>GCC</u> AGGCAGAGCCACGG	CCGTGGCTCTGCCT <u>GGC</u> TGCTAAGGTGTCAGC	TGC to <u>GCC</u>
AvBD9 C2/A	CAGAGCCACGGCTCC <u>GCC</u> TCTTTTGTTCATGC	GCATGCAACAAAAGAG <u>GGC</u> GGAGCCGTGGCTCTG	TGC to <u>GCC</u>
AvBD9 C6/A	TGGGAAGCTGAAATGC <u>GCC</u> AAATGGGCACCCAGC	GCTGGGTGCCATTT <u>GGC</u> GCATTTTCAGCTTCCCA	TGC to <u>GCC</u>
AvBD9 C4/G	TTGACATTGGGACC <u>GGC</u> CGTGGTGGGAAG	CTTCCCACCACGGC <u>GGG</u> TCCCAATGTCAA	TGC to <u>GGC</u>
AvBD9 C3/G	CTCCGCCTCTTTTGTTCAG <u>GCC</u> CGTGCTCC	GGAGCACG <u>GCC</u> TGCAACAAAAGAGGCGGAG	TGC to <u>GGC</u>
AvBD9 C5/G	CCGTGGTGGGAAGCTGAAAG <u>GGC</u> GCCAAATG	CATTTGGC <u>GCC</u> TTTCAGCTTCCCACCACGG	TGC to <u>GGC</u>
AvBD9 W38/G	GGGAAGCTGAAATGCTGCAAA <u>GGG</u> GCACCCAGC	GCTGGGTGCC <u>CCCT</u> TTTGCAGCATTTTCAGCTTCCC	TGG to <u>GGG</u>

Table 2.4 Primers (forward and reverse) designed for site directed mutagenesis.

The underlined sequences are codons of the mutagenised amino acids. AvBD9 C1, 2 and 6 /A represent primers designed to mutagenise cysteines (C1, C2 and C6) to Alanine. AvBD9 C3-5 /G means the primers to replace C3-5 by glycine. AvBD9 W38/G is the substitution of tryptophan (W38) with glycine. TGC (cysteine codon), mutagenised to GCC (Alanine codon) or GGC (Glycine codon). TGG (tryptophan codon), mutagenised to GGG (Glycine codon).

2.16.2. Mutagenesis reaction

The mutagenesis reactions were set up as follows: 2.5 µl of 10 x QuickChange Lightning Multi reaction buffer, 13.5 µl pure molecular grade water, 0.75 µl QuickSolution, 2 µl of recombinant plasmid (50 ng/ µl), 2 µl of each primers, 1 µl dNTPs and 1 µl of QuickChange Lightning Multi enzyme blend. The reactions were incubated in one cycle of (95 °C for 2 minutes); 30 cycles of (95 °C for 20 seconds, 55 °C for 30 seconds and 65 °C for 2.5 minutes); 3 cycles of (65 °C for 5 minutes); and incubated on ice for 2 minutes. The parental DNA (non-mutated, methylated and hemimethylated double stranded DNA) was digested by incubating the reaction with 1 µl of Dpn I restriction enzyme at 37 °C for 5 minutes prior to the transformation step.

2.16.3. Transformation of mutagenised plasmids

The transformation of the mutagenised plasmids was performed by thawing 45 µl of the XL10-Gold ultra-competent cells in a 14-ml Falcon tube on ice, mixing with 2 µl of β-Mercaptoethanol and swirling the tube every 2 minutes for 10 minutes. Dpn I-treated mutagenised plasmids (1.5 µl) were mixed with the thawed cells and incubated on ice for 30 minutes. The mixture was incubated in a 42 °C water bath for 30 seconds, incubated on ice for 2 minutes, followed by the addition of 0.5 ml of preheated NZY broth. The competent cells plus DNA were incubated at 37 °C for 1 hour with shaking on an orbital shaker at 225 rpm. An appropriate volume (1 µl, 10 µl and 100 µl) of the transformed competent cells were plated on the LB-Amp (50 µg/ ml) agar plates and incubated overnight at 37 °C. The mutagenised plasmids were extracted as described in section 2.13.8, and DNA sequenced by Genevision (Section 2.15).

2.17. Hyper expression of AvBD6 and AvBD9

For hyper-expression work recombinant plasmids, pGEX-6P-1+AvBD6 and pGEX-6P-1+AvBD9, were transformed into BL21 (DE3) pLysS and colonies selected on the LB agar plates containing ampicillin (50 µg/ ml) and chloramphenicol (30 µg/ ml). Single colonies were picked and cultured overnight in 10 ml LB containing antibiotics with gentle shaking. The overnight culture (10 ml) was added to 1L of LB containing Ampicillin and Chloramphenicol, shaken at 37 °C for 3.5 hours or until an optical density of 0.8- 1 nm. Peptide production was induced with IPTG (1M) for 2-3 hours. The culture was centrifuged at 5000 rpm at 4 °C for 10 minutes (Beckman Coulter Centrifuge, JA10 rotor). The pellets

were collected and re-suspended in 20 ml sterile 1x PBS and frozen overnight at -80 °C. After thawing, the pellets were sonicated for 2 minutes using a Braun Labsonic U sonicator, set at low intensity ~42 watts and 0.5 second cycling, followed by centrifugation at 15,000 x g, 4 °C for 30 minutes (Beckman Coulter Centrifuge, JA2.5 rotor). Each supernatant was collected, the pellets resuspended in 10 ml PBS and all fractions stored at 4 °C.

2.18. Purification of AvBD peptides

2.18.1. Column chromatography using glutathione sepharose resin

CellThru 10-ml Disposable Columns (Clontech Laboratories, Inc.), were rinsed with 70 % ethanol and prepared by adding 3 ml of Glutathione Sepharose resin (Expedeon Ltd UK). The resin was washed using 10 ml of sterile 1 x PBS; this was followed by 20 ml cell free extract (CFE), 10 ml 1xPBS wash buffer and 5 ml of Tris glutathione elution buffer to obtain GST tagged AvBDs. All eluants were collected in 20 ml tubes for analyses by SDS PAGE.

2.18.2. Desalting by gel infiltration

The PD10 desalting columns (GE Healthcare life Sciences) were prepared by removing the column tips and discarding the storage solution. Three ml of 1 x PBS were passed through the column as an equilibrium agent. The samples (previously eluted using Tris-Glutathione) were put through the columns, followed by 1 x PBS to elute the GST tagged-AvBDs. All eluents were collected separately in 20 ml tubes and analysed by NUPAGE.

2.18.3. Hyperexpression and purification of GST-tagged 3C PreScission protease enzyme

The PreScission protease site is located between the GST gene and BamH1 of the pGEX-6-P-1 vector (Figure 2.1). The enzyme cleaves the recombinant peptides from the GST at Gln and Gly residues position and was produced in house using a recombinant pGEX-6P-1 -3C PreScission protease plasmid (GST-tagged HRV 3C PreScission protease, a kind gift of Professor Harry Gilbert, Newcastle University). After transformation into BL21 (DE3) pLysS was hyper expressed and purified as described previously. This GST tagged enzyme was used to cleave the GST tag from the AvBDs.

2.18.4. Cleaving the peptide from GST by PreScission protease enzyme (cutting off the columns)

To cleave the GST tag from the AvBD peptides, 250 µl of PreScission protease (~0.5 mg), 2 ml of desalted GST tagged AvBD (~50 mg) and 1 ml of cleaving buffer was mixed and incubated overnight at 4 °C. The peptides were eluted with 5 ml cleaving buffer.

2.18.5. Cleaving the peptide from GST by PreScission protease enzyme (Cutting on the columns)

In this procedure the GST was cleaved from the AvBD peptides while the latter were attached to the column. CellThru 10-ml Disposable Columns (Clontech), were rinsed with alcohol and prepared by adding 3 ml of Glutathione Sepharose resin (Expedeon) previously washed using 10 ml of 1 x BPS. This was followed by 20 ml cell free extract (CFE) and 10 ml 1xPBS wash buffer. The GST tags were removed from the AvBD peptides by adding 3 ml of cleaving buffer containing 300 µl of PreScission protease enzyme (~0.5 mg). The columns were left overnight at 4 °C. The peptides were eluted with 7 elutions of either 1 ml cleaving buffer [AvBD9 peptides] or 1x PBS [AvBD6 peptides].

2.18.6. Protein separation by concentrator columns

The cleaved AvBD9 peptides were passed through Vivaspin 20 columns [10 kDa MWCO (Polyethersulfone) membrane] (GE Healthcare Life Sciences, UK) and centrifuged at 3000 x g at 4 °C for 20 minutes (Heraeus Biofuge Stratos centrifuge). This trapped the GST tag and protease enzyme at the top part of the column while the pure AvBD9 passed through and was collected. The pure peptide was desalted as described in section 2.18.2. The cleaved AvBD6 was not put through this column due to solubility issues (discussed in Chapter four).

2.18.7. Freeze drying of the peptide

The desalted purified samples were transferred to microfuge tubes with pinholes in the lid and stored at -80 C° for at least one hour before drying in a freeze dryer (Christ Alpha 1-2, Shropshire, UK) for 2-3 days. The samples were stored lyophilised at 4 °C.

2.19. Synthetic peptides

The synthetic peptides including AvBD6, AvBD9 and AvBD9 W38G were synthesised and supplied by Peptide Synthetics, Peptide Protein Research Ltd (Hampshire, UK), with purities (>95%) as determined by RP-HPLC and electrospray mass spectrometry. The peptides were supplied lyophilized and reconstituted in sterilised grade molecular water to 1 mg/mL. The samples were stored at -20 °C.

2.20. Peptide quantification

Protein/ peptide concentrations were measured using a qBCA kit (Sigma), using bovine serum albumen standards (BSA) ranging from 0 to 30 µg/ml. The freeze dried peptides were reconstituted in molecular grade water, diluted 1:100, 1:200 and 1:400. The qBCA working solution was prepared as per manufacturer instructions by mixing 1 ml solution A, 1 ml solution B and 40 µl solution C. The wells of a 96 well plate were loaded with 150 µl of either diluted peptide or standard and 150 µl of the qBCA working solution. The plate was shaken gently for 5 minutes, incubated either at 37 °C for 2 hours or 60 °C for an hour, and OD₅₆₂ nm measured using a microplate plate reader (POLARstar Omega, BMG LAB TECH LTD). Peptide concentrations were calculated in relation to the BSA standards.

2.21. Identification of the peptide

2.21.1. SDS PAGE

Two volumes of the protein samples (~50 µg cell lysate) were mixed with one volume of SDS loading buffer, and boiled for 10 minutes. SDS PAGE gels (15%) consisted of a Resolving gel (4.7 ml 0.75 M Tris/SDS pH 6.8, 3.5 ml 40% (v/v) acrylamide, 1.13 ml sterile water, 90 µl 10% (w/v) Ammonium persulphate and 30 µl of N,N,N',N'-Tetramethylethylene diamine (TEMED) and stacking gel (1.9 ml 0.25 M Tris/SDS pH 6.8, 0.4 ml 40% (v/v) acrylamide, 1.5 ml sterile water, 60 µl 10% (w/v) Ammonium persulphate and 20 µl TEMED). The resolving gel was poured into the glass plates until one quarter of the space was left and this was topped up using water. When the gel was set the water was poured off, the gel edge dried using filter paper, the stacking gel added and the comb inserted carefully. After setting, the plates were put into a vertical gel tank and the tank filled with 1 X SDS running buffer. The comb was removed from the stacking gel, the samples loaded and gel electrophoresis performed at 100 V for 2 hours. Gels were stained with Instant Blue dye (Expedeon, Cambridge, U.K.) for up to 45 minutes.

2.21.2. NUPAGE

The purified proteins were observed using NUPAGE gel electrophoresis. The NUPAGE materials was purchased from Life Technologies (A Thermo Fischer Scientific brand), which included NUPAGE tank (XCell SureLock™ Mini-Cell Electrophoresis System), precast gels (NuPAGE® 4-12% Bis-Tris Gel 1.0 mm, 12 or 15 wells, Novex®), LDS (Lithium dodecyl sulfate) sample loading buffer (SDS analogue), reducing agents, Novex prestained protein markers, antioxidants and 20 X Mes SDS running buffer.

The protein samples were prepared by mixing 4 µl LDS sample buffer, 1.6 µl reducing agents and 10 µl peptide (5-10 µg) and incubated at 70 °C for 10 minutes. The 1 X NuPAGE running buffer was prepared by mixing 42.5 ml of 20X Mes SDS running and 807.5 ml deionised water and mixed well. NUPAGE gels were washed with distilled water, and the tape and comb carefully removed, followed by rinsing the wells with the 1 X NUPAGE running buffer. The electrophoresis tank was set up with the upper chamber containing 200 ml 1 x NUPAGE running buffer and 0.5 ml antioxidant, and the rest of 1 x NUAPGE buffer poured into the lower chamber. The Novex pre stained protein marker and protein samples were loaded into the wells, the electrophoresis performed at 200 v, 125 mA for 45 minutes and the gels stained with Instant Blue (Expedeon, UK).

2.21.3. MALDI TOF mass spectrometry

Peptides were sent for amino acid sequencing by MALDI TOF Mass spectrometry (Proteomics Laboratory, York University, UK). Peptides were transferred by C18 ziptip into 50 % (v:v) aqueous acetonitrile containing 0.1 % (v:v) trifluoroacetic acid before spotting out (1:1) with 4-hydroxy- -cyano-cinnamic acid (CHCA) matrix, 2,5-dihydroxybenzoic acid (DHB) matrix, or 1,5-diaminonaphthalene (DAN) matrix. The samples were analysed by MALDI-MS and In-Source Decay (ISD) using a Bruker ultraflex-III mass spectrometer.

2.22. Anti-microbial activity assays

Antimicrobial activity (AMA) was analysed using both Radial Immuno-Diffusion (RIDA) and Time-Kill Colony Counting assays (CCA). AvBD peptides tested for antimicrobial activity were solubilized in PBS. To test the proteolytic activity of *E. coli* a protease inhibitor cocktail tablet (Roche Diagnostics Ltd. UK) was dissolved in 10 ml 1X PBS solution and serially diluted (1:10, 1:100, 1:1000, 10000 and 1:100000) in PBS.

2.22.1. Radial immuno-diffusion Assay

Bacterial cultures were grown to mid-log phase [OD_{600} 0.3-0.4], diluted to OD_{600} 0.2 then further diluted 1:50 using 10mM Na phosphate buffer. An underlay gel was prepared by mixing 1% agarose and 0.3mg/ml Tryptone soya broth (TSB) with 100 mM Na phosphate buffer. Following cooling to ~ 50 °C, the gel (4.5 ml) was mixed with 0.5 ml of the diluted bacterial culture (OD_{600} 0.2) and poured into a petri dish. After setting, holes were carefully punched into the agarose gel layer and loaded with 2 μ l of peptide of known concentration (0.5, 1 and 3 μ g/ μ l). The plates were incubated for three hours at 37 °C and then overlaid with 5 ml of an overlay gel [100 mM Na phosphate buffer, 1% agarose and 6% TSB]. The plates were incubated for a further 16 hours at 37 °C. AMA was defined by the presence of halos around each well.

2.22.2. Time-kill colony counting Assay

Colony counting assays were performed as reported by Townes *et al* 2004. Initially the bacteria were cultured over-night at 37 °C in 5 ml of Luria broth (LB). Of the overnight culture, 100 μ l was added into 10 ml of LB and incubated for approximately 1.5 h at 37 °C to obtain mid log phase (0.3-0.4) at OD_{600} . Ten (10 μ l) of the culture was added to 10 ml PBS, and 10 μ l of each peptide or PBS was added to 90 μ l of the diluted bacterial culture, vortexed and incubated for 3 h at 37 °C. The suspensions were serially diluted to 10^{-4} in PBS, and each dilution was spread onto a blood agar plate. All plates were incubated overnight at 37 °C, and the colonies counted. The number of surviving colonies for each dilution plated (10^{-2} , 10^{-3} , 10^{-4}) were determined by multiplying the colony number counted by the dilution factor. The effects of the PBS and peptide treatments were calculated by subtracting the mean bacterial colony number following a 3h incubation with PBS or peptide from the colony number determined at 0 hours of incubation. The % survival was deduced by dividing the (loss/gain) value for the peptide by the (loss/gain) value for PBS. Triplicate plates were used for each test sample and each time-kill experiment was repeated at least twice.

2.23. Calcein leakage assay

A lipid stock solution (50 mg/ml) was prepared by mixing 0.345 g soya bean, type II S Phospholipid powder, L- α - Phosphatidylcholine (Sigma, P-5638, kindly gifted by Professor Jeremy Lakey, Newcastle) with 7 ml hexane (BHD, VWR, UK) and a few drops

(up to 0.5 ml) of ethanol, and kept at -20 °C. 100 mg (2 ml of 50 mg/ml) of the lipid were dried in a round bottom flask using compressed air until the lipid film had attached to the wall of the flask. The lipid film was further dried using a vacuum pump for 2 hours at room temperature to remove any residues of the organic solvent. All drying processes were performed in a fume cabinet.

Calcein solution (20 mM) was prepared by dissolving 62.25 mg of Calcein (Sigma) in 5 ml of 100 mM sodium phosphate buffer and filtered through 0.2 µm membrane. To create Calcein-trapped multilamellar (MLV) vesicles, 2 ml of the Calcein solution was added into the lipid film and shaken with clean glass beads (2.5-3.5 mm) for 20 minutes at room temperature. Unilamellar vesicles (ULV) were prepared by passing the MLV through a miniextruder (Avanti) with 100 nm polycarbonated membrane at least 11 times. Untrapped (free) calcein molecules were removed using a PD-10 desalting column (GE Healthcare), (Hyldgaard *et al.*, 2012), and the column was eluted with 3 x 1 ml of 100 mM sodium phosphate buffer. Calcein leakage from the ULV liposomes was monitored by mixing 5-10 µl of the liposomes with 3 ml Sodium phosphate buffer (100 mM) in a quartz cuvette (1mm thick) containing magnet. The leakage was measured using a fluorescent spectrophotometer (Varian) and Cary Eclipse software, Excitation (493 nm) and emission (505-600nm). TritonX-100 (1% final concentration) was used a 100% leakage positive control. Leakage was calculated using the equation:

$$\text{Leakage \%} = (F_p - F_0) / (F_t - F_0) * 100\%$$

Where F_p is the measurement of fluorescent leakage by the peptides, F_t is the complete leakage by TritonX and F_0 is intact vesicles before adding peptide or TritonX

2.24. Circular dichroism (CD)

Eighty (80 µl) of either peptide (250 µg/ml) or Sodium Phosphate buffer 50 mM or 1% SDS (30 mM) were added to a 0.2 cm Hellma cuvette. Far-UV measurements (250- 185) nm were recorded by Jasco-810 CD spectropolarimeter with interval band width 0.2 nm, data pitch 0.5 nm, scanning speed 100 nm/min, response 10 sec and accumulation 10 at room temperature (Park *et al.*, 2002). Signals detected below 190 nm were removed due to high tension (HT) voltage measurements increasing to >600 V (all HT measurements were required to be <600 V).

After subtraction from the buffer baseline, the data were extracted in millidegree (theta machine unit) using Jascow software, converted to text files and then calculated to $\Delta\epsilon$ ($M^{-1}cm^{-1}$) which is a per residue molar absorption units of circular dichroism. The quantity of secondary structure types such as α -helix, β -sheet, β -turns and disordered structure were predicted using Dichroweb (<http://dichroweb.cryst.bbk.ac.uk/html/home.shtml>). The CD spectra data were inputted and outputted as text files and delta epsilon units from 190-240 nm using SELCON3 and Set4 or K2D. This software quantifies the secondary structures of proteins based on an algorithm (Sreerama and Woody, 2000).

2.25. Immuno-histochemistry (IHC)

2.25.1. Antibodies for IHC

Polyclonal antibody to AvBD9 was prepared by Cambridge Research Biochemicals, through immunising a rabbit with AvBD9 antigen (LASRQSHGS-Ahx-C-amide). The antisera was purified by the Company using affinity chromatography and thiopropyl sepharose 6B coupled to the antigen.

The Rabbit polyclonal anti-body to IL-6, which recognises chicken IL-6 was purchased from Abcam (ab24769, Cambridge, UK).

2.25.2. Tissue processing

Following fixation the avian tissues the samples were processed into paraffin blocks. Tissue was sectioned to a thickness of 4 μm onto SuperFrost Plus slides (Thermo Scientific) and allowed to dry for 24 to 48 hours before staining.

2.25.3. IHC staining and antibody procedure

For immunohistochemistry, slides were dewaxed in xylene, rehydrated through graded alcohols to water and subjected to a hydrogen peroxide block (1.5% in water) for 10 minutes. All antibodies were assessed independently to determine the appropriate antigen retrieval method for use with each stain. Methods assessed were pressure cooking with citrate buffer (pH6.0), pressure cooking with EDTA (pH8.0), enzymatic digest with trypsin (pH7.8 at 38 °C) and no antigen retrieval. For the AvBD9 and IL-6 detecting antibodies, pressure cooking with EDTA worked most effectively (Performed by Dr C Mowbray, Newcastle University). After antigen retrieval, staining was carried out using the Vectastain Elite ABC peroxidase kit (rabbit) (Vector Laboratories) as per manufacturer's instructions. AvBD9 and IL-6 antibodies (0.5 mg/ml) were used at a dilution of 1/70 and 1/120 in TBS

(pH7.6) for 1 hour at room temperature, respectively. The reaction was developed using the peroxidase chromogen DAB (3, 3 diaminobenzidine tetrahydrochloride) (Sigma) as per manufacturer's instructions, and the nuclei counterstained using Mayer's Haematoxylin and Scot's tap water substitute. Sections were dehydrated through graded alcohols and cleared in xylene before mounting using DPX (Sigma).

2.26. Statistical analysis

The real time expression data were analysed using Graph Pad Prism software and one way ANOVA followed by Tukey's multiple comparison tests. The AMA and leakage assay data were managed in Excel and analysed by Minitab 17 statistical software (MINITAB®, Minitab Inc) using one way ANOVA followed by Dunnett's multiple comparison tests. The AMA raw data were statistically analysed for the number of colonies survived.

Chapter 3

3. *In vivo* expression analyses of chicken genes associated with gut innate immunity

3.1. Introduction

In 2008 a bird trial was performed that focussed on a commercial Aviagen broiler chicken line, designated Line X, characterised by its increased susceptibility to gut inflammation. The aim of the trial was to explore the effects of rearing environment on the innate immune responses of Line X birds, particularly the tissue expression of genes encoding avian β -defensin (AvBD) antimicrobial peptides (AMPs).

The Line X birds were reared for 35 days in two contrasting environments pedigree (high hygiene, HH), or sib-test (low hygiene, LH). To achieve the HH environment the rearing barn was subjected to a complete disinfection process between flocks and a tight bio-security control system was enforced. In contrast, the LH environment modelled the conditions of an UK commercial broiler unit.

Previous analyses reported the expression of the AvBD 1, 4 and 10 genes in ten tissues removed from birds reared either in the LH or HH conditions (V. Butler 2010, PhD Thesis). The bird AvBD expression levels were very variable, even between birds within a specific group, but the data supported a distinct trend in that mean duodenal AvBD gene expression values were elevated in birds of line X raised in the LH compared to the HH environment. Thus despite the susceptibility of the birds to gut inflammation these data suggested a robust AvBD1, 4 and 10 gene response.

This Chapter extended the analyses and explored the gene expression of AvBDs 6 and 9, IL-2, IL-6, TGF β 4 and chicken galectin-3 (CG3). AvBDs 6 and 9 were targeted due to the identification of SNPS (Table 3.1), including two SNPs relating to the AvBD6 gene and three SNPs relating to the AvBD9 gene (V. Butler, 2010D Thesis).

Code	AvBD	Gene code	SNP code	SNP	Location	frequency
5	6	ENSGALG00000016668	Rs13526000	T/G	Intronic	0.49
6	6	ENSGALG00000016668	Rs16341514	G/T	Intronic	0.17
10	9	ENSGALG00000019845	Rs3137928	T/C	3'UTR region	0.08
11	9	ENSGALG00000019845	Rs14411786	C/T	Intronic	0.97
12	9	ENSGALG00000019845		T/C	Intronic	0.99

Table 3.1 List of 5 SNPs in an Illumina study that were identified in Aviagen Line X birds.

Frequency is for the presence of the T base in allele designated A. (V. Butler 2010, PhD Thesis).

The expression of cytokines IL-2 and IL-6 were studied as the genes encode pro-inflammatory agents, while TFG β 4 gene expression was analysed as the encoded protein functions as an anti-inflammatory agent. Chicken galectin-3 (CG3) gene expression was also explored as an earlier proteome analysis of the bird gut mucosae using LC-MS specifically identified the chicken galectin-3 peptide, a carbohydrate binding lectin, in the gut extracts of Line X samples thereby suggesting a role in the innate defences of the birds (V. Butler 2010, PhD thesis).

The aim of this chapter was to use Endpoint (RT-PCR) and Real-time (qPCR) to compare the gene expression of AvBD6 and 9, IL-2, IL-6, TFG β 4 and CG3 in tissue samples, excised from young Day 7 (D7) and older Day 35 (D35) Line X Aviagen broiler chickens raised in LH and HH environments. Additionally immunohistochemistry was performed to identify and compare the synthesis and localisation of both AvBD9 and IL-6 in the gut, specifically the duodenal tissues.

3.2.Endpoint PCR analyses of AvBDs 6 and 9, chicken galectin-3, IL-2, IL-6 and TGF β -4 gene expression

Endpoint PCR provided a method to screen samples and establish gene expression before developing methods to quantify the actual levels of tissue expression.

3.2.1. Tissue panels investigating AvBD6 and 9 gene expression in birds raised in Low and High hygiene conditions

AvBD6, 9 and 18S gene expression were studied using end-point PCR and initially an array of Day 7 bird tissues, including thymus, liver, kidney, small intestine, caecum, caecal tonsils, lung, spleen, bursa and testis were analysed. The AvBD6 and AvBD9 primers were

each designed to amplify cDNAs of 126 bp (section 2.10) and the size of the 18S housekeeping cDNA was 500 bp.

The results, shown as panels, are presented in Figures 3.1 and 3.2. The data (Figure 3.1), indicated that the AvBD6 and 9 genes were expressed in all the bird tissues analysed and regardless of the rearing conditions. It was not possible, however, using these data to identify whether gene expression was affected by the different rearing conditions.

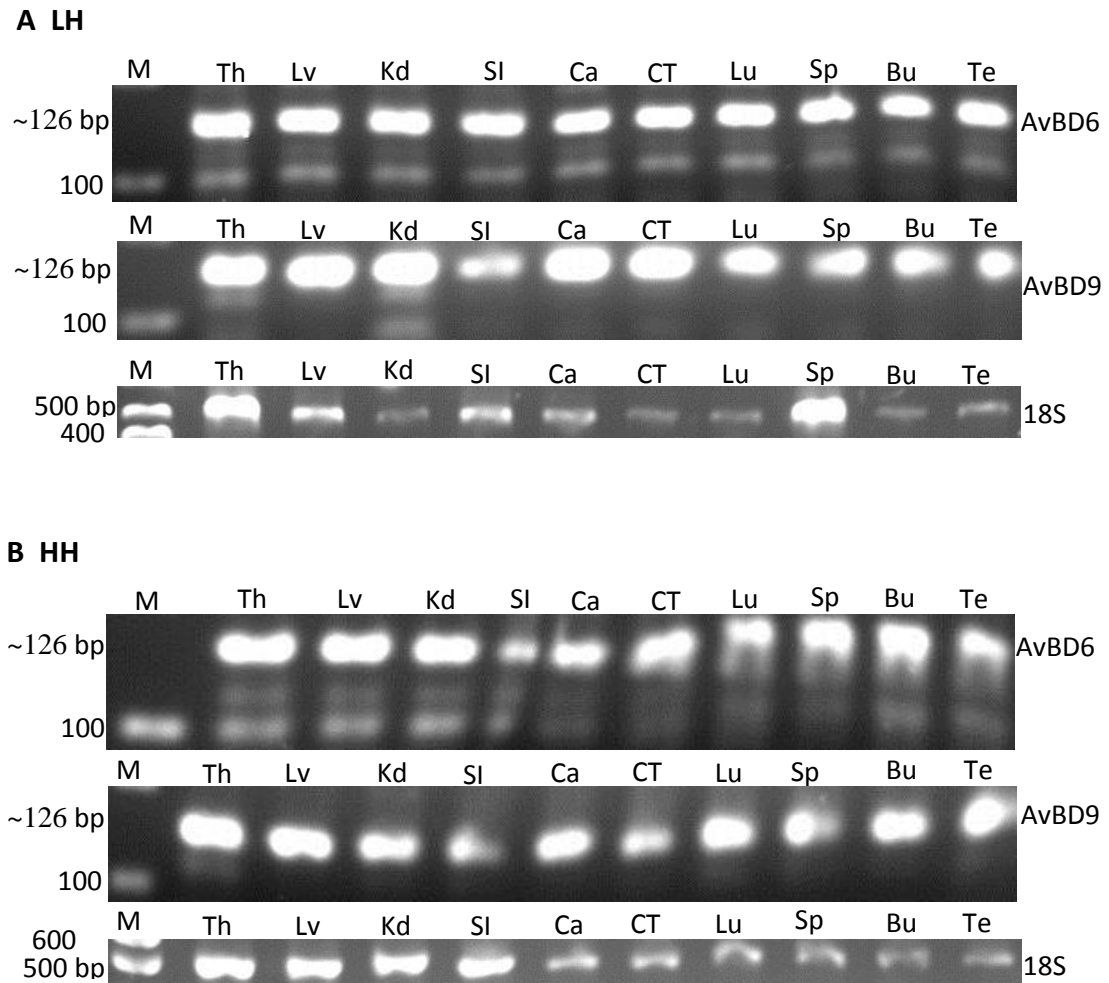


Figure 3.1 AvBD6/ 9 and 18S cDNA expression panels using tissues from a single bird, D7, Line X birds raised in low (A) and high (B) hygiene conditions. Lanes comprise: M=DNA marker 100-1000 bp, Th=thymus, Lv=liver, Kd=kidney, SI=small intestine, Ca= caecum, CT=caecal tonsils, Lu=lung, Sp=spleen, Bu=bursa, Te=testis.

In relation to AvBD6 (Av6) expression (Figure 3.1C), three cDNA bands of approximately 100 bp, 126 bp and 200 bp were amplified. The strong band was of the correct size (126bp) and confirmed as AvBD6 by DNA sequencing. Bands of less than 100bp were due to primer dimers. The negative controls represented the PCR reactions of each set of gene primers, in which cDNA was replaced by molecular grade water.

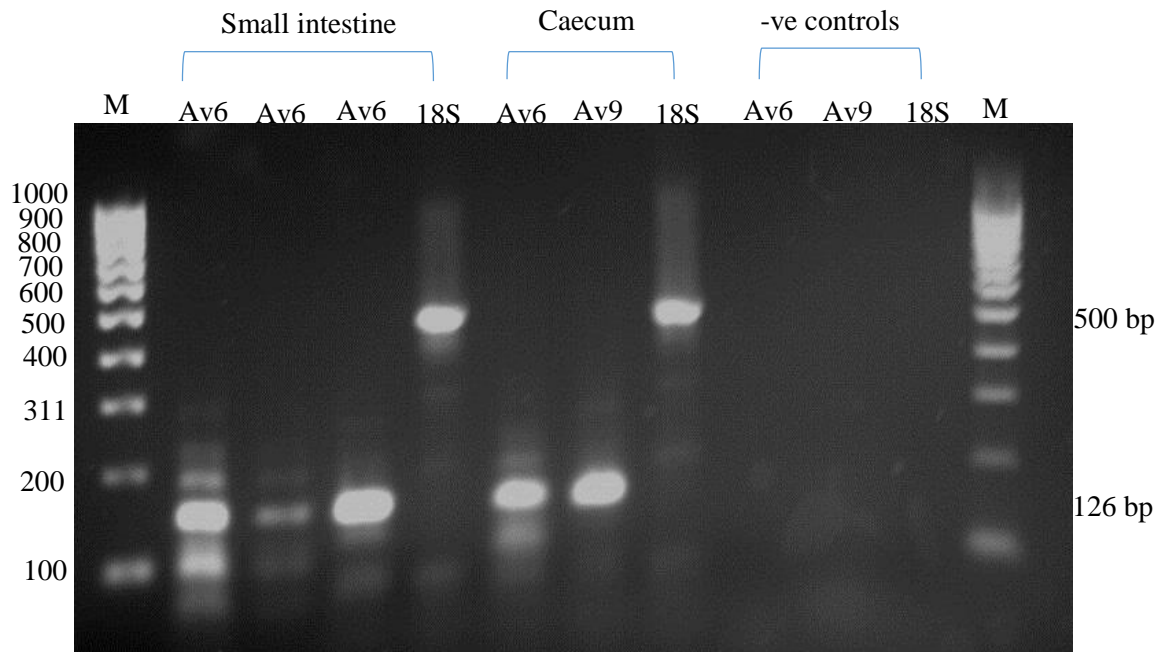


Figure 3.1 C Agarose gel electrophoresis of AvBD6, AvBD9 and 18S PCR products amplified from small intestinal and caecal tissues excised from a single bird, D 7, Line X, HH bird alongside negative controls. AvBD6 (Av6), AvBD9 (Av9), 18S. M= DNA Marker (100-1000bp).

3.2.2. Sequencing results for AvBD6 and 9 cDNA:

To verify that the cDNA bands were AvBD6 and 9, the 126 bp cDNA PCR products were cloned into pGEX-6p-1 and the plasmids sequenced by Genevision, Newcastle, UK using primers shown in Table 2.2.

Figure 3.3 shows the DNA sequences of AvBD6 (panel A) and AvBD9 (panel B) taken from the NCBI (National Centre for Biotechnology) database (<http://www.ncbi.nlm.nih.gov/>) and the sequences of the amplified PCR products. Authenticity of the cDNA products was proven by the 100 % sequence match.

[gb|AY621308.1|](#) **UGM** Gallus gallus beta-defensin 6 (G&L6) mRNA, complete cds
Length=502

A

Identities = 132/132 (100%), Gaps = 0/132 (0%)

```

Query 68 TCCAGCCCTATTCATGCTTGTAGATATCAAAGGGGTGTCTGCATTCTGGGCCATGTCGG 127
          |||
Sbjct 153 TCCAGCCCTATTCATGCTTGTAGATATCAAAGGGGTGTCTGCATTCTGGGCCATGTCGG 212

Query 128 TGGCCATATTACCGGTTGGATCATGTGGCAGTGGACTAAAATCTTGCTGTGTGAGGAAC 187
          |||
Sbjct 213 TGGCCATATTACCGGTTGGATCATGTGGCAGTGGACTAAAATCTTGCTGTGTGAGGAAC 272

Query 188 AGGTGGGCCTGA 199
          |||
Sbjct 273 AGGTGGGCCTGA 284

```

[gb|AY621311.1|](#) **UGM** Gallus gallus beta-defensin 9 (G&L9) mRNA, complete cds
Length=693

B

Identities = 128/128 (100%), Gaps = 0/128 (0%)

```

Query 67 CGCTGACACCTTAGCATGCAGGCAGAGCCACGGCTCCTGCTCTTTTGTTCATGCCGTGC 126
          |||
Sbjct 237 CGCTGACACCTTAGCATGCAGGCAGAGCCACGGCTCCTGCTCTTTTGTTCATGCCGTGC 296

Query 127 TCCTTCAGTTGACATTGGGACCTGCCGTGGTGGGAAAGCTGAAATGCTGCAAAATGGGCACC 186
          |||
Sbjct 297 TCCTTCAGTTGACATTGGGACCTGCCGTGGTGGGAAAGCTGAAATGCTGCAAAATGGGCACC 356

Query 187 CAGCTCCT 194
          |||
Sbjct 357 CAGCTCCT 364

```

Figure 3.2 Sequencing results for AvBD6 (A) and AvBD9 (B) DNA products. ‘Query’ represents the amplified cDNA products. ‘Sbjct’ is the NCBI database gene sequence.

3.2.3. Tissue panels investigating IL-2, IL-6, TGFβ4 and chicken galectin-3 gene expression

Due to the lack of sensitivity of the endpoint PCR analyses and to help conserve the sample RNA material, IL-2, IL-6, TGFβ4 and CG3 gene expression were performed using only selected tissues from birds raised in the LH environment. Figure 3.3 shows the expression of Interleukin-2 (IL-2), Interleukin-6 (IL-6), Transforming growth factor β-4 (TGFβ-4) and Chicken Galectin-3 (CG3) in the selected tissues, which included gut tissues, the thymus and bursa (two primary lymphatic organs) and the spleen (a secondary lymphatic organ). Copy (c) DNA bands of 305 bp (IL-2), 280 bp (IL-6), 332 bp (TGFβ4) and 385 bp (CG3)

were identified in all tissues indicating the expression of the genes of interest. However, two bands of approximately 200 and 305 bp were observed in relation to IL-2 gene expression (Figure 3.3A), and similarly for IL-6 gene expression, two bands of approximately 200 and 280 bp in size were recorded (Figure 3.3B). Thus DNA sequencing of the cDNA bands was performed in each case to confirm the cDNA amplified actually reflected the targeted gene.

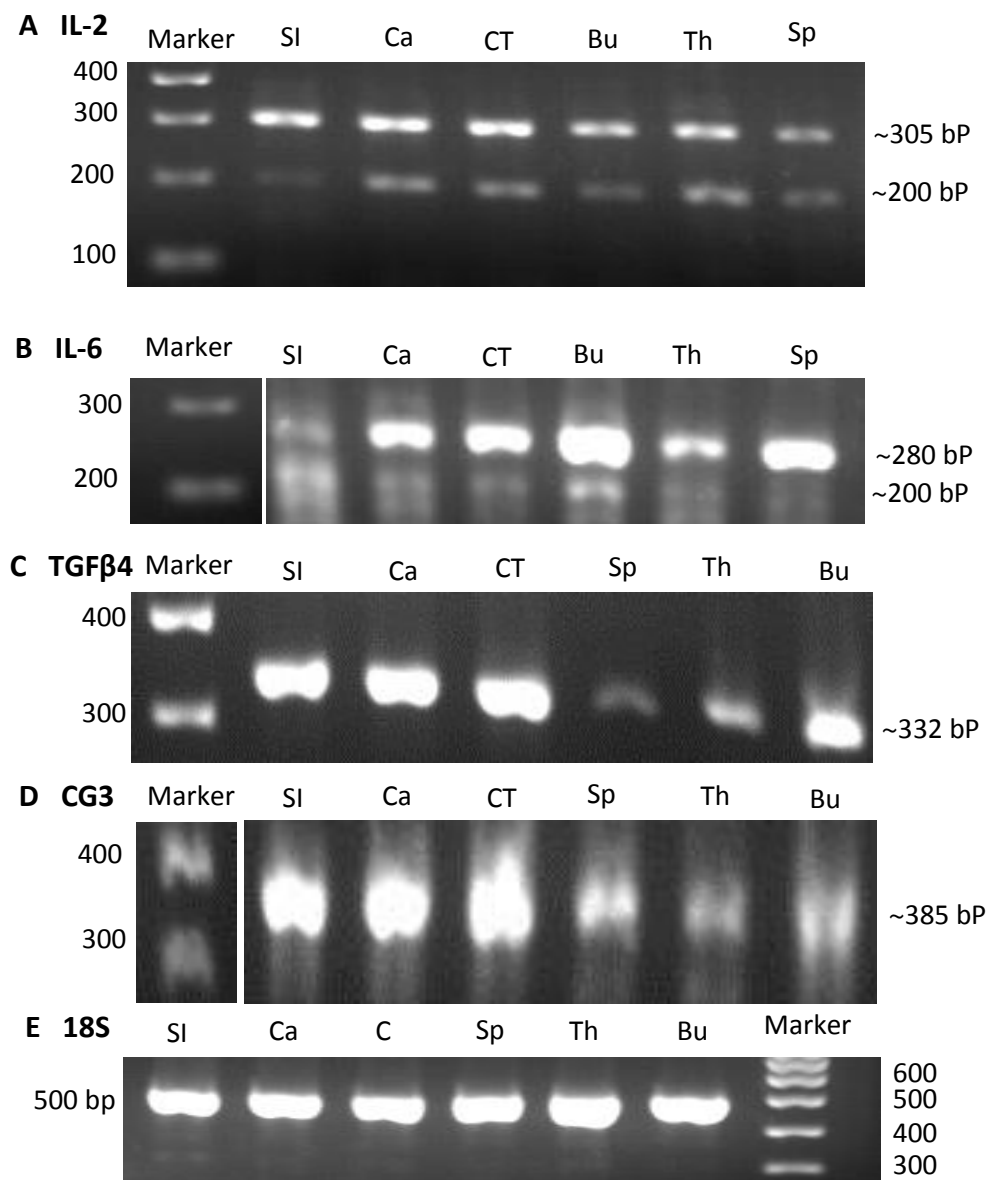


Figure 3.3 IL-2 (A), IL-6 (B), TGFβ4 (C), CG3 (D) and 18S (E) expression panels. Tissues were excised from D7, Line X birds raised in LH conditions. Lanes are M= DNA Marker (100-1000bp), SI=small intestine, Ca=Caecum, CT=Caecal tonsils, Bu=Bursa, Th=Thymus, Sp=Spleen. bp= base pairs.

3.2.4. Sequence results of IL-2, IL-6, TGFβ4 and CG 3 cDNAs

cDNAs obtained using the IL-2, IL-6, TGFβ4 and CG3 primers were cloned into the pGEM T Easy vector and sequenced using the appropriate gene primers shown in Table 2.2.

Figures 3.4 to 3.6 show the results of the DNA sequence analyses. These data indicated 95%, 99%, and 98 % identity to NCBI sequences for IL-2 (305bp band), TGFβ4 and CG3 cDNAs respectively. Putative nucleotide changes highlighted in the sequences reflected either poor quality sequence or potential nucleotide base changes.

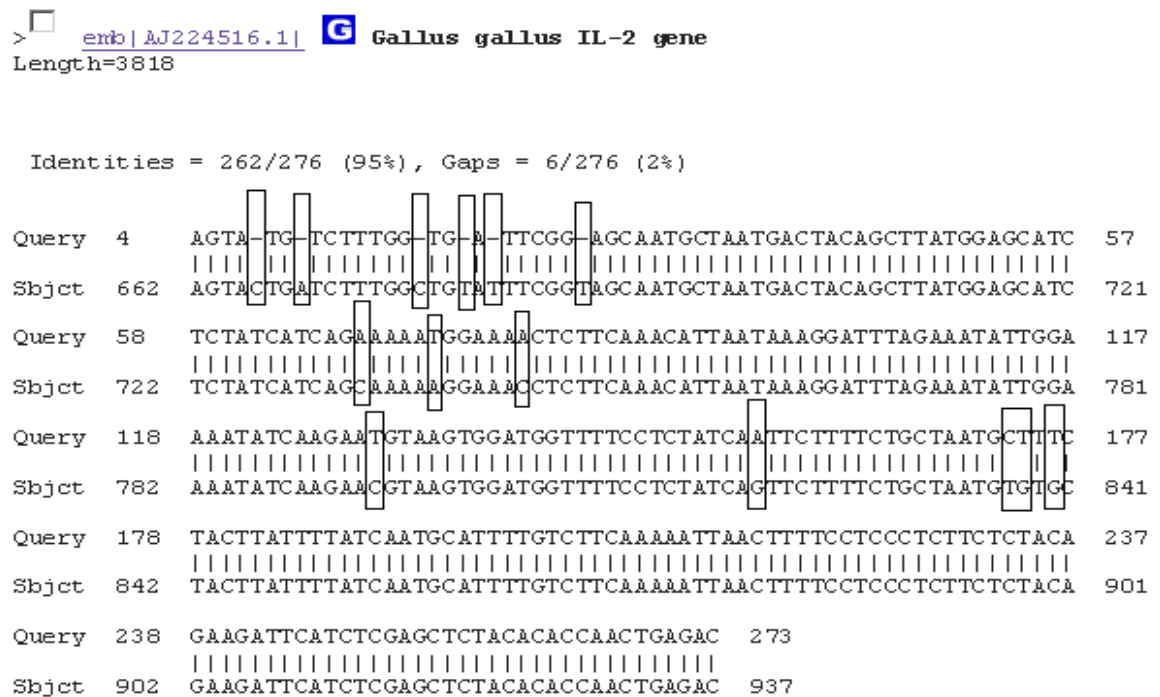


Figure 3.4 A: Sequencing and BLAST results of an IL-2 PCR product amplified from D7 caecum Line X bird. 'Query' is the sequence analysed; 'Sbjct' is the NCBI database gene sequence. The boxes represent either poor quality sequence or potential nucleotide changes.

Figure 3.4B shows the DNA chromatograph of an IL-2 cDNA sequence. The circles represent nucleotides missed by the software due to poor quality sequencing. However, manual reading of the peaks allowed the gaps to be identified; for example, A10 (Green) was recorded as absent, but the peak was present in the chromatograph albeit hidden under the G9 and T11 peaks. The boxes represent potential nucleotide changes and include A70, T75, A81, T131, A157, C174, T175 and T177. However, the DNA was sequenced in one direction only, thus SNPs cannot be confirmed.

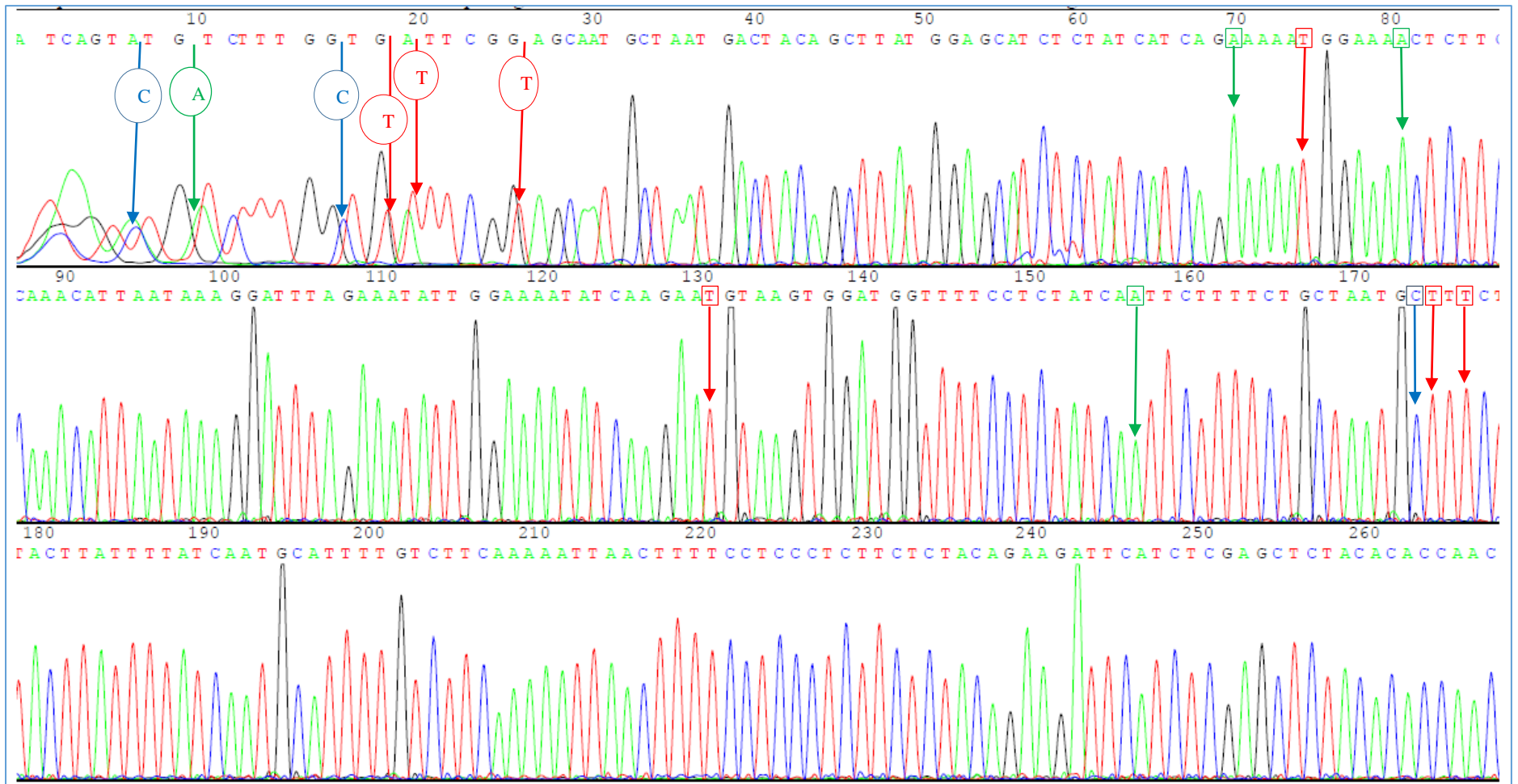


Figure 3.4 B: Sequenced PCR product from a D7 caecum Line X bird showing the poor quality sequence (circles) and the potential nucleotide changes (Boxes) in IL-2. The different bases are colour-coded, A-green, T-red, G-black and C-blue.

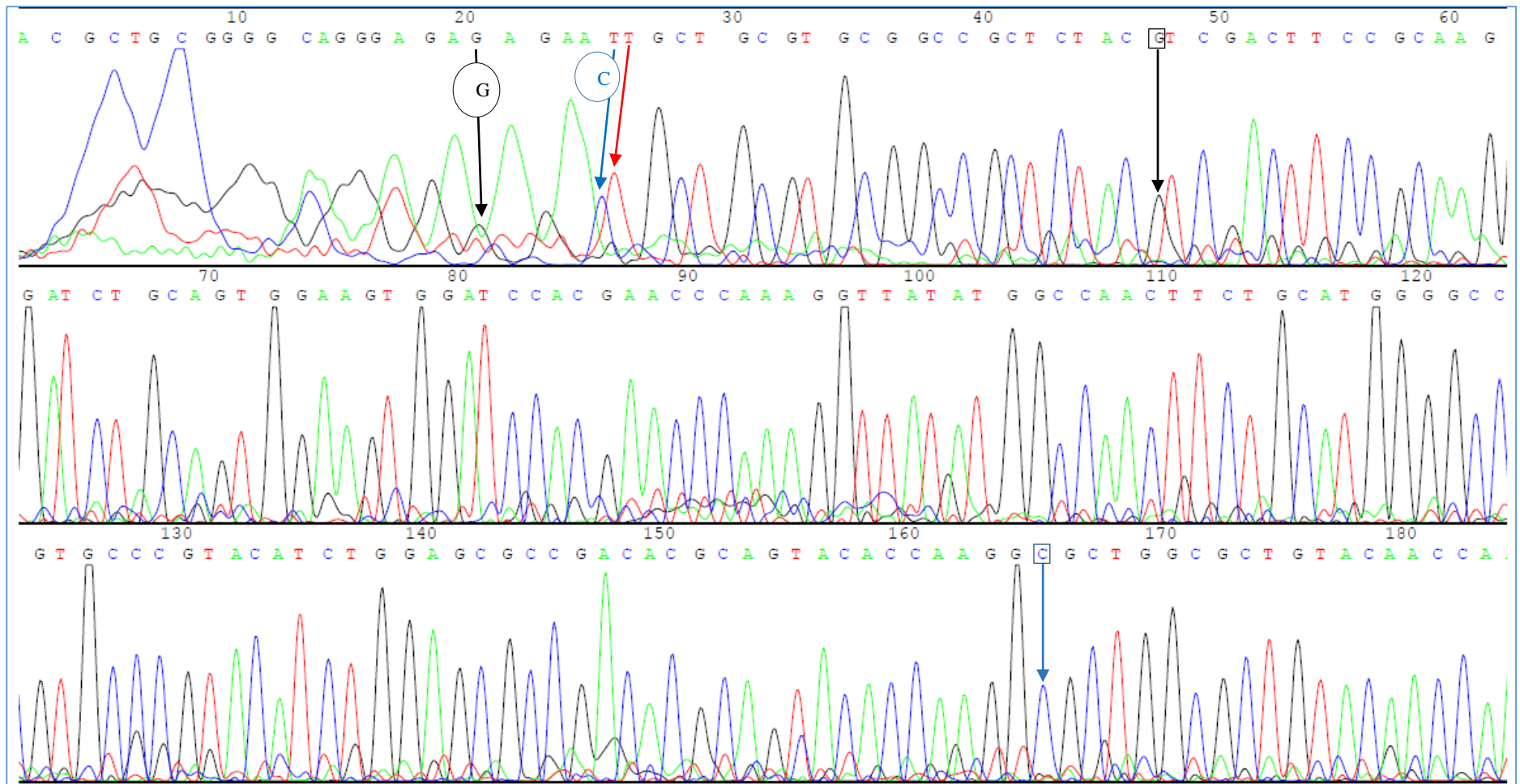


Figure 3.5 B: Sequenced PCR product from a D7, Line X bird (caecum) showing the poor quality sequence (circles) and the potential nucleotide changes (Boxes) in TGF β 4. The different bases are colour-coded, A-green, T-red, G-black and C-blue.

Figure 3.6B shows the poor quality DNA sequence and potential nucleotide changes of a CG3 cDNA product amplified from caecum of a Line X bird. For example, G32 was recorded absent in the CG3 gene sequence but its peak was present in the chromatograph. Potential nucleotide changes include C93, A115 and C231.

```

>  gb|EF429082.1|  Gallus gallus galectin-3 mRNA, complete cds
Length=726

Identities = 348/354 (98%), Gaps = 3/354 (1%)

Query 6 TCTG  AGCT  CAGCCGCTCCACTGAAA  TCCCCTACGATCTGCCCCCTGCCAGCAGGACTC 62
      |||
Sbjct 289 TCTG  AGCT  CAGCCGCTCCACTGAAA  TCCCCTACGATCTGCCCCCTGCCAGCAGGACTC 348

Query 63 ATGCCTCGGCTGCTCATAAACCATCACGGGC  AACTGTAAC TCAAATCCCAAC  AGTTTTC 122
      |||
Sbjct 349 ATGCCTCGGCTGCTCATAAACCATCACGGGC  AACTGTAAC TCAAATCCCAAC  AGTTTTC 408

Query 123 CTGGATTTC AAGAGGGGGCAAAGACATTGCCTTCCACTTTAACCCCGTTTCAAGGAAGAC 182
      |||
Sbjct 409 CTGGATTTC AAGAGGGGGCAAAGACATTGCCTTCCACTTTAACCCCGTTTCAAGGAAGAC 468

Query 183 CACAAAAGGGTCATTGCTGTAAATTC AATGTTCCAAAACAACTGGGGAC  AAGAGGAGAGA 242
      |||
Sbjct 469 CACAAAAGGGTCATTGCTGTAAATTC AATGTTCCAAAACAACTGGGGAC  AAGAGGAGAGA 528

Query 243 ACAGCTCCTAGATTTCCATTTGAACCTGGAACCCCTTCAAGCTCCAGGTGCTCTGCGAG 302
      |||
Sbjct 529 ACAGCTCCTAGATTTCCATTTGAACCTGGAACCCCTTCAAGCTCCAGGTGCTCTGCGAG 588

Query 303 GGGGATCACTTCAAGGTAGCAGTGAACGATGCTCACCTGCTGCAGTTCAACTTC 356
      |||
Sbjct 589 GGGGATCACTTCAAGGTAGCAGTGAACGATGCTCACCTGCTGCAGTTCAACTTC 642

```

Figure 3.6 A: Sequencing and BLAST results of a CG3 PCR product amplified from caecal tissue. 'Query' is the sequence analysed; 'Sbjct' is the NCBI database gene sequence. The boxes represent either poor quality sequence or potential nucleotide changes.

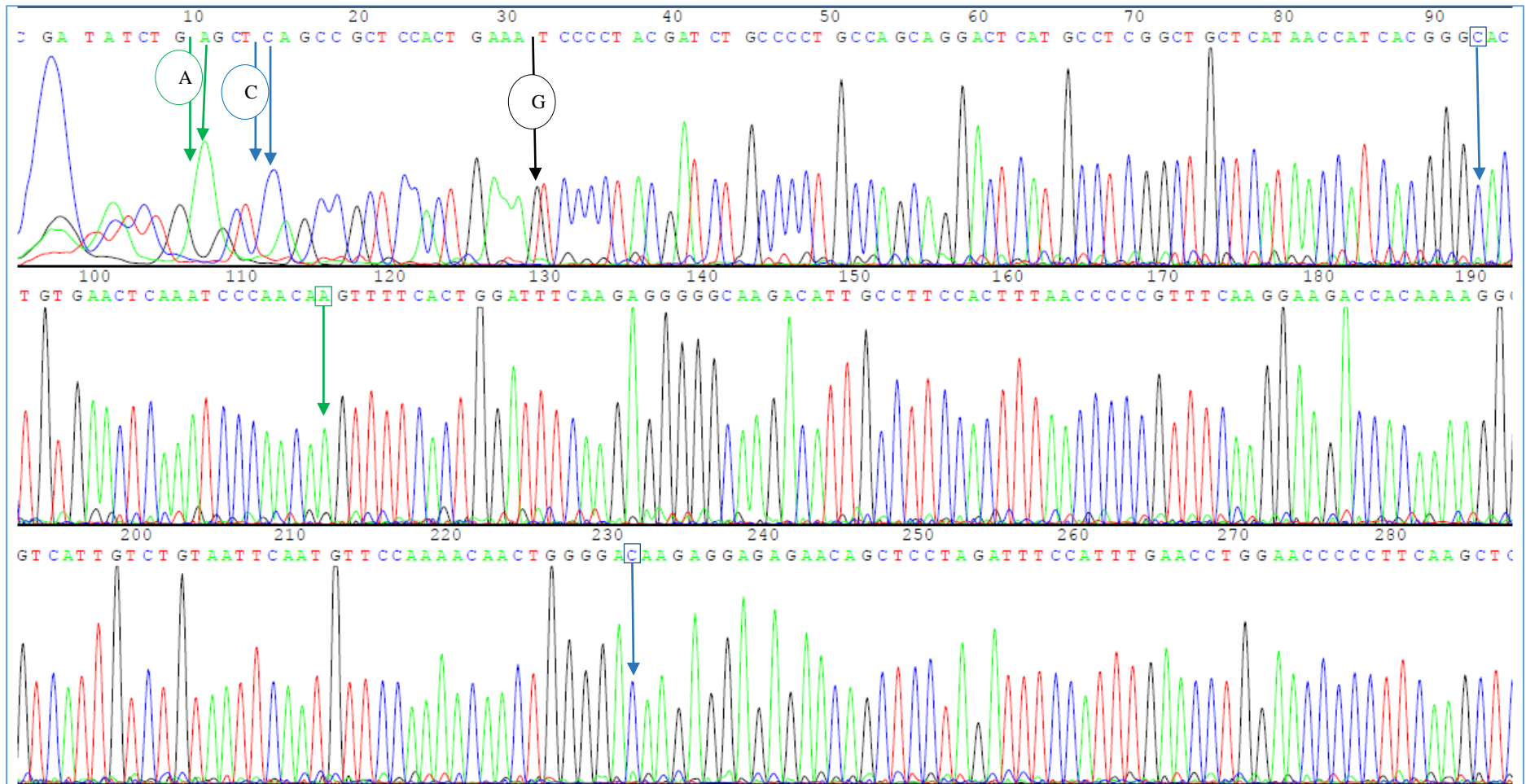


Figure 3.6 B: Sequenced PCR product from a D7, Line X bird (caecum) showing the poor quality sequence (circles) and the potential nucleotide changes (Boxes) in CG3. The different bases are colour-coded, A-green, T-red, G-black and C-blue.

Unlike the data relating to IL-2, TGFβ4 and CG3 the cloned cDNA amplified using the IL-6 primers did not match the NCBI chicken IL-6 gene sequence. The amplified sequence was identified as a hypothetical protein (Figure 3.7).

This non-specific amplification was attributed to the high GC content in the mRNA sequence of the IL-6 gene; in fact the GC content was identified as 79.7 %, 60.5 %, and 53.7% in exons 1-3 respectively. It was predicted that the high GC content in exons 1 and 2 to which the IL-6 primers were designed (Table 2.2) resulted in secondary structure formations that inhibited polymerase activity and encouraged the amplification of non-specific cDNA sequences. To explore this further the RT-PCR analyses were repeated, but using the Qiagen Q solution kit designed to amplify GC rich sequences. However, this did not result in amplification of IL-6 specific cDNA bands suggesting an IL-6 primer design problem.

```

>  emb|AJ720109.1| UEGM Gallus gallus mRNA for hypothetical protein, clone
10m24
Length=4181

Identities = 297/297 (100%), Gaps = 0/297 (0%)

Query 277 AGCTTGGCGTAATCATGGTCATAGCTGTTTCTGTGTGAAATTGTTATCCGCTCACAATT 336
          |||
Sbjct 3885 AGCTTGGCGTAATCATGGTCATAGCTGTTTCTGTGTGAAATTGTTATCCGCTCACAATT 3944

Query 337 CCACACAACATACGAGCCGGAAGCATAAAGTGTAAGCCTGGGGTGCCTAATGAGTGAGC 396
          |||
Sbjct 3945 CCACACAACATACGAGCCGGAAGCATAAAGTGTAAGCCTGGGGTGCCTAATGAGTGAGC 4004

Query 397 TAACTCACATTAATTGCGTTGCGCTCACTGCCCGCTTCCAGTCGGGAAACCTGTCGTGC 456
          |||
Sbjct 4005 TAACTCACATTAATTGCGTTGCGCTCACTGCCCGCTTCCAGTCGGGAAACCTGTCGTGC 4064

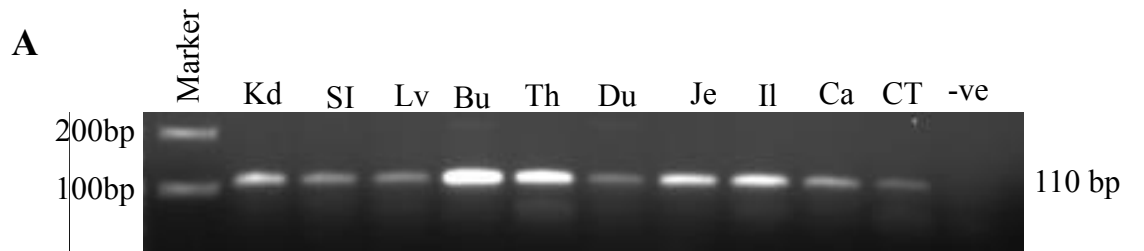
Query 457 CAGCTGCATTAATGAATCGGCCAACGCGCGGGGAGAGGCGGTTTGCCTATTGGGCGCTCT 516
          |||
Sbjct 4065 CAGCTGCATTAATGAATCGGCCAACGCGCGGGGAGAGGCGGTTTGCCTATTGGGCGCTCT 4124

Query 517 TCCGCTTCCTCGCTCACTGACTCGCTGCGCTCGGTCGTTCCGGCTGCGGCGAGCGGTA 573
          |||
Sbjct 4125 TCCGCTTCCTCGCTCACTGACTCGCTGCGCTCGGTCGTTCCGGCTGCGGCGAGCGGTA 4181

```

Figure 3.7 Sequencing and BLAST results of a putative IL-6 PCR product D7 Line X bird (caecum). 'Query' is the sequence analysed; 'Sbjct' is the NCBI database gene sequence.

To address this a new set of IL-6 primers (Table 2.3) were designed to cross the second and third exons, and used for the endpoint analyses. The expression of IL-6, using the new primers, in the Day 7 tissues including kidney, spleen, liver, bursa, thymus, duodenum, jejunum, ileum, caecum and caecal tonsil tissues is shown in Figure 3.8A. DNA sequencing indicated the authenticity of the amplified cDNA sequence (Figure 3.8B).



B

Gallus gallus interleukin-6 (IL6) mRNA, complete cds

Sequence ID: [gb|HM179640.1](#) Length: 762

Score	Expect	Identities	Gaps	Strand
204 bits(110)	1e-51	110/110(100%)	0/110(0%)	Plus/Plus
Query 1	CTTCGACGAGGAGAAATGCCTGACGAAGCTCTCCAGCGGCCTGTTTCGCCTTTCAGACCTA	60		
Sbjct 391		450		
Query 61	CCTGGAATTCATTCAAGAGACTTTCGATAGCGAAAAGCAGAACGTCGAGT	110		
Sbjct 451		500		

Figure 3.8 Panel (A): End point PCR for IL-6. kidney (Kd), Spleen (Sp), Liver (Lv), Bursa (Bu), Thymus (T) Duodenum (Du), Jejunum (Je), Ileum (Il), Caecum (Ca), and Caecal tonsils (CT) of LH, Day 7 birds. Marker is a 100 bp-1000 bp.

Panel (B): Sequencing and BLAST result for IL-6. Query represents the amplified and sequenced product. Sbjct is the NCBI database gene sequence. (PCR and BLAST Analyses performed by Dr. Catherine Mowbray, Newcastle University).

3.3. Real time PCR analyses of AvBD6, AvBD9, chicken galectin-3, IL-6 and TGFβ4 expression in line X bird tissues

The end-point PCR data supported expression of all the genes investigated in the Line X bird tissues. To allow direct comparisons between gene expression in the different tissues of D7 and D35 birds reared in the different environments ie (LH and HH) quantitative real-time assays were used.

3.3.1. qPCR assay development

Quantitative assays were developed for AvBD6, AvBD9 and IL-6 gene expression by Dr. Catherine Mowbray (Newcastle University). The housekeeping or reference genes SDHA and SF3A1 (chicken GEnorm kit, PrimerDesign, UK) were selected following GEnorm analysis of chicken RNA material and utilised throughout the study to normalise the expression data. The GEnorm analysis data is shown in Figure 3.9, and indicated that of the six housekeeping genes analysed in relation to gene expression in chicken tissues ie (GAPDH, YWHAZ, ACTB, UBC, SDHA & SF3A1). SDHA and SF3A1 had the lowest GEnorm M values, which reflected the stability of their expression. Normalization of all qPCR expression data was performed using the two stably expressed reference genes SDHA and SF3A1.

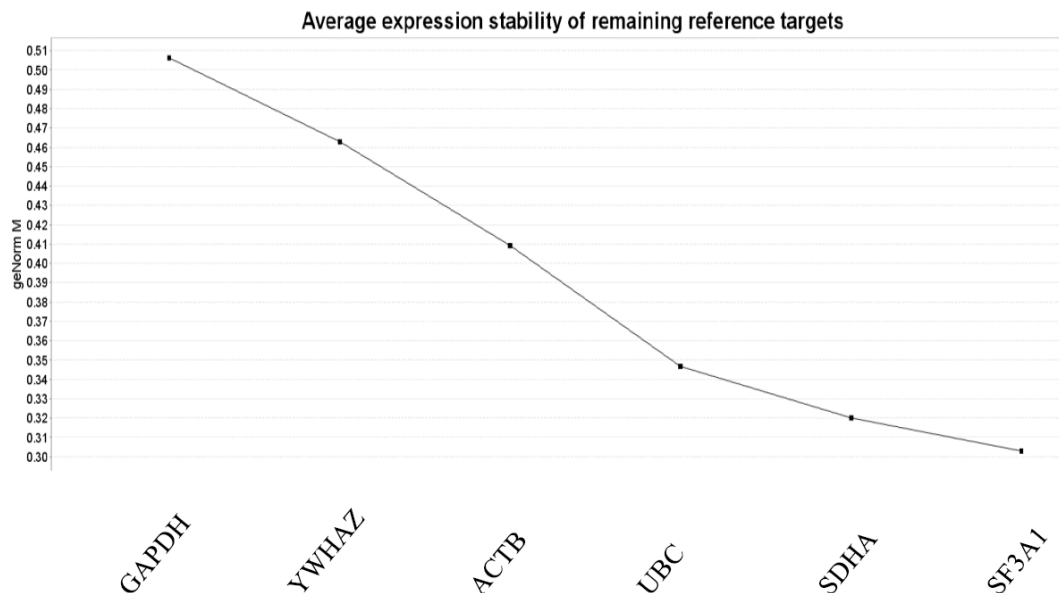


Figure 3.9 GeNorm analysis showing the most appropriate genes for real-time qPCR in avian tissues (Kevin Cadwell, 2014, PhD Thesis).

Quantitative assays for chicken galectin-3 and TGF β 4 were not available and were developed as follows. The amplification, melting and standard curves for chicken galectin-3 and TGF β 4 were constructed using 1:10 serial dilutions of the recombinant plasmids containing each of the targeted genes and a Roche Lightcycler 480 (Figures 3.10-3.15). To minimise errors, two curves were prepared for each dilution of the plasmid. The amplification curve relating to the highest concentration of plasmid relates to the lowest number of cycles while the curve relating to the lowest concentration of plasmid relates to the highest number of cycles (Figures 3.10 and 3.13). Melting curves represented by a single peak indicated the specificity of the primers (Figures 3.11 and 3.14). These data were supported by robust standard curves with the efficiency of the CG3 standard curve being 1.97 with error 0.02 (Figure 3.12) and the efficiency of that for TGF β 4 being 1.89 and error 0.02 (Figure 3.15).

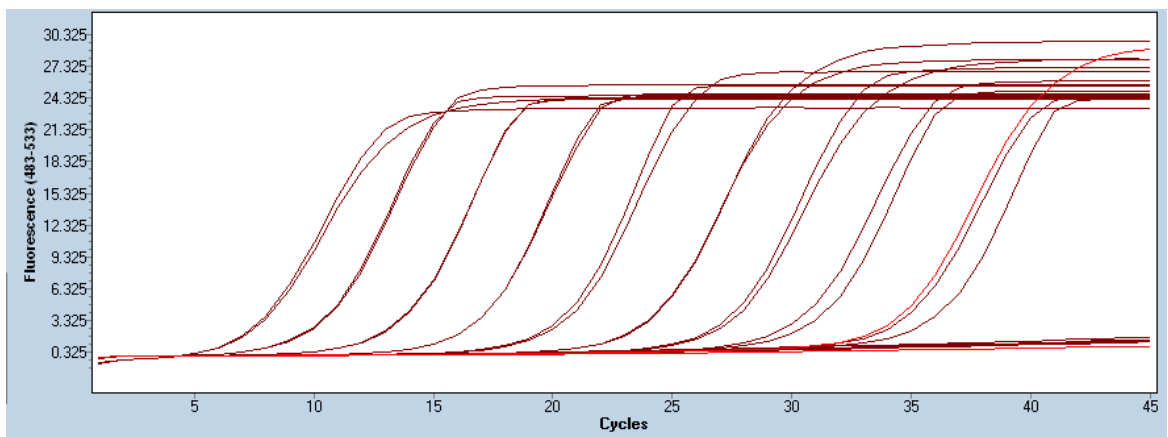


Figure 3.10 Amplification curves of diluted chicken galectin-3 plasmids. The dilutions of each plasmid relate to arbitrary units ie one gene cannot be directly compared to another.

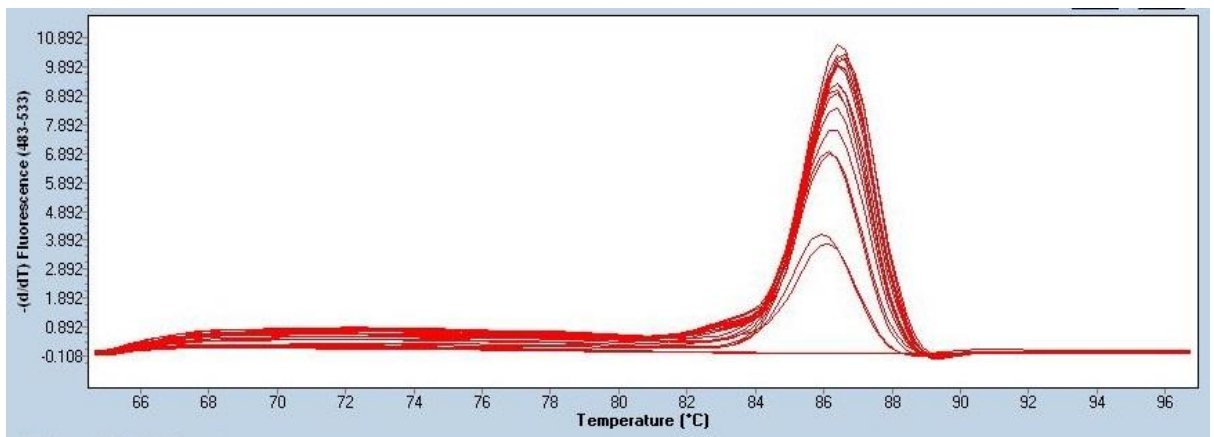


Figure 3.11 Melting curves for diluted chicken galectin-3 plasmids. The dilutions of each plasmid relate to arbitrary units ie one gene cannot be directly compared to another.

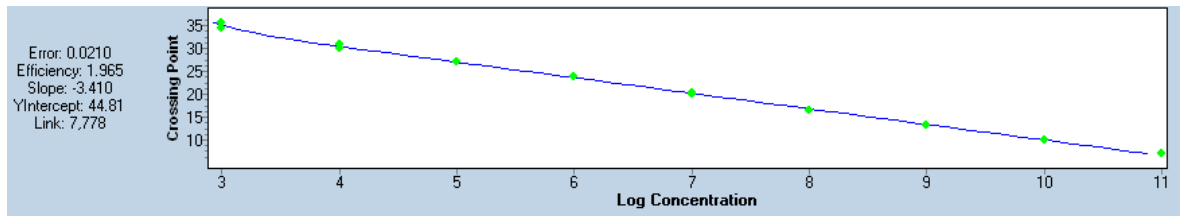


Figure 3.12 Standard curve of diluted chicken galectin-3 plasmids. Each green point represents a dilution of the plasmid. The dilutions of each plasmid relate to arbitrary units ie one gene cannot be directly compared to another

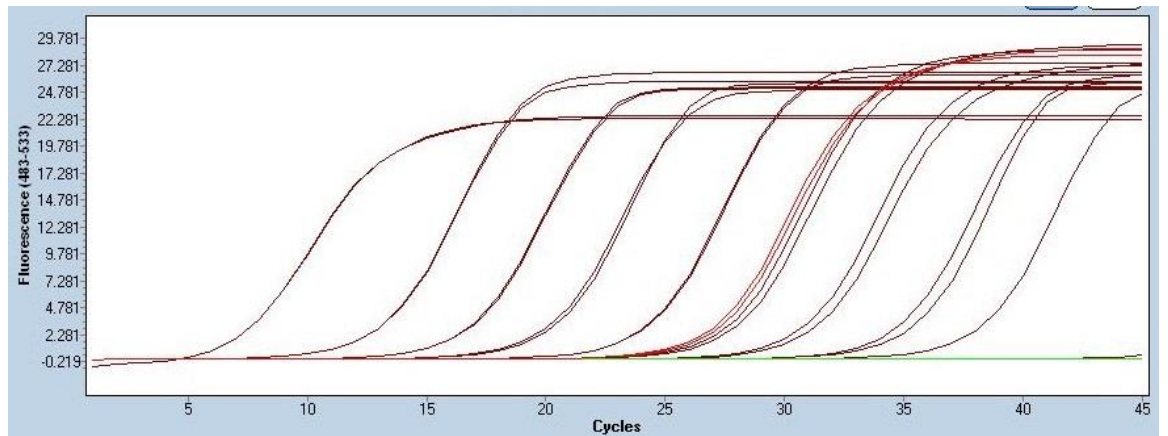


Figure 3.13 Amplification curves of diluted TGFβ4 plasmids. The dilutions of each plasmid relate to arbitrary units ie one gene cannot be directly compared to another

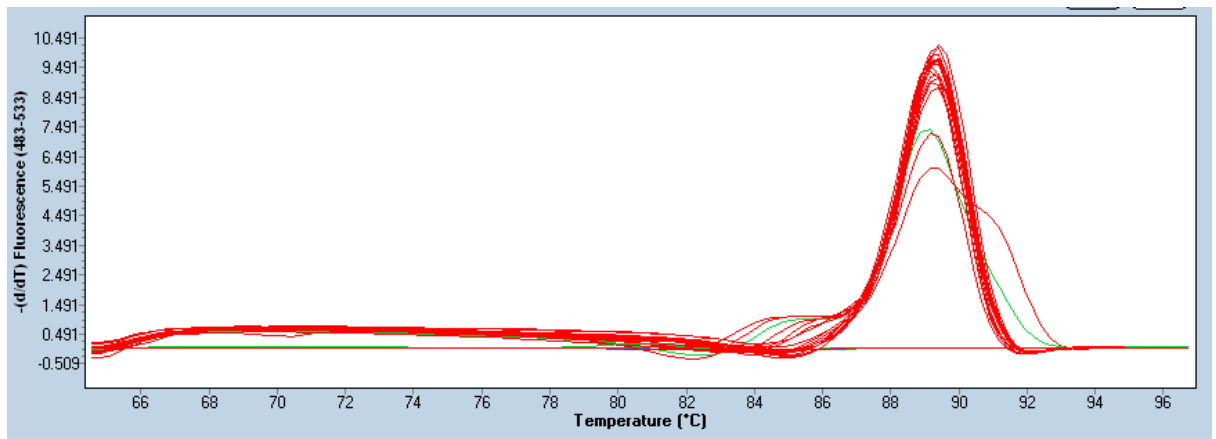


Figure 3.14 Melting curves of diluted TGFβ4 plasmids. The dilutions of each plasmid relate to arbitrary units ie one gene cannot be directly compared to another.

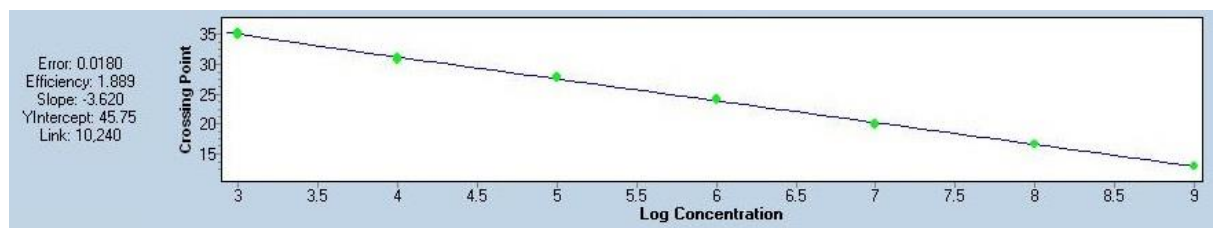


Figure 3.15 Standard curve of diluted TGFβ4 plasmids. Each green point represents a dilution. The dilutions of each plasmid relate to arbitrary units ie one gene cannot be directly compared to another.

3.3.2. Real time PCR

Using the standard curves and reference genes described real time PCR analyses were performed to quantify the tissue expression of AvBD6, AvBD9, IL-6, TGF β 4 and chicken galectin-3 gene (CG3). Gene expression was determined in Day 7 (D7) gut, liver, kidney and lung tissues, and Day35 (D35) liver, kidney and lung tissues excised from birds raised in either LH or HH conditions. Gut and lung tissues were chosen as these are exposed, directly, to microbes in the environment, while the liver and kidneys are exposed to microbial pathogen associated molecular patterns, or PAMPs, which include lipopolysaccharide and peptidoglycan.

3.3.2.1. AvBD6 mRNA expression by real time PCR

Figure 3.16 shows the AvBD6 expression data in relation to the gut, kidney, liver and lung tissues. In D7 birds raised in LH conditions, five samples relating to small intestine, caecal tonsils, kidney and liver were analysed, but only four samples relating to lung and three relating to caecum were available. In D7 birds raised in HH conditions five samples relating to liver were analysed but only four samples relating to kidney, lung and caecal tonsils and two tissues relating to small intestine and caecum were available. For D35 birds raised in both LH and HH, three samples relating to kidney, liver and lung were analysed.

The data sets were compromised by the small number of bird samples analysed and no statistically significant differences were found between AvBD6 expression in gut, kidney and lung tissues analysed from D7 and D35 birds raised in LH and HH conditions. However, liver AvBD6 expression (Figure 3.16C), was significantly suppressed ($p < 0.001$) in D7 compared to D35 birds raised in the HH environments. Additionally, liver AvBD6 expression was significantly reduced ($p < 0.01$) in D35 birds raised in LH compared to HH conditions.

The expression values were marked by their variability. For example in the small intestine and caecal samples, AvBD6 values ranged from 1 to 25 arbitrary units (AU), although one caecum value of 777 AU was recorded. Interestingly regardless of rearing environment the D7 gut data supported increased AvBD6 expression in the caecal tonsils compared to the small intestinal tissues ($p < 0.05$), which suggested a key role for the secondary lymphoid organ in the innate responses of the gut. In D7, AvBD6 expression values ranged from 6-125AU in kidney, 4- 28AU in liver and 48- 958AU in lung, with the two highest recorded values in kidney and lung respectively linked to the same bird. These individual variations

probably reflected the immune responses of individual birds to their different rearing environments. In D35, AvBD6 expression values ranged from 2-34 AU in kidney, 6-546 AU in liver and 47-307 AU in the lung.

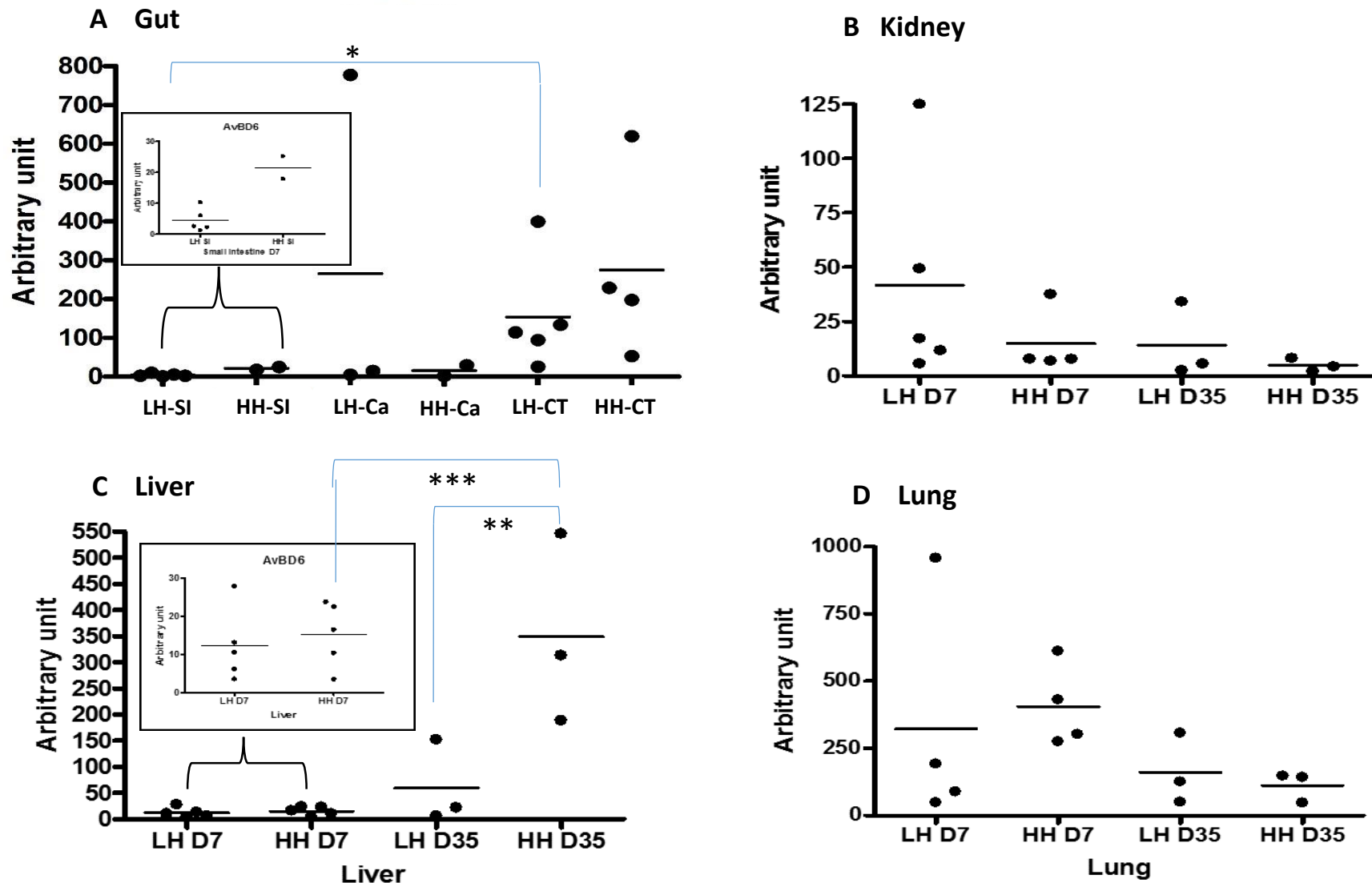


Figure 3.16 Dot plots showing AvBD6 expression in chicken tissues as measured by qPCR. Gut (A), kidney (B), Liver (C) and Lung (D). LH= low hygiene, HH=high hygiene. D7, D35= ages of the birds in days. SI=small intestine, Ca=caecum, CT= caecal tonsils, each black point represents an individual expression value. Solid lines show mean values. * $P < 0.05$, ** $P < 0.01$, *** $P < 0.001$. Data analysed by one way ANOVA, followed by Tukey's multiple comparison test.

3.3.2.2. AvBD9 mRNA expression by real time PCR

Figure 3.17 shows the AvBD9 mRNA expression data relating to bird gut, kidney, liver and lung tissues. As with AvBD6, the AvBD9 expression values recorded were marked by their variability. Unlike AvBD6 no patterns relating to AvBD9 expression were observed along the gut. Moreover, no statistically significant differences reflecting either bird age and/or rearing environment were identified apart from in the kidney where the expression values increased significantly ($p < 0.05$), with age and regardless of environment. What was interesting was the AvBD9 values recorded in the different tissues: in D7 bird tissues expression values ranged between 2- 30 AU in small intestine, 1-90AU in caecum, 1-32AU in caecal tonsils, but 20-841AU in lung, 85-802 AU in kidney and 34,511- 236,391AU in liver. In fact, the values in the liver were 10^5 times greater than those of the gut. Increased expression values were also seen in older birds. For example, in D35 birds, the expression levels ranged from 451-8,501 AU in kidney; 3,143-223,385 AU in liver and 74-263 AU in lung tissues.

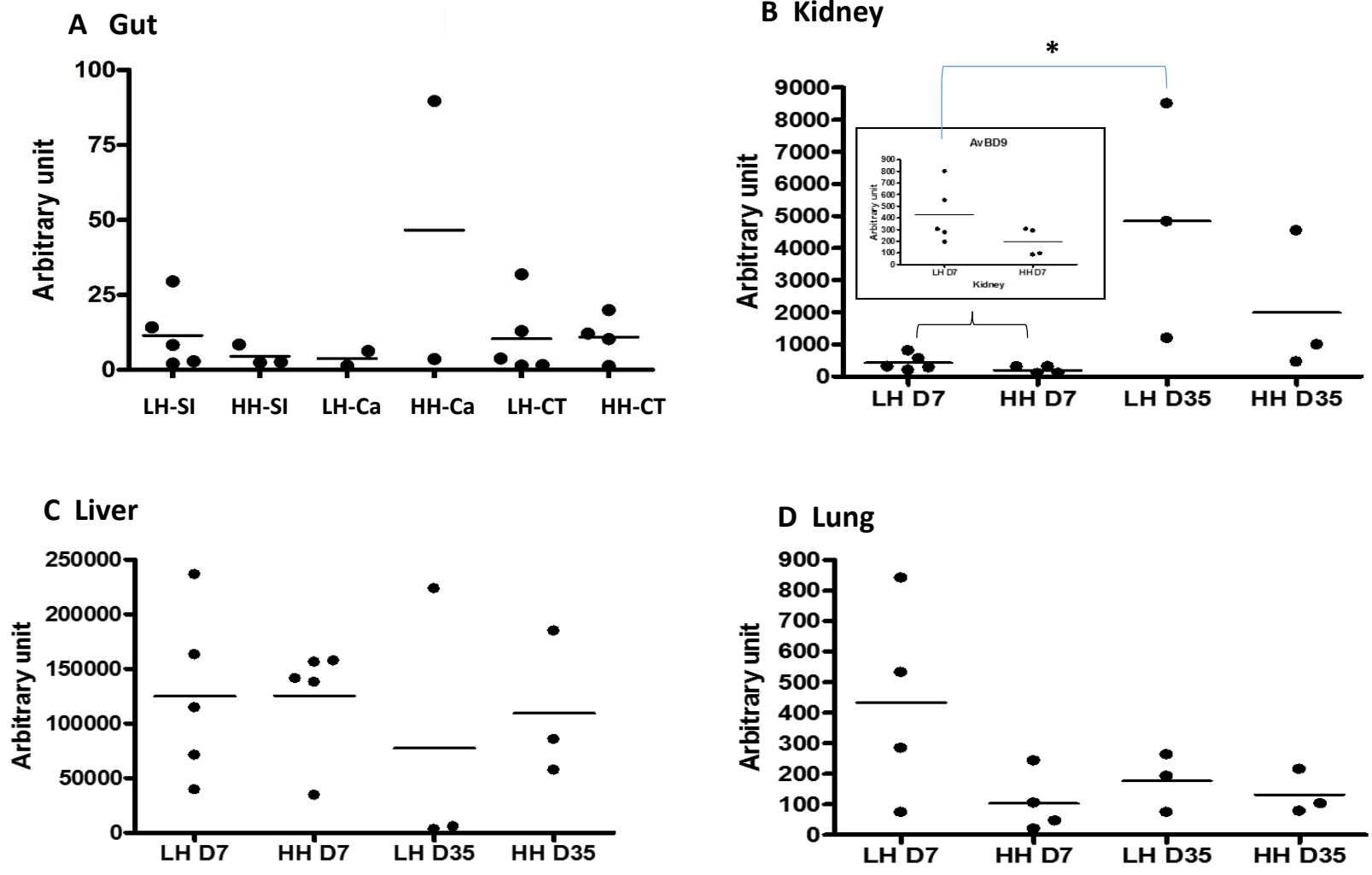


Figure 3.17 Dot plots showing AvBD9 expression in chicken tissues as measured by qPCR. Gut (A), kidney (B), Liver (C) and Lung (D). LH= low hygiene, HH=high hygiene. D7, D35= ages of the birds in days. SI=small intestine, Ca=caecum, CT= caecal tonsils, each black point represents an individual expression value. Solid lines show mean values. * P < 0.05. Data analysed by one way ANOVA, followed by Tukey's multiple comparison test.

3.3.2.3. Chicken galectin-3 mRNA expression by real time PCR

The chicken galectin-3 (CG3) gene expression data are shown in Figure 3.18 A-D. In the D7 birds studied CG3 small intestinal expression values ranged from 148-507 AU compared to 52-1242 AU in the caecal tissues and 127-2216AU in the caecal tonsils. The values were less variable in the other tissues ranging from 25-42 AU in the kidney, 12-58 AU in the liver and 23-76 AU in the lung. In tissues analysed from D35 birds, the expression values ranged from 34-424 AU in the kidney, 33-351 AU in the liver and 75-484 AU in the lung.

Although compromised by small sample numbers no distinctive patterns relating to CG3 expression were observed along the horizontal axes of the bird guts. However, the mean CG3 values recorded in both kidney and liver tissues were significantly increased ($P < 0.01$) in D35 birds compared to D7 birds reared in high hygiene conditions (Figure 3.18 B and C). Additionally, the mean CG3 expression values of both the kidney and liver tissues were significantly reduced ($P < 0.05$) in LH D35 reared birds compared to those reared in HH conditions. In contrast no significant differences were detected in the lung CG3 expression values (Panel D).

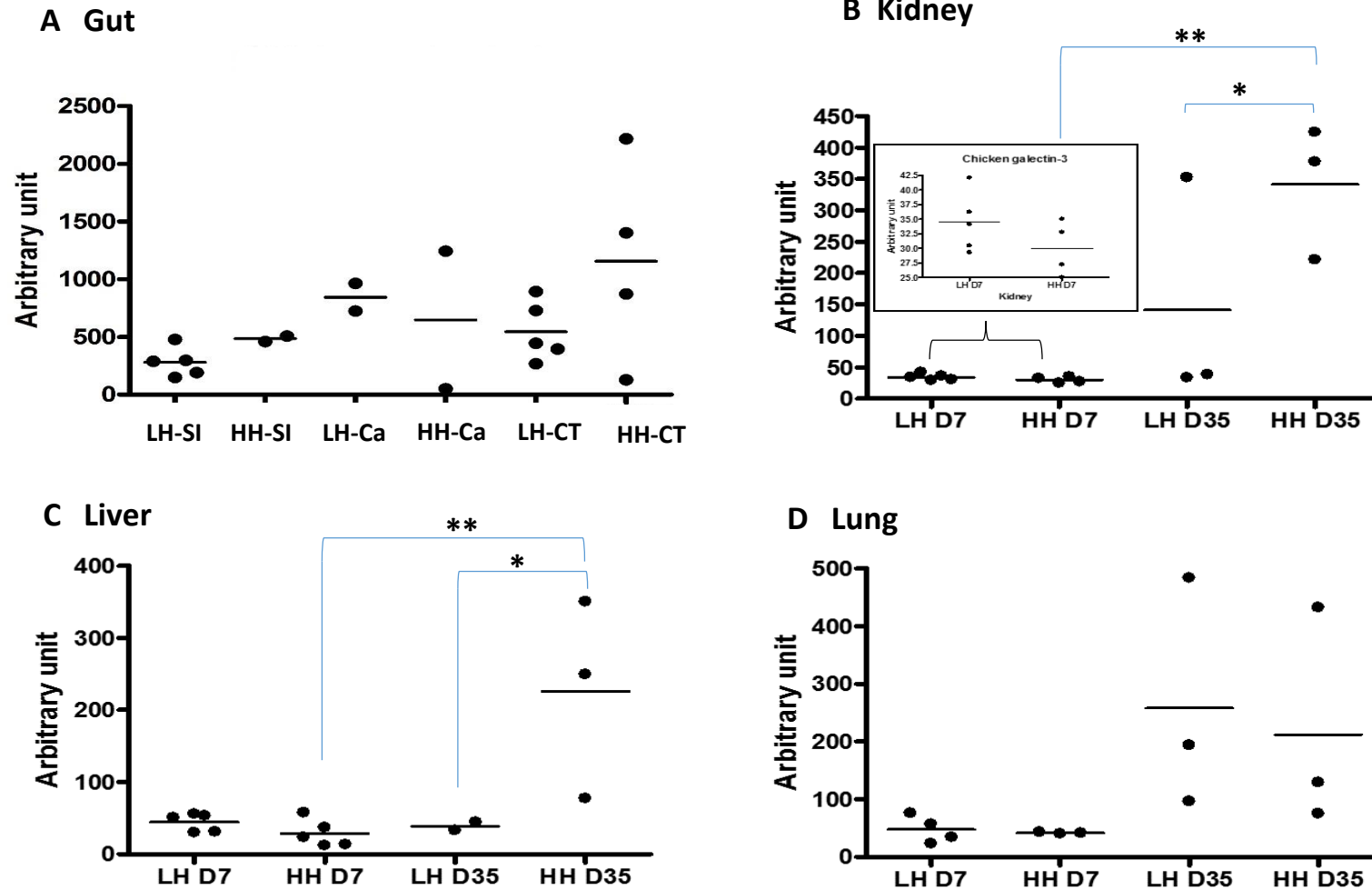


Figure 3.18 Dot plots showing CG3 expression in chicken tissues as measured by qPCR. Gut (A), kidney (B), Liver (C) and Lung (D). LH= low hygiene, HH=high hygiene. D7, D35= ages of the birds in days.SI=small intestine, Ca=caecum, CT= caecal tonsils, each black point represents an individual expression value. Solid lines show mean values. * $P < 0.05$, ** $P < 0.01$. Data analysed by one way ANOVA, followed by Tukey's multiple comparison test.

3.3.2.4.IL-6 mRNA expression by Real time PCR

Expression of the gene encoding the pro-inflammatory molecule IL-6 was also assessed and the data are shown in Figure 3.19. Again sample numbers meant that statistical analyses of the gut data was limited, although the mean value of IL-6 expression was significantly higher ($P < 0.05$) in the caecal tonsil samples of LH raised birds compared to the LH small intestinal samples (Panel A). There was also the suggestion of IL-6 expression being suppressed in the caecal tonsils of the HH raised birds although the LH data was skewed by one outlier value of 126 AU.

The panels B to D show IL-6 mRNA expression in the kidney, liver and lung tissues. No significant differences in expression were found between age equivalent LH and HH raised birds. However, in the kidney samples (Figure 3.19B), IL-6 was significantly increased in D35 birds compared to D7 birds reared in LH conditions ($P < 0.01$) and HH conditions ($P < 0.05$). Although not statistically significant similar patterns were identified for the liver and lung tissues.

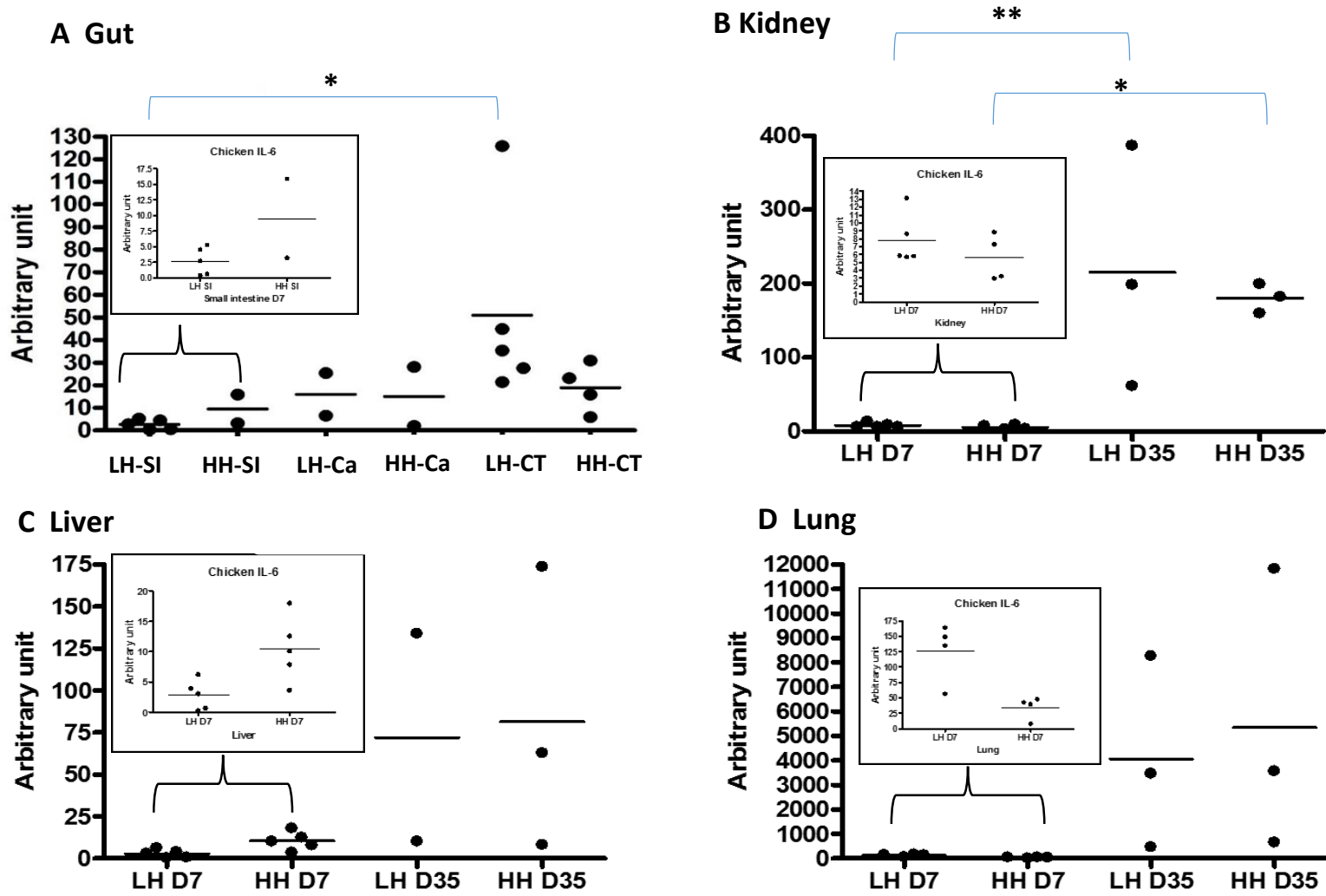


Figure 3.19 Dot plots showing IL-6 expression in chicken tissues as measured by qPCR. Gut (A), kidney (B), Liver (C) and Lung (D). LH= low hygiene, HH=high hygiene. D7, D35= ages of the birds in days.SI=small intestine, Ca=caecum, CT= caecal tonsils, each black point represents an individual expression value. Solid lines show mean values. * P < 0.05, ** P < 0.01. Data analysed by one way ANOVA, followed by Tukey's multiple comparison test.

3.3.2.5. TGFβ4 mRNA expression by real time PCR

Figure 3.20 shows the data relating to the expression of the TGFβ4 gene, which encodes an anti-inflammatory molecule. In the kidney a significant ($P<0.01$) age related response was detected with TGFβ4 mRNA expression being increased in D35 birds although this was limited to the HH raised birds. A similar, but non-significant trend ($p=0.057$) was suggested in the LH raised birds. There was also a significant increase ($P<0.01$) in TGFβ4 expression in the D35 HH raised birds compared to those raised in LH conditions.

Similar data were observed for the liver tissues, although the D35 LH versus HH data was skewed by a D35 LH value of 3431 compared to the other values of 156 and 189. In the lung (Figure 3.20 D), TGFβ4 mRNA was significantly increased ($P<0.01$) in D35 compared to D7 birds regardless of the rearing environment indicating an age effect.

The D7 TGFβ4 mRNA expression levels in the gut (Figure 3.20A) were comparable to those recorded in the liver, lung and kidney. Although compromised by the sample numbers there was a suggestion of increased TGFβ4 expression in the caeca ($P<0.01$) and caecal tonsils ($P<0.001$) of LH raised birds compared to the small intestinal tissue. Additionally, expression levels were reduced ($P<0.01$) in the caecal tonsils of HH compared to LH raised birds.

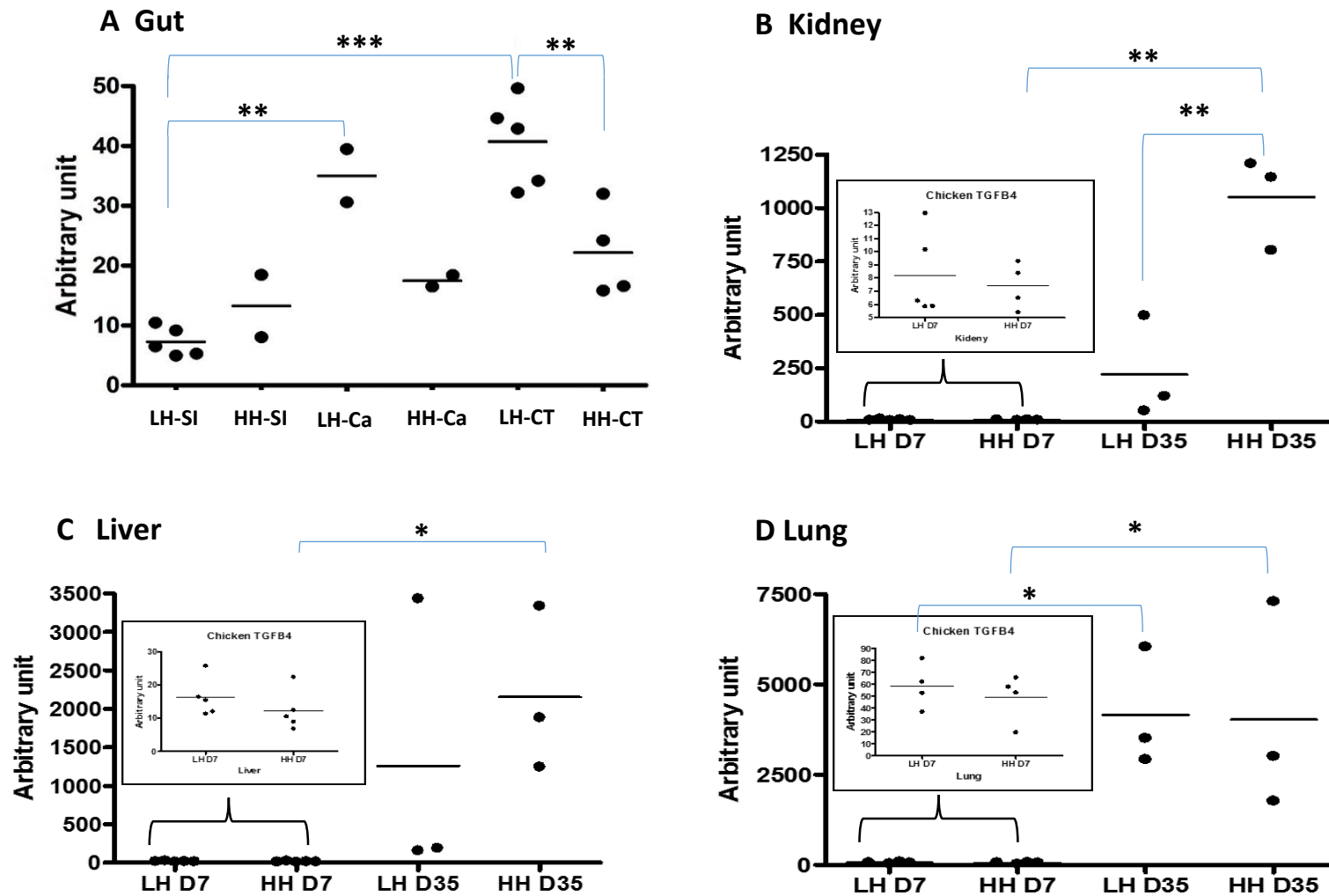


Figure 3.20 Dot plots showing TGFβ4 expression in chicken tissues as measured by qPCR. Gut (A), kidney (B), Liver (C) and Lung (D). LH= low hygiene, HH=high hygiene. D7, D35= ages of the birds in days. SI=small intestine, Ca=caecum, CT= caecal tonsils, each black point represents an individual expression value. Solid lines show mean values. * P < 0.05, ** P < 0.01, *** P < 0.001. Data analysed by one way ANOVA, followed by Tukey's multiple comparison test.

3.4. Immuno-histochemical examination of gut tissues:

The data presented indicated the expression of AvBD6 and 9 in the gut, kidney, liver and lung tissues. The major interest of this project was the gut tissues and to further explore the synthesis and localisation of the AvBD, and cytokines in the gut tissues, immunohistochemistry was performed. These analyses described in section 2.25 were performed in collaboration with Dr. Catherine Mowbray (PhD, Newcastle University). AvBD9 and IL-6 were selected for immunohistochemistry as examples of an antimicrobial peptide and pro-inflammatory cytokine.

3.4.1. Localisation of AvBD9 by immunohistochemistry

Fixed duodenal tissue sections from Line X D7 birds were stained with a custom synthesised AvBD9 antibody (Cambridge Research Biochemicals). The control and AvBD9 staining results are shown in Figure 3.21 A-D. AvBD9 immunoreactivity was localised to the enterocytic cells and the staining was intense on the brush border (Figure 3.21 B & C) and the luminal surfaces of the intestinal crypts (Figure 3.21 B & D) suggesting AvBD9 is synthesised by and involved in the defence of the gut epithelium.

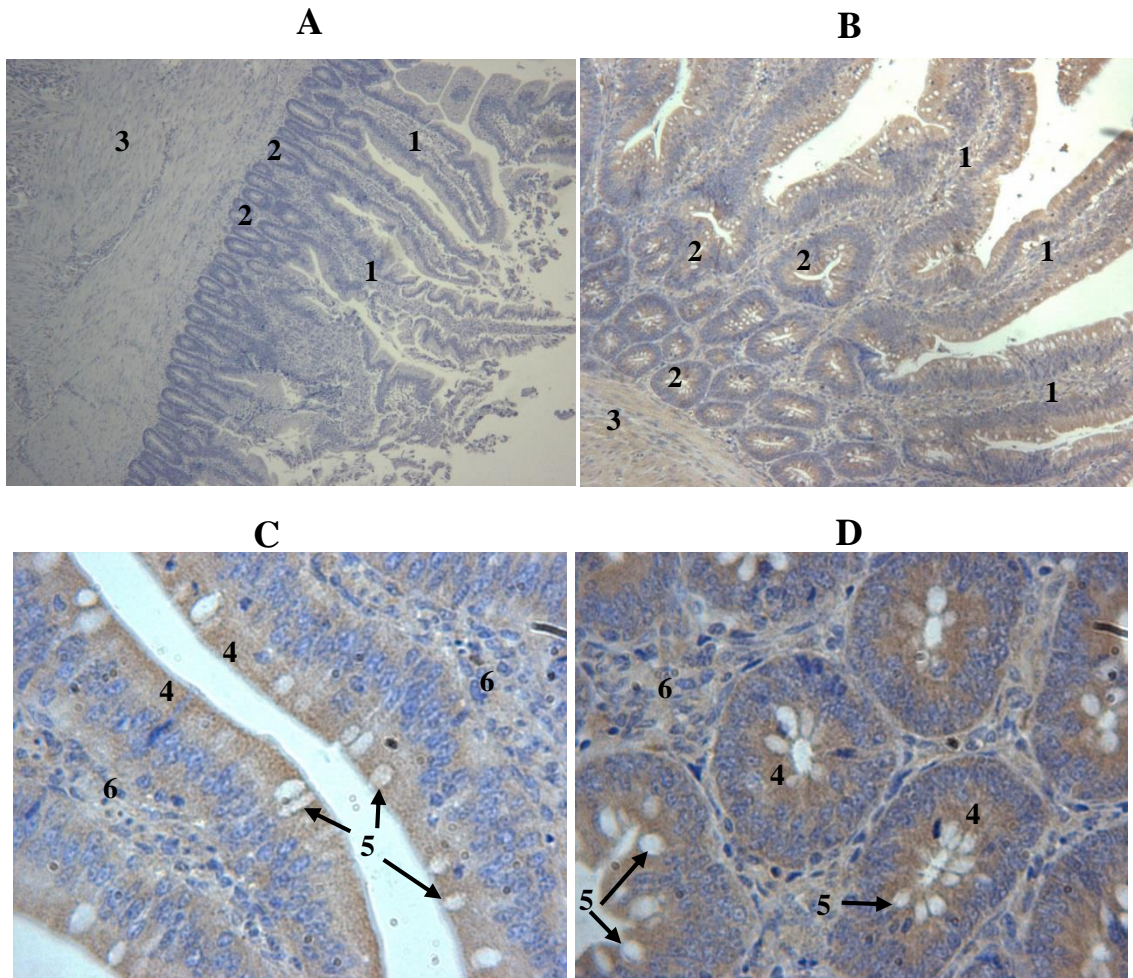


Figure 3.21 Immunolocalisation of AvBD9 in duodenal tissues from D7, Line X birds. Antibody was at 1:70 dilution in EDTA).

Negative control with no primary antibody (x40) (A); AvBD9 antibody (1:70 dilution in EDTA) immunostaining in duodenum (x100) (B); mucosal epithelium longitudinal section (x400) (C) and mucosal crypts with cross sections (x400)(D).

Mucosal villus (1), mucosal crypts (2), muscular layer (3), brush borders (4), goblet cells (5), lamina propria (6). (Dr. Catherine Mowbray, Newcastle University).

3.4.2. Immunolocalisation of chicken IL-6 in gut tissues

The duodenal tissues were also stained with rabbit poly clonal Anti-IL-6 antibody (Abcam) and the control and IL-6 staining results are shown in Figure 3.22 A-C.

Staining was comparable to AvBD9 with a more intense signal observed in the apical surfaces ie brush border and intestinal crypts of the epithelium. These data suggested that AvBD9 and IL-6 were synthesised and secreted from similar cells of the gut epithelium.

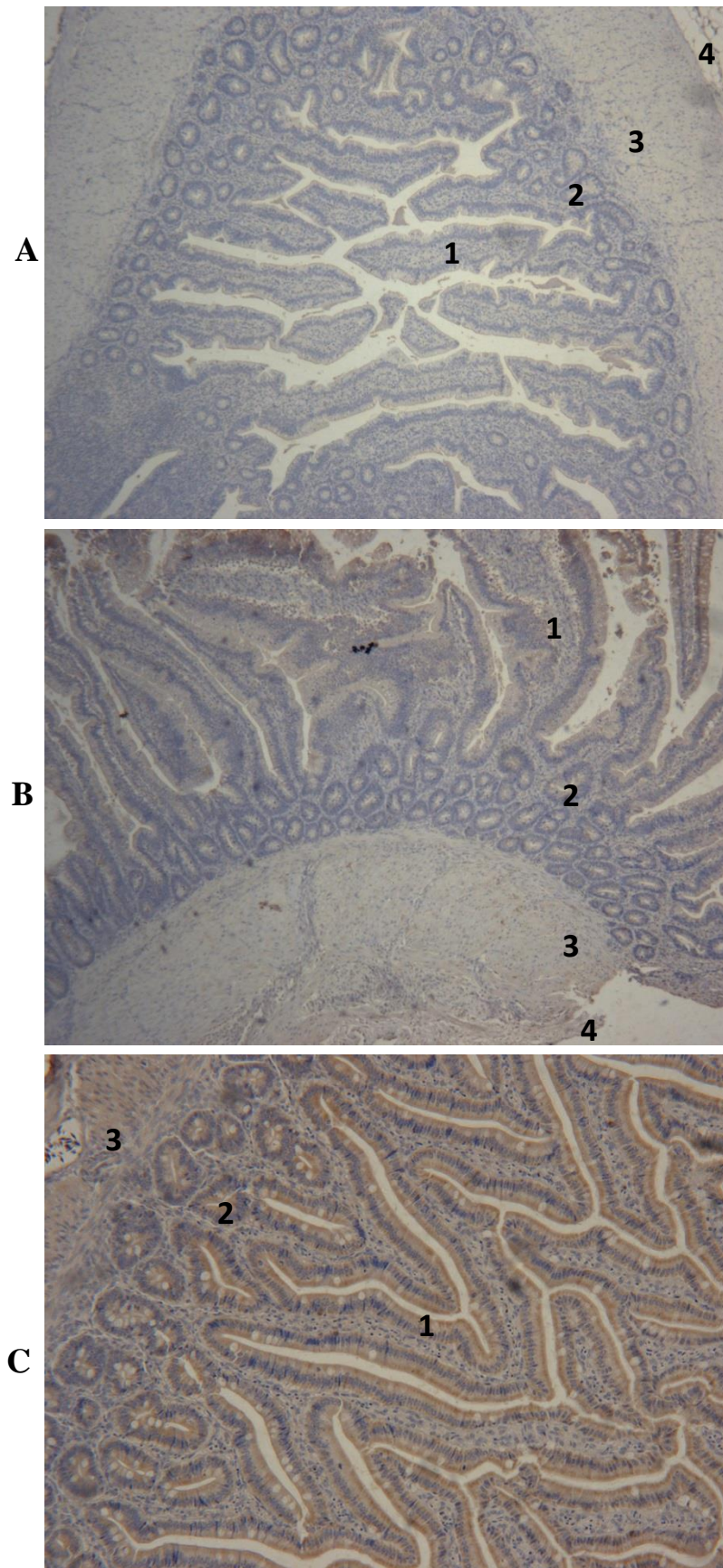


Figure 3.22 Immuno-localisation of IL-6 (dilution 1:120 in EDTA) in duodenal tissues from D7, Line X birds. Negative control with no primary antibody (X 40) (A); IL-6 immunostaining (x40 & x100) (B & C). Mucosal villi epithelium with brush borders (1), intestinal crypts (2), muscular layer (3) and serosa (4). (Dr. Catherine Mowbray, Newcastle University).

3.5. Discussion

The tissue samples analysed in this study were isolated from a line of genetically related chicken broilers with increased susceptibility to gut inflammation. The birds were originally raised in LH and HH environments with the premise that the environmental conditions would challenge the birds' immune systems and hence provide clues as to their susceptibility to inflammation.

The AvBDs are part of the innate immune response and therefore a first line defence mechanism in protecting epithelia from microbial assault. Previous studies had analysed the Line X bird tissues for AvBD1, 4 and 10 gene expression. It was found that expression of the AvBD1 and 4 genes was elevated in LH compared to HH conditions (Butler 2010, PhD thesis), although AvBD10 expression was not affected by the rearing environment. It was therefore decided to analyse these bird samples for AvBD6 and 9, IL-6, CG3 and TGF β 4 gene expression to explore whether there were specific patterns in the responses of the birds to their rearing environments. The hypothesis was that the gut epithelia of these birds would not be able to respond efficiently to the LH rearing conditions resulting in their increased susceptibility to inflammation.

There are 14 AvBD genes; the original choice to study AvBD 1 expression was directed by the presence of SNPs in Exon 1 of the gene coding sequence. These SNPs were not expected to affect expression per se, but it was hypothesised that they could affect the functionality of the encoded peptides and this is discussed further in Chapter 5 II. The choice of AvBD4 was directed by presence of a SNP in the 3'UTR of the gene, which it was hypothesised could impact on its expression. In this study the choice of the AvBD6 and 9 genes was again directed by the presence of SNPs although these were intronic for AvBD6 and intronic/3'UTR located for AvBD9 (Table 3.1). Thus the aim of this study was to extend the AvBD expression profile at Day 7 (D7) when the innate immune response of the young birds is key to their survival and at Day 35 (D35), when the adaptive immune system dominates to investigate if AvBD6 and 9 expression were compromised.

Initially endpoint PCR analyses of mRNA isolated from D7 bird tissues were performed and the results indicated that AvBD6 and AvBD9 were expressed in all tissues (thymus, liver, kidney, small intestine, caecum, caecal tonsils, lung, spleen, bursa and testis) of the D7 Line X birds. These results were comparable to data reported by others, but using different bird genetic lines and ages. For example, AvBD6 (Gal4) was expressed in the

small intestine, large intestine, bursa, lung, kidney and testis of Day 21 Cobb 500 broilers (Lynn *et al.*, 2004), in caecal tonsils of Day 1 ‘local hatchery’ chicks (Akbari *et al.*, 2008), and in lung tissues of Day 5 Goldline chicks (Milona *et al.*, 2007). Similarly AvBD9 expression was identified in the small intestine, caecum, caecal tonsils, bursa, testis, kidney, liver, thymus, lung, and spleen of 6 week old Ross 308 broilers (van Dijk *et al.*, 2007), and the lung, kidney, spleen, testis, large intestine, but not small intestine of 21 day old Cobb 500 broilers (Lynn *et al.*, 2004). Furthermore, AvBD9 was expressed in Day 14 Chinese painted quail lung, small intestine, caecum, caecal tonsil, spleen and thymus tissues, but neither in liver nor kidney tissues (Wang *et al.*, 2010b). It is interesting that the intestinal expression of the genes appeared variable; eg AvBD9 was not identified in Cobb broilers (Lynn *et al.*, 2004), which may reflect the redundancy of the encoded peptide in the defence of the bird gut.

The end point PCR analyses were not quantitative so it was not possible to identify any differences or trends in expression between the LH and HH rearing conditions. To address this, quantitative PCR assays were developed with normalisation of the targeted gene data using the two housekeeping genes SDHA and SF3A1, which were the most appropriate of a panel tested for chicken tissue analyses (Figure 3.9). This contrasts to other studies where β -actin (Ma *et al.*, 2012a) or GAPDH (Sunkara *et al.*, 2014) were used for normalisations. However, analyses performed in this study indicated that the β -actin and GAPDH housekeeping genes showed significant variability and therefore was not used. Also the end point PCR analyses indicated 18S variability, which precluded the use of this gene in the qPCR analyses.

The quantitative PCR analyses were compromised by the small number of samples, but the data confirmed AvBDs 6 and 9 expression and suggested variability with outliers evident amongst the data (Figures 3.16 and 3.17). However, overall no significant effects of environment were observed on the gut (SI, caecal and CT) expression of the genes. It is possible that the individual variations in expression, particularly the outlier values, might be correlated to presence of the SNPs, including intronic SNPs affecting expression. This has been reported for human β -defensin1 with individuals carrying a 5’UTR homozygous polymorphism showing increased salivary peptide concentrations (Polesello *et al.*, 2015). However, there were no correlations that connected the samples eg in relation to AvBD6 the outlier related to a LH caecal sample, but no other gut samples relating to this bird were elevated. Additionally, the outliers observed in relation to lung and kidney expression (LH

environment) were also linked to different bird samples. This hinted at environmental rather than genomic effects although further investigation of all the genomic sequences of the birds is required to confirm this. In relation to AvBD9 gut expression there was one outlier that related to a HH caecal sample. Other 'high' expression values were recorded for the kidney, liver and lung tissues, but again there were no consistent patterns relating specifically to individual birds. The AvBD9 gene contains a SNP in the 3'UTR which potentially may affect expression through mRNA stability, as shown in sheep β -defensin 1 (Monteleone *et al.*, 2011). However, the majority of 'high' values were detected in the LH environment, and without any supporting genomic data it is impossible to state whether these values were due an environmental, genomic or an environmental/genomic effect. Thus the AvBD6 and 9 data contrasted to that of AvBD1 and 4 that showed elevated expression in D7 birds raised in LH compared to HH conditions.

AvBD6 and 9 expression values varied according to the actual tissue studied. For example in HH D7 kidney samples AvBD6 baseline expression was <50 AU compared to >250 AU in the lung. Similarly the AvBD9 baseline expression values were increased in the kidney and liver tissues compared to those of the lung and gut. Previous studies have also reported AvBD expression variability in different tissues (Meade *et al.*, 2009a; Wang *et al.*, 2010a; Ma *et al.*, 2012b; Ma *et al.*, 2013; Peng *et al.*, 2013; Lu *et al.*, 2014). In the lung the elevated AvBD6 baseline expression could have been linked to microbial exposure although the gut (apart from caecal tonsil) expression values, <50AU, do not support this. Similarly it is difficult to explain the higher baseline expression of AvBD9 in kidney and liver compared to the lung or gut using this argument. Multiple roles for mammalian defensins have been reported, including in wound healing and immunomodulation (Steinstraesser *et al.*, 2011; Semple and Dorin, 2012), but apart from the duck Apl_AvBD2 defensin, which has been shown to have chemotactic functions other immunomodulatory properties have not been described for avian peptides.

The data shown in Figure 3.16A showed that AvBD6 expression was particularly variable in the caecal tonsils compared to the caecum. The caecal tonsils are a pair of lymphoid nodules rich in both T and B lymphocytes, and suggested to play a role in the adaptive response through the production of antigen-specific antibodies (Casteleyn *et al.*, 2010). Data, shown in this study, indicate a potential role for this secondary lymphoid tissue in the innate defences of the chicken gut. In support it has been reported that infection of one-

day-old chicks with *Salmonella* serovar *Typhimurium* also increased AvBD6 as well as AvBD1, 2 and 4 expression in the caecal tonsils (Akbari *et al.*, 2008).

The AvBD expression data were compromised by the small number of samples, but generally no age related effects were observed. A significant increase in AvBD6 gene expression was observed in the D35 livers of the HH raised birds compared to D7, but an environmental effect was also observed in that increased liver expression was associated with the HH conditions. Why HH conditions should favour increased AvBD6 expression is difficult to explain, but it may indicate potential roles for the peptide in the physiology of liver cells. It has been reported that chicken liver expressed peptide 2 (cLEAP-2) mRNA expression is upregulated in liver and small intestine in response to salmonella infection indicating direct and systemic exposure (Townes *et al.*, 2004). The immunological properties of human LEAP-2 was also explored using *in vitro* cell lines modelling the liver and gut epithelia, and immunohistochemistry showed that the peptide has a role in innate immunity in response to lipopolysaccharides, and the peptide was localised in the epithelial cytoplasm (Howard *et al.*, 2010). A significant increase in AvBD9 expression was detected in the kidneys of the D35 LH raised birds compared to D7, but this was not observed in the HH raised birds. This is challenging to explain as the kidneys are not directly exposed to microbes although it may have reflected systemic exposure to microbial PAMPs including lipopolysaccharides that stimulate defensin expression pathway (Sadeyen *et al.*, 2004; Derache *et al.*, 2009a). Dietary factors including butyrate can also impact on AvBD9 expression (Sunkara *et al.*, 2014), but it is unlikely that these gut metabolites would be in sufficient concentration systemically to have caused a localised kidney effect.

As AvBD6 and 9 gut expression appeared unaffected in the birds despite the different rearing conditions the expression of genes encoding pro-inflammatory (IL-6) and anti-inflammatory (TGF β 4) molecules was explored. The gut microbiota interact naturally with the host epithelia resulting in physiological inflammation (Crhanova 2011), which involves the controlled synthesis of pro and anti-inflammatory cytokines. When this homeostasis becomes imbalanced pathological conditions, including chronic inflammation, result. The molecular data showed that IL-6 was expressed in the gut epithelia of the Line X birds and synthesis was supported by IHC. No significant differences in D7 gut IL-6 expression were observed that could explain the susceptibility of the birds to inflammation, although these data were again compromised by small numbers. Also the lack of D35 gut samples meant the long term effects could not be reported. Trends were observed in the D35 kidney, liver

and lung samples that supported increased IL-6 levels regardless of rearing environment but these increases were matched by TGFβ4 expression patterns, which overall supported a controlled and hence physiological inflammatory response.

The gut TGFβ4 expression patterns measured in the LH caecal and caecal tonsil tissues were interesting as these were reduced in the birds raised in HH conditions supportive of reduced inflammation. Although the sample numbers were small TGFβ4 gene expression was elevated in the caecal tissues of birds raised in LH compared to small intestinal tissues. Although not mirrored by the IL-6 data these TGFβ4 results may link to the increased microbial numbers residing naturally in the bird caecum.

In this study the LH reared birds were challenged by higher bacterial and coccidian loads than the HH birds (Butler, 2010). Interestingly in response to coccidiosis (*Eimeria maxima*) infection, IL-6 upregulation in chicken intestinal intraepithelial lymphocytes was reported while TGFβ4 expression was not changed (Hong *et al.*, 2006). Although these data relate to lymphocytes they do conflict with the results of this study. However, another report in which chickens were challenged with coccidian parasites, detected increased IL-6 expression only in older, 3 week old birds, suggesting age related effects (Zhang *et al.*, 2012).

Galectin-3 functions as an opsonin facilitating microbial destruction through attachment to the lipopolysaccharide (LPS) of the bacteria cell membrane and phagocyte surface glycoproteins (Almkvist and Karlsson, 2004). It also has chemo-attractive properties, attracting macrophages and stimulating monocyte migration (Sano *et al.*, 2000). In mice galectin-3 participates in the inflammatory process via degranulation of mast cell contents (Dhirapong *et al.*, 2009). Little is known of galectin's role in the avian gut although it has been reported to activate dendritic cells via glycan binding and toll-like receptors (de Geus and Vervelde, 2013; Van Crombruggen *et al.*, 2013). In the guts of D7 birds no significant differences in CG3 expression were observed despite the different rearing environments. It was noted that the baseline CG3 expression levels were elevated compared to other tissues supporting a link between gene expression and microbial presence.

AvBD9 synthesis was localised by IHC to gut enterocytes. There are few IHC studies showing AvBD localisation probably due to the lack of commercial antibodies and those published have focused on the reproductive tract. For example, the importance of AvBD3 in the protection of sperm presumably against infection before and after ejaculation has been reported (Shimizu *et al.*, 2008). Furthermore, positive staining for AvBD11 and

AvBD12 in the chicken epididymis and testis, suggests the production of these AvBDs in both organs (Watanabe *et al.*, 2011), although their functions require further clarification. Research has shown that mammalian host defense peptides synthesised in epididymis play roles in maturation of sperm and protection against infection (Dorin and Barratt, 2014). Immunostaining for gallin, an egg defensin, in the tubular glands and ciliated cells of magnum, and shell glands of the oviduct also supports the activity of this AMP in the egg white and shell to help protect the embryo against potential pathogens (Gong *et al.*, 2010). The chicken gut lacks Paneth cells (Nile *et al.*, 2004) and in the current study, synthesis and secretion of AvBD9 was detected in the intestinal crypts and brush borders (Figure 3.21). This supported the concept that enterocytes in the basal part of the crypts secrete the peptide to limit the invasion of the gut mucosa by both commensals and pathogens. In addition, the comparable localisation of IL-6 and AvBD9 in the gut suggest the peptides function collectively to control commensal numbers and help protect the gut epithelium from damage from potential pathogens.

3.6.Conclusions

Although the data were compromised by small sample numbers and variable expression real time PCR assay data showed the IL-6, TGF β 4, and CG3 genes were expressed in all bird tissues including the gut tissues. Overall no marked trends were detected and where elevated IL-6 tissue expression was detected this was matched by TGF β 4 suggesting physiological as opposed to pathological inflammation. Although only D7 data were available for the gut samples, AvBD6 and AvBD9 gene expression were detected in all samples examined with rearing environment having no significant effects on expression. These data, which suggested almost constitutive expression, contrasted to the AvBD1 and 4 data, and suggested the reduced importance of AvBD6 and 9 in the AvBD hierarchy in the protection of the gut. The original hypothesis was that the gut epithelia of these birds would not be able to respond efficiently to the LH rearing conditions resulting in their increased susceptibility to inflammation. The data reported did not support this hypothesis suggesting factors as yet unknown play a role in the pathology.

To date it is assumed that the AvBD6 and AvBD9 gene encoded products have antimicrobial activity. To explore this further the peptides were synthesised *in vitro* and their activity against Gram positive and negative bacteria examined.

Chapter 4

4. *In vitro* synthesis and analyses of the anti-microbial properties of AvBD6 and AvBD9 peptides

4.1. Introduction

Although the sample numbers were small the data presented in Chapter 3 confirmed the gene expression of AvBD6 and AvBD9, and AvBD9 peptide synthesis in Aviagen broiler chicken tissues including those of the gastrointestinal tract. Mammalian defensins are known, classically as host defence peptides due to their immunomodulatory as well as anti-microbial activities (Bowdish *et al.*, 2006). Compared to the mammalian defensins little is known about the properties of the AvBDs. However, AvBD expression and synthesis in the chicken gut tissues, populated naturally by microbes including commensals and potential pathogens, does suggest a key role for the AvBDs in the protection of the avian gut epithelium from potential microbial damage. Central to such a role is that the AvBDs exhibit bacterial killing or antimicrobial properties.

Mammalian α -defensins such as Human Neutrophil Peptide-1 (HNP-1) are synthesised containing a N-terminal pro-piece composed of 40 to 45 amino acids. This hydrophilic anionic peptide is proposed to function in subcellular sorting and peptide folding, and reduces the toxicity of the peptide during cell storage; proteolytic removal is essential for peptide activation (Wu *et al.*, 2003). AvBDs, like mammalian β -defensins, contain no or short pro-pieces and the functions of any of these small peptides remain unknown (Ganz, 2004; Cuperus *et al.*, 2013). The AvBD6 and AvBD9 primary amino acid sequences predict short pro-sequences comprising the amino acids GQPYFS and AYSQED respectively (Figure 4.1).

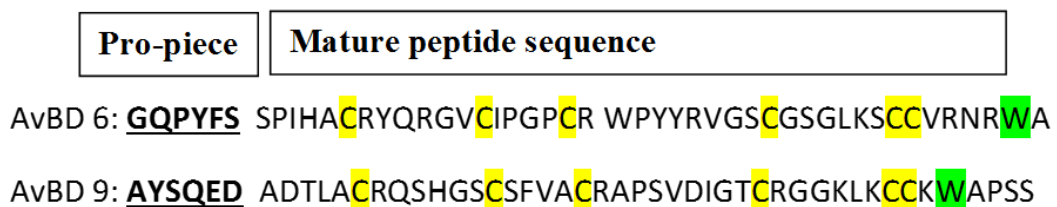


Figure 4.1 Amino acid composition of AvBD6 and 9 including pro and mature sequences. The pro- pieces are bold and underlined. Cysteines (Yellow); C-terminal tryptophan (Green).

This Chapter focussed on exploring the potential antimicrobial properties of AvBD6 and 9. To address this an *in vitro* approach was used in which recombinant AvBD peptides were produced and their antimicrobial properties studied using Gram negative and positive bacterial strains isolated from commercially reared broiler chickens. Recombinant AvBD6 and AvBD9 peptides were prepared that included and excluded the hexapeptide N-terminal pro-piece sequences. Defensin molecules are characterised by 6 C amino acids (Figure 4.1), which form three intramolecular disulphide bonds. To investigate the potential importance of the cysteine amino acids, variants of recombinant AvBD9 with either three or no cysteines were synthesised and used in the antimicrobial assays (AMAs). The family of AvBDs, apart from 8, 10, 12 and 13, all contain a C-terminally located tryptophan (Figure 4.1). Thus to determine the significance of this amino acid in the antimicrobial activity of the AvBD9 peptide a recombinant variant was synthesised lacking the C-terminal tryptophan and its AMA tested.

4.2. Recombinant AvBD synthesis

Initially the AvBD6 and 9 peptides were prepared as recombinant peptides using a GST hyper-expression system.

4.2.1. AvBD6 and AvBD9 cloning

Avian (Av) BD 6 and 9 cDNAs encoding both pro and mature peptides amplified from RNA isolated from D7 Line X birds and the expression vector pGEX-6P-1 were each digested with BamH1 and EcoR1 restriction enzymes (Figure 4.2A). After ligation of the cDNAs into the vector and transformation into *E. coli* DH5 α , recombinant colonies were selected and plasmid DNA prepared (Figure 4.2B). The cDNA inserts were confirmed by PCR (Figure 4.2C) and DNA sequencing (Figure 4.3).

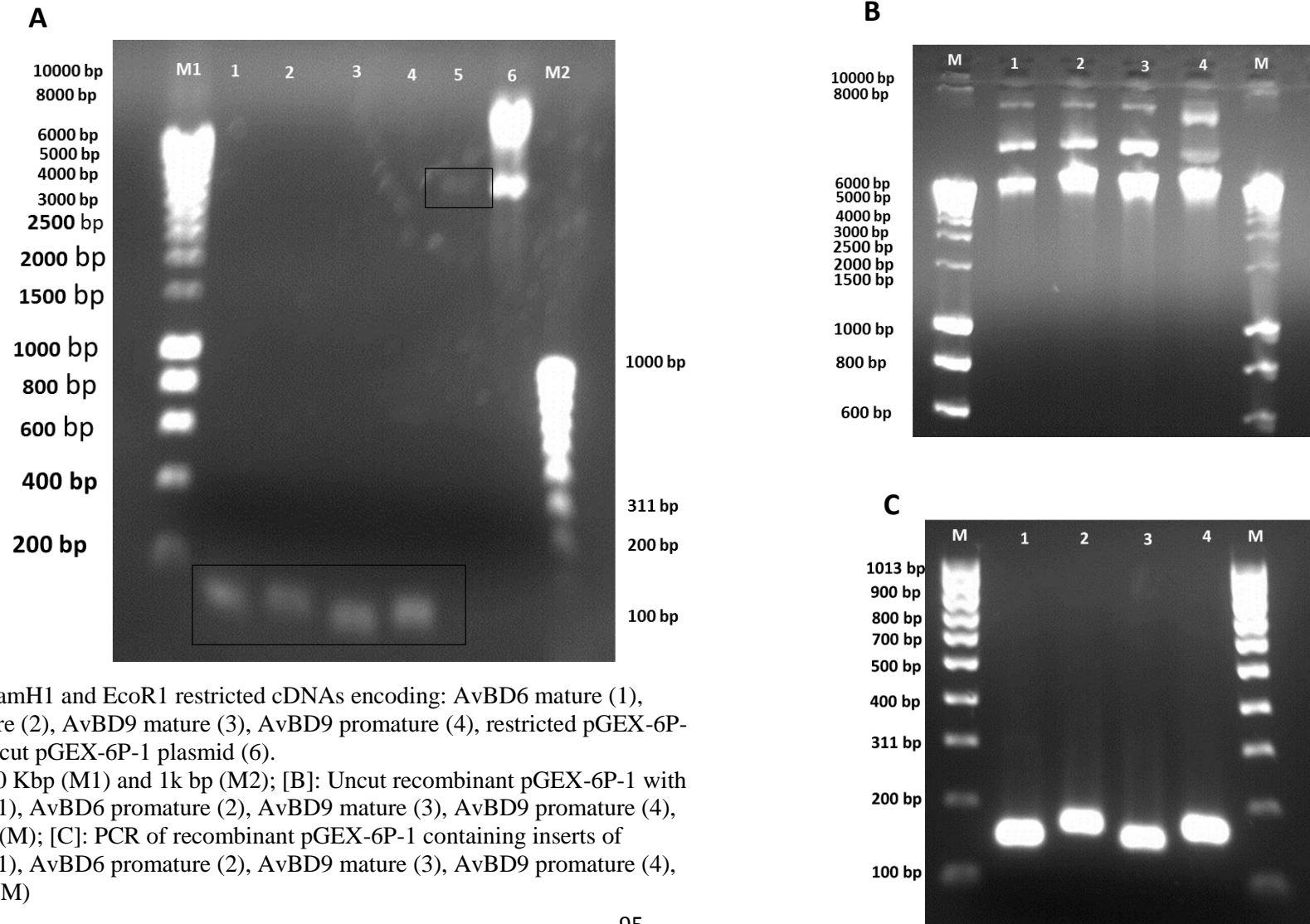


Figure 4.2[A]: BamH1 and EcoR1 restricted cDNAs encoding: AvBD6 mature (1), AvBD6 promature (2), AvBD9 mature (3), AvBD9 promature (4), restricted pGEX-6P-1 plasmid (5), uncut pGEX-6P-1 plasmid (6). DNA markers, 10 Kbp (M1) and 1k bp (M2); [B]: Uncut recombinant pGEX-6P-1 with AvBD6 mature (1), AvBD6 promature (2), AvBD9 mature (3), AvBD9 promature (4), Markers 10 Kbp (M); [C]: PCR of recombinant pGEX-6P-1 containing inserts of AvBD6 mature (1), AvBD6 promature (2), AvBD9 mature (3), AvBD9 promature (4), Markers, 1 Kbp (M)

gb|AY621308.1| **UGM** Gallus gallus beta-defensin 6 (GAL6) mRNA, complete cds
Length=502

A

Identities = 132/132 (100%), Gaps = 0/132 (0%)

```

Query 68  TCCAGCCCTATTCATGCTTGTAGATATCAAAGGGGTGCTGCATTCTGGGCCATGTCGG 127
          |||
Sbjct 153  TCCAGCCCTATTCATGCTTGTAGATATCAAAGGGGTGCTGCATTCTGGGCCATGTCGG 212

Query 128  TGGCCATATTACCGGGTTGGATCATGTGGCAGTGGACTAAAATCTTGCTGTGTGAGGAAC 187
          |||
Sbjct 213  TGGCCATATTACCGGGTTGGATCATGTGGCAGTGGACTAAAATCTTGCTGTGTGAGGAAC 272

Query 188  AGGTGGGCCTGA 199
          |||
Sbjct 273  AGGTGGGCCTGA 284
  
```

gb|AY621311.1| **UGM** Gallus gallus beta-defensin 9 (GAL9) mRNA, complete cds
Length=693

C

Identities = 128/128 (100%), Gaps = 0/128 (0%)

```

Query 67  CGCTGACACCTTAGCATGCAGGCAGAGCCACGGCTCCTGCTCTTTTGTTCATGCCGTGC 126
          |||
Sbjct 237  CGCTGACACCTTAGCATGCAGGCAGAGCCACGGCTCCTGCTCTTTTGTTCATGCCGTGC 296

Query 127  TCCTTCAGTTGACATTGGGACCTGCCGTGGTGGGAAGCTGAAATGCTGCAAAATGGGCACC 186
          |||
Sbjct 297  TCCTTCAGTTGACATTGGGACCTGCCGTGGTGGGAAGCTGAAATGCTGCAAAATGGGCACC 356

Query 187  CAGCTCCT 194
          |||
Sbjct 357  CAGCTCCT 364
  
```

gb|AY621308.1| **UGM** Gallus gallus beta-defensin 6 (GAL6) mRNA, complete cds
Length=502

B

Identities = 147/147 (100%), Gaps = 0/147 (0%)

```

Query 70  GGTACAGCCCTACTTTTCCAGCCCTATTCATGCTTGTAGATATCAAAGGGGTGCTGCATT 129
          |||
Sbjct 138  GGTACAGCCCTACTTTTCCAGCCCTATTCATGCTTGTAGATATCAAAGGGGTGCTGCATT 197

Query 130  CCTGGGCCATGTCGGTGGCCATATTACCGGGTTGGATCATGTGGCAGTGGACTAAAATCT 189
          |||
Sbjct 198  CCTGGGCCATGTCGGTGGCCATATTACCGGGTTGGATCATGTGGCAGTGGACTAAAATCT 257

Query 190  TGCTGTGTGAGGAACAGGTGGGCCTGA 216
          |||
Sbjct 258  TGCTGTGTGAGGAACAGGTGGGCCTGA 284
  
```

gb|AY621311.1| **UGM** Gallus gallus beta-defensin 9 (GAL9) mRNA, complete cds
Length=693

D

Identities = 145/145 (100%), Gaps = 0/145 (0%)

```

Query 62  GCCTTACAGCCAAGAAAGACGCTGACACCTTAGCATGCAGGCAGAGCCACGGCTCCTGCTCT 121
          |||
Sbjct 220  GCCTTACAGCCAAGAAAGACGCTGACACCTTAGCATGCAGGCAGAGCCACGGCTCCTGCTCT 279

Query 122  TTTGTTGCATGCCGTGCTCCTTCAGTTGACATTGGGACCTGCCGTGGTGGGAAGCTGAAA 181
          |||
Sbjct 280  TTTGTTGCATGCCGTGCTCCTTCAGTTGACATTGGGACCTGCCGTGGTGGGAAGCTGAAA 339

Query 182  TGCTGCAAAATGGGCACCCAGCTCCT 206
          |||
Sbjct 340  TGCTGCAAAATGGGCACCCAGCTCCT 364
  
```

Figure 4.3 Sequencing results of recombinant pGEX-6P-1 plasmid. It contains inserts of AvBD6 mature peptide (A), AvBD6 promature peptide (B), AvBD9 mature peptide (C), and AvBD9 promature peptide (D). ‘Query’ represents the amplified and sequenced products. ‘Sbjct’ relates to the NCBI database gene sequences. The black box shows the pro-peptide sequences (18 bp). Blue boxes indicate the partial sequence (s) of the restriction site, BamH1 (GGATCC).

4.2.2. Hyper expression of AvBD6 and AvBD9 peptide variants

The four AvBD6/9 recombinant plasmids were each transformed into *E. coli* BL21 (DE3) pLysS, grown to an OD₆₀₀ of 0.8 at 37 °C and expression induced for up to 3h by the addition of 1 M IPTG. Cell free extract (CFE) and pellet fractions were prepared as described in Section 2.17.

Figure 4.4A shows the synthesis of the AvBD6 peptides at 37 °C with the tagged GST peptides migrating at 31 kDa. All gels (a typical example is shown in [A]) showed more protein to be located in the pellet (lanes 2 and 4) than the CFEs (lanes 1 and 3), which suggested that at 37 °C the peptides were less soluble in the CFE. To try and address the AvBD6 solubility issues the bacteria were grown more slowly at 16 °C and 25 °C respectively (panel B), and induced using 0.1M IPTG, as opposed to 1M. These adjustments helped to improve the solubility of the recombinant peptides with the suggestion of increased protein identified in the CFE (Figure 4.4B lanes 5 and 7) compared to the pellet (lanes 6 and 8) fractions. A protein band of ~26 kDa was observed below the GST tagged AvBD6, which from its size was predicted to be GST protein due to proteolysis of the recombinant proteins.

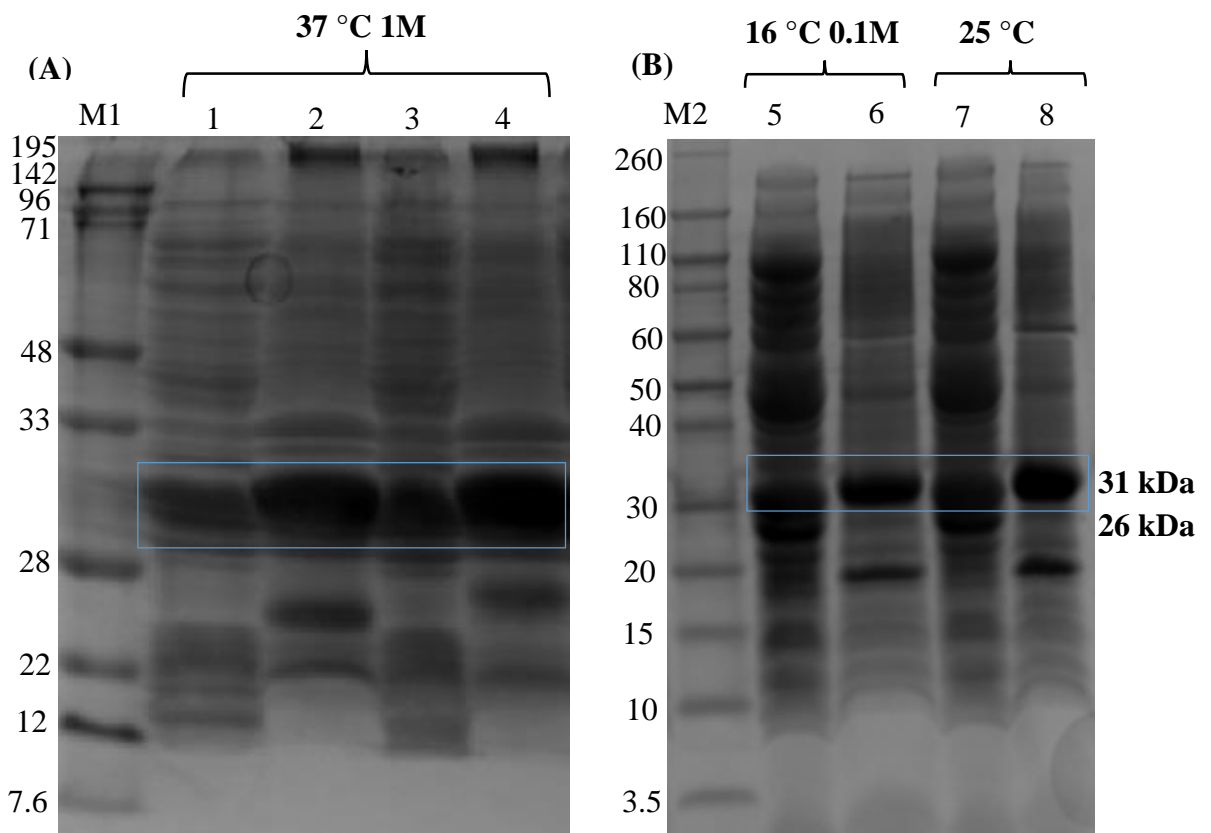


Figure 4.4 SDS PAGE (A) and NUPAGE (B) gels of recombinant pGEX-6P-1/AvBD6 induced by IPTG with 1M at 37 °C (A) and 0.1M at 16 and 25 °C (B), and stained with Instant blue. AvBD6 mature CFE (1, 5, and 7), AvBD6 mature pellet fraction (2, 6, and 8), AvBD6 promature CFE (3), and AvBD6 promature pellet fraction (4). ClearPAGE protein marker (M1) and Novex sharp prestained protein marker (M2).

AvBD9 peptide was also hyperexpressed. As shown in Figure 4.5 the 37 °C/1M IPTG conditions supported the synthesis of a 30.5 kDa soluble AvBD9 GST tagged protein. In fact the GST tagged AvBD9 peptide proved soluble using growth temperatures of either 37 °C or 25 °C (Panels A and B), with the suggestion of increased protein in the CFEs (lanes 1, 3 and 5) compared to the pellet fractions (lanes 2, 4 and 6).

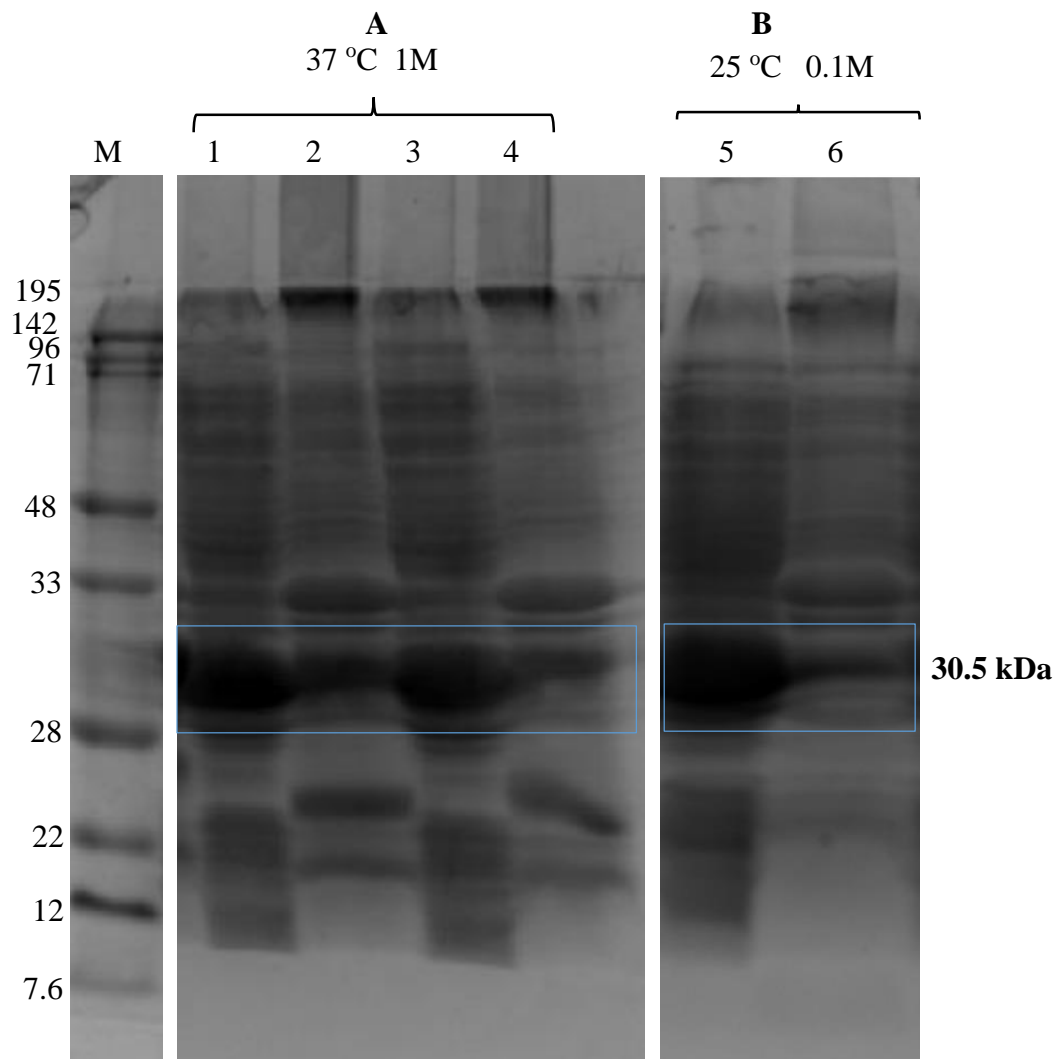


Figure 4.5 SDS PAGE gels of hyperexpressed pGEX-6P-1 BL21/AvBD9 induced by IPTG with 1M 37 °C (A) and 0.1M 25 °C (B), and stained with Instant blue.

AvBD9 mature CFEs (1 and 5), AvBD9 mature pellet fractions (2 and 6), AvBD6 promature CFE (3), AvBD6 promature pellet fraction (4). ClearPAGE protein marker (M1).

4.2.3. Purification of AvBD6 and AvBD9 peptides

Purification of the AvBD6 and 9 peptides was performed as described in Section 2.18. Two procedures were used: in the first the GST proteins were cleaved from the GST tagged AvBD peptides following elution of the tagged AvBD peptides from the CellThru 10-ml Disposable Columns (Clontech Laboratories, Inc.). This is termed ‘cleaving off the column’. In the second procedure the GST tags were cleaved while the peptides were still attached to the column resin. This is known as ‘cleaving on the column’.

4.2.3.1.Purification: cleaving off the column

Purification focussed initially on the AvBD9 peptide due to its increased solubility. The AvBD9 cell free extracts (CFE) (Figure 4.6, lanes 1 and 5) were applied to a glutathione resin packed CellThru column and the GST tagged AvBD9 peptides (30.5 kDa) eluted using Tris glutathione buffer (20 mM reduced L- Glutathione and 50 mM Tris base pH 8) (Figure 4.6, lanes 2 and 6). The GST tags were removed by incubating the tagged fusion protein (50 mg) with 0.5 mg of 3C protease enzyme (GST-tagged HRV 3C PreScission protease) in cleaving buffer (50 mM Tris-HCl, 150 mM NaCl, 1 mM EDTA, 1 mM DTT pH 7.5) overnight at 4 °C (lanes 3 and 7). Pure peptide was separated and collected using a 10 kDa Vivaspin column (Vivaspin 20 columns, GE Healthcare Life Sciences, UK), (lanes 4 (4.5 kDa) and 8 (5 kDa)). The purified peptides were desalted using PD-10 desalting columns (GE Healthcare life Sciences) to remove Tris glutathione buffer and concentrated by freeze-drying. Lyophilised AvBD9 peptide was reconstituted in sterilised molecular grade water when required. Removal of the cleaving buffer by desalting was necessary as the buffer chemicals interfered with the protein concentration measurements, which were performed using a QuantiPro™ BCA Assay Kit (Sigma Aldrich).

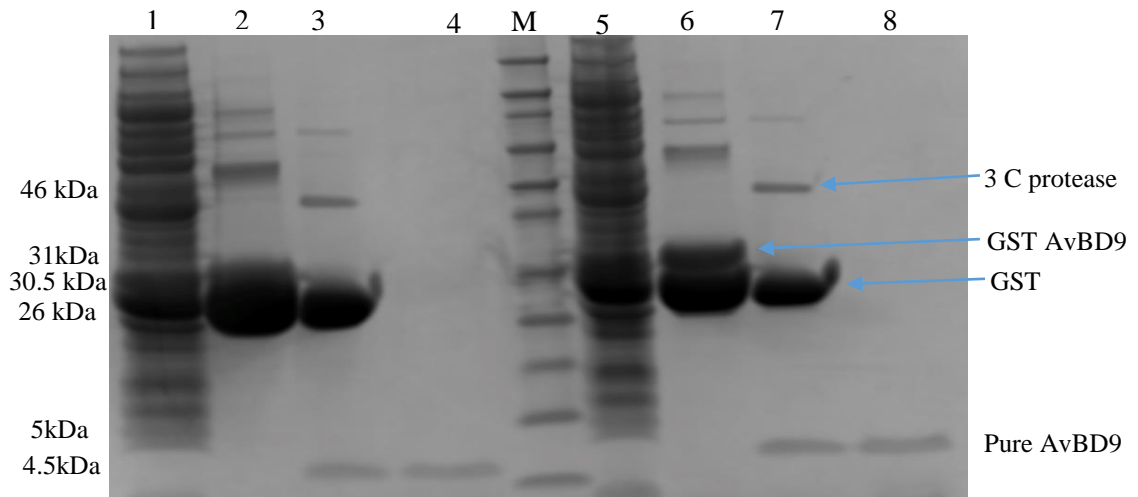


Figure 4.6 NUPAGE gel stained with Instant Blue showing AvBD9 purification (cleaving off the column). CFEs (1 and 5). GST tagged AvBD9 (2 and 6). GST cleaved by 3C protease (3 and 7). Pure AvBD9 (4 and 8). AvBD9 mature (1-4) and AvBD9 promature (5-8). Novex sharp prestained protein marker (M).

The purification procedures were repeated for AvBD6. However, using the ‘cutting off the column’ procedure, the yield of AvBD6 peptide was consistently poor as evidenced by the absence of pure peptide in Figure 4.7, lane 4. Therefore, to try and overcome the problem of poor yields a ‘cutting on the column’ procedure was used.

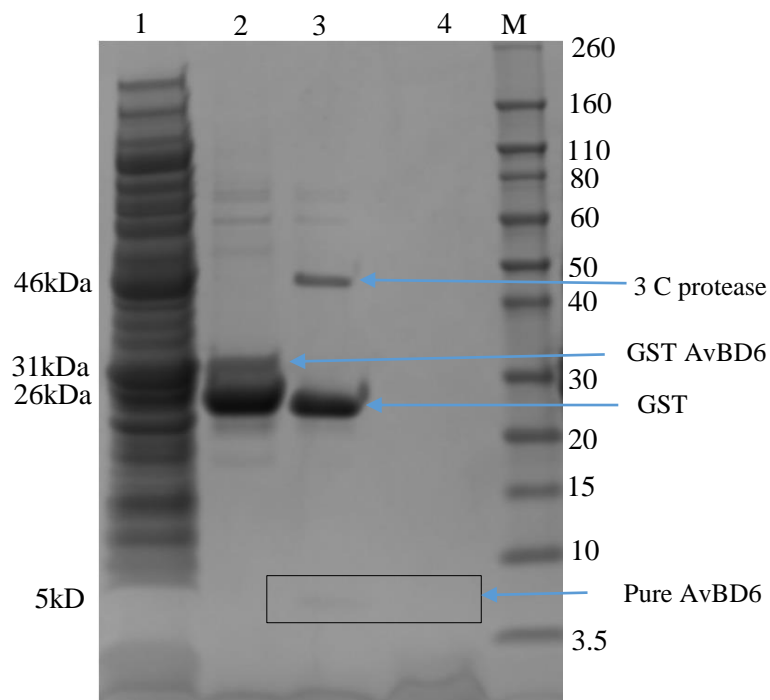


Figure 4.7 NUPAGE gel stained with Instant Blue showing AvBD6 purification (cleaving off the column). CFE (1). GST tagged AvBD6 (2). GST cleaved by 3C protease (3). Pure AvBD6 (4). Novex sharp prestained protein marker (M).

4.2.3.2. Purification: cleaving on the column

In this procedure, the CFEs containing GST tagged peptides on the glutathione resin packed CellThru were left overnight with 3C protease enzyme at 4 °C to allow cleavage on the column and then eluted with cleaving buffer. The eluent was applied to a 10 kDa Vivaspin column to facilitate separation of the GST, 3C protease and other bacterial proteins. The cleaving on the column procedure increased the yield and purity of the mature and promature AvBD9 peptides as shown in the NUPAGE gel, Figure 4.8. The data showed that the impure proteins were trapped at the top of the 10 kDa Vivaspin columns (Lanes 1 and 4). The pure AvBD9 peptides were desalted (section 2.18.2) to remove the Tris and EDTA of the cleaving buffer (Lanes 3 and 6), lyophilised and reconstituted with sterilised molecular grade water.

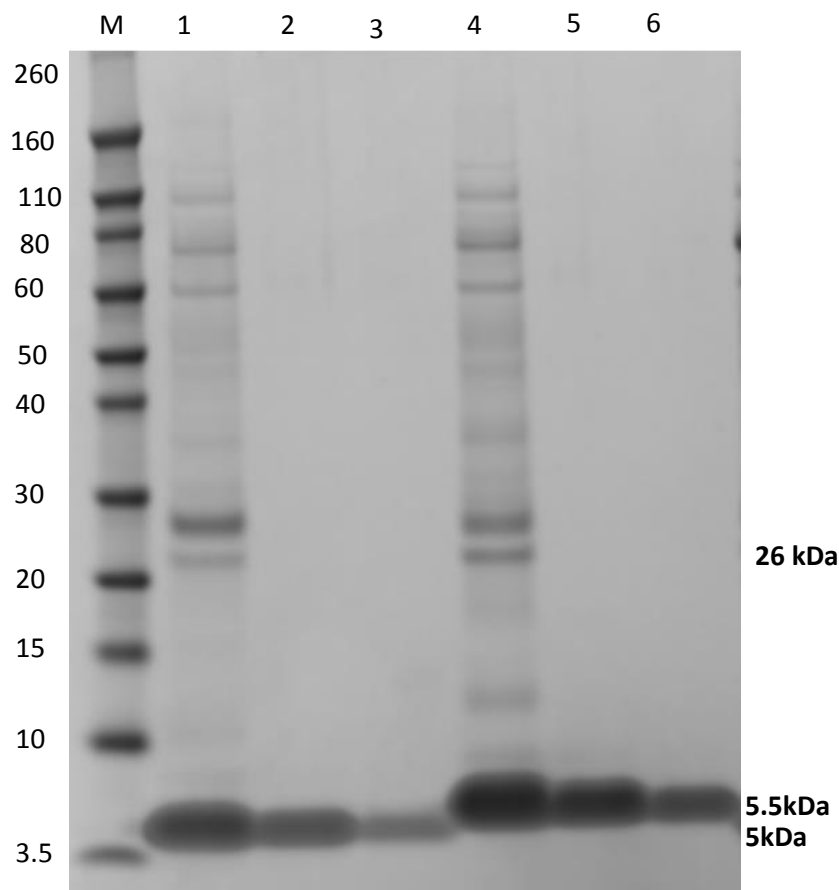


Figure 4.8 NUPAGE gel stained with Instant Blue showing AvBD9 purification (cleavage on the column).

The impure peptides removed by Vivaspin column (1 and 4). Pure AvBD9 in cleavage buffer (2 and 5). Desalted pure AvBD9 (3 and 6). AvBD9 mature (1, 2 and 3) and AvBD9 promature (4, 5 and 6). Novex sharp prestained protein marker (M).

The procedure was repeated using GST tagged AvBD6 promature and mature CFEs (Figure 4.9, lanes 1, and 5). As previously, the peptides and 3C protease were applied to the glutathione resin packed CellThru column, incubated overnight at 4 °C with 3C protease and the peptides eluted with cleaving buffer. Lanes 2 and 6 show the cleaved GST tagged peptides. The peptides were passed through 10kDa Vivaspin columns to separate the GST and 3C protease, but these procedures were unsuccessful with no pure peptide collected in the bottom of the 10kDa columns (lanes 4 and 8). These results suggested that most of the AvBD6 peptide was trapped on the Vivaspin column (Lanes 3 and 7).

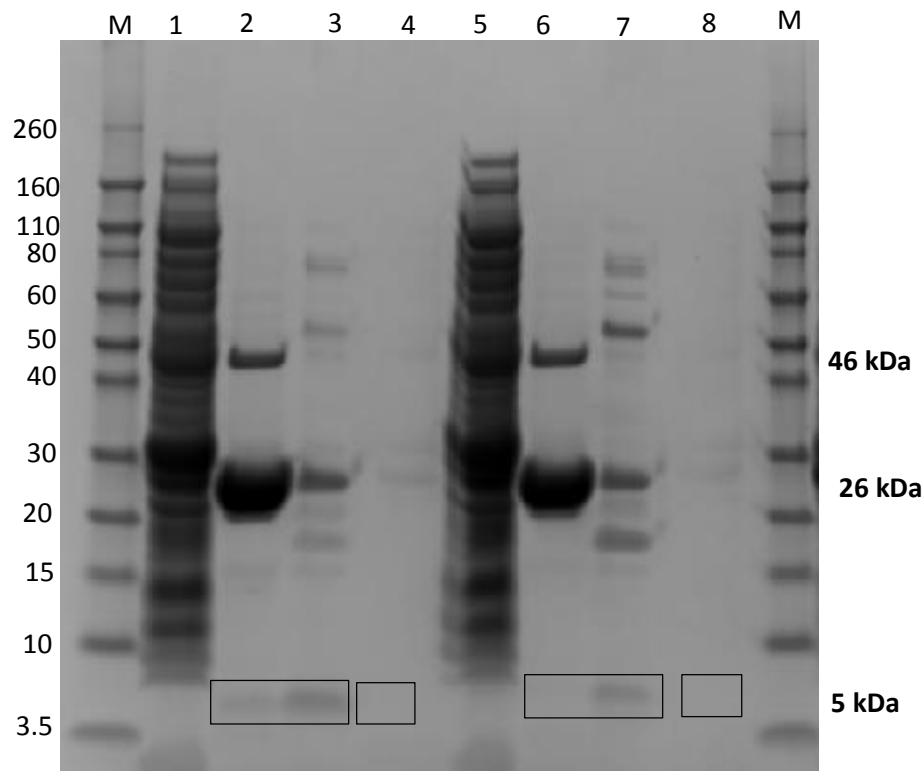


Figure 4.9 NUPAGE gel stained with Instant Blue showing AvBD6 purification (cleaving on the column).

AvBD6 mature (Lane 1-4) and AvBD6 pro (Lane 5-8). CFE (1 and 5). Cleaved GST tagged AvBD6 (2 and 6), GST, 3C protease and AvBD6 peptides trapped on the Vivaspin columns (3 and 7). Pure AvBD6 (5 and 8). Novex sharp prestained protein marker (M).

To address this problem the cleaved AvBD6 peptides were eluted from the resin packed CellThru column using 1x PBS, instead of the cleavage buffer. The idea was that both GST and 3C proteases remained attached to the resin and the cleaved AvBD peptides were eluted with PBS, removing the need for the 10 kDa Vivaspin and desalting steps. While the elution with 1x PBS increased the yield of peptides (Figure 4.10, lanes 3-7), the final purity of the peptides was reduced due to contamination with GST and 3C protease residues. However,

recognising the GST/protease contamination, the eluents from lanes 5, 6 and 7 were collected, freeze dried and when required reconstituted in sterilised molecular grade water.

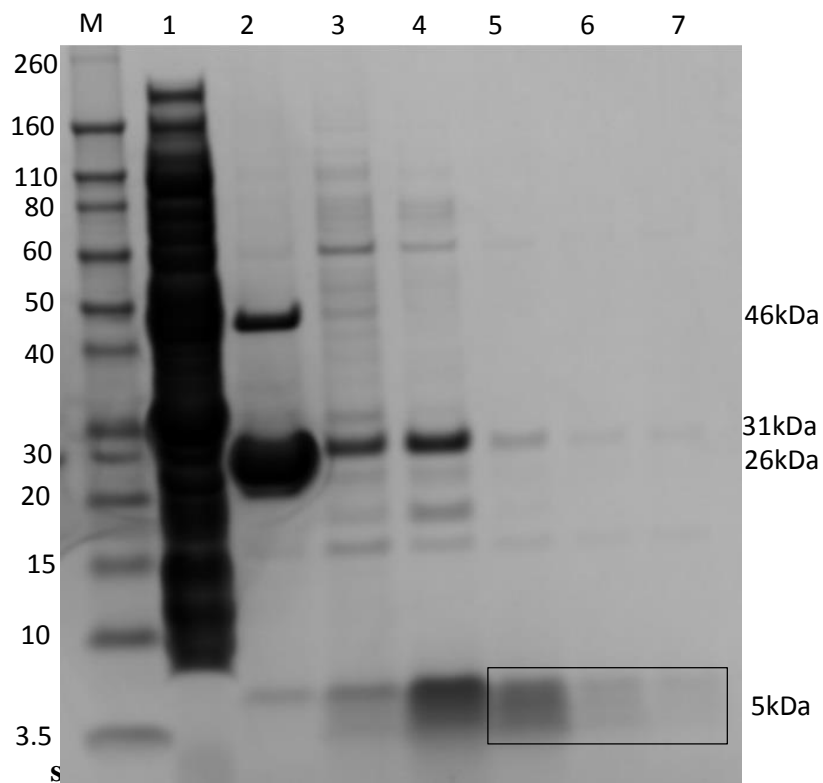


Figure 4.10 NUPAGE gel stained with Instant Blue showing AvBD6 purification (cleaving on the column eluting with PBS).

CFE (1). Cleaved GST tag from AvBD6 by 3C protease (2). Eluents with PBS (3-7). Novex sharp prestained protein marker (M).

The yield of pure lyophilised AvBD6 and AvBD9 variants was in the range 0.1 to 0.6 mg/L bacterial growth media.

4.2.4. MALDI TOF mass spectrometry

To ensure authenticity of the peptides the amino acid sequence of one purified peptide - AvBD9 (promature) - was analysed by peptide mass-spectrometry (York University) using CHCA, DHB and DAN matrices and these data are shown in Figures 4.11 A, B and C, respectively. The analyses resulted in a N terminal amino acid sequence of GPLGSAYSQEDADTLACRQSHGSCSFVACR with the pentamer GPLGS sequence representing the remaining residues of the GST tag (26 kDa) following cleavage, and the underlined hexamer the pro region. DHB matrix was used to reduce the number of salt and peptide adducts, and the data showed the derived sequence GPLGSAYSQEDADTLA at 1594.6 m/z (Figure 4.11 B). Other sequences (including QSHGSCSFVACR) were detected using DAN matrix and MALDI-In Source Decay (ISD) spectrum (Figure 4.11 C).

From the MALDI-MS/MS analyses (Figure 4.11 A) the single peak with the greatest deflection indicated a peptide with a mass of 5456.2 m/z, which supported the predicted mass of 5325.2 Da for the AvBD9 promature peptide. The multiple peaks shown in panel A were thought to be adducts of sodium ions or peptide components remaining in the sample during the purification processes.

Overall these data authenticated the AvBD9 promature peptide produced *in vitro* and it was inferred from these data that the primary amino acid sequences of all the other peptides produced *in vitro* were authentic.

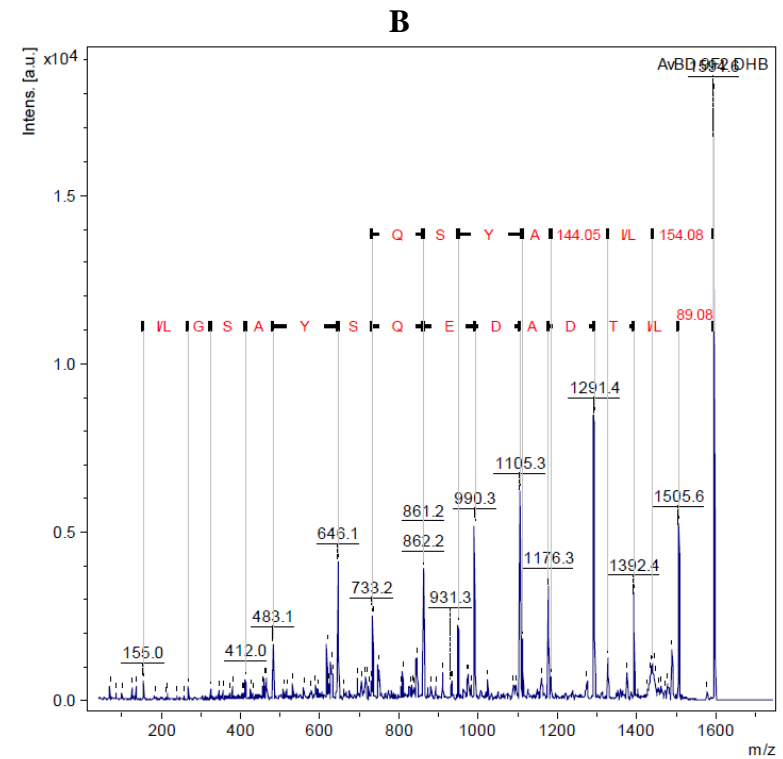
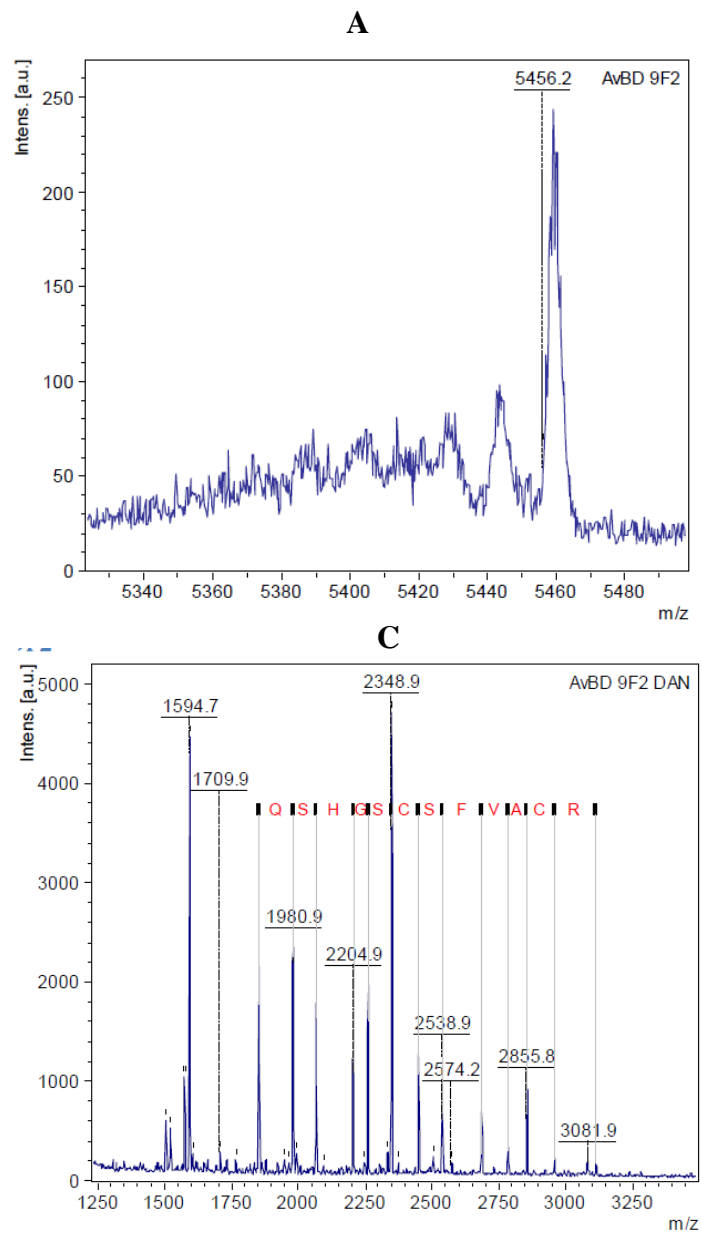


Figure 4.11 A sample of purified AvBD9 promature peptide analysed by MALDI-MS/MS using CHCA (A), DHB (B) and DAN matrices (C).

4.3. AvBD9 site directed mutagenesis

Once the purified peptides had been produced *in vitro*, the aim was to explore their antimicrobial activities (AMA). The amino acid sequences of the AvBDs, like all vertebrate defensins, are characterised by six cysteines. The AvBDs 1 -7, 9, 11, and 14 are also characterised by a distinctive C-terminal tryptophan (Figure 4.12).

Studies on the cysteines in the AMAs of the defensins have generated conflicting findings. Kluver *et al.* (2005), reported that mutating the cysteines in human (H) BD3 had no significant effects on its AMA (Kluver *et al.*, 2005). In contrast, more recent reports have indicated that mutagenesis of the HBD3 cysteines reduces the peptide's AMA properties presumably through conformational changes (Chandrababu *et al.*, 2009; Wanniarachchi *et al.*, 2011). Additionally, Maemoto *et al.* (2004) reported that mutagenizing cysteines of Crp4 (mouse α -defensin) increased its AMA, although they also reported that the peptide was more susceptible to proteolytic degradation (Maemoto *et al.*, 2004).

The literature is less confusing in relation to the roles of hydrophobic amino acids in defensin antimicrobial function. AvBD amino acid structures contain a number of aromatic hydrophobic amino acids (2-7 residues per mature peptide), and *in silico* and molecular site directed mutagenesis of the duck defensin Apl-AvBD2 has confirmed their importance in bacterial killing (Soman *et al.*, 2010). Tryptophan 26, located at the C-terminus of HNP-1, a mammalian α -defensin, has also been reported to be crucial for its activity, essentially directing interactions of the peptide with target molecules (Wei *et al.*, 2010). Thus it was hypothesised that the C-terminal tryptophan functions in the bacterial killing mechanisms of those AvBDs in which it is found.

To investigate the potential roles of the cysteine and tryptophan amino acids in AvBD9 antimicrobial activity, the cysteines and C-terminal tryptophan of the molecule were mutated using site directed (SD) mutagenesis to either glycines or alanines and the bacterial killing properties of the mutated peptides analysed. AvBD6 was not investigated because of the potential problems linked to peptide purification.

AvBD 1: MRIVYLLLPFILLLAQGAAGSSQALGRKSDCFRKS^{FC}AF^{LK}CPSLTISGKCSRFL^{LCKR}W^G

AvBD 2: MRILYLLSLLFLALQVSPGLSSPRRDML^{CK}GGSC^{HF}GG^{CS}HLIKVGS^{CF}FR^{SCCK}WP^{WNA}

AvBD 3: MKILYLLIPFFLLFLQGAAGTATQCRRIRGGFCRVGS^{CR}PHIAI G^{KCAT}FIS^{CC}GRAYEVDALNSV^{RTSP}WLLAPGNPH (no pro)

AvBD 4: MKIL^{CFF}IVLLFVAV^HGAVG^{FSRS}PR^{YH}MO^{CG}YR^{GT}FC^{TPG}K^{CP}HGNAYLGL^{CRPKY}^{CCR}WL

AvBD 5: MQILPLLFAVLLMLRAEPGLSLARGLPQDCERRGGFC^{SHR}SCPPGIGRIGL^{CKED}^{FCCR}SRWYS

AvBD 6: MRILYLLLSVLFVVLQGVAGQPYFSSPIHACRYQ^{RGV}CIPGP^{CR}W^{PYYR}VGS^{CG}SLK^{CC}VRNRWA

AvBD 7: MRILYLLLSVLFVVLQGVAGQPFIPRPID^{CR}LRNGI^{CF}PGI^{CRR}Y^WIGT^{CN}NGIGS^{CC}ARG^{WRS}

AvBD 8: MKILYFLLAVLLTVLQSSLGFM^{RV}PNNEAQCEQAGGIC^{SKD}H^{CF}HL^HTRAF^{GH}C^{QR}GV^{PCCR}TV^{YD}

AvBD 9: MRILFFLVAVLFFLQAAPAYSQEDADTL^{CR}QSHGSC^{FV}AC^{RAPS}V^DIGT^{CR}GG^{KL}^{CK}WAPSS

AvBD 10: MKILCLLFAVLLFLFQAAPGSADPL^{PD}TVAC^{RT}QGN^{FC}RAGAC^{PPT}FTISGQ^{CH}GGLLN^{CCA}KIPAQ

AvBD 11: MKLFSCLMALLLFLQAVPGLGLPRD^{TS}RCV^{GH}Y^CIRSKV^{CP}KPFAAF^{GT}CS^{WR}O^{KT}CC^{VD}TTSD^{FH}TC^QDKGG^{HC}VSP^{KIRC}EEQLGL^{CPL}KRW^{CC}KEI

AvBD 12: MRNLCFVFIFISLLAHGSTH^{GP}DS^{CN}H^{DR}GL^{CR}VGN^{CN}PEYLA^{KYCF}EPVIL^{CK}PLSPTPTKT (no pro)

AvBD 13: MRILQLLFAIVVILLQDAPARG^{FS}DSQL^{CR}NNH^{GC}R^{RR}L^{CF}H^{ES}WAGSC^{MN}GR^{LR}^{CCR}FSTKQP^{SNP}K^HS^VL^HTAE^{QD}PSPSLGGT

AvBD 14: MGIFLLFLVLLAVPQAAPESD^{TV}T^{CR}K^MK^G^KCS^{FL}^{CF}FK^{RR}SSGT^{CY}NGLAK^{CCR}PF^W (no pro)

Figure 4.12 AvBDs 1 – 14 primary amino acid sequences. Cysteines are highlighted (yellow), aromatic hydrophobic residues (green). Cationic (blue) and anionic (red). Underlined (propiece) which separate the signal sequence from mature sequence. Modified from xiao *et al.*, 2004 and NCBI website.

4.3.1. Mutagenesis of cysteine residues

The three cysteines (C1, C2 and C6) of AvBD9, shown in Figure 4.13, were proposed to be involved in disulphide bond formation, and to explore this further were each mutagenized to an alanine. This variant was named AvBD9 3CA and it was predicted that the alterations in sequence would cause disruption of the three di-sulphide bonds in the encoded peptide. The DNA sequencing results confirmed the SD mutagenesis had been successful (Figure 4.14 B-D). For the second construct (AvBD9 C6A/G) the remaining three cysteines (C3, C4 and C5) of AvBD9 3CA, were mutagenised to glycines (Figure 4.14 E-G).

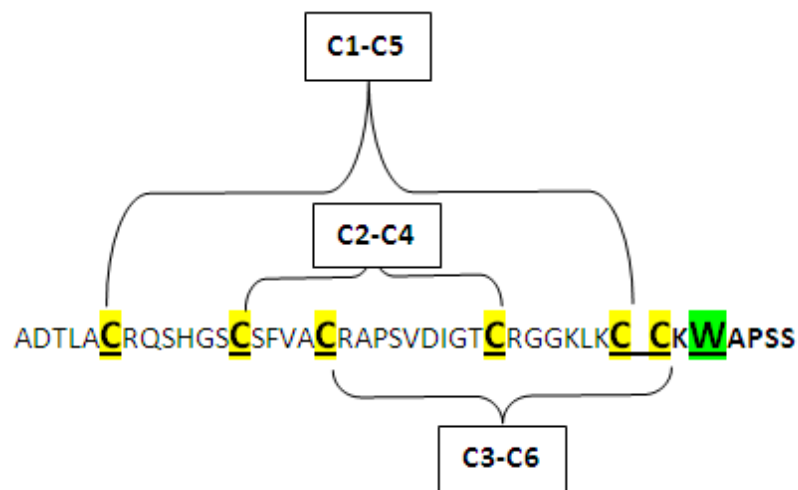


Figure 4.13: Suggested disulphide bond arrangement of AvBD9 between each three pairs of cysteines (C1-C5), (C2-C4) and (C3-C6)

4.3.2. Site directed mutagenesis of C- terminal tryptophan residue

To explore the role(s) of the C-terminal tryptophan in the AvBDs, Tryptophan number 38 [W38] of the AvBD9 mature amino acid sequence was mutagenised to glycine (Figure 4.14 panel H).

A AvBD9 mature

GAGGCCGTTTTGGTGGTGGCGACATCCTCAAATCGGATCTGGAAGTTCTGTTCCAGGGGCCCTGG
A D T L A C R Q S H G S C S F V A C R A
GATCCGCTGACACCTTAGCATGCAGGCAGAGCCACGGCTCTTGCTCTTTTGTTCATGCCGTGCT
P S V D I G T C R G G K L K C C K W A P S
CCTTCAGTTGACATTGGGACCTGCCGTGGTGGGAAGCTGAAATGCTGCAAATGGGCACCCAGC
S *
TCCTGAGAATTC CCGGGTCTGACTCGAGCGGCCGCATCGTGACTGACTGACGATCTGCCTCGCGCGTT

B AvBD 9 C1A Cysteine number 1 to Alanine

ACCAAAGTGTGGTGGTGGCGACATCCTCAAATCGGATCTGGAAGTTCTGTTCCAGGGGCCCTG
A D T L A A R Q S H G S C S F V A C R A
GGATCCGCTGACACCTTAGCA GCCAGGCAGAGCCACGGCTCTTGCTCTTTTGTTCATGCCGTGCT
P S V D I G T C R G G K L K C C K W A P S
CCTTCAGTTGACATTGGGACCTGCCGTGGTGGGAAGCTGAAATGCTGCAAATGGGCACCCAGC
S *
TCCTGAGAATTC CCGGGTCTGACTCGA

C AvBD 9 C1A C2A Cysteine number 1 and 2 to Alanines

TGGGCAGTTTTGGTGGTGGCGACATCCTCAAATCGGATCTGGAAGTTCTGTTCCAGGGGCCCT
A D T L A A R Q S H G S A S F V A C R
GGGATCCGCTGACACCTTAGCA GCCAGGCAGAGCCACGGCTCCGCCCTCTTTTGTTCATGCCGT
A P S V D I G T C R G G K L K C C K W A P
GCTCCTTCAGTTGACATTGGGACCTGCCGTGGTGGGAAGCTGAAATGCTGCAAATGGGCACCC
S S *
AGCTCCTGAGAATTC CCGGGTCTGACTCG

D AvBD 9 C1A-C2A C6A Three Cysteines to Alanines (AvBD9 3C A)

TGCCCAAGTTTTGTGTGGTGGCGAACATCCTCAAATCGGATCTGGAAGTTCTGTTCCAGGGGCCCT
A D T L A A R Q S H G S A S F V A C R
TGGGATCCGCTGACACCTTAGCA GCCAGGCAGAGCCACGGCTCCGCCCTCTTTTGTTCATGCCGT
A P S V D I G T C R G G K L K C A K W A P
GCTCCTTCAGTTGACATTGGGACCTGCCGTGGTGGGAAGCTGAAATGCCGCCAAATGGGCACCC
S S *
AGCTCCTGAGAATTC CCGGGTCTGACTCG

- E AvBD 9 C1A-C2A-C6A C4G Three Cysteines to Alanines. Cysteine 4 to glycine**
GGAGTCTTTTTGGTGGTGGCGACATCCTCCAAATCGGATCTGGAAGTTCTGTTCCAGGGGCCCTGG
A D T L A A R Q S H G S A S F V A C R A
GATCCGCTGACACCTTAGCA GCCAGGCAGAGCCACGGCTCCGCCCTCTTTTGTGTCATGCCGTGCT
P S V D I G T G R G G K L K C A K W A P
CCTTCAGTTGACATTGGGACCGGCCGTGGTGGGAAGCTGAAATGCGCCAAATGGGCACCC
S S *
AGCTCCTGAGAATCCCGGGTCTGACTCGA
- F AvBD 9 C1A-C2A-C6A-C4G -C3G Three Cysteines to Alanines. Cysteines 3 and 4 to Glycines**
AGGACCTTTTTGGTGGTGGCGACATCCTCCAAATCGGATCTGGAAGTTCTGTTCCAGGGGCCCTGG
A D T L A A R Q S H G S A S F V A G R
GGATCCGCTGACACCTTAGCA GCCAGGCAGAGCCACGGCTCCGCCCTCTTTTGTGTCAGGCCGT
A P S V D I G T G R G G K L K C A K W A
GCTCCTCAGTTGACATTGGGACCGGCCGTGGTGGGAAGCTGAAATGCGCCAAATGGGCA
P S S *
CCCAGCTCCTGAGAATCCCGGGTCTGACTCGA
- G AvBD 9 C1A-C2A-C6A-C4G -C3G-C5G Six Cysteines to Alanine/Glycines (AvBD9 6CA/G)**
TGAATTTTGATGCTGGCGACATCCTCCAAATCGGATCTGGAAGTTCTGTTCCAGGGGCCCTGGAT
A D T L A A R Q S H G S A S F V A G R A P
CCGCTGACACCTTAGCA GCCAGGCAGAGCCACGGCTCCGCCCTCTTTTGTGTCAGGCCGTGCTCCT
S V D I G T G R G G K L K G A K W A P S
TCAGTTGACATTGGGACCGGCCGTGGTGGGAAGCTGAAAGGCCGCCAAATGGGCACCCAGC
S *
TCCTGAGAATCCCGGGTCTGACTCGAGC
- H AvBD 9 W38G Tryptophan number 38 to Glycine (AvBD9 W38G)**
AGGGAATTTGTTTTGTGGTGGCGACATCCTCCAAATCGGATCTGGAAGTTCTGTTCCAGGGGCCCC
A D T L A C R Q S H G S C S F V A C R
TGGGATCCGCTGACACCTTAGCATGCAGGCAGAGCCACGGCTCCGCTCTTTTGTGTCATGCCGT
A P S V D I G T C R G G K L K C C K G A P
GCTCCTCAGTTGACATTGGGACCTGCCGTGGTGGGAAGCTGAAATGCTGCAAAAGGGGCACCC
S S *
AGCTCCTGAGAATCCCGGGTCTGACTCG

Figure 4.14 A-H: DNA sequencing results of mutagenised plasmids.

AvBD9 3CA variant (panel D) was performed by replacement of AvBD9 mature (Panel A) cysteines C1 (panel B), C2 (panel C) and C6 (panel D) to Alanine. AvBD9 6CA/G variant (panel G) was acquired by substitution of the rest cysteines of AvBD9 3CA variant, C4 (panel E), C3 (panel F) and C5 (panel G) to glycines. AvBD9 W38G variant was constructed by changing tryptophan 38 of AvBD9 mature peptide to glycine (panel H). The highlighted colours: BamH1 and EcoR1 restriction sites (Grey). The mutagenised codon sequences, Alanine (red) and Glycine (pink). Turquoise highlights are the name of the variants produced. Non-mutagenised residues, cysteines (yellow) and tryptophan (green).

Attempts to mutagenise the three cysteines, C3, C4 and C5 to alanines was unsuccessful. This was probably due to the GC rich mutagenesis primers (Table 4.1) either failing to anneal to the DNA sequences or mis-priming. To address this the three cysteines were mutated to glycines.

Primers	Forward	Reverse	Change
AvBD9 C3A	GGCTCCTGCTCTTTTGTGCA <u>GCCCGTGCTCCTT</u>	AAGGAGCACGG <u>GGCT</u> GCAACAA AAGAGCAGGAGCC	TGC to GCC
AvBD9 C4A	GTTGACATTGGGACC <u>GCCCG</u> TGGTGGGAAGCT	AGCTTCCCACCACG <u>GGC</u> GGTCC CAATGTCAAC	TGC to GCC
AvBD9 C5A	GTGGTGGGAAGCTGAA <u>AAGCC</u> TGCAAATGGGCACC	GGTGCCCATTTGCAG <u>GGC</u> TTTCA GCTTCCCACCAC	TGC to GCC

Table 4.1 Primers used to mutagenise cysteines, C3, C4 and C5 of AvBD9 to Alanines.

Once the plasmids encoding the amino acid mutations were engineered they were transformed into BL21 (DE3) pLysS, the GST tagged proteins hyper-expressed and the peptides purified as described for mature AvBD9.

The mutagenised variants were visualised using NUPAGE gels stained with Instant Blue. Figures 4.15 and 4.16 show purification of the AvBD9 3CA, and AvBD9 6CA/G and AvBD9 W38G peptides, respectively, and the yields are shown in Table 4.2.

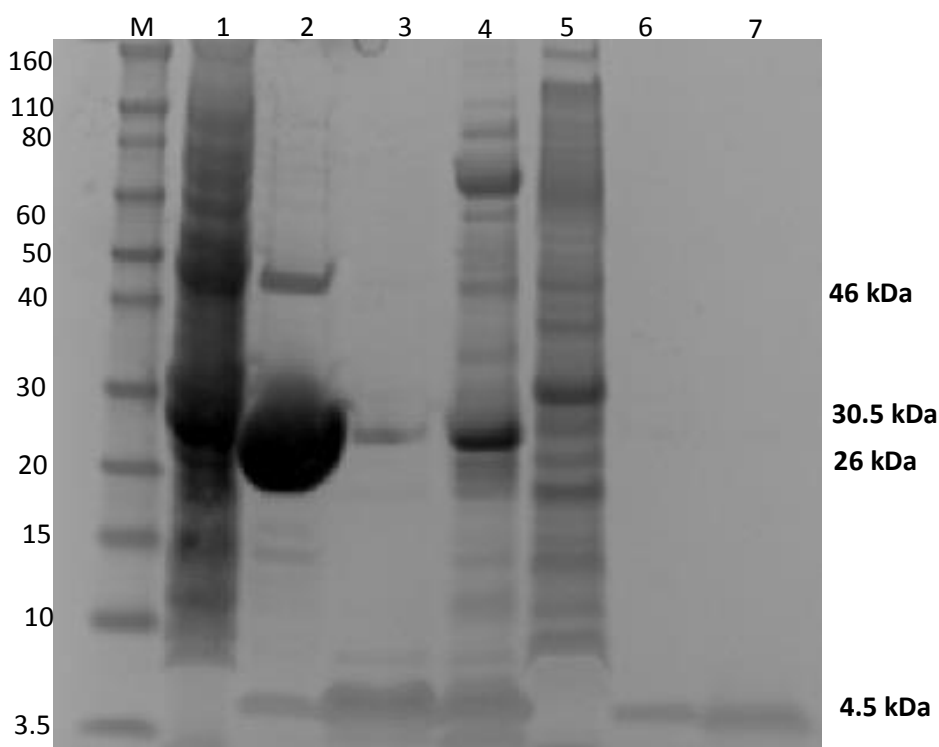


Figure 4.15 NUPAGE gel stained with Instant Blue showing AvBD9 3CA purifications. CFE contains GST tagged AvBD9 (1). Cleaved GST tag from AvBD9 by 3C protease (2), eluted with cleaving buffer (3). Impure proteins trapped in the top of Vivaspin columns (4). Pellets (5). Desalted pure peptide (6). Freeze dried peptides reconstituted with water (7). Novex sharp prestained protein marker (M).

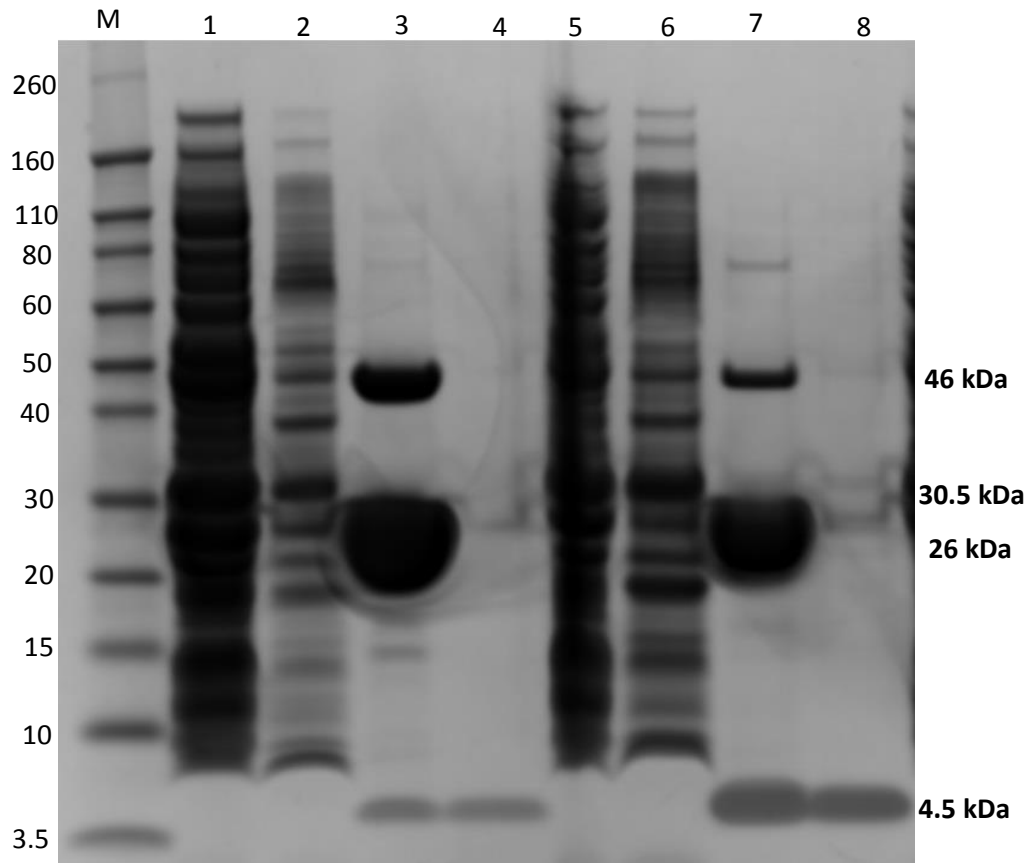


Figure 4.16 NUPAGE gel stained with Instant Blue showing AvBD9 6CA/G (Lanes 1-4) and AvBD9W38G (Lanes 5-8) purifications. CFE contains GST tagged AvBD9 (1 and 5). Cleaved GST tag from AvBD9 by 3C protease (3 and 7). Pure peptides (4 and 8). Pellets (2 and 6). Novex sharp prestained protein marker (M).

AvBDs	Mean±SEM (mg/L)	n
9 mature	0.33± 0.03	7
9 promature	0.64± 0.12	3
9 3C A	0.35± 0.05	8
9 6C AG	0.42± 0.06	8
9 W38G	0.30± 0.06	8
6 mature	0.16± 0.03	4
6 promature	0.15± 0.01	2

Table 4.2 Yields of AvBD9 recombinant peptides (mg/L bacterial growth culture). n is the number of purifications. Mean± SEM.

4.4. Antimicrobial activities of the AvBD peptides

To test the antimicrobial activities of the wild-type AvBD6 and 9 peptides and mutated variants of AvBD9 two anti-microbial assay systems were used. Initially, a radial immunodiffusion assay (RIDA) was used, which allowed bacterial killing properties to be identified quickly but did not support reproducible and accurate quantification of the antimicrobial data. The use of time-kill colony counting assays (CCA) allowed the bacterial killing to be quantitated.

4.4.1. Radial immuno-diffusion assay (RIDA) for AvBD6 and AvBD9 peptides against E. coli

The radial immuno-diffusion assay used in the current study was adapted from the method described by Schroeder *et al.* (2011) and described in Section 2.22.1. These authors, investigating properties of human β -defensin-1, used concentrations of 0.5, 1 and 2 $\mu\text{g}/\mu\text{l}$. A similar approach was adopted in this study using three peptide concentrations of 0.5, 1 and 4 $\mu\text{g}/\mu\text{l}$. To quantify the antimicrobial activity, the percentage of bacterial inhibition was determined by measuring the clear zone created by the AvBD peptide treatments relative to a positive control peptide. The diameters of the wells were considered as baselines and subtracted from the zone measurements. Two positive controls with known AMA, lysozyme (Schroder and Harder, 2006) and cecropin (Lu *et al.*, 2012) were used routinely, but unless stated otherwise the positive control data relate to cecropin as its antimicrobial activity was more consistent in the RIDA than that of lysozyme.

A typical example of the *E. coli* radial diffusion assay results for AvBD6 is shown in Figure 4.17. These data indicated that AvBD6, at 4 $\mu\text{g}/\mu\text{l}$, was antimicrobial causing an *E. coli* zone of inhibition comparable to that of the positive controls, cecropin (4 $\mu\text{g}/\mu\text{l}$) and lysozyme (10 $\mu\text{g}/\mu\text{l}$). The antimicrobial data were less clear for AvBD6 at concentrations of 0.5 and 1 $\mu\text{g}/\mu\text{l}$.

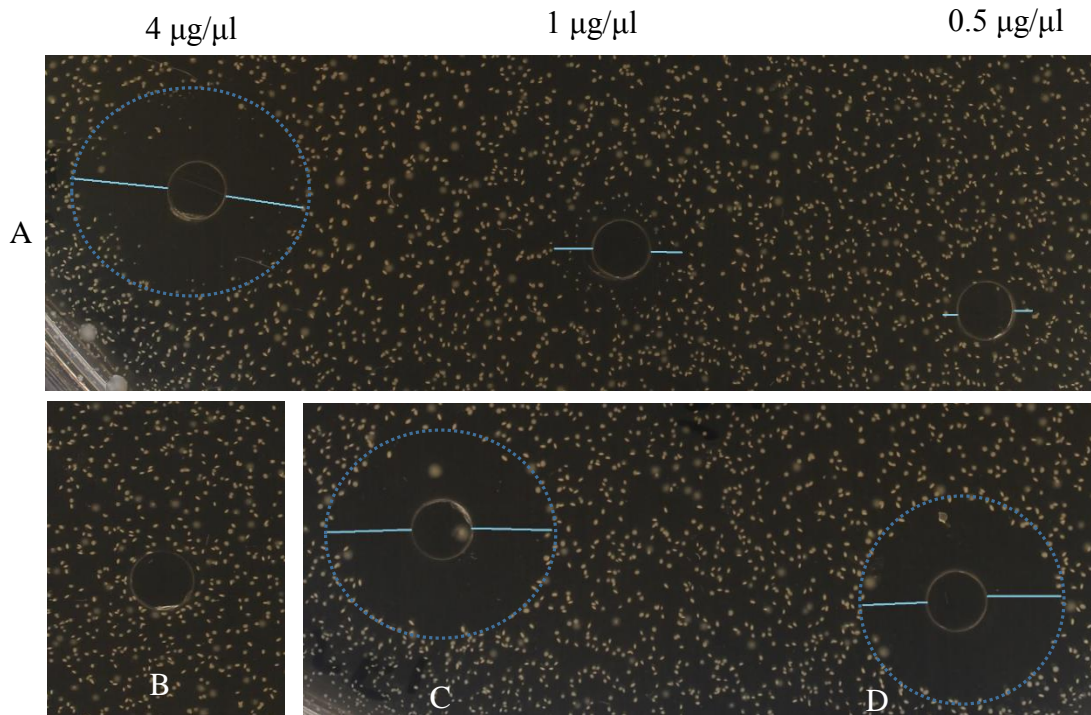


Figure 4.17 Radial immunodiffusion assay results following incubation of 0.5, 1 and 4 $\mu\text{g}/\mu\text{l}$ recombinant AvBD6 mature peptide (A). PBS (B); 10 $\mu\text{g}/\mu\text{l}$ Lysozyme (C) and 4 $\mu\text{g}/\mu\text{l}$ Cecropin (D) with an *E. coli* lawn. *E. coli* grown on TSB agar. 2.3 X magnification

A typical example of the *E. coli* radial diffusion assay results following incubation of AvBD9 mature, promature and AvBD9 3CA peptides with *E. coli* at concentrations of 0.5, 1 and 3 $\mu\text{g}/\mu\text{l}$ is shown in Figure 4.18. Clear halos or zones of inhibitions were observed at 1 and 3 $\mu\text{g}/\mu\text{l}$, indicating that the peptides had antimicrobial properties against *E. coli*. Moreover the percentages of inhibition for 3 $\mu\text{g}/\mu\text{l}$ AvBD9 mature, promature and AvBD9 3CA peptides were comparable at 100, 90 and 110% (where AvBD9=100%)

Figure 4.19 shows the semi-quantitative analyses of the inhibition zones resulting from using 3 $\mu\text{g}/\mu\text{l}$ AvBD9 mature, AvBD9 promature and AvBD9 3CA peptides. These data indicated no significant differences in the zones of inhibition and suggested comparable *E. coli* killing between the variants ($100\pm 0\%$ (mean \pm SEM) killing for AvBD9 mature, $83\pm 8\%$ using AvBD9 promature and $88\pm 22\%$ using AvBD9 3CA).

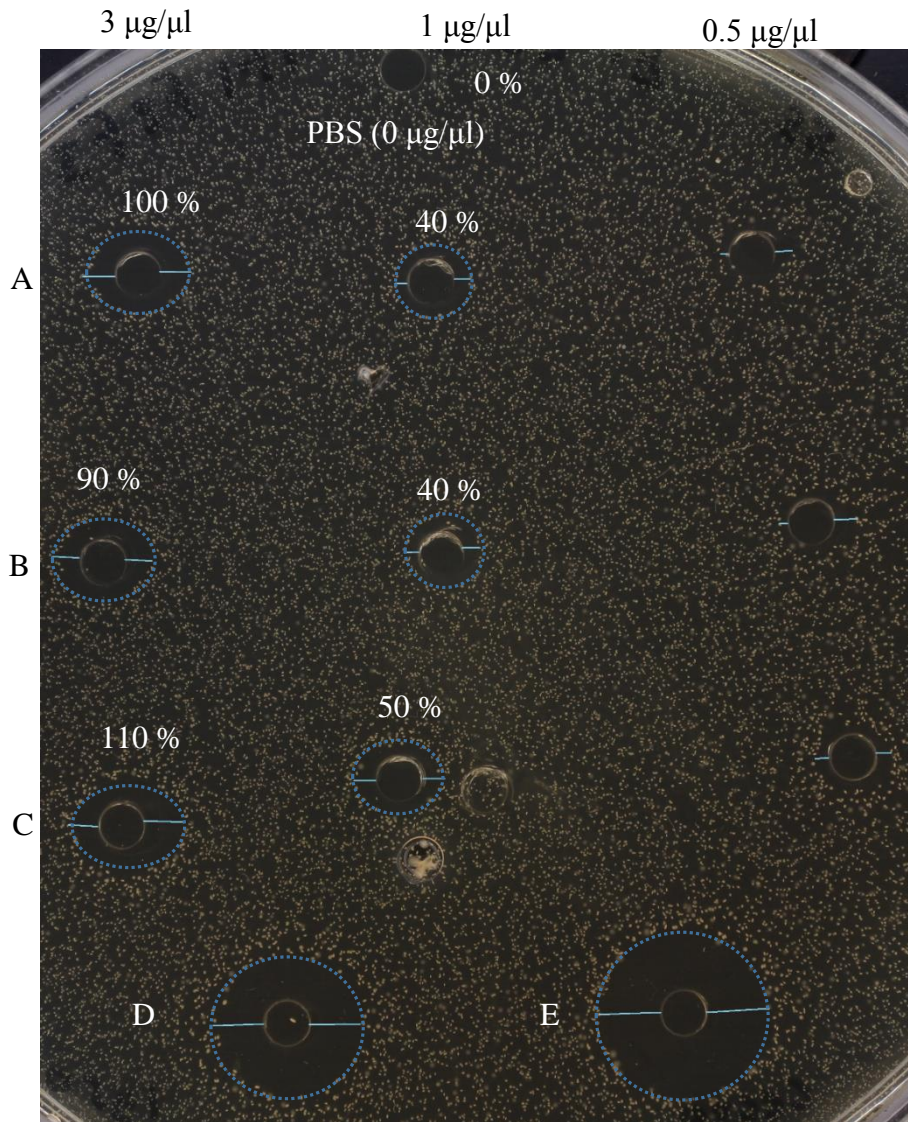


Figure 4.18 Radial immuno-diffusion assay of recombinant AvBD9 peptides using lawn of *E. coli* grown on TSB agar. AvBD9 mature (A); AvBD9 promature (B); AvBD9 3CA (C). The positive controls were Lysozyme 10 $\mu\text{g}/\mu\text{l}$ (D) and Cecropin 4 $\mu\text{g}/\mu\text{l}$ (E). PBS was used as the negative control. % represents percentage of inhibition zones compared to the AvBD9 mature as 100% inhibition. 2X magnification.

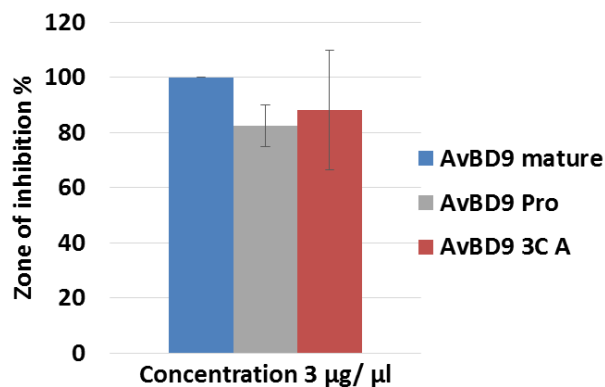


Figure 4.19 Percentage inhibition zone created using 3 $\mu\text{g}/\mu\text{l}$ of AvBD9 promature and 3CA peptides compared to AvBD9 mature. Mean \pm SEM. Experiments =2. Replicates =4. AvBD9 mature was used as a 100 % inhibition.

Zone of inhibition data relating to the variants containing either no cysteines AvBD9 6CA/G or no C-terminal tryptophan AvBD9 W38G are shown in Figures 4.20 and 4.21. The 3 $\mu\text{g}/\mu\text{l}$ data indicated that the AvBD9 6CA/G and AvBD9 W38G variants had bacterial killing properties with zones of inhibition comparable to that of the mature peptide. Minimal or no killing was observed at 1 $\mu\text{g}/\mu\text{l}$ and 0.5 $\mu\text{g}/\mu\text{l}$. The quantification of inhibitory zones is shown in Figure 4.21 using AvBD9 data as 100% inhibition, 81 \pm 9 % inhibition was recorded for both AvBD9 6CA/G and AvBD9 W38G with no statistical differences.

The inhibitory zone experiments were quick and the data useful in that they indicated whether or not the AvBD peptides were antimicrobial. However, the disadvantage of the methodology was that the inhibitory zone measurements were very subjective and essentially provided only qualitative data.

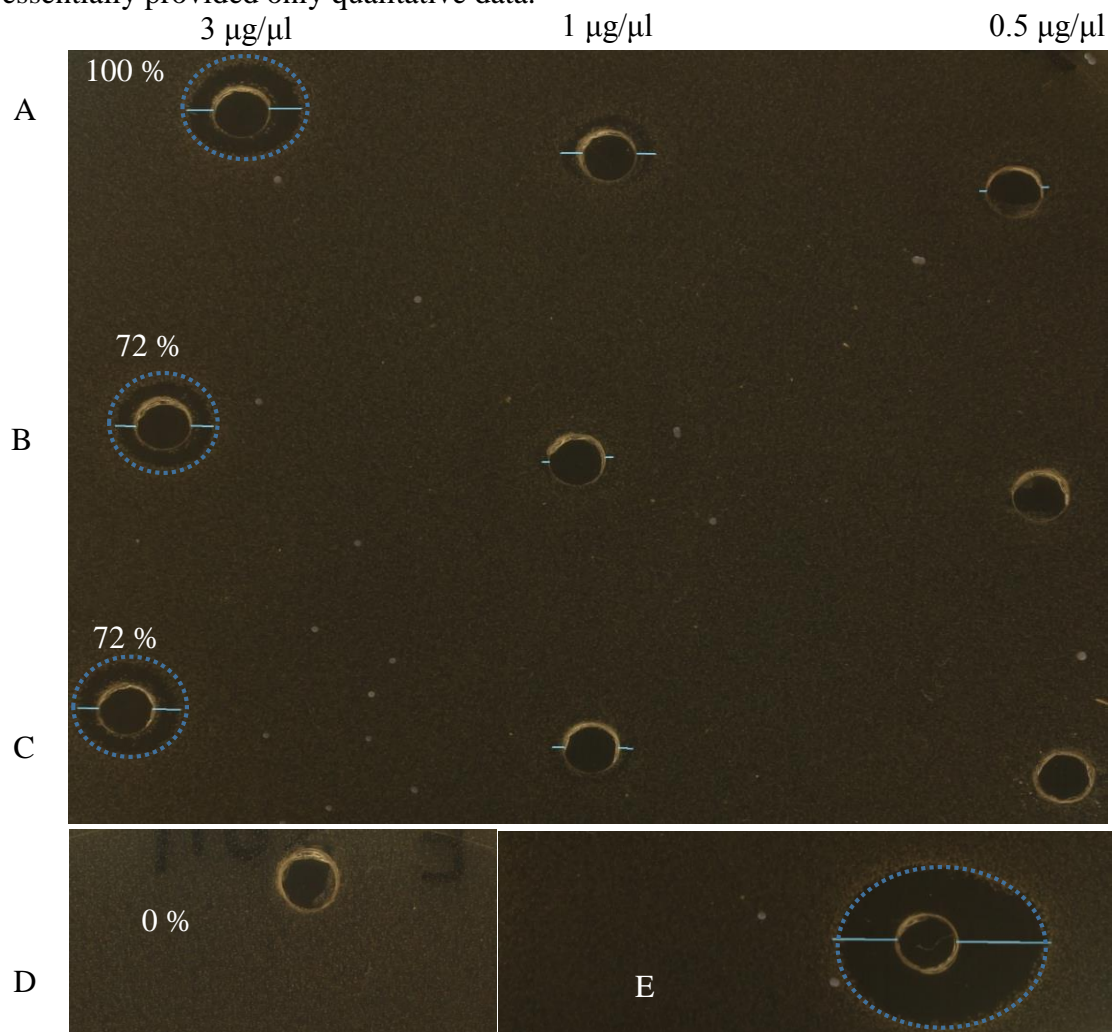


Figure 4.20 Radial immune-diffusion assay of rAvBD9 peptides in different concentrations against *E. coli* grown on TSB agar. AvBD9 mature (A). AvBD9 6CA/G (B). AvBD9 W38G (C). PBS as a negative control (D). Cecropin (E), 4 $\mu\text{g}/\mu\text{l}$. % represents percentage of inhibition zones compared to the AvBD9 mature as 100% inhibition. 2.2 X magnification.

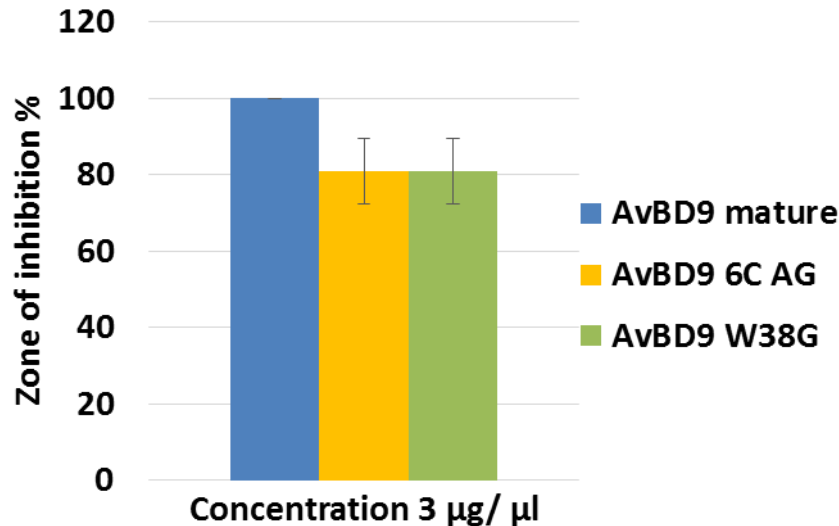


Figure 4.21 Percentage inhibition zone created by 3 µg/µl of AvBD9 6CA/G and W38G peptides compared to AvBD9 mature against *E. coli*. Data presented as mean ± SEM. Experiments=2, Replicates=4. AvBD9 mature was used as a 100 % inhibition.

4.4.2. Time kill-colony counting assay

To secure more quantitative data a time-kill colony counting assay was adopted.

This method was adapted from that described by Townes *et al.* (2005), and explained in section 2.22.2. This assay is based on counting bacterial colonies following incubation with a peptide and hence the data are quantitative.

4.4.2.1. rAvBD6 peptide AMA against *E. coli*

The kill curves of the AvBD6 mature compared to the AvBD6 promature peptides are shown in Figure 4.22. These data revealed no statistically significant differences in the *E. coli* killing activities of the two peptides. For example, 15.9 % *E. coli* killing (84.1±10.8 % survival) was recorded using 2.5 µg/ml of mature AvBD6 compared to 13.2 % killing (86.8±12.8 % survival) using the promature peptide. Similarly 44.4 % (55.6±7.1 % survival) of *E. coli* colonies were killed using 25 µg/ml of mature AvBD6 compared to 55.7 % (44.3±17.9 survival) using pro-mature AvBD6. These data suggested that the short pro-piece hexamer amino acid sequence had no effect, *in vitro*, on the *E. coli* AMA properties of AvBD6.

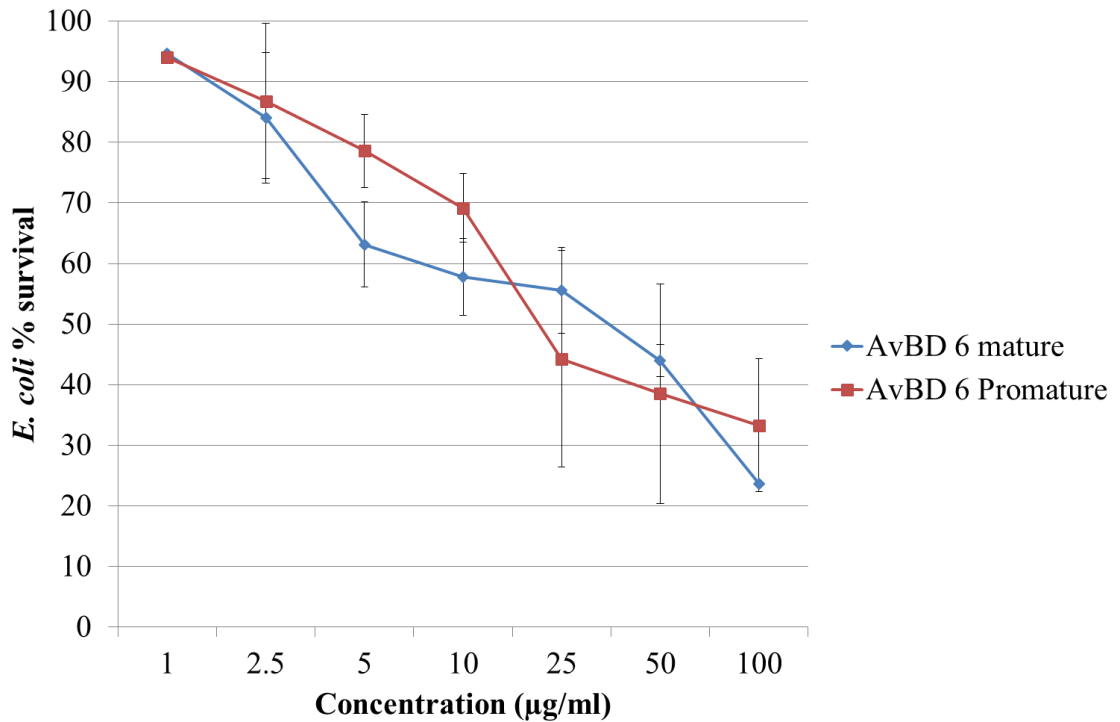


Figure 4.22 Time-kill assay data comparing *E. coli* killing by rAvBD6 mature and promature peptides. Data presented as Mean±SEM. Experiments=3, Replicates=9.

4.4.2.2. AvBD6 AMA against *E. faecalis*

The time-kill assays were repeated using *E. faecalis*, a Gram positive bacterium, isolated from the gut of an Aviagen broiler chicken and these data are presented in Figure 4.23. As the previous data indicated that the hexamer pro sequence had no effects on AvBD6 killing the assay was performed using only the mature AvBD6 peptide. *E. faecalis* killing was observed and the killing curve was comparable to that of *E. coli*. For example at 100 µg/ml, the peptide killed 84 % (16.0±6.5 % survival) of the *Enterococci* compared to 76.4% (23.6±2.3 % survival) of *E. coli*. However, at concentrations <5 µg/ml, the AvBD6 peptide was not anti-microbial and indeed bacterial survival values >100% were observed reproducibly, suggesting that at this concentration the bacteria were using the peptide as a nutrient source for growth. Complete killing of *E. faecalis* was observed at 250 µg/ml.

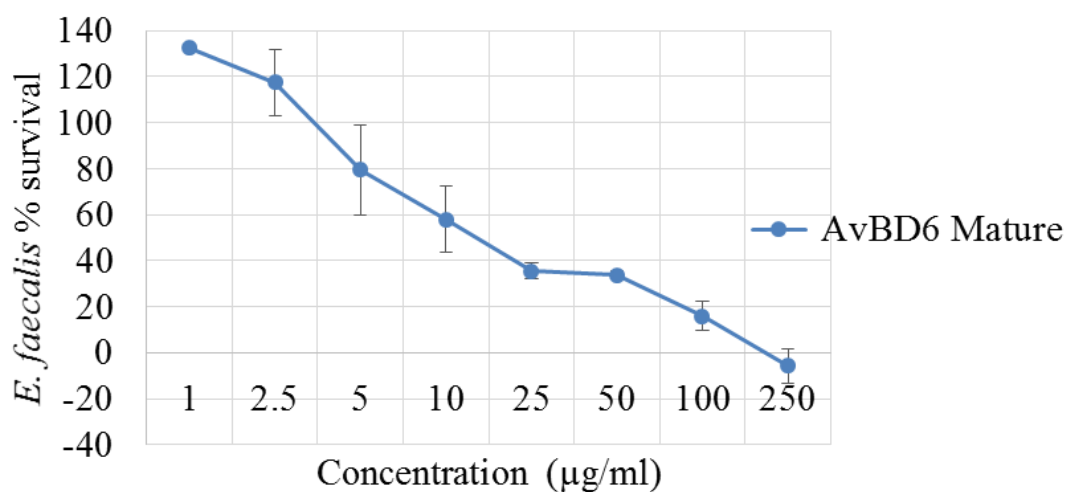


Figure 4.23 Time-kill assay data comparing *E. faecalis* killing by rAvBD6 mature peptides. Data presented as Mean±SEM. Experiments=3, Replicates=9

4.4.2.3. AvBD9 AMA against *E. coli*

The curve showing the killing of *E. coli* by the AvBD9 mature peptide is presented in Figure 4.24A. As marked *E. coli* killing was observed at 25 µg/ml 29.4 % (70.6±2.3 % survival) this concentration, as well as 50, 100, 250 and 500 µg/ml, was chosen to compare the killing properties of the wild-type and mutated AvBD9 peptides. These data are shown in Figure 4.24B. *E. coli* killing did not differ significantly when equivalent concentrations of the mature, promature and AvBD9 3CA peptides were used (Figure 4.24B: blue, grey & red columns). These data suggested that, *in vitro*, the pro-piece of AvBD9 had no impact on the AMA of the peptide against *E. coli* and that AvBD9 3CA retained its AMA activity. However, mutation of the six AvBD9 cysteines to alanines and/or glycines (AvBD9 6CA/G), and the C-terminal tryptophan to glycine (AvBD9 W38G), significantly reduced the killing capabilities of the resulting peptides against *E. coli*. For example incubating *E. coli* with 50 µg/ml AvBD9 6CA/G and AvBD9 W38G resulted in ≥100% bacterial survival (112.3±5.8) and (154.8±15.1) while increasing the dose five-fold to 250 µg/ml resulted in only 35.3 % (64.7±15.4 % survival) and 25.9 % (74.1±13.7 % survival) killing (Figure 4.24B: yellow and green columns). These data indicated that the presence of six cysteine amino acids and a C-terminal tryptophan residue are important in the AMA of AvBD9 against *E. coli*.

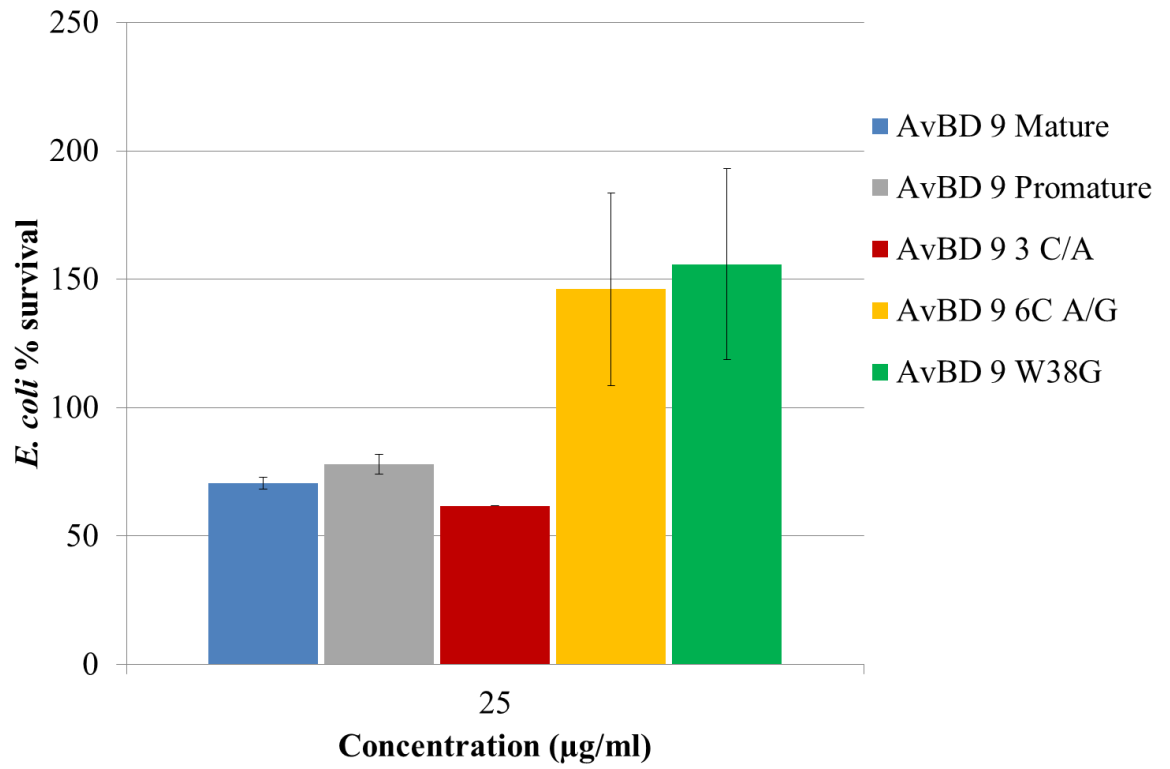


Figure 4.24 A: Time-kill assay data comparing *E. coli* killing by rAvBD9 peptides. Experiments=2, Replicates=6. Mean±SEM. Data were compared to the number of bacterial colonies observed using PBS.

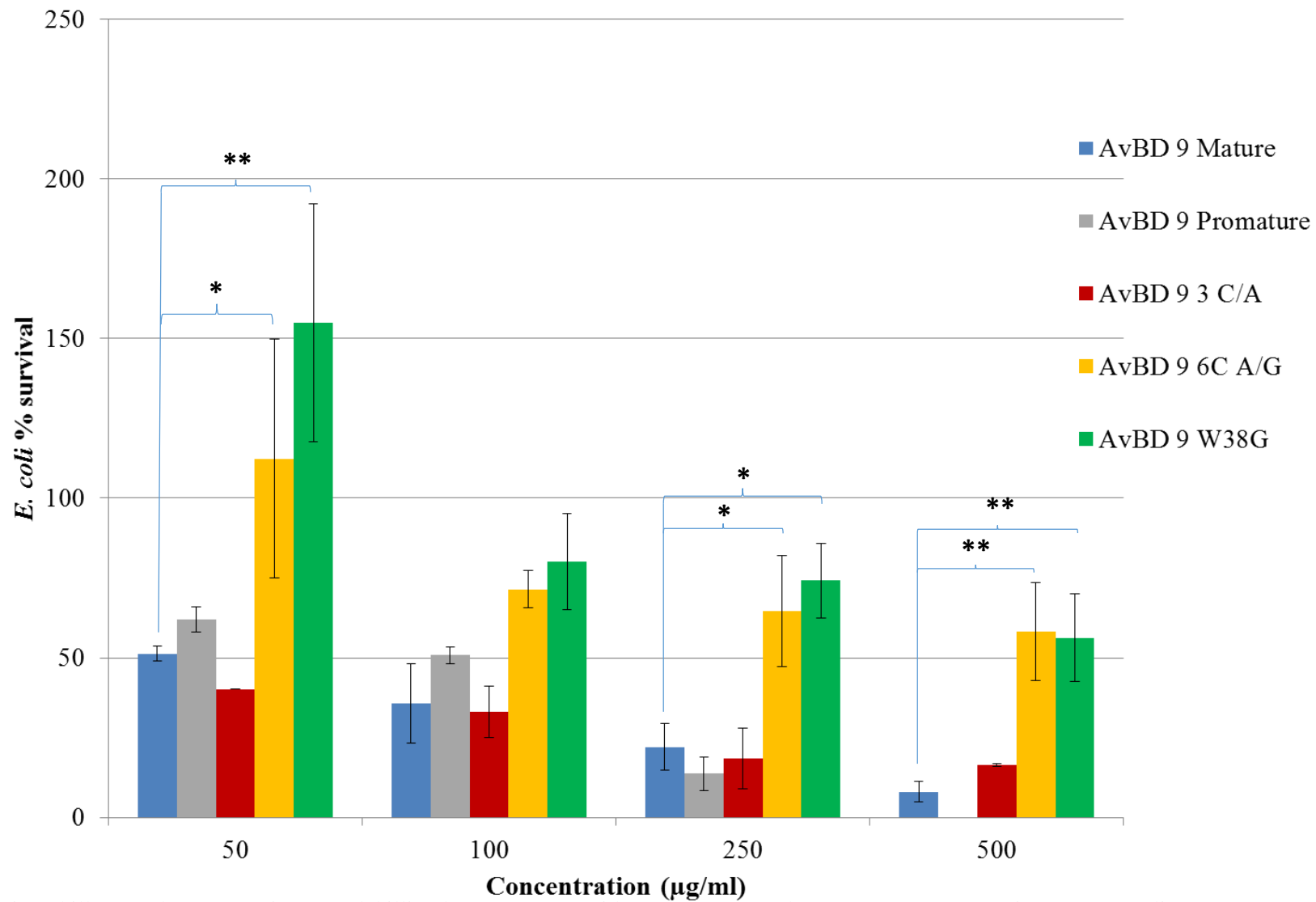


Figure 4.24B: Time-kill assay data comparing *E. coli* killing by rAvBD9 peptides. Data presented as Mean±SEM. Experiments=2, Replicates=6. * P<0.05. ** P<0.01. Data were analysed using one way ANOVA, followed by Dunnett's multiple comparison test.

At concentrations of 25 and 50 $\mu\text{g/ml}$ pro-microbial activity, $>100\%$ *E. coli* survival, was recorded when AvBD9 6CA/G and AvBD9 W38G peptides were used in the time-kill assay. To explore whether the bacteria were utilising the recombinant peptides as a nutrient source, two non-antimicrobial proteins, bovine serum albumin (BSA) and the recombinant GST tagged 3C enzyme (GST-3C), were used at 25 $\mu\text{g/ml}$ along with AvBD9 and AvBD9 W38G in the time-kill assay. The resultant data shown in Figure 4.25 showed that all three, AvBD9 W38G, BSA and GST-3C, enhanced the growth of *E. coli* with survival recorded as 140 ± 26 , $125 \pm 1.0\%$ and $119\pm 1.0\%$. These data suggested that in the absence of antimicrobial peptide killing effects, the *E. coli* were able to exploit the recombinant peptides as a nutrient source, hence the $>100\%$ values.

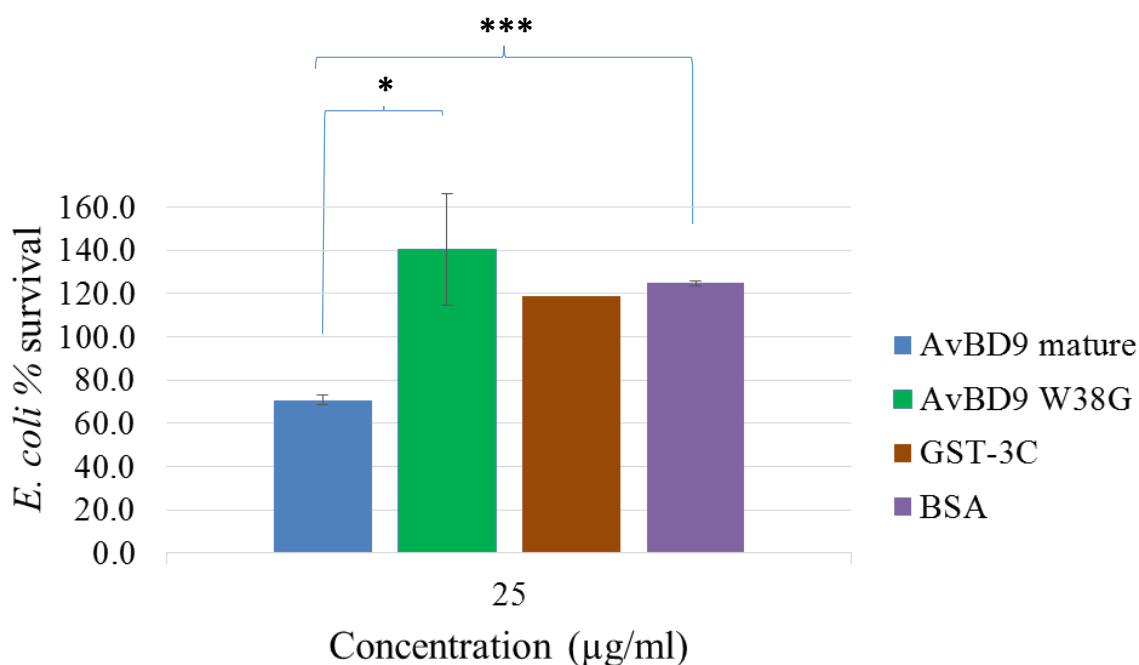


Figure 4.25 Time-kill assay data comparing *E. coli* killing by rAvBD9 mature, rAvBD9 W38G; GST-3C and BSA. Experiments=2, Replicates=6. Mean \pm SEM, $P<0.05$. *** $P<0.001$. Data were analysed using one way ANOVA, followed by Dunnett's multiple comparison test.

4.4.2.4. Dimerization of AvBD9 3CA

Mutagenesis of cysteines C1, C2 and C6 to alanines did not affect the antimicrobial effectiveness of the AvBD9 peptide. Previous work (Campopiano *et al.*, 2004) focussed on mouse defensin, Defr1, explained the antimicrobial activity of this five cysteine molecule through the formation of intermolecular disulphide bonds and a dimer tertiary structure. To explore the possibility of AvBD9 C3A dimer formation through intermolecular disulphide bond formation, the AvBD9 C3A peptide was analysed using NUPAGE following

incubation for 10 minutes in either reducing or non-reducing conditions. AvBD9 wild type was used as the control. The results, Figure 4.26, showed that AvBD9 wild type migrated as a single band in non-reducing conditions (Lane 1), compared to the AvBD9 3CA variant, which migrated as two bands (Lane 2). In reducing conditions (Lanes 3 and 4), both peptides migrated as single bands with molecular weights of approximately 4.5 kDa. The double bands of 4.5 and 9 kDa (Lane 2) suggested that the AvBD9 C3A peptides formed dimers, with inter molecular disulphide bond formation occurring between the free cysteines of the two peptide molecules.

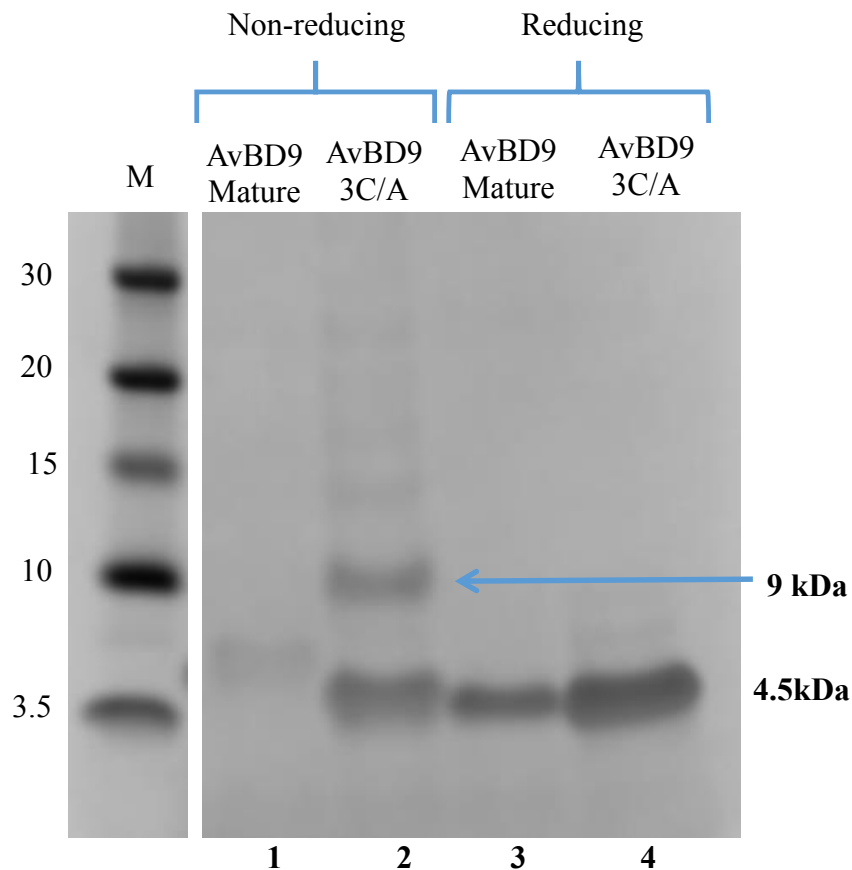


Figure 4.26 NUPAGE gel stained with Instant Blue and comparing AvBD9 mature and AvBD9 3CA in both reducing (1 and 2) and non-reducing (3 and 4) conditions. Novex sharp prestained protein marker (M).

However, as AMAs were not performed under reducing conditions it was not possible to directly relate the AMA of AvBD9 3CA to the formation of the tertiary molecule.

4.4.2.5. AvBD9 AMA against *E. faecalis*

The AMAs of the mature and mutated AvBD9 peptides were also tested against *E. faecalis*. As data indicated that the hexamer pro-piece sequence had no effects on killing the assays did not include the AvBD9 promature peptide. The results are shown in Figure 4.27.

The pro-microbial activities recorded at 10 µg/ml suggested that, as observed with *E. coli*, the *E. faecalis* bacteria were using the recombinant peptides as a nutritional growth source. At 25 µg/ml the data were characterised by large error bars, but statistically the AvBD9 6C A/G and AvBD9 W38G peptides showed no antimicrobial activity. However, both the AvBD9 mature and AvBD9 3CA peptides were antimicrobial resulting in 20.8% (79.2±34.4% survival) and 69% (41.0±12.5% survival) *E. faecalis* killing. The significant reduction in AvBD9 6CA/G AMA compared to AvBD9 3CA further supported the significance of the dimer molecules, via intermolecular disulphide bonding, in *E. faecalis* killing.

No statistical differences in AMA were observed between the AvBD9 variants at 50 µg/ml, although again these data were characterised by large error bars. Of note was the reduced AMA of the AvBD9 W38G peptide 15.1 % (84.9±20.5 % survival) compared to that of the mature AvBD9 53.3 % (46.7±20.1% survival). This difference in AMA was significant ($P < 0.05$) at 100 µg/ml and supported the importance of the AvBD9 C-terminal tryptophan in bacterial killing.

The antimicrobial activities of all the AvBD9 variants were similar at the highest concentration tested, 250 µg/ml.

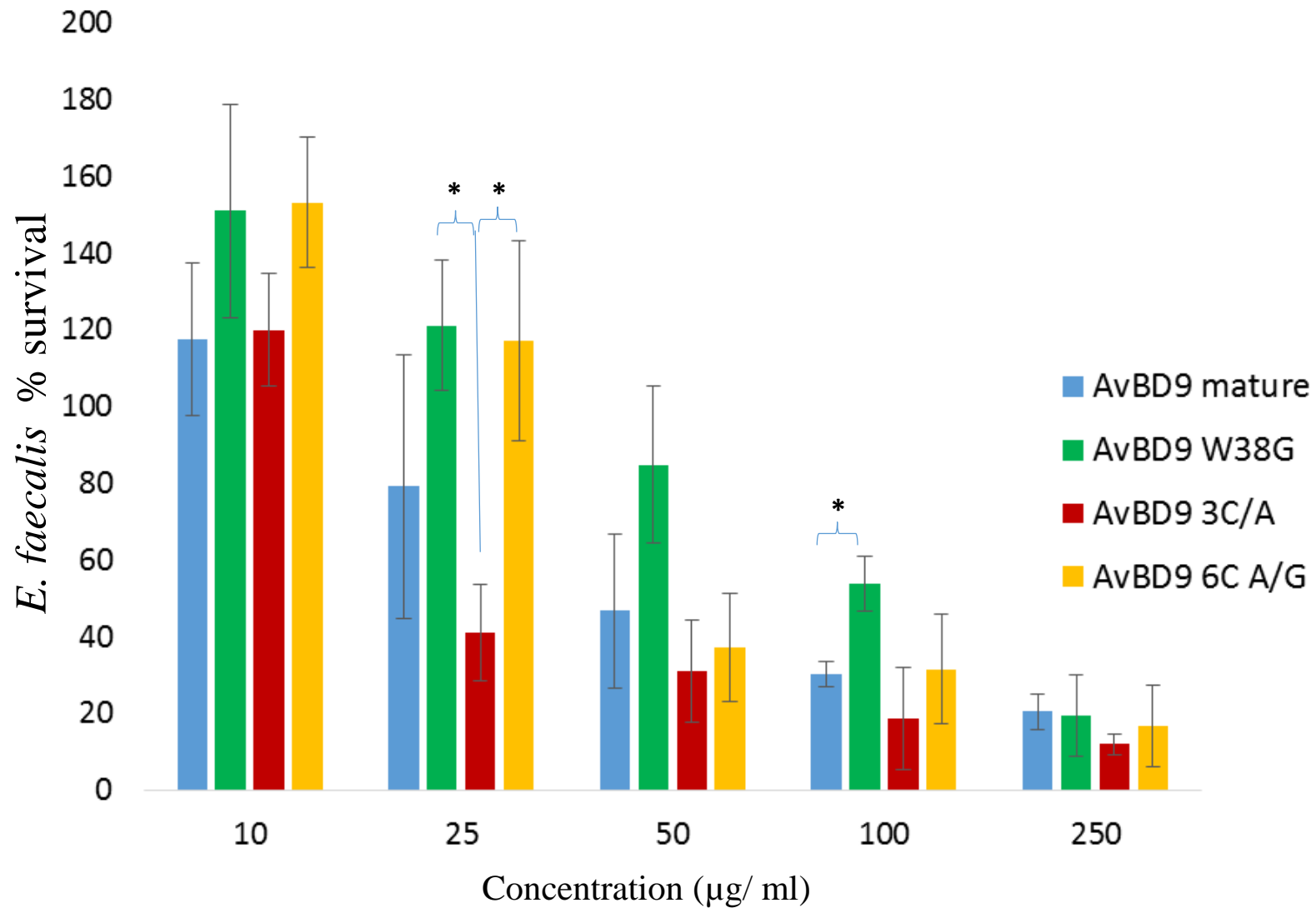


Figure 4.27 Time-kill assay data comparing *E. faecalis* killing by rAvBD9 peptides. Data presented as Mean±SEM. Experiments=3, Replicates=9. * P<0.05. Data were analysed using one way ANOVA, followed by Dunnett's multiple comparison test.

4.4.3. Recombinant AvBD10 production and AMA

The AMA data highlighted the potential importance of the C-terminal tryptophan in the AMA of AvBD9. AvBD10 has no tryptophan at its C-terminal or indeed within its primary sequence of 46 amino acids (Figure 4.12). Thus to further explore the importance of the C-terminal tryptophan in bacterial killing the C-terminal alanine of AvBD10 was replaced by a tryptophan and the impact of the aromatic hydrophobic residue on AvBD10 A45W explored.

4.4.3.1. AvBD10 site directed mutagenesis:

The recombinant plasmid for mature AvBD10 was previously constructed by colleagues Kevin Caldwell and Vanessa Butler (PhDs, Newcastle University) and the DNA sequence is shown in Figure 4.28A. In this study, and using site-directed mutagenesis, a tryptophan was substituted for Alanine 45 in the AvBD10 primary sequence (Figure 4.28B). Both mutagenised and mature AvBD10 plasmids were transformed into BL21, the GST tagged proteins hyperexpressed and the peptides purified as described previously for AvBD9. Results of the purification are shown in Figure 4.29.

A AvBD10 wild type

AGGGACAGTTTTGGTTGGTTGGCGACATCCTCCAAATCGGATCTGGAAGTTCTGTTCCAGGGGCCCC
D P L F P D T V A C R T Q G N F C R A G
TG**GGATCC**GACCCACTTTTCCCTGACACCGTGGCATGCAGGACTCAGGGGAATTTCTGCCGTGCTGG
A C P P T F T I S G Q C H G G L L N C C A K
GGCATGCCCCCCCACCTTCACCATCTCTGGGCAGTGCCATGGGGGGCTGTAAACTGCTGTGCCAAG
I P **A** Q
ATTCCG**GCG**CAG**GAATTC**CCGGGTCGACTCGAGCGGCCGCATCGTGACTGACTGACGATCTGCCTC
GCGCGTTTCGGTGATGACGGTGA

B AvBD10 A45W

AGGGACAGTTTTGGTTGGTTGGCGACATCCTCCAAATCGGATCTGGAAGTTCTGTTCCAGGGGCCCC
D P L F P D T V A C R T Q G N F C R A G
TG**GGATCC**GACCCACTTTTCCCTGACACCGTGGCATGCAGGACTCAGGGGAATTTCTGCCGTGCTGG
A C P P T F T I S G Q C H G G L L N C C A K
GGCATGCCCCCCCACCTTCACCATCTCTGGGCAGTGCCATGGGGGGCTGTAAACTGCTGTGCCAAG
I P **W** Q
ATTCCG**TGG**CAG**GAATTC**CCGGGTCGACTCGAGCGGCCGCATCGTGACTGACTGACGATCTGCCTC
GCGCGTTTCGGTGATGACGGTGA

Figure 4.28 AvBD10 DNA sequences of the mature (A) and mutagenized plasmids (B). Restriction sites (BamH1) and (EcoR1) are highlighted in grey. The green sequence shows the mutated codon changed from Alanine (GCG) to Tryptophan (TGG).

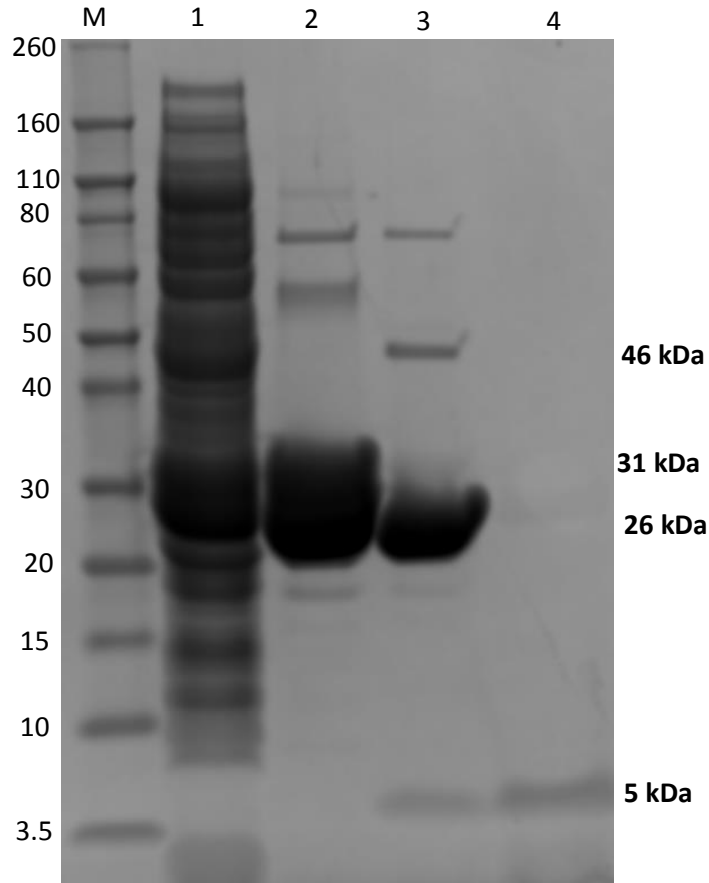


Figure 4.29 NUPAGE stained by Instant Blue showing purification of AvBD10 recombinant peptides. CFE (1); GST tagged AvBD10 (2); AvBD10 (5 kDa) cleaved from GST tag (26 kDa) by 3 C enzyme (46 kDa) (3); Purified AvBD10 (4). Novox pre-stained marker (M).

The average yields of AvBD10 and AvBD10 A45W were 0.13 and 0.09 mg/L (Table 4.3).

AvBDs	Mean±SEM (mg/L)	n
10 wild type	0.13± 0.04	3
10 A45W	0.09± 0.02	3

Table 4.3 Final yields of AvBD10 and AvBD10 A45W (mg/L bacterial growth media) purification. Mean±SEM. n is number of purifications.

4.4.3.2. AvBD10 AMA against *E. coli*

Radial immuno-diffusion and time-kill colony counting assays were used to compare the AMAs of the mature AvBD10 and AvBD10 A45W recombinant peptides. The immuno-diffusion assay was performed to quickly verify AMA and the data relating to *E. coli* is shown in Figure 4.30.

Both the mature and mutated AvBD10 peptides showed antimicrobial activity against *E. coli* and although the analyses was subjective no obvious differences were observed between the two peptides.

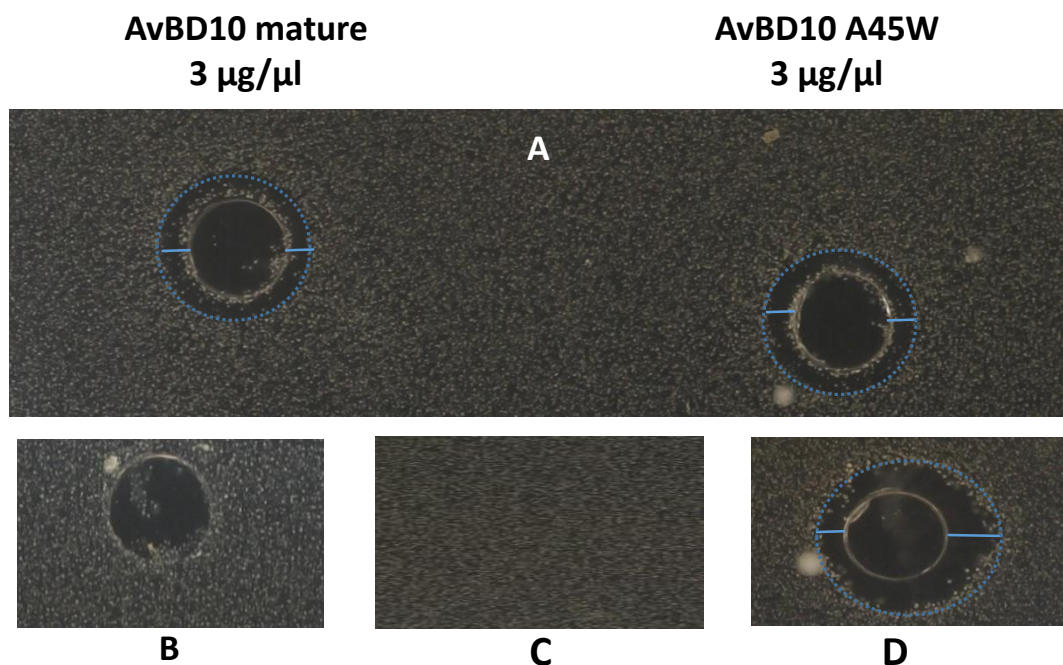


Figure 4.30 Radial immuno-diffusion assay comparing the AMAs of AvBD10 mature and AvBD10 A45W (A) using *E. coli* grown on TSB (C). PBS negative control (B). Cecropin, 1 $\mu\text{g}/\mu\text{l}$, positive control (D). 4 X magnifications.

The time-kill assay data relating to the AvBD10 peptides and *E. coli* survival is shown in Figure 4.31. The kill curves relating to AvBD10 and AvBD10 A45W were comparable and in fact almost super-imposed. However, these data indicated that the mature and A45W mutant peptides were poor antimicrobial agents. For example 50 $\mu\text{g}/\text{ml}$ doses of mature and A45W mutant peptides killed <10% *E. coli* [4.3 % (95.7 \pm 34.1 % survival) and 6.9 % (93.1 \pm 38.9 % survival) respectively]. Moreover the AMAs of both peptides remained constant at 100, 250 and 500 $\mu\text{g}/\text{ml}$ and did not even reach 75% killing; at the highest concentration tested, 500 $\mu\text{g}/\text{ml}$, AvBD10 and AvBD10 A45W achieved only 69.3% and 74.1 % *E. coli* killing (31.7 \pm 7.1 % and 25.9 \pm 8.1 % survival), which compared to >90% (92%) for AvBD9 (Figure 4.24B). These data indicated that AvBD10, characterised by reduced numbers of positively charged amino acids, is less active in killing gram negative bacteria.

No statistical differences were observed between the AMA of mature AvBD10, which has no tryptophan at its C terminus, and the mutant AvBD10 A45W in which the C-terminal alanine 45 was changed to a tryptophan. These data indicated that the tryptophan had not increased the AMA of AvBD10 against *E. coli*.

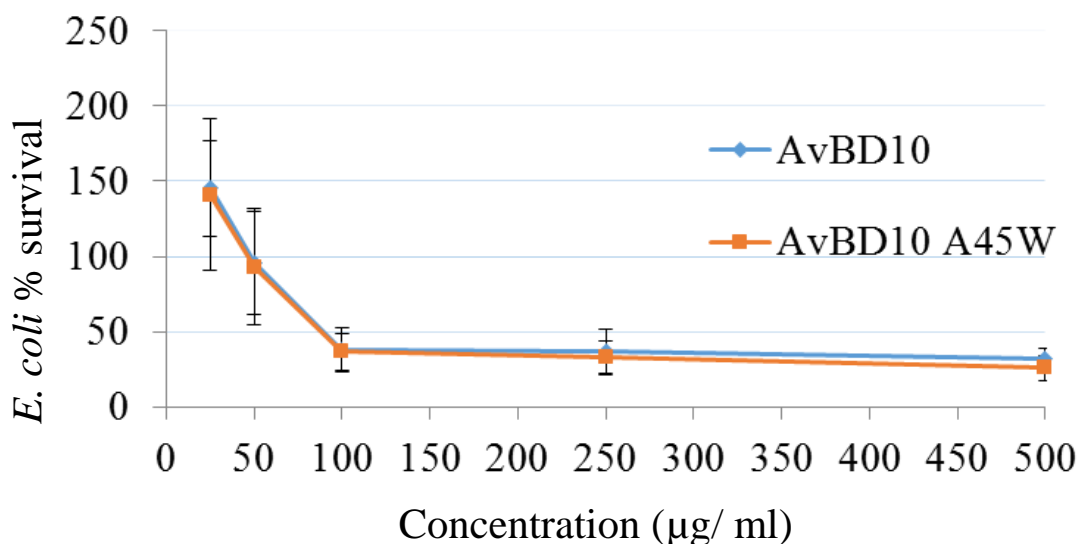


Figure 4.31 Time-kill assay data comparing *E. coli* killing by rAvBD10 mature and AvBD10 A45W peptides. Data presented as Mean±SEM. Experiments=3, Replicates=9.

4.4.3.3. AvBD10 AMA against *E. faecalis*

Similar results were observed in relation to the effects of AvBD10 and AvBD10 A45W on the survival of the gram positive isolate *E. faecalis* (Figure 4.32), with the kill curves again comparable and in fact over-lapping. These data also suggested that a C-terminal tryptophan is not important for the killing of *E. faecalis* by AvBD10. However, in contrast to the *E. coli* killing curves, these data showed increased bacterial killing at lower peptide concentrations. For example using 10 µg/ml AvBD10 and AvBD10A45W peptides, killing was recorded as 45.0 % and 61.9 % (55.0±5.1 % and 39.1±15 % survival) respectively, which compared to >100% survival with *E. coli* (Figure 4.31).

Using 50 µg/ml, 83.4 % and 84.1 % *E. faecalis* killing (17.6±4.0 % and 15.9±3.0 % survival) was recorded using the mature and mutant AvBD10 peptides. Following a five-fold increase in the peptides to 250 µg/ml the killing values reached only 88 % (12.0±5.1 % survival) and 87.4 % (12.6±5.8 % survival), but again were greater than those observed for *E. coli*. Overall, these data suggested that the AvBD10 peptides had increased activity

against gram positive organisms, but that the C-terminal tryptophan residue had no impact on AvBD10 AMA against *E. faecalis*.

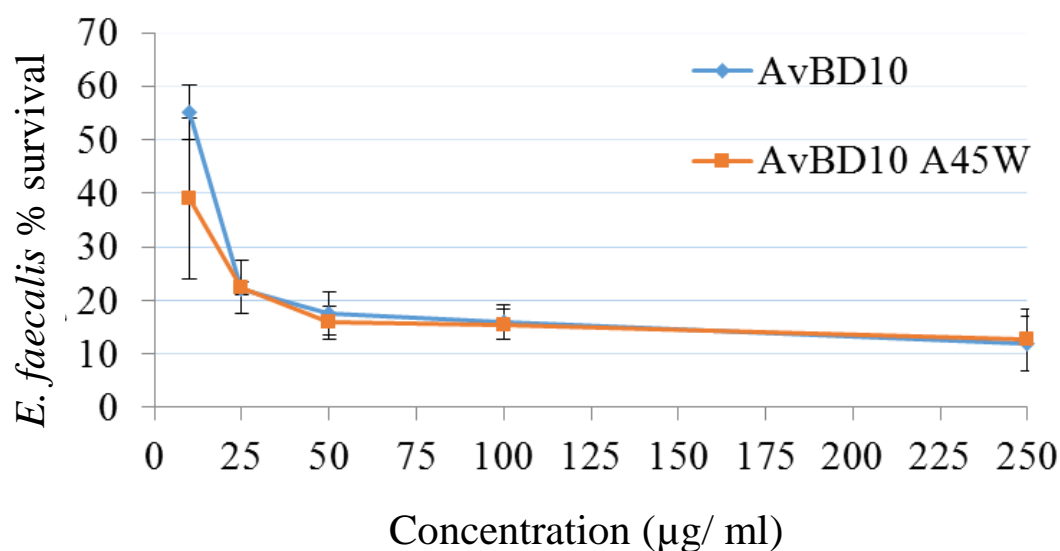


Figure 4.32 Time-kill assay data comparing *E. faecalis* killing by AvBD10 mature and AvBD10 A45W peptides. Experiments=3, Replicates=9. Mean±SEM.

4.5. Time-kill assays using synthetic AvBD peptides

In addition to using recombinant peptides in the time-kill antimicrobial assays three synthetic peptides were also used, but with the knowledge that these peptides were synthesised and supplied as linear molecules. The three linear synthetic AvBD peptides were sAvBD6 mature, sAvBD9 mature and sAvBD9 W38G; these peptides were HPLC purified and 95% pure.

The HPLC data provided by Protein Peptide Research Ltd shows the purity of the sAvBD6, sAvBD9 and sAvBD9 W38G fractions and their collection times, 8.1, 9.5 and 7.3 minutes post injection (Figures 5.33-35).

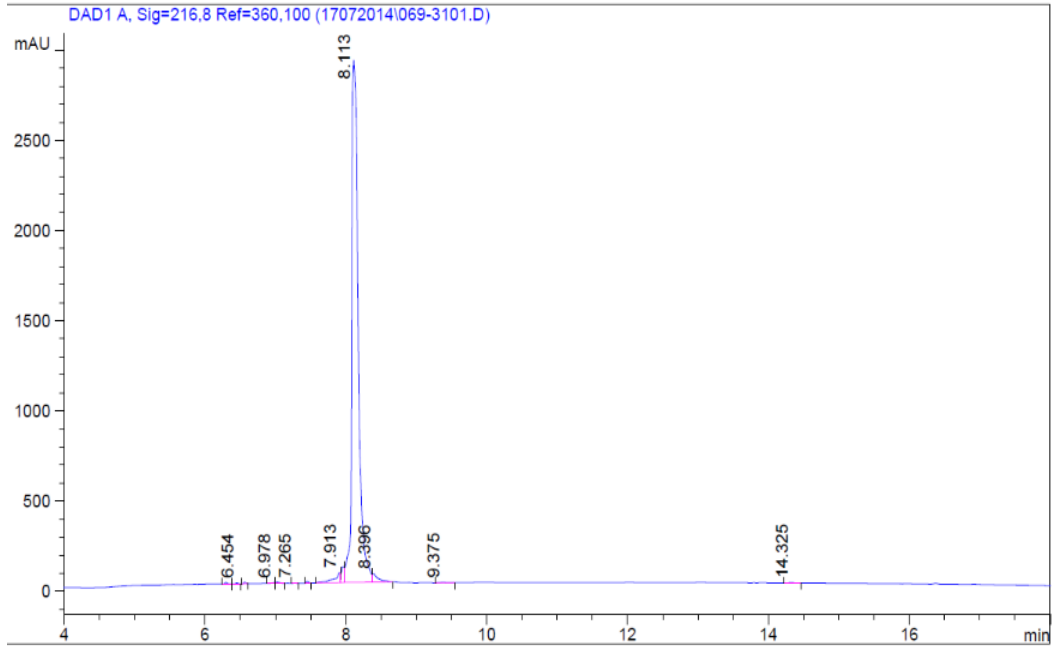


Figure 4.34 HPLC analysis of mature sAvBD6

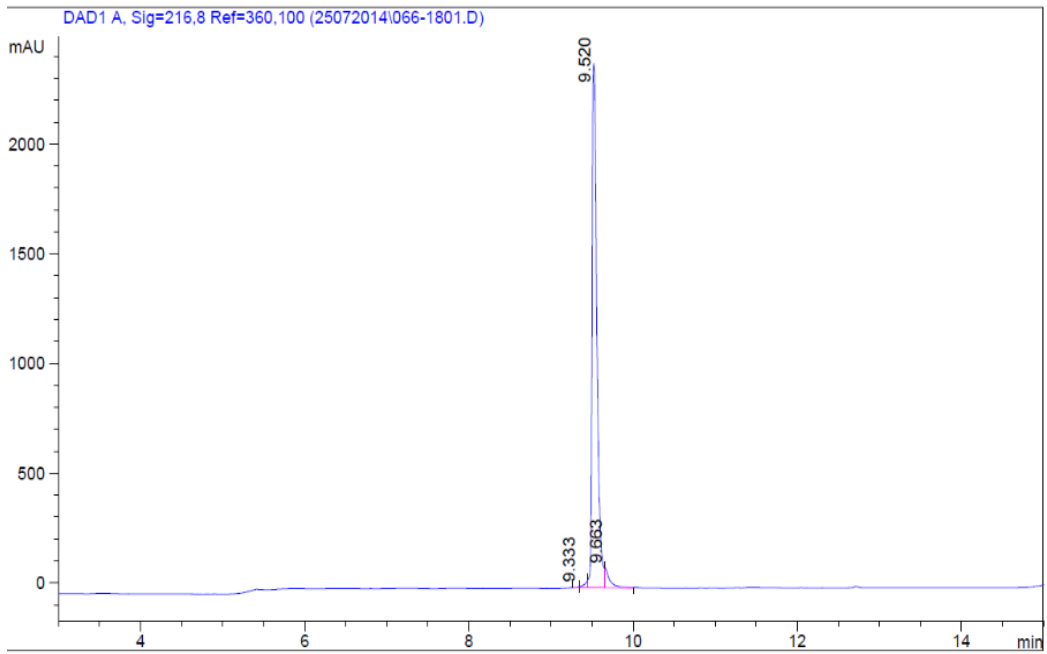


Figure 4.33 HPLC analysis of mature sAvBD9

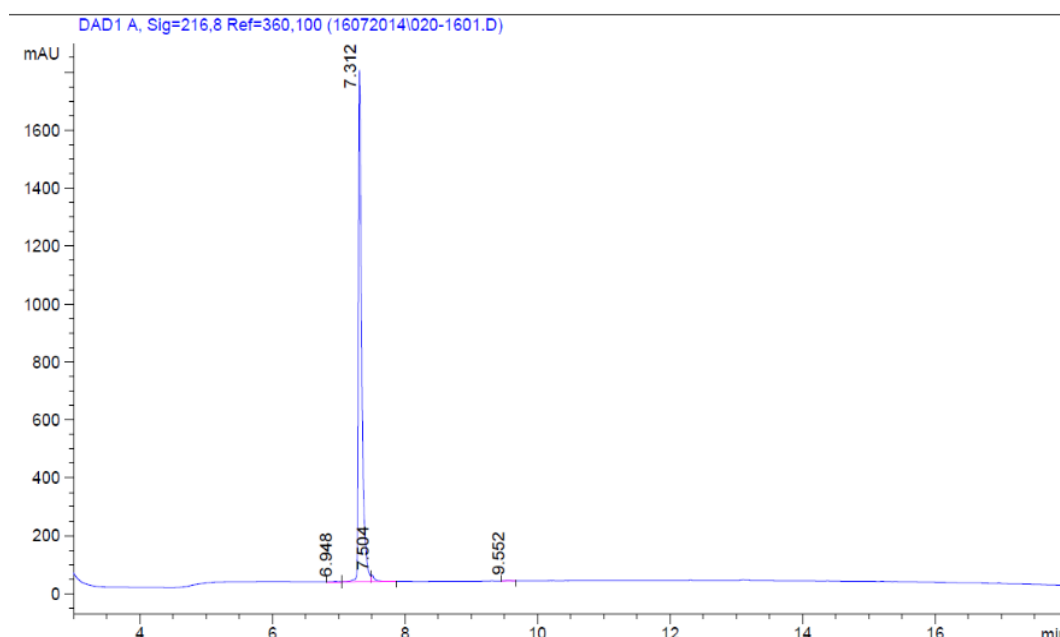


Figure 4.35 HPLC analysis of AvBD9 W38G

4.5.1. Comparison of synthetic and recombinant AvBD6 mature, AvBD9 mature and AvBD9 W38G peptide AMAs against *E. coli*

The AMAs of the synthetic and recombinant peptides against *E. coli* were compared at 50 and 100 µg/ml (Figure 4.36). Using 50 µg/ml (Figure 4.36 A), the recombinant AvBD6 and 9 mature peptides killed 56% and 50% (44.0±2.6 and 51.3±12.4 % survival) of the *E. coli*, but surprisingly the synthetic peptides appeared inactive with *E. coli* survival reproducibly >100%.

This result was also observed at 100 µg/ml, where the *E. coli* survival rates following incubation with the recombinant AvBD mature peptides, AvBD6 and AvBD9 mature, were 31.1±7.3 % (78.9 % killing) and 35.7±7.2 % (74.3 % killing), while the survival rates relating to the synthetic peptides, sAvBD6 and sAvBD9 were again >100% (Panels B and C). Bacterial survival >100% suggested degradation of the synthetic peptides and the bacterial usage of the amino acid/peptide fragments as growth nutrients. A similar pattern (Panel D) was observed using AvBD9 W38G with recombinant (r)AvBD9 W38G killing 19.9 % *E. coli* (80.1±11.6 % survival) while synthetic AvBD9 W38G actually supported bacterial growth (>100% survival).

These data suggested that the synthetic linear AvBD peptides were inactive against *E. coli*.

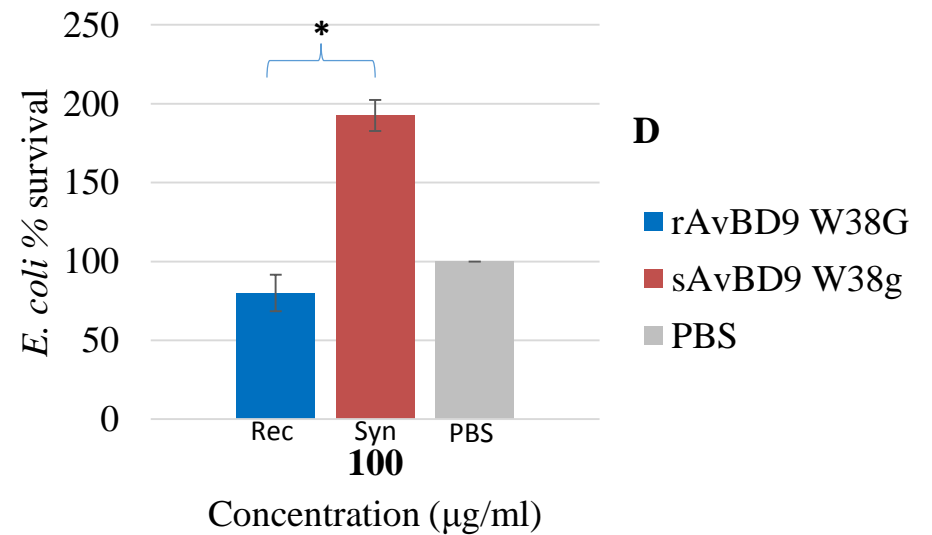
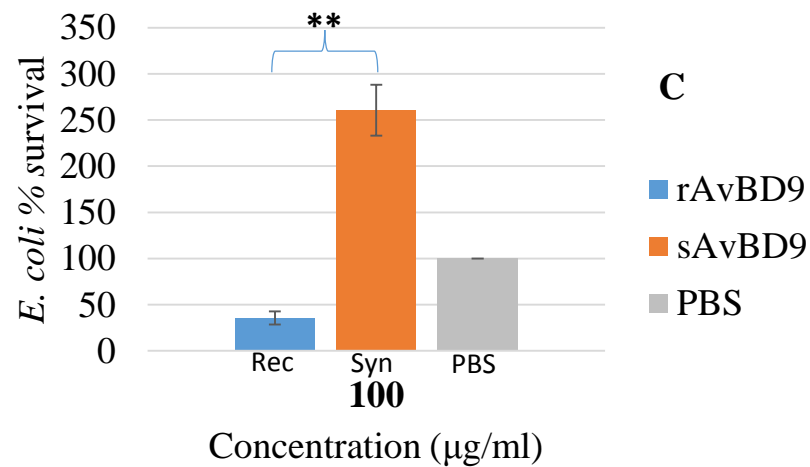
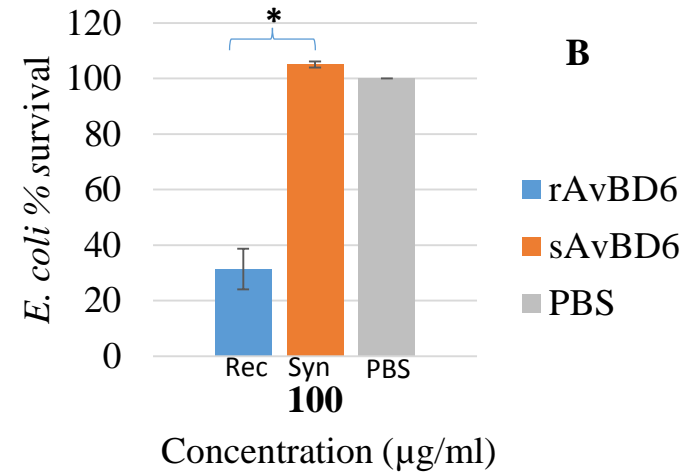
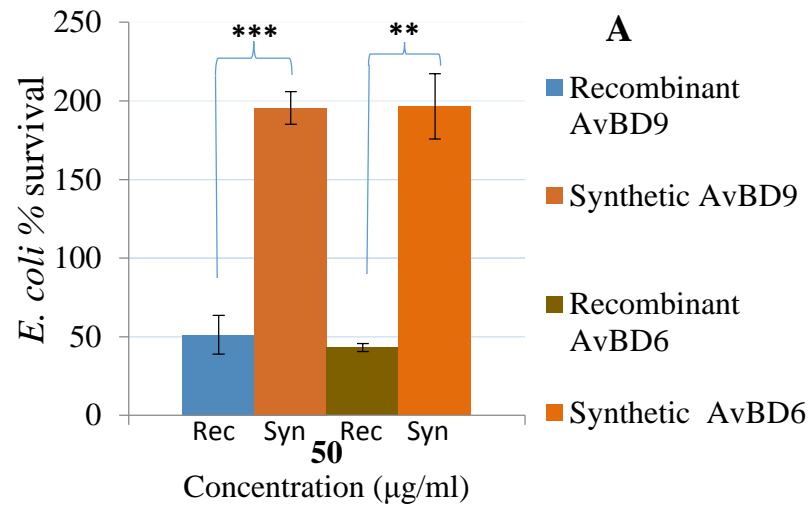


Figure 4.36 Time-kill assay data comparing *E. coli* killing by synthetic and recombinant peptides. AvBDs 6 and 9 at 50 µg/ml (A); AvBD6 at 100 µg/ml (B); AvBD9 at 100 µg/ml (C); AvBD9 W38G at 100 µg/ml (D). Data presented as Mean±SEM. Experiments=2, Replicates=6. *P<0.05, ** P<0.01 and *** P<0.001.

4.5.2. Comparison of synthetic and recombinant AvBD6 mature, AvBD9 mature and AvBD9 W38G peptide AMAs against *E. faecalis*

In contrast to the *E. coli* data, there were no significant differences between the killing activities of the recombinant and synthetic peptides when *E. faecalis* was used in the time-kill assays (Figure 4.37). For example using rAvBD6 and rAvBD9 mature peptides at 50 $\mu\text{g/ml}$, 66.2% (33.8 ± 1.6 % survival) and 53.3 % (46.7 ± 20.1 % survival) *E. faecalis* killing was observed. At the same concentrations, the synthetic peptides, sAvBD6 and sAvBD9 killed 47.5 % (52.5 ± 11.4 % survival) and 19.2 % (80.8 ± 13.9 % survival) *E. faecalis*. These data suggested that both recombinant and linear synthetic AvBDs were active against *E. faecalis* but that the recombinant peptides were the more potent killing agents. However, using synthetic AvBD9 W38G resulted in >100% *E. faecalis* survival. The data using the recombinant peptide supported only weak killing, 15.1 % (84.9 ± 20.5 % survival), which again supported a role for the C-terminal tryptophan in *E. faecalis* killing.

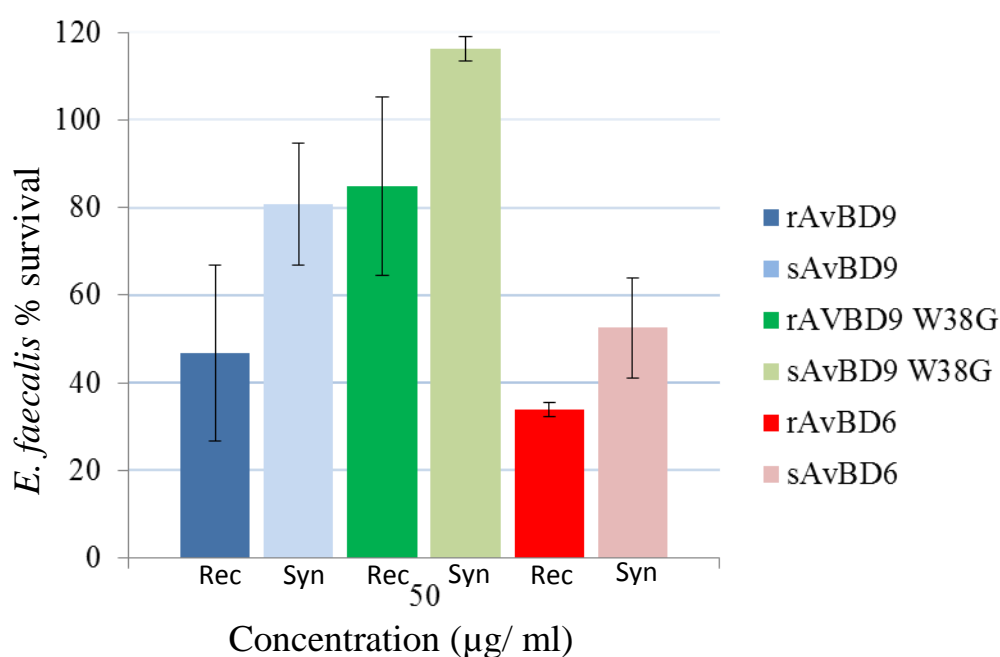


Figure 4.37 Time-kill assay data comparing *E. faecalis* killing by synthetic and recombinant peptides. AvBDs 6 and 9 at 50 $\mu\text{g/ml}$ (A); AvBD6 at 100 $\mu\text{g/ml}$ (B); AvBD9 at 100 $\mu\text{g/ml}$ (C); AvBD9 W38G at 100 $\mu\text{g/ml}$ (D). Experiments=2, Replicates=6. Mean \pm SEM.

4.5.3. Effect of proteases and buffer ionic strength on sAvBD6/9 and rAvBD6/9 AMAs against *E. coli*

Section, 4.5.1 showed that using the synthetic peptides in the time-kill assays involving *E. coli*, resulted in bacterial growth as opposed to killing and suggested that the linear synthetic peptides were easily degraded in the assay. It was hypothesised that this occurred due to production and activity of bacterial proteases with the amino acids, and peptide fragments, exploited nutritionally by the bacteria for growth. That the time-kill assay data supported *E. faecalis* killing by the synthetic peptides (section 4.5.2), suggested that the gram positive bacteria were unable to produce such proteases.

To explore the protease idea further, the *E. coli* BL21 strain, which lacks the outer membrane proteases OmpT and Lon was used in the AMA assays instead of the original *E. coli* clinical isolate. Additionally protease inhibitors were employed as well as sodium phosphate (NaP) buffer (10 mM), which contained no sodium chloride. Sodium chloride has been proposed to reduce the AMA of defensins (Bals *et al.*, 1998; Garcia *et al.*, 2001). The data (Figure 4.38) showed that sAvBD6 (100µg/ml) was inactive ($p < 0.05$) against the chicken *E. coli* clinical isolate compared to rAvBD6 (Panel A). Interestingly however, sAvBD6 was as active as rAvBD6 against *E. coli* BL21, which lacks the two major outer membrane proteases (Panel B). Furthermore, using protease inhibitors (Panels C and D) described in section 2.22, and sodium phosphate buffer (NaP) (Panels E and F) significantly increased the AMA of sAvBD6 and resulted in complete killing of both the clinical and BL21 *E. coli* strains at 100 µg/ml. Less marked effects were observed with the rAvBD6 peptide.

These data suggested that both bacterial proteases and the ionic strength of the assay buffer had negative effects on the AMA of the synthetic but not the recombinant AvBD6 peptide.

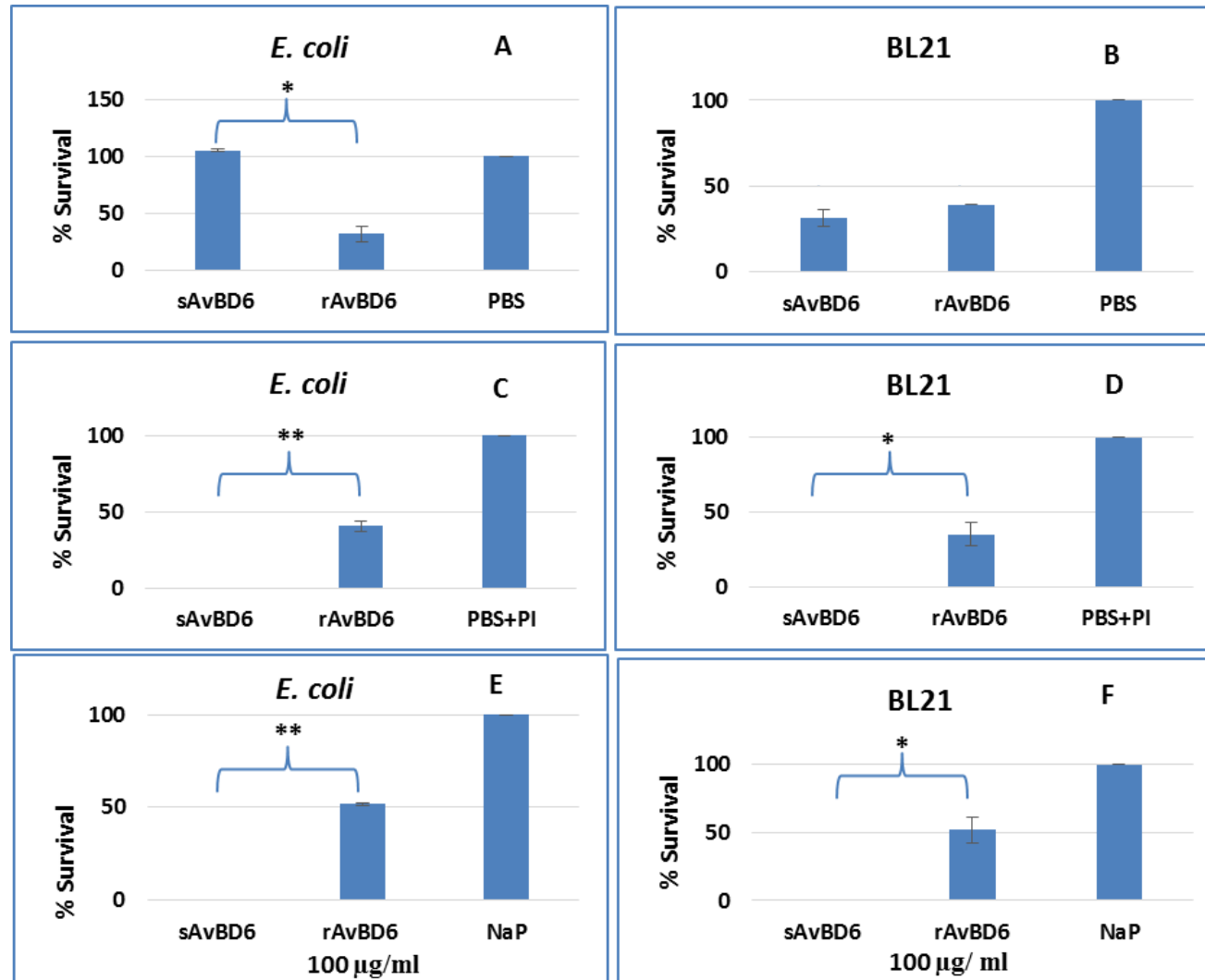


Figure 4.38 Time-kill assay data using 100 µg/ml of synthetic and recombinant AvBD6 peptides against *E. coli* clinical isolate (A, C and E) and BL21 (B, D and F) in PBS (A and B), protease inhibitors (C and D), and sodium phosphate (NaP) buffer 10 mM (E and F). Experiments= 2, Replicates=6 Mean±SEM. *P<0.05 and **P<0.01

Using rAvBD9 and AvBD9 W38G at 100 µg/ml against *E. coli* (Figure 4.24B) detected 64.3 % (35.7±7.2% survival) and 19.9 % (80.1±11.6 % survival) killing, compared to 0% killing using sAvBD9 and sAvBD9 W38G (Figure 4.39, Panel A). However, unlike sAvBD6, sAvBD9 and its variants still showed no AMA against the *E. coli* BL21 strain (Panel B). Moreover, replacing PBS buffer with sodium phosphate buffer (Panels E and F) did not alter the data. This suggested that decreasing the buffer salt concentration had no impact on the AvBD9 killing mechanisms. Using a cocktail of protease inhibitors did not affect the activity of sAvBD9 against the *E. coli* clinical isolate (Panel C), but it did rescue the AMA of the peptide against BL21 (Panel D), with 54.1% (45.9±1.2 % survival) killing recorded. Additionally 12.8 % killing (87.2±7.3 survival) was observed for sAvBD9 W38G respectively (Panel D). These data suggested that proteases, in addition to OmpT and Lon, were involved in the degradation and thus inactivation of sAvBD9. Additionally, the significant difference ($p < 0.05$) in the AMA of sAvBD9 and sAvBD9W38G against BL21 in presence of protease inhibitors (Panel D), suggested that the C-terminal tryptophan does play a role in AvBD9 bacterial killing.

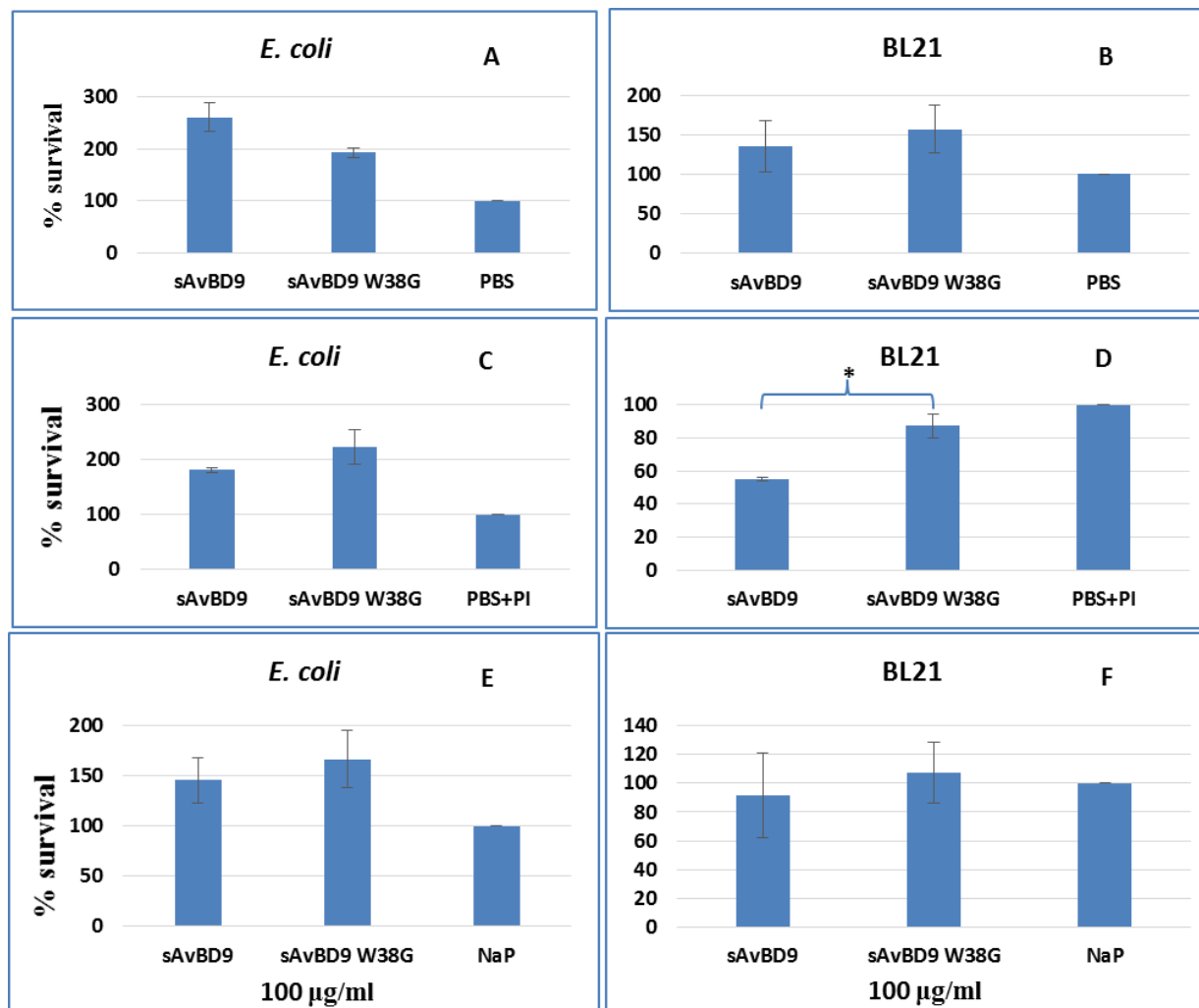


Figure 4.39 Time-kill assay comparing synthetic AvBD9 peptides against *E. coli* clinical isolate (A, C and E) and BL21 strain (B, D and F) in PBS (A and B), protease inhibitors (C and D), and sodium phosphate (NaP) buffer 10 mM (E and F). Experiments=2, Replicates=6 Mean±SEM *P<0.05

4.6. Discussion

The previous chapter indicated that the gut expression of the AvBD6 and 9 genes by Aviagen broiler chickens was not affected by the rearing environment. These data suggested that the encoded defensin peptides were little importance in the host defences and in controlling the gut microbiota.

The AvBD peptides, because of their primary amino acid sequences, which contain six cysteines as well as cationic and hydrophobic residues, are predicted to be antimicrobial agents, but their AMA has still to be proven. Thus the aim of this chapter was to synthesise recombinant AvBD6 and 9 peptides and explore their AMA against Gram negative and Gram positive bacteria, focussing particularly on bacteria isolated from the chicken gut.

The procedure used to produce the recombinant (r) AvBD6/9 peptides involved a GST hyper-expression system and was relatively successful. The recombinant peptides were purified without their GST tags, which compared favourably to other studies in which the researchers utilized GST or His tagged peptides in their peptide functionality studies (Milona *et al.*, 2007; van Dijk *et al.*, 2007; Wang *et al.*, 2010b). During the procedures, rAvBD6 was identified as less soluble than rAvBD9, which was probably due to protein misfolding or partial folding resulting in inclusion body formation (Villaverde and Carrio, 2003), and this made AvBD6 purification challenging. In fact the inability to completely remove GST protein from the AvBD6 peptide preparations (Figure 4.10) was probably due to presence of a large number of both hydrophobic and cationic residues in the peptide affecting its solubility (Figure 4.40) and hence reducing the efficiency of GST cleavage. It was however interesting that the presence of a six hexamer pro-piece increased the yield of AvBD9 (AYSQED) but not AvBD6 (GQPYFS). This was probably due to the presence of aromatic hydrophobic residues (YF) in the latter and anionic residues (ED) in the pro-piece of the former peptide.

AvBD9: AYSQEDADTLACRQSHGSCSFVACRAPSVDI GT CRGGKLCCKWAPSS
AvBD6: GQPYFS SPIHACRYQRGVCIPGP CRWPYYRVGSCGSLKSCCVRNRWA

Figure 4.40: amino acid sequences of AvBD6 and 9. Yellow: cysteine, blue: cationic, red: anionic, green: aromatic hydrophobic, grey: glycine and underline: pro piece

To assess the bacterial killing functions of the recombinant peptides two antimicrobial assays were used. The first, a radial immuno-diffusion assay system used bacterial lawns, involved small amounts of peptide and killing was assessed by observing circles or zones of cleared bacteria (Figure 4.17). The technique involved measuring the diameter of the

zones, and equating each value to bacterial killing, but because of poor assay reproducibility, often due to the thickness of the bacterial lawn, it was difficult to quantitate the resultant data. Thus this method was very subjective and qualitative. Therefore, a quantitative time-kill colony counting assay (Townes *et al.*, 2004) was used to confirm all the data. All peptide variants were successfully tested and their bacterial killing properties compared using this method.

Previous work has suggested that the pro-piece of an AMP, which is generally anionic, reduces the AMA of the peptide, for example mouse α -defensin, cryptdin-4 (Figueredo *et al.*, 2009). In fact *in vivo*, pro-pieces are generally cleaved to activate the peptide (Lynn *et al.* 2004, van Dijk *et al.* 2008). However, the predicted pro-pieces of the AvBDs are either absent or small (6 amino acids) and to date it is not known whether or not they are cleaved *in vivo* (Xiao *et al.* 2004, van Dijk *et al.* 2007). However, the fact that the AMAs of the promature and mature (no pro-piece) AvBD6 and 9 peptides were similar against *E. coli* (Figures 4.22 and 4.24) probably relates to the small sizes of each pro-piece and the rarity of negatively charged amino acids reducing the anionic charge. Moreover, these two pro-pieces contain hydrophobic amino acids e.g., A, F, P and Y that may function in facilitating membrane perforation and disruption (Soman *et al.*, 2010; Tai *et al.*, 2014).

AvBDs, like all β -defensins, have six conserved cysteines, which are reported as necessary for structural conformation (van Dijk *et al.*, 2008). However, their contribution to peptide antimicrobial activity is still debatable (Maemoto *et al.*, 2004; Chandrababu *et al.*, 2009; Derache *et al.*, 2012; Zhao *et al.*, 2012). It was not known whether the rAvBD6 and AvBD9 peptides synthesised in this study and containing 6 Cys (C) were correctly folded ie C1-C5, C2-C4 and C3-C6. None-the-less, mutagenising three of the cysteines of AvBD9 ie C1, C2 and C6 to alanines did not affect its AMA profile (Figures 4.24 and 4.27). As the mutagenesis did not significantly affect the charge of the peptide (+3.8 to 4) (Innovagen peptide property calculator: <http://pepcalc.com/>), the data suggested that a correctly folded structure is not essential for AMA. Following mutagenesis, each AvBD9 3CA peptide had 3C and based on the report of a mouse defensin, Defr1 with 5 cysteines it was predicted that two of these 3C could form, naturally an internal di-S bond leaving one free C (Campopiano *et al.*, 2004). The free C of one AvBD9 3CA molecule could then form a disulphide bond with the free C of another AvBD9 3CA molecule, thus creating a dimer molecule (Figure 4.41). Gel electrophoresis (Figure 4.26) confirmed this occurred *in vitro* and these data suggested the dimer molecules were contributing to the observed AMA. This

was further supported by the fact that removal of all cysteines resulted in reduced *E.coli* killing (Figure 4.24). Yet, the AvBD9 6CA/G peptide was still active against *E. faecalis* (Figure 4.27), which suggested that peptide folding was more important for AvBD9 AMA against gram negative than gram positive microbes. Interestingly, this result contrasted to that found for AvBD2, in which disulphide bonds were required for its AMA against gram positive compared to gram negative bacteria (Cuperus *et al.*, 2013). Collectively, these data indicate that the impact of the C amino acids on the functionality of the AvBDs cannot be generalised. Folding however produces a globular molecule that is more protected than a linear one from proteolysis caused for example by bacterial proteases. Indeed data relating to the AMA of linear AMP peptides may reflect the ability of the bacteria studied to synthesise degradative proteases.

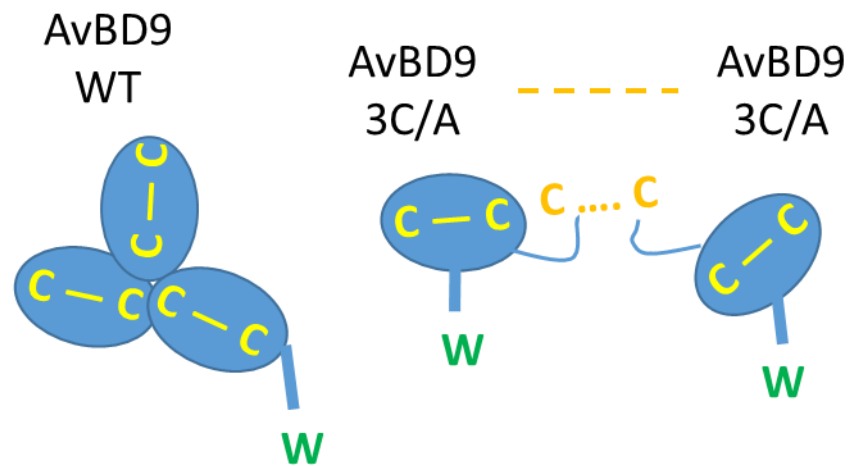


Figure 4.41: Predicted inter molecular disulphide bonds between two monomers of AvBD9 3CA leading to dimer formation

The identification of evolutionarily conserved amino acids has been linked to the functional activity of the defensin peptides (Yeaman and Yount, 2003). Interestingly, the four amino acids, CCKW, located at the C-terminal end of AvBD9 (Figure 4.12) also appear conserved in the predicted AvBD9 peptide sequences of other avian species including pheasant and quail (Kannan *et al.*, 2013). Moreover, ten out of the 14 AvBDs have a C-terminal tryptophan (Figure 4.12) suggesting a critical role for this amino acid in AMP function. Additionally as the C-terminal location of the tryptophan promotes its flexibility and the fact that tryptophans are known to help anchor peptides into membranes which facilitates membrane permeation (Kluver *et al.*, 2005; Kim *et al.*, 2013) argues strongly for a role of

the C-terminal tryptophan (W38) in AvBD9 AMA. In fact the argument strengthens as mutagenising the C-terminal W in the mature peptide to a glycine resulted in the loss of AvBD9 AMA (Figures 4.24 and 4.27). Disappointingly, however, engineering AvBD10 to contain a C-terminal tryptophan did not enhance its AMA properties. Only AvBDs 8, 10, 12 and 13 do not contain a C-terminal tryptophan and interestingly all have charge at pH7 of ≤ 2 . Previous studies have shown baseline AvBD10 expression to be significant in tissues such as the kidney and testes (Butler, 2010), that are not exposed continuously to microbes, thus it is feasible that an increased overall charge is just as important as a C-terminal tryptophan in AMA and both together are not required for AvBD AMA.

The inability to completely purify AvBD6 prompted the use of custom synthesised peptides, the disadvantage being that the peptides were supplied as linear and not pre-folded molecules. Surprisingly, however, when the synthetic peptides were used against *E. coli* they appeared pro-microbial (Figure 4.36) ie supporting rather than decreasing bacterial growth, although antimicrobial activity was detected against *E. faecalis* (Figure 4.37).

Previous studies have found that there are several mechanisms through which microbes, particularly human pathogens, can acquire resistance to AMPs and one such mechanism is the secretion of proteolytic enzymes that degrade linear peptides (Nizet, 2006). For example, the heat shock serine protease DegP increases the survival of *E. coli* and *S. aureus* against killing by Lactoferricin B (Ulvatne *et al.*, 2002; Yeaman and Yount, 2003). Similarly, the outer membrane protease, OmpT, also plays an important role in the degradation of AMPs with an *E. coli* OmpT mutant strain showing increased sensitivity to protamine (Yeaman and Yount, 2003). In this study, the promicrobial data suggested proteolytic degradation of the linear peptides by enzymes synthesised by the chicken gut *E.coli* isolate and the use of the resultant amino acids as a nutrient supply. This was supported by the sAvBD6 killing of protease (OmpT and lon) negative *E.coli* mutant strains and these data also highlighted potential pathogenicity factors ie proteases, synthesised by the chicken *E.coli* isolate.

Two studies have examined the impact of high salt buffers on the antimicrobial properties of AvBDs. For example, a high salt concentration (150 mM NaCl) reduced the AMAs of duck AvBD1, 3, 5, 6, and 16 against *Micrococcus tetragenus* and *Pasturella multocida*, and geese AvBD1, 3 and 6 against *S. aureus* and *P. mirabilis* (Ma *et al.* 2012, Ma *et al.* 2013). Similarly, synthetic linear ostrich AvBD2 and 7 showed decreased AMA at 100 mM, and no AMA at 150 mM, salt concentration, against *E. coli* and *S. aureus*, and to

explain this the authors suggested the ionic strength of the buffer was inhibiting peptide binding to the bacterial membrane (Lu *et al.*, 2014). In this study, a similar effect was noted for AvBD6 as the linear synthetic AvBD6 exhibited reduced AMA in PBS compared to NaP buffer although this effect was not observed for sAvBD9. It is difficult to explain these data but may relate to the high charge (+7) of the AvBD6 peptides at pH 7. Interestingly the AMA of folded AvBD9 against both Gram positive and negative bacteria has been reported to be inactivated in high salt (150 mM), but rescued using sodium phosphate buffer (10 mM) or low salt buffer (20 mM) (van Dijk *et al.*, 2007). However, the rAvBD9 used in this study and presumably at least partially folded, was highly active against *E. coli* in PBS (Figure 4.24).

4.7. Conclusions

rAvBD6 and 9, both promature and mature peptides, were hyperexpressed and purified *in vitro* and shown to have AMA against two isolates, Gram negative *E. coli* and Gram positive *E. faecalis*, isolated from the chicken GI tract.

The synthesis and purification of mutant peptides AvBD9 3CA, AvBD9 6CA/G, AvBD9 W38G, indicated the functional importance of the cysteine and C-terminal tryptophan amino acids in AMA.

rAvBDs 6 and 9 were shown to have AMA against bacteria isolated from the chicken gastrointestinal tract thus supporting their *in vivo* roles as host defence molecules.

The next chapter will investigate the secondary structure and membrane disruptive ability of the AvBD6 and 9 using CD spectra and calcein-entrapped liposomes.

Chapter 5

5. AvBD structure-membrane interactions (Part I)

5.1. Introduction

In Chapter four, AvBDs 6 and 9 were shown to have antimicrobial activity against *E. coli* and *E. faecalis*. Moreover, the data using recombinant and chemically synthesised peptides suggested the importance of the disulphide bonds, and the C-terminal tryptophan in AvBD killing.

Cationic peptides have been reported as killing microbes through mechanisms involving membrane interactions that can be described by one or more of four models namely the aggregate, toroidal pore, barrel stave and carpet models (Jenssen *et al.*, 2006). Fundamentally each model exploits the cationic and hydrophobic amino acid structure of the AvBDs; the cationic charge facilitates electrostatic interaction with negatively charged bacterial membranes and the hydrophobicity enables insertion of the defensin molecule into the membrane causing its disruption and bacterial cell death (Jenssen *et al.*, 2006).

To further explore the actual interactions of AvBD6 and 9 with bacterial cell membranes *in vitro* models were adopted. The first *in vitro* system utilised sodium dodecyl sulphate (SDS), which forms a negatively charged micelle that mimics the microbial membrane. The AvBD peptides were each mixed with the micelles and any structural changes occurring in the peptides following this interaction were determined using circular dichroism (CD).

The second *in vitro* system, known as a calcein leakage assay, used calcein entrapped liposomes to explore the membrane destructive ability of the AvBD peptides. The liposomes used in this study represented a mixture of phospholipids including phosphatidylcholine, phosphatidylethanolamine and inositol phosphatides, a class of phosphatidylglycerol, with the latter two phospholipids being major components of the *E. coli* lipid membrane (Ruiz *et al.*, 2006). Calcein is a self-quenched fluorescent dye, which can be trapped inside the liposomes and its release, following peptide addition, is detected using fluorimetry.

The aim of this chapter was to use the *in vitro* systems described to further explore the mechanisms underpinning the microbial killing properties of AvBD6 and 9. This work was performed in collaboration with Professor Jeremy Lakey (Newcastle University).

5.2. Secondary structure-membrane interaction activities of recombinant AvBD9 peptides

The reduced purity of rAvBD6, caused by GST contamination (Figure 4.10), meant that rAvBD6 could not be used in any of the following analyses. However, the structure/membrane interactions of rAvBD9, rAvBD9 3CA, rAvBD9 6CAG and rAvBD9 W38G were investigated using (i) SDS micelles and CD analyses and (ii) leakage assays employing calcein entrapped liposomes.

5.2.1. CD spectra of recombinant AvBD9 peptides

The freeze dried rAvBD9 peptides were reconstituted in water to 500 µg/ml, mixed with either 50mM sodium phosphate buffer (NaP) or 1% SDS at a final peptide concentration of 250 µg/ml and the CD spectra measured using a Jasco-810 CD spectropolarimeter at a range (250-185nm). The CD measurements of the machine (θ) in millidegree were changed to delta epsilon ($\Delta\epsilon$), which is the per residue molar absorption unit ($M^{-1}cm^{-1}$) directed by the following equation:

$$\Delta\epsilon = \theta X (0.1 * MRW) \\ (P * CONC) * 3298$$

Mean residue weight ((MRW) =protein mean weight (in atomic mass units/ daltons)/ number of residues) for the protein, path length (P) in cm and protein concentration (CONC) in mg/ml: (<http://dichroweb.cryst.bbk.ac.uk/html/userguide.shtml>).

Typical peptide conformations are shown in Figure 5.1 (Woody, 2010). An α -helix displays as two negative absorption bands at 208 and 222 nm, and a positive absorption band below 200 nm (Line A). A β -sheet structure displays as a negative absorption band at 217 nm and a positive absorption band below 200 nm (Line B). A β -turn structure displays a broad negative absorption band between 205-220 nm and a positive absorption band at 200 nm (Line C). Unordered peptides display as a positive absorption band at 212 nm and a negative band at 195 nm (Line D).

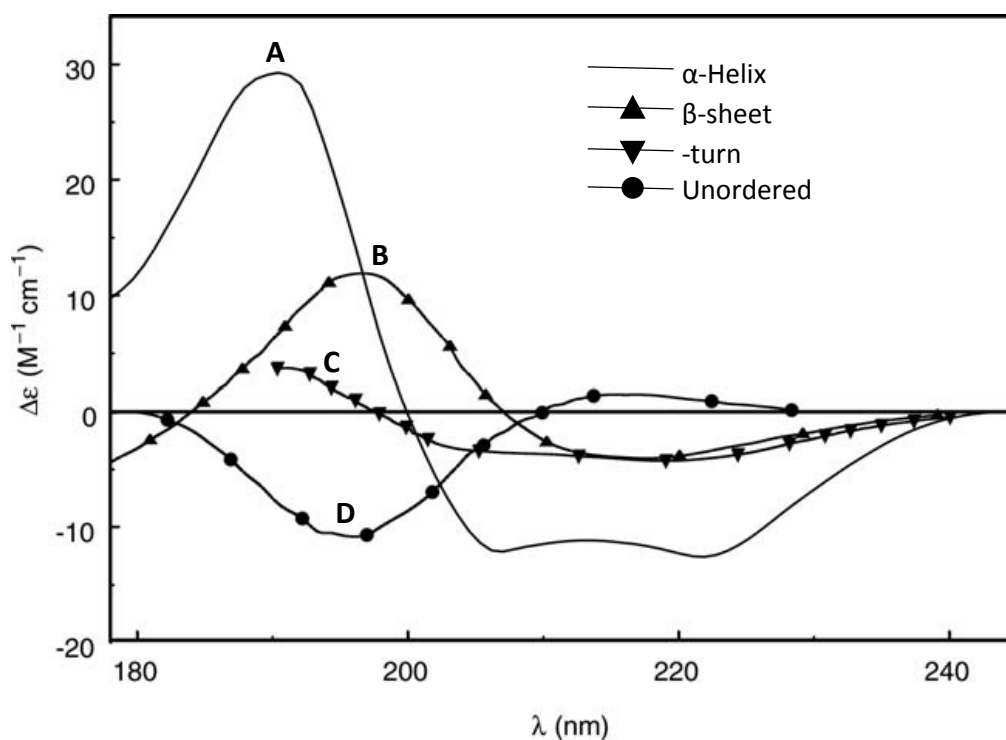


Figure 5.1 CD spectra of standard peptide conformations A-helix (A), β -sheet (B), type I β -turn (C), Unordered (D). (Woody, 2010).

The CD spectrum of rAvBD9 mature peptide (blue) (250 $\mu\text{g/ml}$) in 50 mM NaP buffer is shown in Figure 5.2 A. The spectrum displays as a broad negative absorption band from 195 to 215 nm with maximum absorption at 203 nm ($-2.5 \text{ M}^{-1}\text{cm}^{-1}$). These data suggested that the peptide was folded and contained a mixture of β -sheet, α - helices, β -turns and unordered structures. The CD spectra also supported the rAvBD9 3CA peptide (red) being more folded than either the rAvBD9 W38G (purple) or rAvBD9 6CA/G (green) peptides. This was deduced because rAvBD9 3CA showed maximum absorption at 200 nm ($-4.3 \text{ M}^{-1}\text{cm}^{-1}$), while the latter peptides rAvBD9 W38G and rAvBD9 6CA/G both displayed maximal absorption at 199 nm ($-5.2 \text{ M}^{-1}\text{cm}^{-1}$) and ($-7.0 \text{ M}^{-1}\text{cm}^{-1}$) respectively.

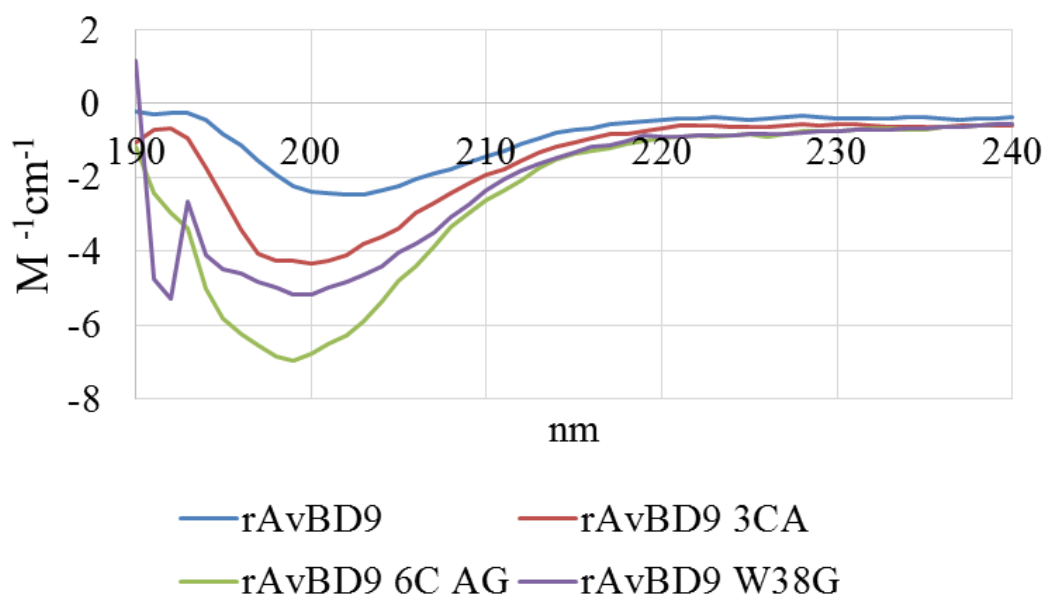


Figure 5.2 CD spectra of recombinant AvBD9 variants in 50 mM Na P buffer

To quantitate the secondary structures of the rAvBD9 peptides an online software programme, Dichroweb (<http://dichroweb.cryst.bbk.ac.uk/html/process.shtml>), was used (Whitmore and Wallace, 2004; Whitmore and Wallace, 2008) as described in Section 2.24. The results are shown in Table 5.1 and Figure 5.2 B.

These data supported folding of the rAvBD9 mature peptide and predicted 52.4 % β -sheet, 19.4 % α -helix, 20.2% β -turns and 7.9% unordered structure. In comparison rAvBD9 3CA, which contains only three cysteines was predicted to contain 29.6 % β -sheet and 31.7% unordered structure, which suggested only partial folding of the peptide. Interestingly, these data were comparable to that of rAvBD9 W38G, which contained all six cysteine amino acids. The CD spectra data indicated 40.1% unordered structure for the rAvBD9 6CAG variant. The lack of cysteines was therefore associated with a predominantly disordered structure.

Peptides	α -Helices %	β -Strands %	β -Turns %	Unordered %
rAvBD9	19.4	52.4	20.2	7.9
rAvBD9 3CA	15.5	29.6	23.2	31.7
rAvBD9 6CAG	12.9	24.4	22.5	40.1
rAvBD9 W38G	12.1	27.7	24.7	35.4

Table 5.1 Dichroweb quantification of CD secondary structures (%) including α -helices, β -strands, β -turns and unordered structure following exposure of rAvBD9 variants to 50 mM NaP buffer.

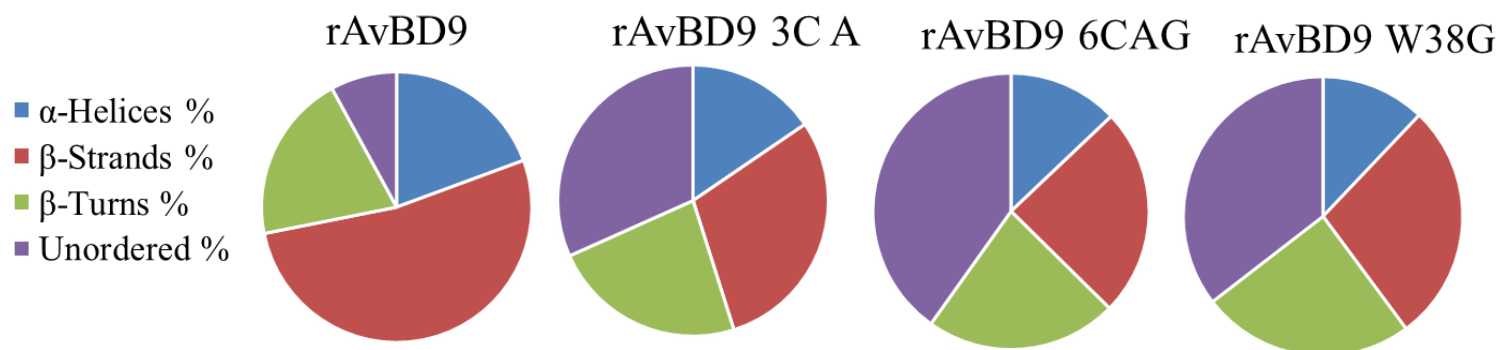


Figure 5.2 B: Pie charts showing quantification of CD secondary structures (%) including α -helices (Blue), β -strands (Red), β -turns (Green) and unordered (Purple) following exposure of rAvBD9 variants to 50 mM NaP buffer.

Sodium dodecyl sulphate (SDS) is an anionic detergent, which spontaneously forms micellar structures each with a hydrophobic core and hydrophilic exterior thereby mimicking the negatively charged phospholipid bilayer of bacterial membranes (Lindberg and Graslund, 2001). Therefore, to investigate AvBD peptide interactions with bacterial membranes, the rAvBD peptides were exposed to 30 mM (1%) SDS micelles (section 2.24) as described previously (Hu *et al.*, 2013; Bi *et al.*, 2014).

The resultant data are shown in Figure 5.3 A. Qualitatively both rAvBD9 mature (Blue) and rAvBD9 3C A (Red) displayed disordered structures as evidenced by the absorption bands ($-6.9 \text{ M}^{-1}\text{cm}^{-1}$) and ($-10.1 \text{ M}^{-1}\text{cm}^{-1}$) detected at 197 nm. In contrast, rAvBD9 6CAG (Green) showed absorption bands at 201 nm ($-11.7 \text{ M}^{-1}\text{cm}^{-1}$) and 222 nm ($-3.6 \text{ M}^{-1}\text{cm}^{-1}$) respectively, indicating the ability of these peptides, lacking disulphide bonds, to adopt an α -helical conformation. However, the secondary structure of rAvBD9 W38G (Purple) was comparable to previous observations (Figure 5.2) with its maximum absorption, $-8.9 \text{ M}^{-1}\text{cm}^{-1}$, recorded at 200 nm.

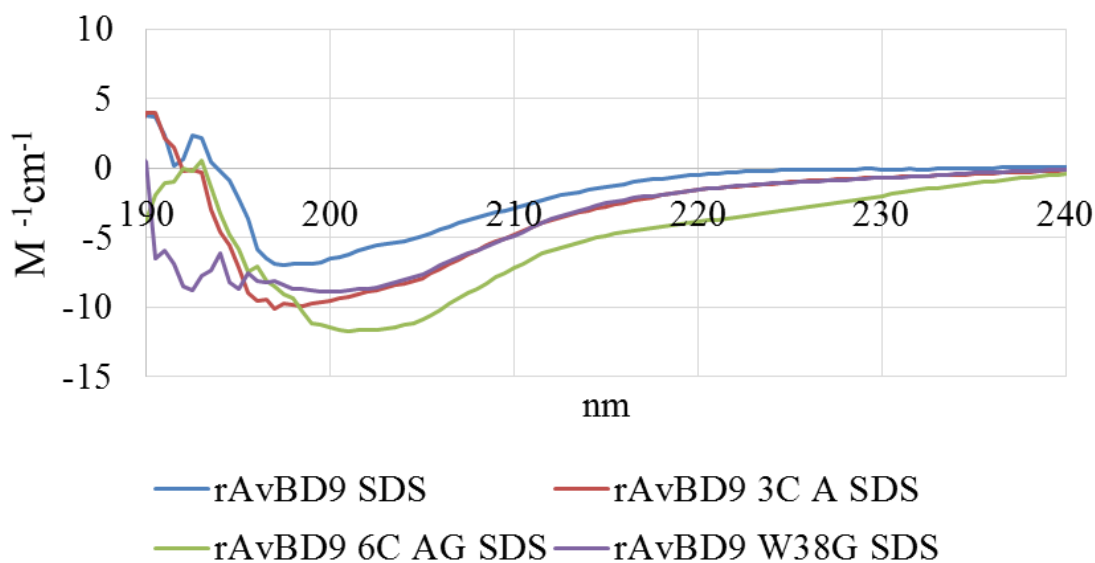


Figure 5.3 A: CD spectra of recombinant AvBD9 variants in 1% SDS micelles

Quantification of the CD data is shown in Table 5.2 and Figure 5.3 B. These data showed that in the presence of the SDS micelles the β -strand component of rAvBD9 was reduced from 52.4 to 31.3 % while the unordered structure increased from 7.9 to 31.9 %. These values therefore indicated that exposure to the SDS micelles disrupted the disulphide bonds of the rAvBD9 molecule. Interestingly, mixing rAvBD9 6CAG with the micelles resulted in β -strand component of 8.6%, which was three to four times less than the other AvBD9 variants, but an α -helix structural component of 35.9%, which was three times higher. The secondary structures of rAvBD9 3CA and rAvBD9 W38G remained relatively unchanged in the presence of the SDS micelles.

Peptides+SDS	α -Helices %	β -Strands %	β -Turns %	Unordered %
rAvBD9	13.6	31.3	23.2	31.9
rAvBD9 3CA	13.8	33.1	19.3	33.8
rAvBD9 6C AG	35.9	8.6	21.8	33.7
rAvBD9 W38G	11.8	25.1	23.8	39.5

Table 5.2 Quantification of CD secondary structures (%) including α -helices, β -strands, β -turns and unordered structure following exposure of rAvBD9 variants to 1% SDS micelle solution.

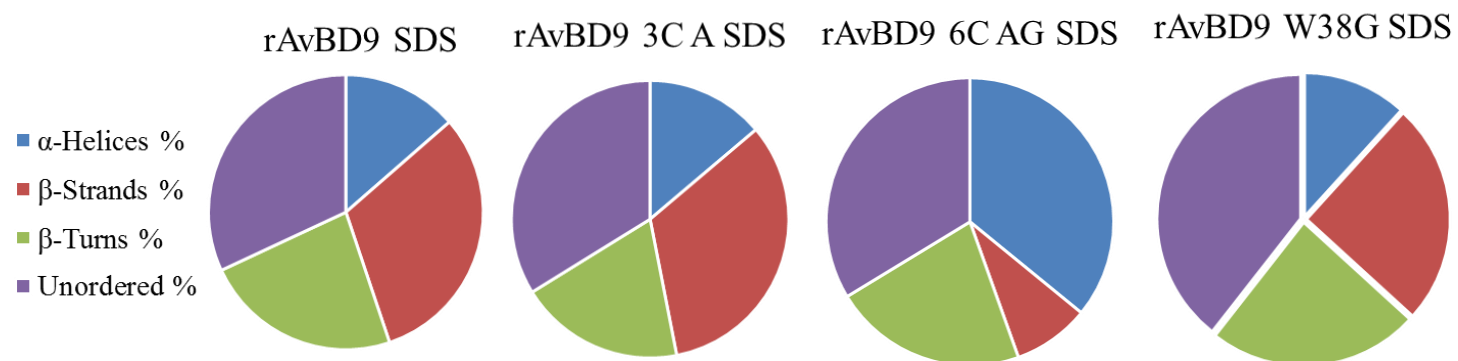


Figure 5.3 B: Pie charts showing quantification of CD secondary structures (%) including α -helices (Blue), β -strands (Red), β -turns (Green) and unordered (Purple) following exposure of rAvBD9 variants to 1% SDS micelle solution.

5.2.2. Investigations of rAvBD9 peptide/ bacterial membrane interactions using calcein leakage assays

Focussing specifically on the membrane destructive activities of the peptides, rAvBD9 and the variants rAvBD9 3CA, rAvBD9 6CA/G and rAvBD9 W38G (10 µg/ml), were exposed to calcein dye-entrapped liposomes prepared with phospholipids to resemble the *E. coli* lipid bilayer (Section 2.23). The liposomes were incubated with the rAvBD9 peptides and any calcein leakage monitored using a Varain fluorescent spectrophotometer set to excitation (493 nm) and emission (505-600nm). The positive control was Triton X-100 (1% final concentration).

As shown in Figure 5.4A, there was no detectable calcein leakage from the liposomes during a 60 min incubation period in 50mM NaP at room temperature. These data indicated that the calcein loaded liposomes were stable up to a minimum of one hour. Figure 5.4 Panel B shows the results of adding Triton X to the liposomes to a final concentration of 1%. Immediately on adding the detergent the calcein leakage changed from 42.5 AU, which was considered as 0 % leakage to 94.7 AU, which was stable up to 5 minutes and regarded as 100% leakage.

The experiments were repeated using the rAvBD9 peptides and the following equation was used to calculate any leakage.

$$\text{Leakage \%} = (F_p - F_0) / (F_t - F_0) * 100\%$$

Where F_p is the measurement of fluorescent leakage after treating the calcein entrapped liposomes with the peptides, F_t is the complete leakage measurement by TritonX and F_0 is intact vesicles before adding peptide or TritonX (Bi *et al.*, 2013).

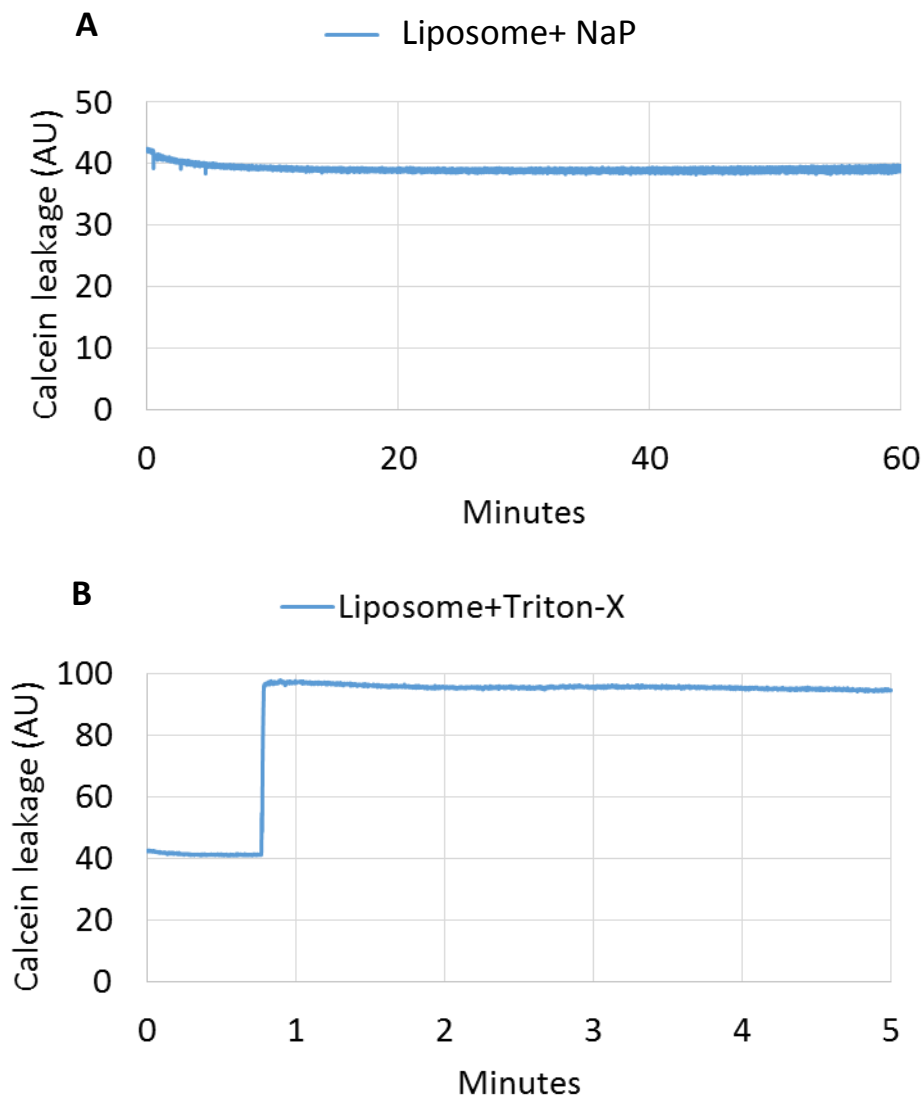


Figure 5.4 Calcein leakage recorded using entrapped liposomes incubated for 60 minutes at room temperature in 50 mM NaP buffer (A); following the addition of 10 % Triton X 100 (1% final concentration) (B).

The results of the calcein leakage assays at 2 to 5 minutes following the addition of the rAvBD9 peptides (10 µg/ml final concentration) are shown in Figure 5.5. Calcein leakage (mean) within two minutes of peptide addition were: AvBD9 (4.7%), AvBD9 3CA (4.9%), AvBD9 6CAG (3.0%) and AvBD9 W38G (2.7). Within 5 minutes the leakage values were AvBD9 (14.4%), AvBD9 3CA (15.5%), AvBD9 6CAG (12.6%) and AvBD9 W38G (13.3%). These data were characterised by poor reproducibility and no differences between the peptides were detected.

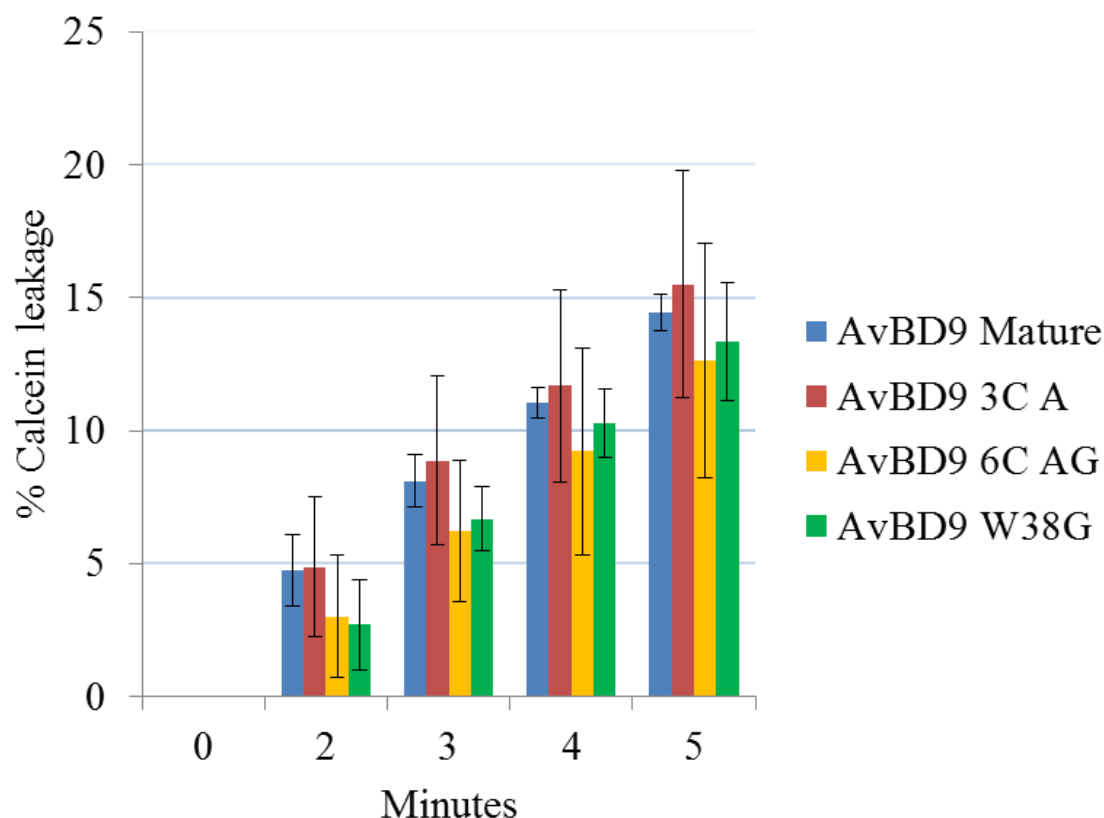


Figure 5.5 Calcein leakage assay following addition of rAvBD9 and variants to dye-entrapped liposomes. Mean (range). Experiments=2; replicates=2.

5.3.Secondary structure-membrane interaction activity of synthetic AvBDs

The CD spectra described in section 5.2.1 suggested that changes in rAvBD9 and rAvBD9 6CAG peptide secondary structures were associated with the peptides interacting with target membranes. It was therefore disappointing that the leakage assay data did not differentiate between any of the rAvBD9 peptides. However, these assay data were compromised by large error bars that may have masked any significant differences. The reasons for the large error bars were not known, but the actual purity of the rAvBD9 peptides, which were not HPLC purified, was a concern. It was also frustrating that due to purity issues rAvBD6 secondary structure and membrane interaction properties could not be analysed.

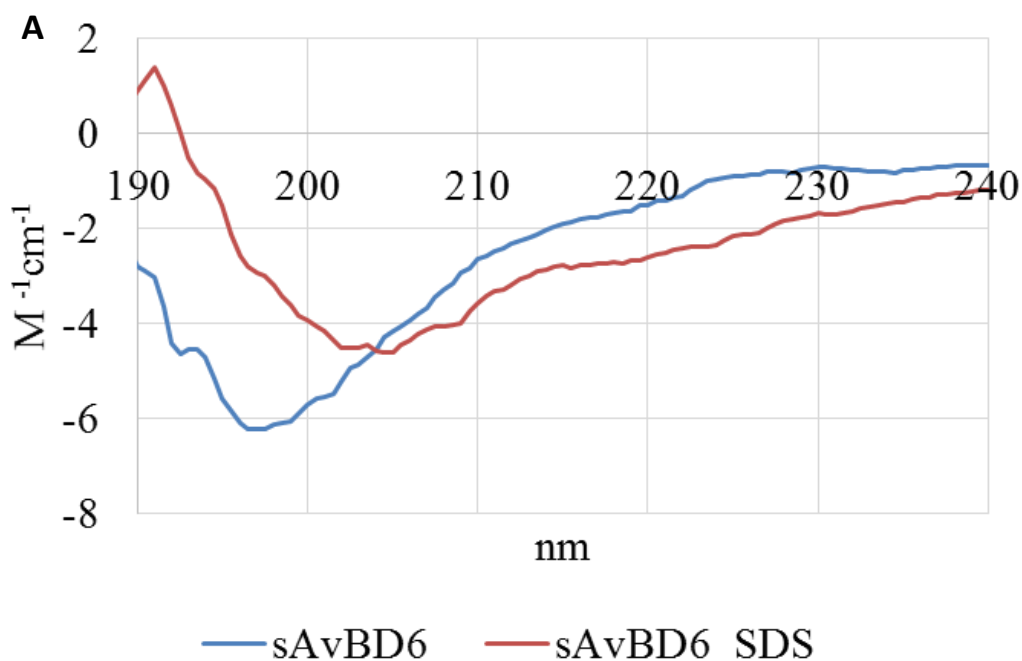
It was therefore decided to use the AvBD6 and 9 synthetic peptides whose purity was guaranteed to further explore the potential activity of the AvBDs to cause membrane damage and hence cytoplasmic leakage.

5.3.1. Circular dichroism of the synthetic peptides

Although it was acknowledged that the sAvBD6, sAvBD9, sAvBD9 W38G peptides were in a linear rather than folded form they were subjected to and analysed by CD as previously described for the recombinant peptides.

5.3.1.1. CD spectra for synthetic AvBD6 peptide

The CD spectrum for sAvBD6 (250 $\mu\text{g}/\text{mL}$) in NaP buffer and shown in Figure 5.6 (blue line) revealed a disordered structure (38.4%) with a negative absorption band at 197.5 nm ($-6.2 \text{ M}^{-1}\text{cm}^{-1}$) although β -sheet (25.9%) and β -turn secondary structures (25.1%) were also predicted. However, in the presence of SDS micelles mimicking the bacterial membrane (red line) the sAvBD6 structure was characterised by two negative absorption bands at 204.5 nm ($-4.6 \text{ M}^{-1}\text{cm}^{-1}$) and 220 nm ($-2.6 \text{ M}^{-1}\text{cm}^{-1}$), and a single positive band at 191 nm ($+1.4 \text{ M}^{-1}\text{cm}^{-1}$), which predicted a mix of α -helix (25.6%), disordered (33.9%) and β -turn (23.6%) secondary structure conformations.



B

Peptides	Helices%	β -Strands %	β -Turns %	Unordered %
sAvBD6	10.8	25.9	25.1	38.4
sAvBD6 SDS	25.6	17.0	23.6	33.9

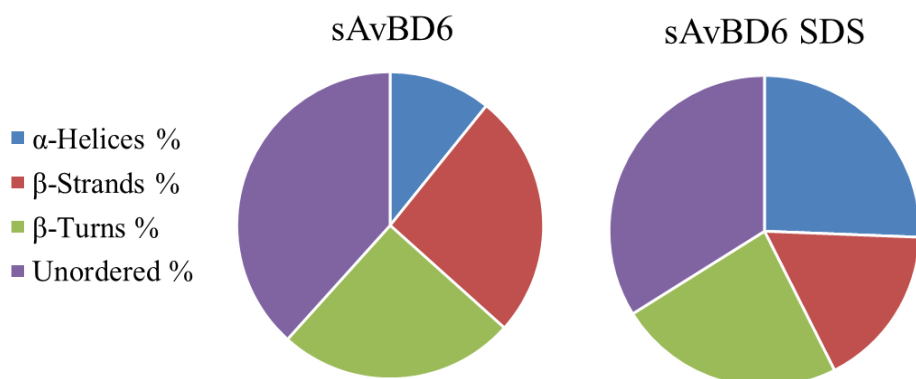
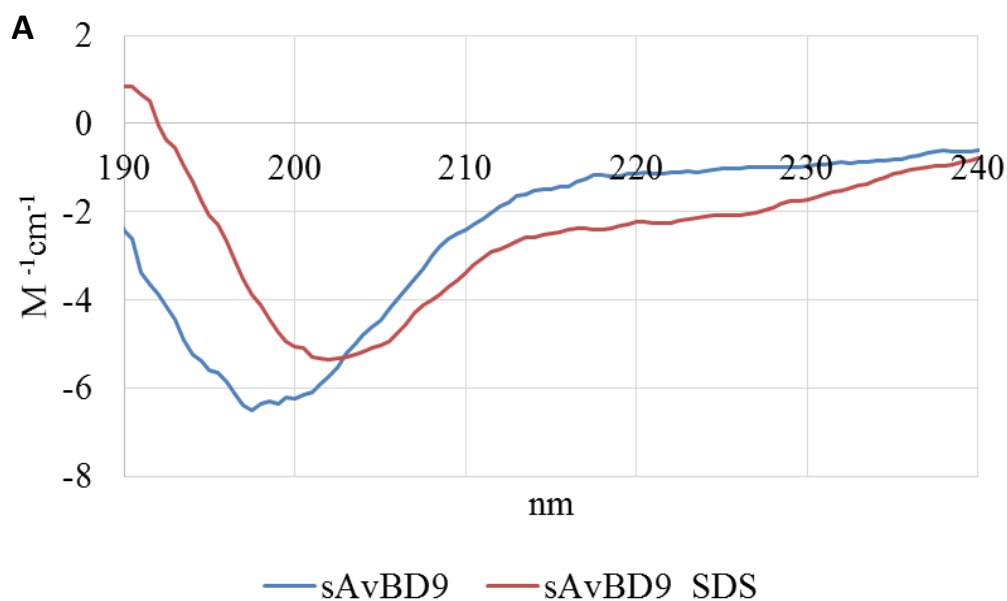


Figure 5.6: A: CD spectra of sAvBD6 in NaP buffer (Blue) and 1% SDS micelle solution (Red).

B: Table and Pie charts show quantification of CD secondary structures (%) including α -helices (Blue), β -strands (Red), β -turns (Green) and unordered (Purple) following exposure of sAvBD6 to NaP and 1% SDS micelle solution.

5.3.1.2. CD spectra for synthetic AvBD9 variants

The CD spectra for sAvBD9 (250 $\mu\text{g/mL}$) in NaP buffer and SDS are shown in Figure 5.7. In NaP buffer (blue line) the spectrum, characterised by a negative absorption band at 197.5 nm ($-6.5 \text{ M}^{-1}\text{cm}^{-1}$), supported a disordered structure (42.4%), but as observed with sAvBD6, β -sheet (22.2%) and β -turn secondary structures (24.8%) were present. In the presence of SDS (red line), the spectrum was characterised by two negative absorption bands at 202 nm ($-5.4 \text{ M}^{-1}\text{cm}^{-1}$) and 220 nm ($-2.2 \text{ M}^{-1}\text{cm}^{-1}$) and a weak single positive band at 192 nm ($+0.8 \text{ M}^{-1}\text{cm}^{-1}$). As observed for AvBD6 disordered structure again predominated (31.9%), but the secondary structure also changed in SDS towards an α -helical conformation (10.5% to 25.1%).



B

Peptides	Helices%	β -Strands %	β -Turns %	Unordered %
sAvBD9	10.5	22.2	24.8	42.4
sAvBD9 SDS	25.1	18.3	24.7	31.9

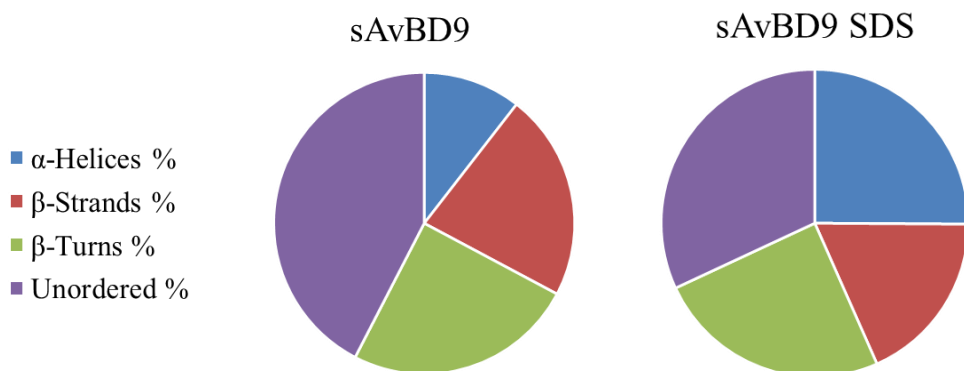
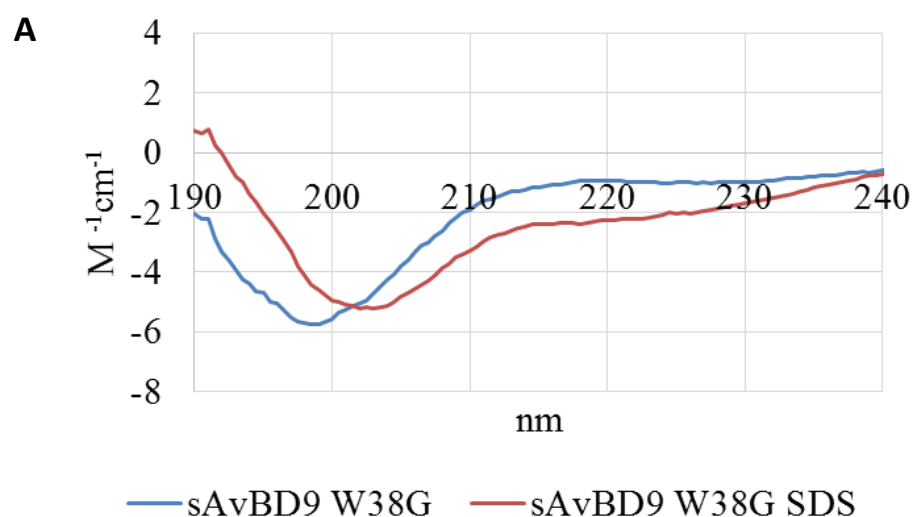


Figure 5.7 **A**: CD spectra of sAvBD9 in NaP buffer (Blue) and 1% SDS micelle solution (Red).

B: Table and Pie charts show quantification of CD secondary structures (%) including α -helices (Blue), β -strands (Red), β -turns (Green) and unordered (Purple) following exposure of sAvBD9 to NaP and 1% SDS micelle solution.

Figure 5.8 shows the CD spectra for sAvBD9 W38G in NaP buffer (blue line) and 1% SDS (red line). The peptide also formed a disordered structure (44.9%) in NaP buffer with single negative band at 198.5 nm ($-5.8 M^{-1}cm^{-1}$). As observed previously β -sheet (19.1%) and β -turn secondary structures (24.2%) were also present. Following exposure to 1% SDS two

negative bands at 203 nm ($-5.3 \text{ M}^{-1}\text{cm}^{-1}$) and 220 nm ($-2.2 \text{ M}^{-1}\text{cm}^{-1}$) and a weak single positive band at 190 nm ($+0.7 \text{ M}^{-1}\text{cm}^{-1}$) were observed. This was linked to a reduction in disordered structure (44.9% v 32.5%) and increase in α -helix (11.7% to 24.0%). Again no changes in either β -sheet (19.1% v 18.9%) or β -turn (24.2% v 24.5%) components were predicted from the CD data.



B

Peptides	Helices%	β -Strands %	β -Turns %	Unordered %
sAvBD9 W38G	11.7	19.1	24.2	44.9
sAvBD9 W38G SDS	24.0	18.9	24.5	32.5

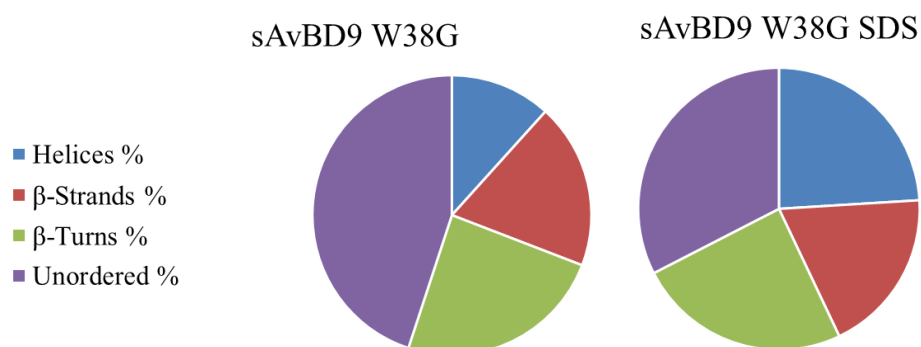


Figure 5.8 A: CD spectra of sAvBD9 W38G in NaP buffer (Blue) and 1% SDS micelle solution (Red).

B: Table and Pie charts show quantification of CD secondary structures (%) including α -helices (Blue), β -strands (Red), β -turns (Green) and unordered (Purple) following exposure of sAvBD9 to NaP and 1% SDS micelle solution.

In summary, the secondary structures of the synthetic linear AvBDs were essentially unordered, but they did respond to the presence of SDS micelles, mimicking bacterial membranes, by an increase in the α -helix content.

5.3.2. Calcein leakage assay: sAvBD6 and sAvBD9

As reported in section 4.5.1, the synthetic sAvBD6 and 9 peptides (100 μ g/ml) were not active against the *E. coli* chicken gut isolate when the time-kill assays were performed in PBS. However, complete killing was observed with sAvBD6 when the buffer was replaced with NaP (Figure 4.38 E). In contrast neither sAvBD9 nor sAvBD9 W38G were active against the *E.coli* strain in NaP buffer (Figure 4.39 E). These data suggested different mechanism actions for each of the two peptides that potentially related to their membrane interactive abilities.

Thus to assess the membrane destructive activities of the linear peptides calcein leakage assays were performed. A range of synthetic peptide concentrations, 1 to 10 μ g/ml, were used and the pore forming AMP, melittin specific to the honey bee, was used as the positive control at a final concentration of 1.5 μ g/ ml. As previously sodium phosphate buffer (50 mM) and 10 % Triton X100 (final concentration 1%) were used to define 0 and 100% leakage.

5.3.2.1. Leakage assay and AvBD6

The results of the leakage assays performed using sAvBD6 (1.5 μ g/ml) and melittin are shown in Figure 5.9 A&B. The positive control, melittin (blue line), induced 92.9 \pm 4.4% leakage within 6 seconds of its application, which remained constant (94.3 \pm 3.4 %) for up to two minutes (Figure 5.9B). In contrast sAvBD6 caused 47.2 \pm 6.4% leakage of calcein-entrapped liposome within 6 seconds of its application (Figure 5.9A), but leakage increased to a peak of 60.3 \pm 6.3 % at two minutes (Figure 5.9B). These data strongly indicated that AvBD6 was able to cause membrane damage.

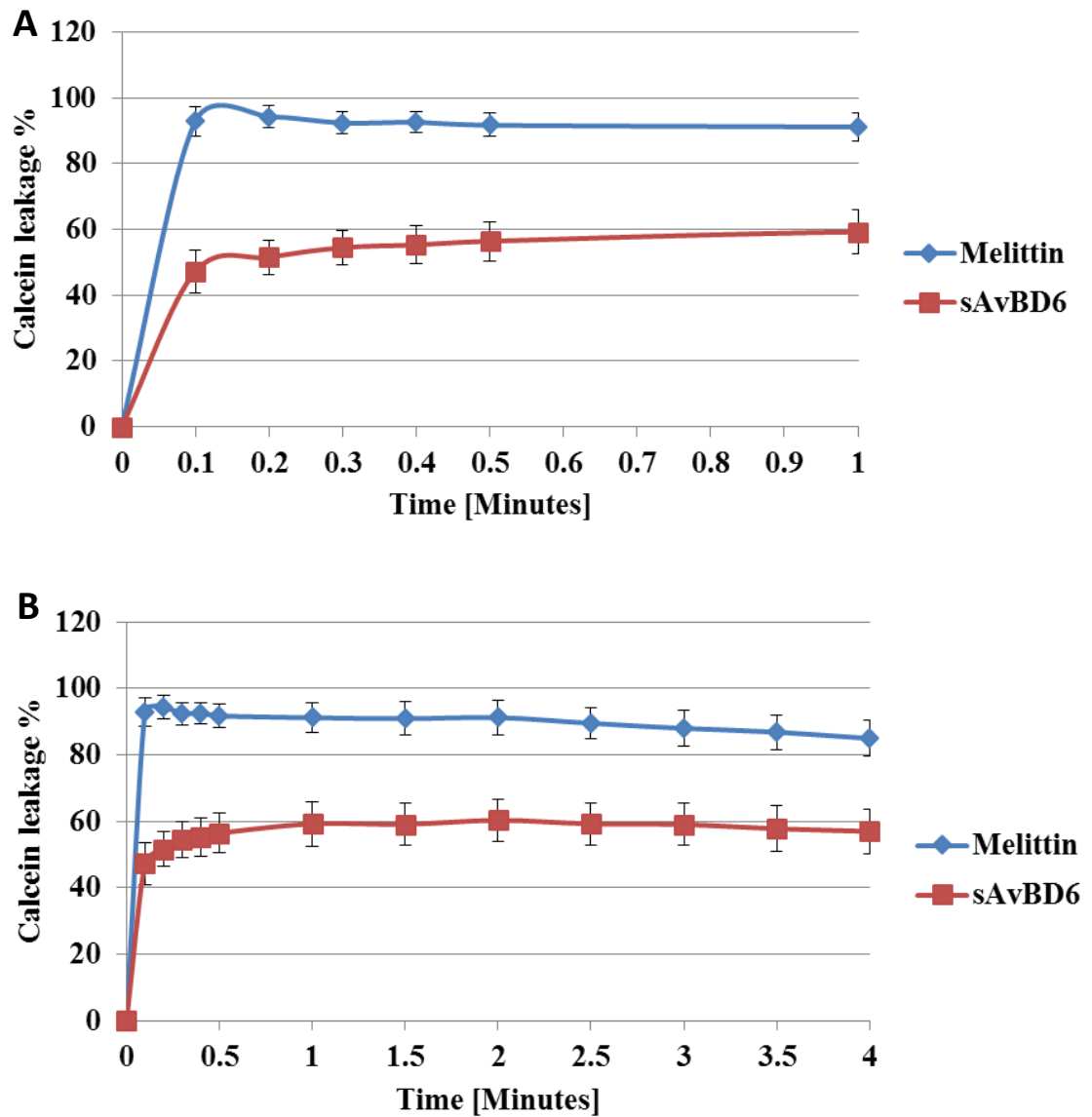


Figure 5.9 Calcein leakage recorded using entrapped liposomes incubated for up to 1 minute (A) and 4 minutes (B) at room temperature in 50 mM NaP buffer and either 1.5 $\mu\text{g}/\text{ml}$ sAvBD6 (red line) or melittin (blue line). Experiments = 4; Replicates =4. Mean \pm SEM.

5.3.2.2. Leakage assay and AvBD9 peptides

Calcein leakage relating to the membrane disruptive capacities of the sAvBD9 peptides at concentrations of 1.5, 3 and 10 $\mu\text{g}/\text{ml}$ are shown in Figures 5.10 & 5.11. It is acknowledged that these three sets of data each relate to only one experiment. However, six seconds following the addition of either 1.5 $\mu\text{g}/\text{ml}$ sAvBD9 (blue line) or AvBD938G (green line) calcein leakage was detected (Figure 5.10A), but at 3.0 % it was reduced markedly compared to the levels observed using AvBD6 (47.2%). While the fluorescence levels increased with time (Figure 5.10B) the maximum leakage detected for the AvBD9 treatment was only 11.5% (compared to 60.3% for AvBD6). In contrast, calcein leakage in response to sAvBD9 W38G treatment did not increase above 4%, which suggested either the inability of sAvBD938G to penetrate the liposomes fully to cause leakage or the immediate reorganisation of the liposomes following damage. To explore this further the concentrations of the peptides were increased to 3 and 10 $\mu\text{g}/\text{ml}$ and the experiments repeated.

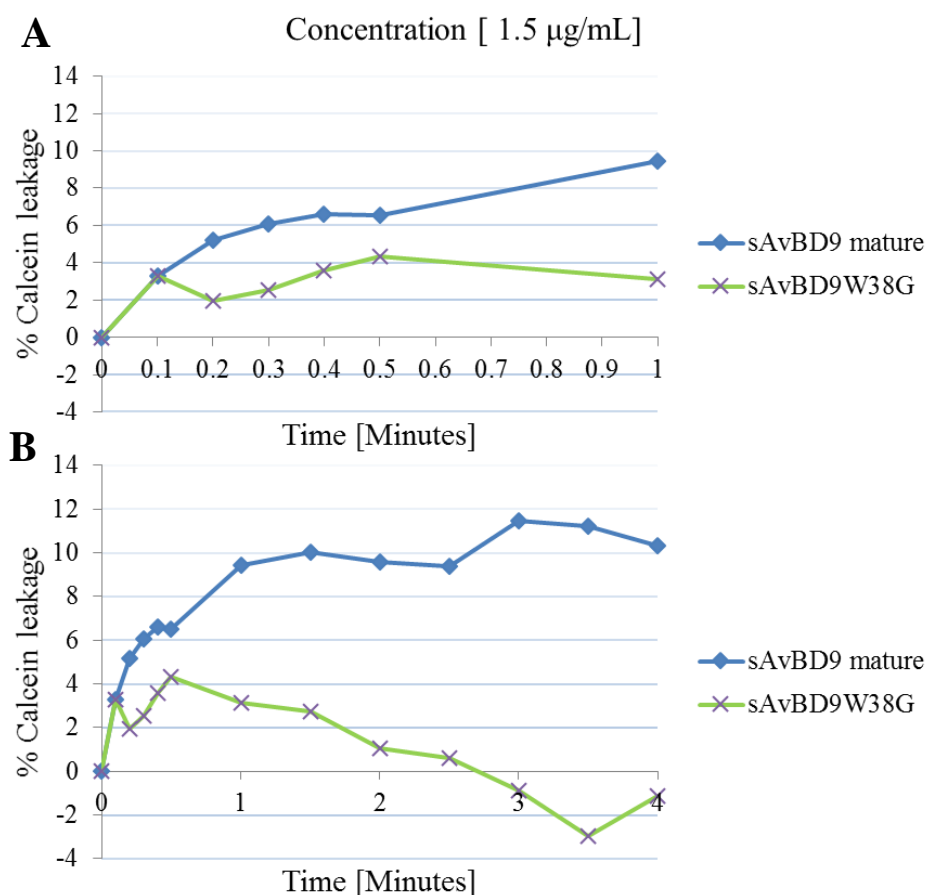


Figure 5.10 Calcein leakage recorded using entrapped liposomes incubated for up to 1 minute (A) and 4 minutes (B) at room temperature in 50 mM NaP buffer and either 1.5 $\mu\text{g}/\text{ml}$ sAvBD9 (blue) or sAvBD9 W38G (green). n=1

At 3 $\mu\text{g/ml}$ the data (Figure 5.11A) were similar to previous as sAvBD9 (blue) and sAvBD9 W38G (green) peptides were associated with 4.3 % and 1.3 % calcein leakage at six seconds, and 14.5 % and 4.7 % within one minute. At 4 minutes the leakage relating to sAvBD9 was 17.9% compared to that for sAvBD9 W38G which remained <5% (Figure 5.11B). Increasing the peptide concentrations to 10 $\mu\text{g/ml}$ (Figure 5.11C) resulted in AvBD9 being associated with 12.6 % leakage (6 seconds), but again sAvBD9 W38G had little effect with <5% leakage detected. Similar to previous leakage data activity associated with sAvBD9 increased gradually, in this case to a maximum of 22.3 % at four minutes (Figure 5.11D), but leakage associated with sAvBD9 W38G still remained at <5%. These data indicated that overall the ability of sAvBD9 to penetrate the liposomes was poor, and that the C-terminal tryptophan was important for the leakage activity of sAvBD9. Using these liposomes 2.5 $\mu\text{g/ml}$ melittin (positive control) resulted in $94.4\pm 2.9\%$ ($n=3$) calcein leakage while BSA (negative control) resulted in 0 leakage.

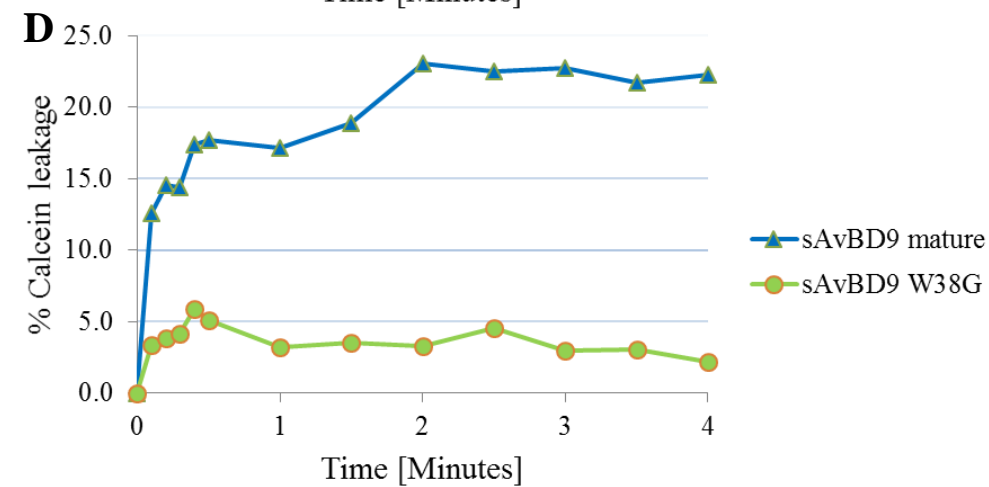
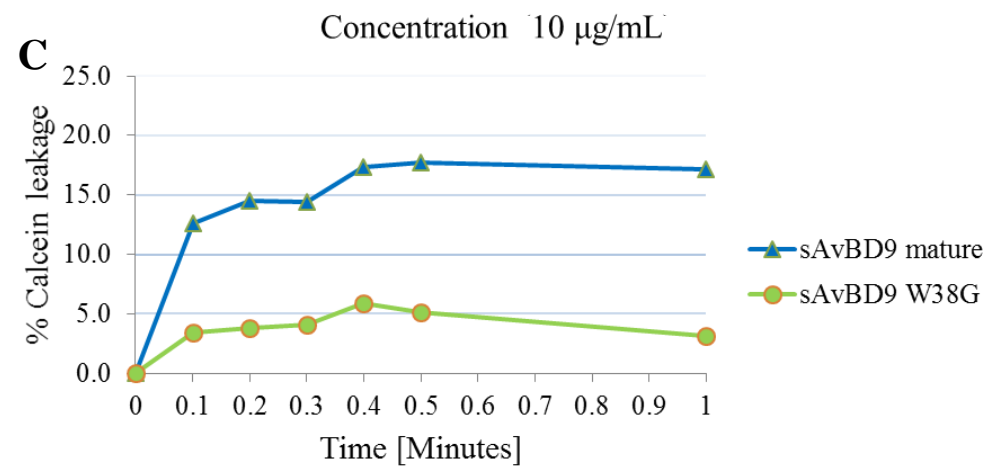
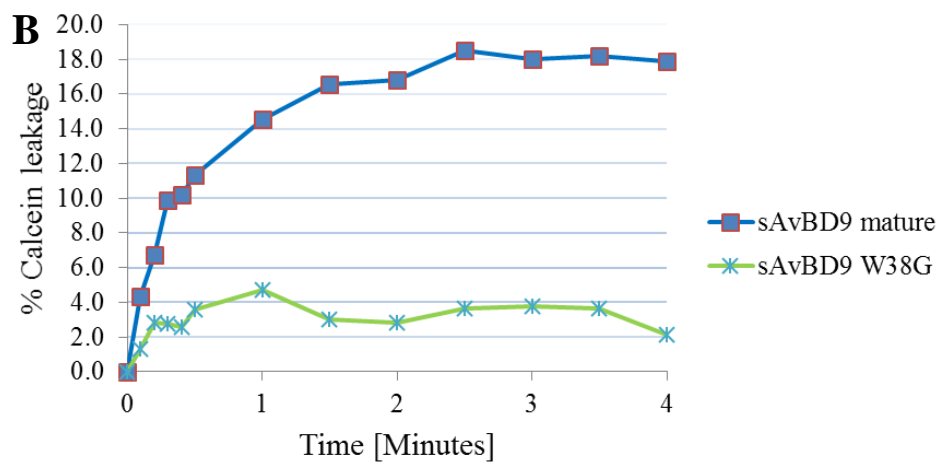
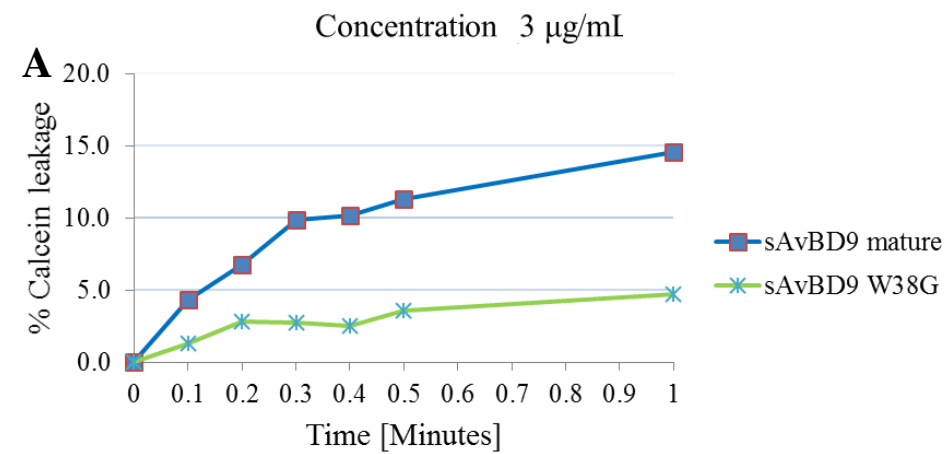


Figure 5.11 Calcein leakage recorded using entrapped liposomes incubated for up to 1 minute (A & C) and 4 minutes (B & D) at room temperature in 50 mM NaP buffer and either 3 (A & B) or 10 $\mu\text{g/ml}$ (C & D) sAvBD9 (blue) or sAvBD9 W38G (green). N=1 for each.

The AvBD6 and 9 data shown in Figures 5.9 to 5.11 support the activity of sAvBD6, but not sAvBD9 as an acute acting membrane permeabilising agent. To investigate this further calcein leakage data were recorded for up to one hour following the addition of the sAvBD9 and sAvBD9 W38G peptides to the calcein loaded liposomes and these data are summarised in Figure 5.12. Essentially sAvBD9 [2.5, 5 and 10 $\mu\text{g/ml}$] induced $8.5\pm 3.5\%$, $12.2\pm 3.0\%$ and $10.2\pm 5.2\%$ leakage, while sAvBD9 W38G induced $1.8\pm 1.8\%$, $4.3\pm 4.3\%$ and $2.4\pm 1.3\%$ leakage. Mellitin ($2.5\ \mu\text{g/ml}$) and BSA ($2.5\ \mu\text{g/ml}$) were used as the positive and negative controls, and at 60 minutes leakage was measured at 97.8 ± 5.5 and 0% respectively.

These 60 min leakage data were consistent with the values recorded at 4 min indicating that the sAvBD9 and sAvBD9 W38G peptides were unable to penetrate and/or disrupt the liposome membranes. Although not statistically significant the mean leakage data of the sAvBD9 W38G peptide was lower (6 - 8%) than that of sAvBD9, which hinted that the AvBD9 C terminal located tryptophan plays a role in membrane disruption.

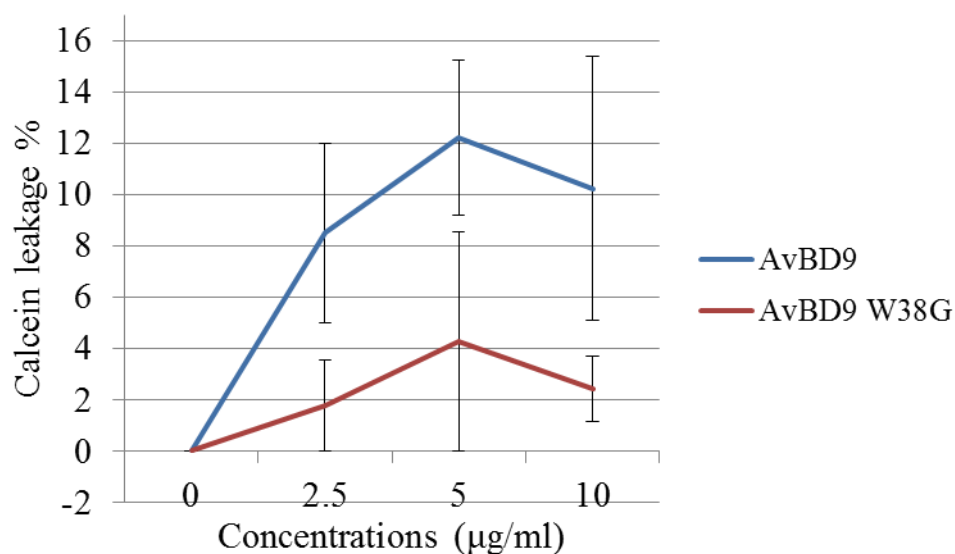


Figure 5.12 Calcein leakage assay of sAvBD9 and sAvBD9 W38G at 2.5, 5 and 10 $\mu\text{g/ml}$ incubated with the vesicles for 1 hour. $n=3$. Mean \pm SE.

In summary these data support different mechanisms of action of the synthetic AvBD6 and AvBD9 peptides in disrupting bacterial membranes with sAvBD6 causing immediate and major membrane disruption compared to sAvBD9. Furthermore, these data also suggested that the AvBD9 C-terminal located tryptophan plays a role in the membrane disruption process.

5.4. AvBD6 and 9 structure modelling

To try and further understand the mechanisms of action of the AvBD6 and 9 peptides their structures were modelled using Raptor X online software (<http://raptorx.uchicago.edu/>) (Peng and Xu, 2011). The three dimensional structure prediction used the Penguin AvBD 103b (Spheniscin-2) structure as its template, which had been solved by two dimensional NMR (Landon *et al.*, 2004). Using this tool the structures of AvBD6 and 9 were predicted to include three β -strands connected by three disulphide bonds and N-terminal α -helices (Figures 5.13 and 5.14).

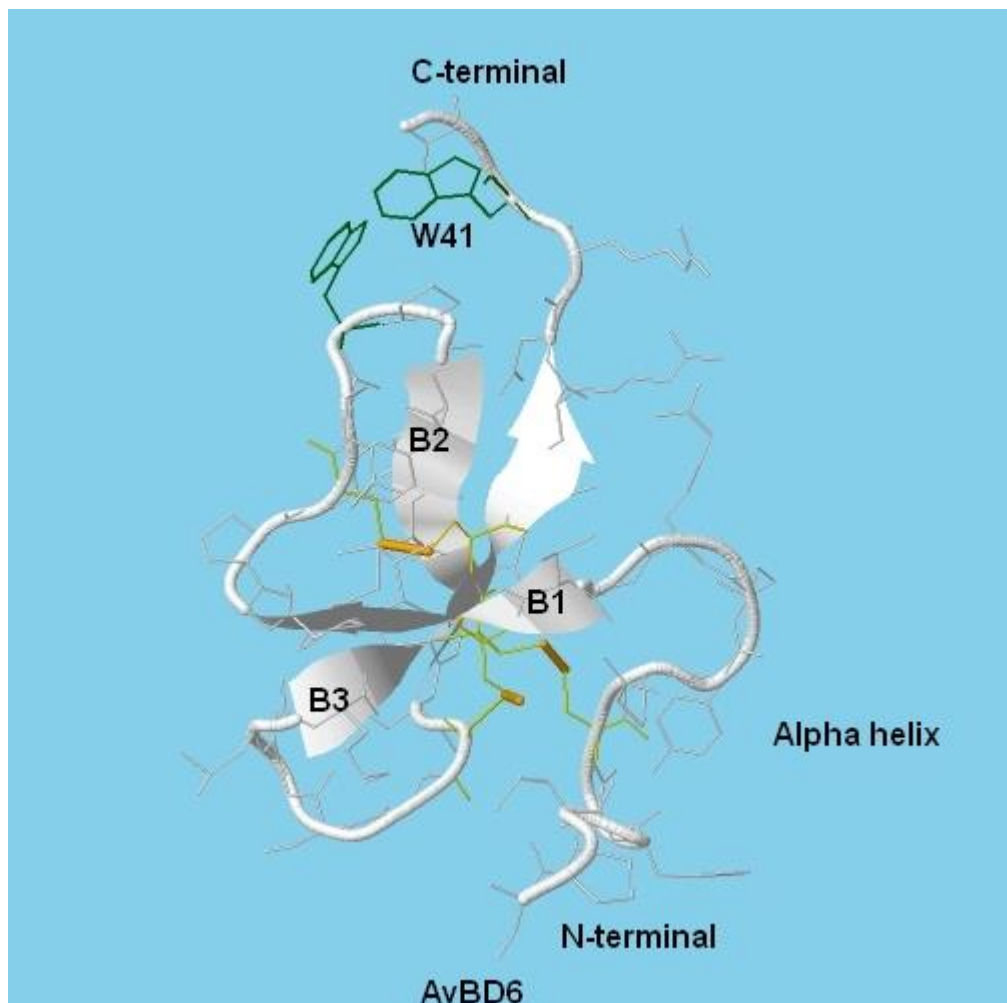


Figure 5.13 Predicted structure of AvBD6. Disulphide bonds (orange). C-terminal and middle tryptophan (green) (<http://raptorx.uchicago.edu/>)

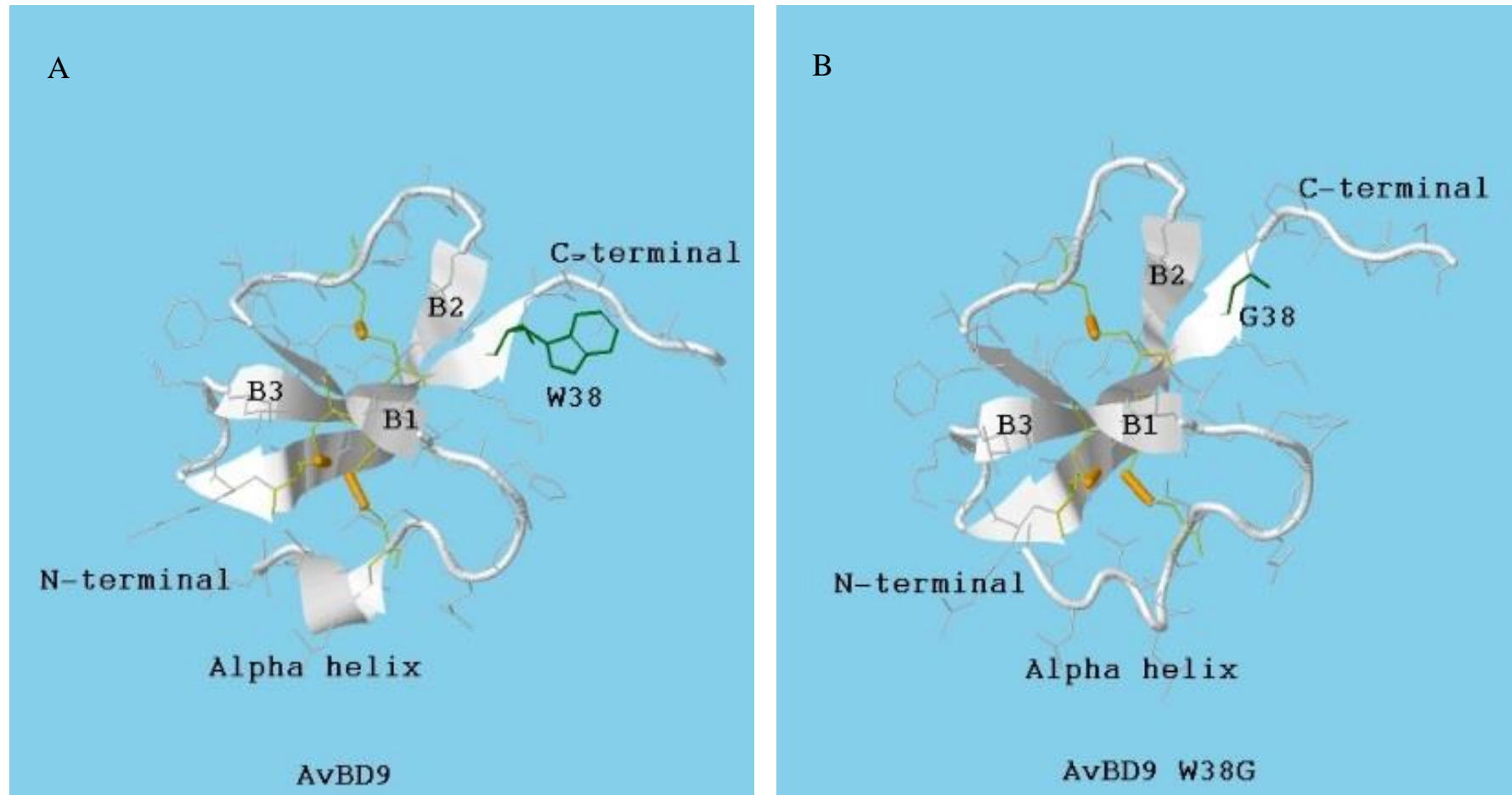


Figure 5.14 Predicted structures of AvBD9 (A) and AvBD9 W38G (B). (<http://raptorx.uchicago.edu/>) Disulphide bonds (orange). C-terminal tryptophan and glycine (green).

The three dimensional configurations of AvBD6 and 9 were also simulated using the Raptor X online service and these data are presented in Figures 5.15-16. In the AvBD6 model (Figure 5.15) specific clustering of positively charged amino acids was predicted. For example, arginine residues R10, R38 and R40 formed a cluster with the C-terminal tryptophan 41 (W41), while K33, R24 and R19 formed a contiguous bunch with tryptophan 20 (W20). Connecting the clusters were the aromatic residues, Y22 and Y23, with this connection creating a foramen hook-like structure. Interestingly in this model the arginine R7 side chain is buried with the cysteines toward the centre of the molecule.

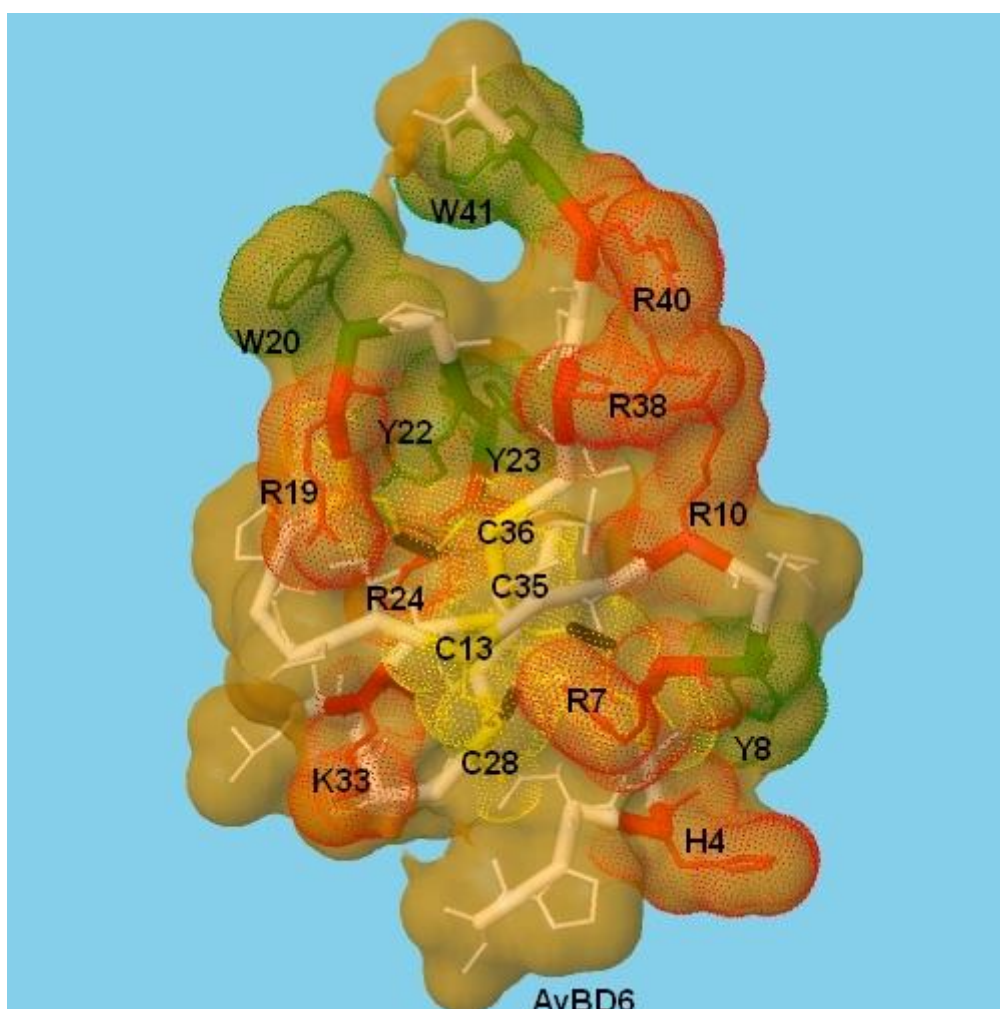


Figure 5.15 Simulated 3D structure of AvBD6. Aromatic amino acids including tryptophan (W) and Tyrosine (Y) are highlighted in green; cationic residues such as arginine (R), lysine (K) and histidine (H) in red; cysteines in yellow and disulphide bonds in orange

Figures 5.16A and B, show the predicted three dimensional conformations of AvBD9 and AvBD9 W38G peptides, respectively. The tertiary structures of both peptides appeared similar with the positively charged (red) R7, R19, R29, H10 and K32 residues and negatively charged (purple) D2 residue surface exposed. The two hydrophobic aromatic residues, W38 and F15 (green) were also exposed on the AvBD9 surface (Figure 5.16A). Interestingly, the model predicted the lysines, K34 and K37, (yellow) to be embedded in the molecule. Unlike AvBD6 however, no hook-like foramen structure was predicted. Substitution of the C-terminal tryptophan (W38) with glycine (G38) reduced the hydrophobicity of the molecule, but also appeared to impact on the orientation of the arginine 19 (R19) side chain (Figure 5.16B).

In summary, the AvBD6, AvBD9 and AvBD9 W38G 3D models indicated that both aromatic and cationic residues were exposed to the peptide exteriors and the cysteines were located to the centre of the peptides, forming three intra molecular disulphide bonds. These models although basic were consistent with other β -defensins, including the mammalian defensins.

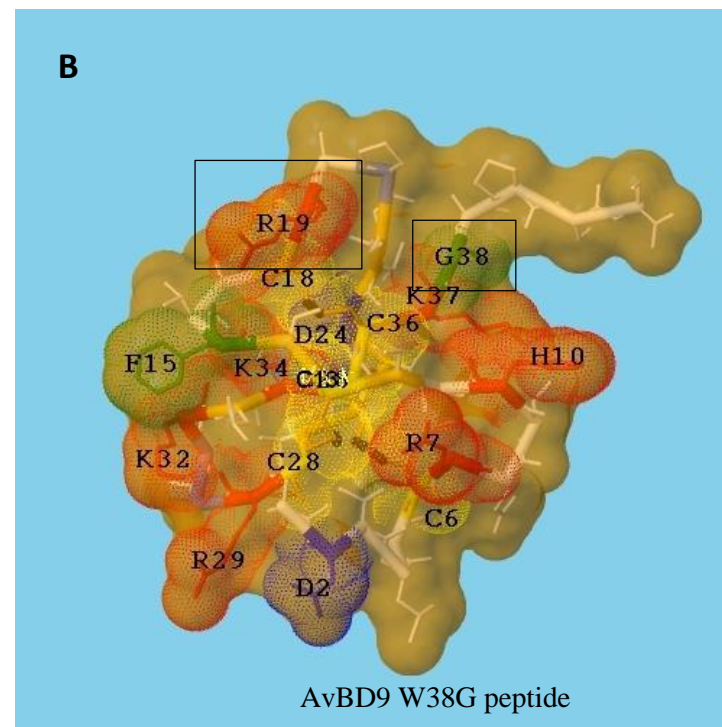
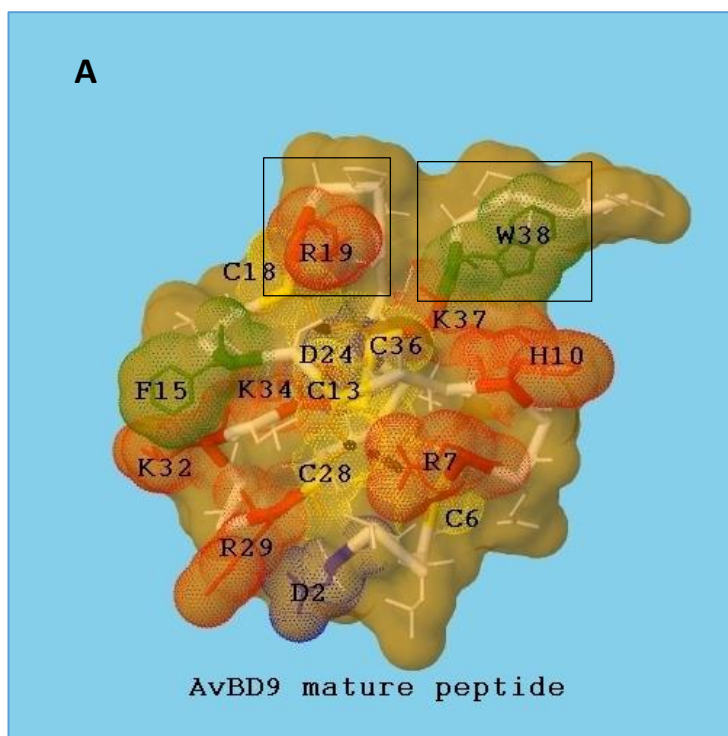


Figure 5.16 Simulated 3D structures of AvBD9 (A) and AvBD9 W38G (B). Aromatic amino acids including tryptophan (W) and phenylalanine (F) are highlighted in green; cationic residues including arginine (R), lysine (K) and histidine (H) in red; anionic residue aspartic acid (D) in purple; cysteines in yellow and disulfide bonds in orange. In (B) tryptophan W38 was replaced by glycine (G38) which is also highlighted in green.

5.5. Discussion

The defensin killing mechanism of action is predicted to involve the interaction of the cationic peptide with a negatively charged bacterial membrane and insertion of the peptide, facilitated by its hydrophobic structure, into the membrane resulting in bacterial membrane depolarisation and death (Ganz, 2003). The aim of this chapter was to explore the mechanisms of action of AvBD6 and 9 by investigating their secondary structure conformations and membrane interactive properties.

The lack of purity for rAvBD6, due to contamination with the 26 kDa GST protein, meant that clear reproducible CD spectra could not be obtained. However, the CD spectral analyses of rAvBD9 was successful and predicted β -sheet structure (52%) consistent with disulphide bond formation (three anti-parallel β -sheets characterise the β -defensins (van Dijk *et al.*, 2008)); α -helix presumably linked to amino acids at the N-terminus as modelled in Figures 5.13 and 5.14; β -turns presumably linking areas of secondary structure to produce a compact and globular protein, and unordered structure. The fact that the rAvBD9 3CA and 6CAG peptides showed reduced β -sheet structure, 29.6% and 24.4% respectively, also supported disulphide bond formation in the mature 6 C rAvBD9. The peptide folding was native and not chemically produced via oxidation thus the experimental data did not allow confirmation of the expected C1-C5, C2-C4 and C3-C6 bonding pattern. To verify this, NMR spectral analyses similar to that used to investigate AvBD2 is required (Derache *et al.*, 2012). The secondary structure data relating to rAvBD9 W38G was more difficult to explain as the only amino acid mutated was the C-terminal tryptophan and thus the percentage of β -sheet structure calculated from the spectral data (27%) was unexpected. In fact although the encoded peptide contained six C the β -sheet content was more equivalent to that of rAvBD9 3CA. This reduced β -sheet content was also not supported by the modelling data (Figures 5.14 & 5.16), but changing the tryptophan for a glycine appeared *in vitro* to affect the folding of the AvBD9 molecule and moreover the CD spectral data indicated a major negative impact on disulphide bond formation.

To model the interactions of the rAvBD9 peptides with bacterial membranes a SDS micelle model system, which consists of a negatively charged outer surface and a hydrophobic inner core was adopted. A comparable system used to investigate Alyteserin-1c, a 23 amino acid AMP secreted by toad skin indicated that the peptide, in the membrane mimicking environment, assumed an α -helical structure (Subasinghage *et al.*, 2011). The exposure of

the rAvBD9 mature peptide to a 1% SDS micelle solution resulted in a reduction in β -strand structure and an increase α -helix, which predicted that the AvBD9 peptide adopted an α -helical conformation in the presence of bacterial membranes. α -helicity is proposed to be important for defensin/membrane interactions, with the α -helix structure facilitating the embedding of hydrophobic residues into the membrane (Yeaman and Yount, 2003). α -helicity is also associated with the bacterial killing activity of an antimicrobial peptide (Sudheendra *et al.*, 2015), and this was supported by the data reported in Chapter 4, where rAvBD9 was shown to have potent antimicrobial activity against *E.coli*.

Exposing the rAvBD9 peptides to SDS, also increased the percentage of disordered structure (Figure 5.3 and Table 5.2), indicative of the reduction and hence loss of the disulphide bonds. In fact the unordered structure observed following SDS exposure was comparable to that calculated for the rAvBD9 6CA/G peptides, lacking cysteines and hence disulphide bonds, in NaP buffer. In addition, the spectral characteristics of rAvBD9 W38G, which lacks its C-terminal tryptophan, were relatively unchanged following SDS micelle exposure, which highlighted a strategic role of the bulky aromatic residue in the folding of the AvBD9 peptide.

The increase in α -helicity following exposure of the peptide to SDS micelles is also an indicator of a pore forming mechanism. Models predict that binding of the peptide initially involves the helical axis lining up parallel to the membrane surface, followed by insertion into the bilayer and disruption of membrane permeability (Jenssen *et al.*, 2006). However, the majority of studies exploring and modelling AMP/membrane interactions have actually focussed on small linear α -helical peptides and not complex peptides such as the defensins.

Pistolesi *et al.* (2007), using spin labelling EPR spectroscopy determined the interaction of a 15 amino acid linear hybrid cecropin-melittin molecule with a membrane bilayer. The authors found no evidence of peptide-peptide interactions <20 Å eliminating a barrel-stave mechanism and proposed a toroidal pore mechanism in which the peptides were separated by intervening phospholipids (Pistolesi *et al.*, 2007). Investigations reporting defensin-lipid interactions are less common, but indicate that the mechanisms reported often reflect the peptide concentrations employed. For example, work with the HBD3 and helical peptides suggests that at low peptide concentrations a thinning or destabilisation of the membrane occurs, explained by the ‘sand in a gear-box theory’ (Derache *et al.*, 2012), but with higher concentrations pore formation is the more probable mechanism of action (Bonucci *et al.*, 2013). The actual mechanisms by which AvBD9 interacts with bacterial membranes are

not known, but probably involves an initial binding step in which the N-terminal α -helix of the molecule lines up parallel to the membrane surface, followed by insertion of the peptide into the bi-layer and disruption of membrane permeability through pore formation.

Data from Chapter 4 indicated that the AvBD6 and 9 peptides caused bacterial killing and to further explore the potential membrane destructive capacity of the peptides, calcein entrapped artificial vesicles mimicking the bacterial lipid bilayer were exploited. The initial data using rAvBD9 was disappointing as it lacked reproducibility (Figure 5.5), which was attributed to purity issues caused by pooling several different recombinant peptide preparations. This and the fact that rAvBD6 could not be used underpinned the use of synthetic peptides. The disadvantage was that the synthetic peptides were linear, ie oxidative folding was not performed, but the CD spectral data analyses supported an increase in α -helicity was observed in the presence of SDS micelles, which mimicked the patterns observed with the recombinant peptides.

The use of sAvBD6 resulted in 47% calcein leakage within six seconds compared to 3% for sAvBD9, which suggested that the mechanisms by which the peptides interacted with the lipid membrane were different. Interestingly despite the original concerns the sAvBD9 data were comparable to that using rAvBD9. However, a mechanism of AvBD9 action where it has little membrane damaging activity does not fit with the AMA data and suggests a model in which the AvBD9 peptide has additional killing properties, for example a DNA inhibitory function once inside the bacterial cell (Wilmes, 2012). In support previous electron microscopic studies have shown that AvBD9 peptides lead to granulation of intracellular materials, irregular septum formation in dividing cells, cytoplasmic retraction and cell lysis at the cell septa (van Dijk *et al.*, 2007). This appears a novel property of the AvBDs as others such as ostrich AvBD1 and AvBD2 have also been reported to cause little membrane leakage, but to have high DNA binding ability (Sugiarto and Yu, 2007b), and penguin AvBD103b has both membrane disruption and nucleic acid binding abilities that appear to be involved in its mechanism against *Salmonella enteritidis* (Teng *et al.*, 2014). These data indicate that bacterial killing by the AvBD family is complex.

The leakage data showed that the absence of the AvBD9 C-terminal tryptophan was linked to minimal or no calcein release. Furthermore, the negative data relating to AvBD9 W38G (Figure 5.10 B) may have been due to the inability of the peptide to insert into the vesicles. Interestingly, the C-terminal tryptophan of human α -defensin HNP-1 has been shown to be involved in the penetration of the peptide through a membrane bilayer (Bonucci *et al.*,

2013), which lends further support to a critical role for this amino acid in bacterial killing. The 3D modelling of the two structures did not help explain why the tryptophan was as important as the tertiary structures of both AvBD9 and AvBD9 W38G appeared similar although the large aromatic tryptophan made the surface of the wild type more hydrophobic.

Modelling did reveal potential differences in AvBD6 and 9 structures which may help explain their different membrane disruption properties and AMAs. Most marked was the clustering of positively charged amino acids and presence of a 'claw-like' structure in AvBD6 (Figure 5.15), the latter involving the large bulky side chains of two tryptophan amino acids. This structure has also been observed in Apl_AvBD2 and suggested to function as a 'prehensile grasp' mechanism presumably functioning in attaching the peptide to lipid bilayers (Soman *et al.*, 2010). It is feasible that this structure enhanced the membrane permeating abilities of AvBD6 compared to AvBD9 although such analyses requires further experimentation.

5.6.Conclusions

CD spectra showed that rAvBD9 was folded and exhibited β -sheet structure consistent with di-sulphide bond formation.

Membrane leakage experiments suggested $sAvBD6 > sAvBD9$, which indicated that AvBD9 may have other properties related to bacterial killing.

Synthetic sAvBD6, rAvBD9 and sAvBD9 variants responded to a SDS environment mimicking a bacterial membrane via increased α -helical structure, indicative of a pore-forming mechanism of action.

The C-terminal tryptophan appears critical for AvBD9 folding, membrane permeation and antimicrobial function.

Chapter 5 (Part II)

AvBD1 structure-membrane interactions

5.7.Introduction

In addition to ABDs 6 and 9, AvBD1 belongs to the AvBD family. The AvBD1 peptide is predicted to be highly hydrophobic (52.5%) and cationic, with a net positive charge of 8 at pH 7, which compares to 7 for AvBD6 and 4 for AvBD9. AvBD1 is of particular interest as analyses of Aviagen birds identified SNPs within the AvBD1 coding regions of two different commercial broiler chicken lines resulting in the synthesis of three AvBD1 variants, NYH, NYY and SSY (Figure 5.17) (Butler 2010, PhD thesis), with the NYH variant acknowledged as the ‘wild-type’ peptide. SNPs resulting in non-synonymous amino acid changes are relatively rare in host defence peptides as they can impact on the function of that encoded peptide and expose the host to microbial assault and infection. Overall however, the amino acid changes underpinning the NYY and SSY variants did not appear to significantly affect either the overall charge of the variants (+8) or their hydrophobicity (50%).

These observations suggested that the amino acid changes would not affect the functionality of the peptides, but to verify this time-kill anti-microbial assays were performed. Initially, in house hyperexpression and purification of the AvBD1 peptides was attempted, but this proved difficult technically due to their hydrophobicity and charge, thus linear peptides (Figure 5.17) were custom synthesised and utilised in determining and comparing the antimicrobial properties against *E. coli* (Cadwell, 2014, PhD thesis).

sAvBD1 NYH: GRKSD^YCFR^KNG^FCAFLK^CP^YLT^LISGK^CSR^FHL^CCKRI^WWG
sAvBD1 SSY: GRKSD^YCFR^KS^GGFCAFLK^CP^SLT^LISGK^CSR^FYL^CCKRI^WWG
sAvBD1 NYY: GRKSD^YCFR^KNG^FCAFLK^CP^YLT^LISGK^CSR^FYL^CCKRI^WWG

Figure 5.17 Amino acid sequences of synthetic AvBD1 SNP peptides. Pink: amino acids encoded by SNPs. Green: C- terminal tryptophan. Yellow: cysteine residues.

Interestingly, the data (Figure 5.18 A & B; Cadwell, 2014, PhD thesis) indicated that the AvBD1 NYH peptide was more potent than AvBD1 SSY, which in turn was more active than AvBD1 NYY. Thus to further investigate the peptides and their interactions with bacterial membranes the synthetic AvBD1 variants were analysed by CD spectra and using the calcein leakage assay.

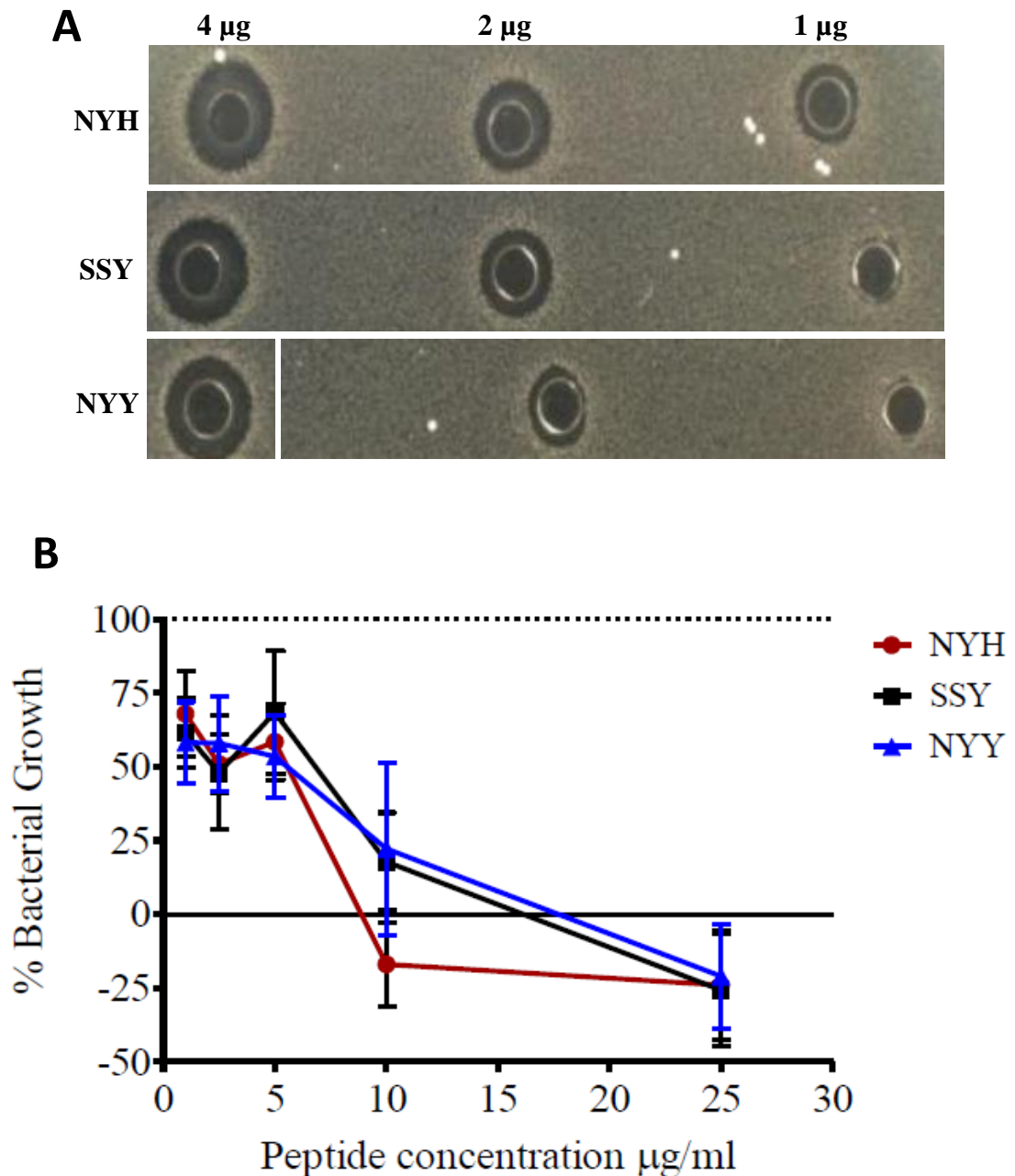


Figure 5.18 A: Radial diffusion assay showing the inhibitory effect of AvBD1 variants ‘NYH’, ‘SSY’ and ‘NYY’ at 4, 2 and 1µg. B: Time-kill assay showing percentage bacterial (*E. coli*) growth following 2 h incubation of *E. coli* (1/1000 dilution) with NYH, SSY and NYY AvBD1 peptides.

All percentage growth is shown relative to PBS (dotted line). Percentage values < 0% indicate fewer colonies after 2 h than at 0 h and hence, indicate bacterial killing. Mean ± SEM from three experiments. (Cadwell, 2014, PhD thesis).

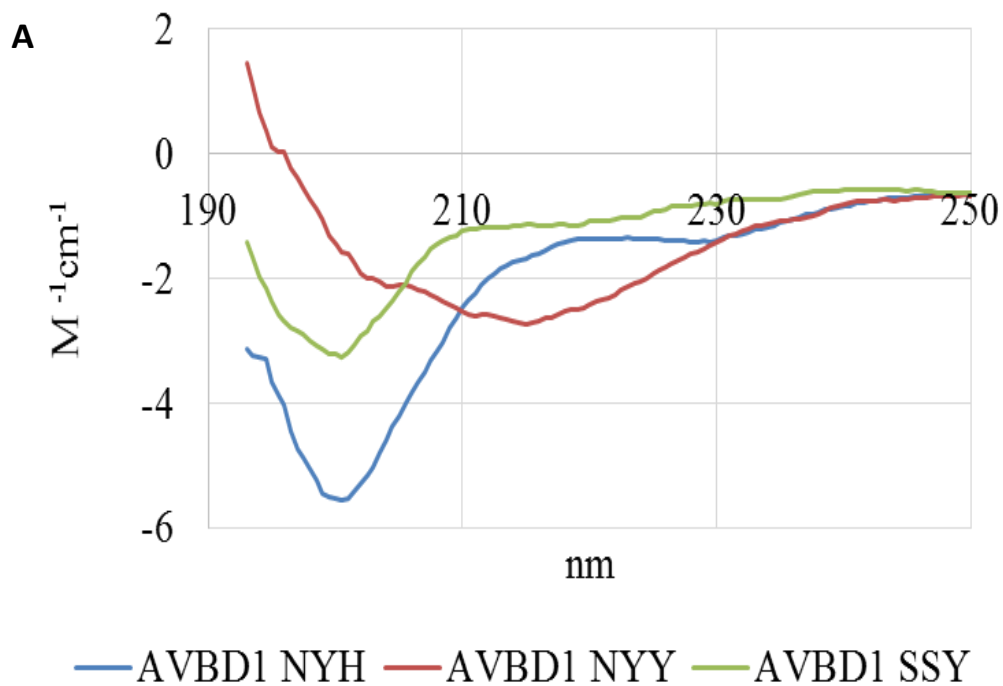
5.8. CD analyses of synthetic AvBD1 Peptides

The three synthetic AvBD1 peptides were each available as 1 mg/ml solutions reconstituted in PBS (kind gift by Kevin Cadwell, PhD Newcastle University). The peptides were further diluted either in NaP (50 mM) or 1% SDS to final concentrations of 250 µg/ml.

The results of the CD analyses performed in NaP buffer and 1% SDS, the latter to mimic the bacterial membrane, are shown in Figures 5.19 and 5.20. In NaP buffer (Figure 5.19 A) both AvBD1 NYH and AvBD1 SSY formed disordered structures as evidenced by the single absorption bands ($-5.5 \text{ M}^{-1}\text{cm}^{-1}$) and ($-3.3 \text{ M}^{-1}\text{cm}^{-1}$) observed at 200.5 nm. In contrast AvBD1 NYY displayed negative absorption bands ($-2.2 \text{ M}^{-1}\text{cm}^{-1}$ and $-2.7 \text{ M}^{-1}\text{cm}^{-1}$) at 207 and 216 nm respectively, and a positive absorption band ($+1.5 \text{ M}^{-1}\text{cm}^{-1}$) at 193 nm, which supported a mixture of α -helix and β -sheet conformations.

The sAvBD1 peptides were originally reconstituted in PBS solution, which meant the preparations contained chloride ions. Chloride ions absorb strongly below 200nm (Kelly *et al.*, 2005). Despite using NaP for the subsequent dilutions the lowest wavelength relating to the CD spectral analyses was 193nm. Because of this quantification of the data was performed using K2D as opposed to Selcon3 software.

The quantitative results are shown in Figure 5.19 B. As expected these data indicated that the peptides contained significant unordered structure (48 to 63%). β -sheet and α -helical conformations were also predicted with NYY containing 15 % α -helix compared to 9 % and 8% for NYH and SSY.



B

Peptides	α -helix %	β -sheet %	Unordered %
AvBD1 NYH	9	28	63
AvBD1 NYY	15	30	55
AvBD1 SSY	8	44	48

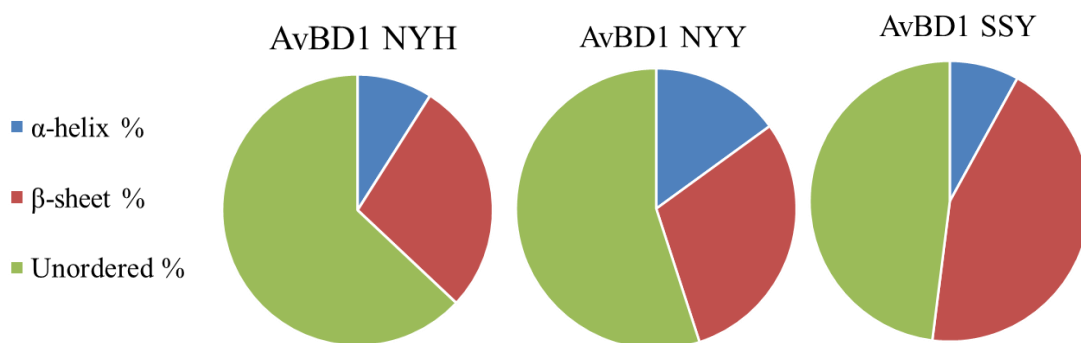


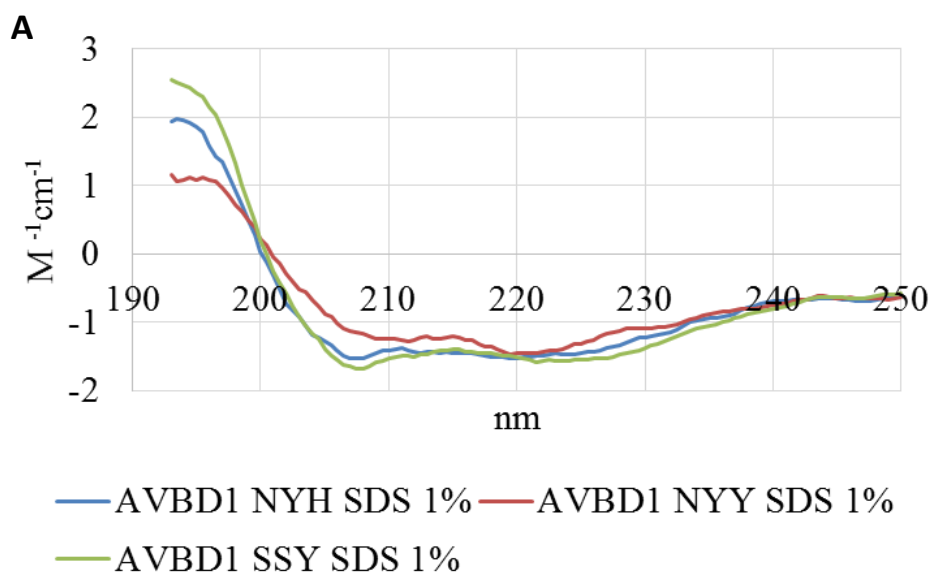
Figure 5.19 A: CD spectra of sAvBD1, NYH (Blue), NYY (Red) and SSY (Green).

B: Table and Pie charts show quantification of CD secondary structures (%) including α -helices (Blue), β -sheet (Red), and unordered (Green) following exposure of sAvBD1 to NaP (50 mM).

In 1% SDS (Figure 5.20 A) the NYH (blue) and SSY (green) sAvBD1 peptides formed α -helix conformations, as characterised by two negative absorption bands at 208 nm and 222 nm, and a positive band at 193 nm.

Values for the two negative absorption bands of the NYH variant were $-1.5 \text{ M}^{-1}\text{cm}^{-1}$, while the two bands relating to SSY were recorded as -1.7 and $-1.6 \text{ M}^{-1}\text{cm}^{-1}$; the positive absorption bands observed for NYH and SSY were $+2$ and $+2.5 \text{ M}^{-1}\text{cm}^{-1}$. The two negative absorption bands for NYY were at 211 nm ($-1.3 \text{ M}^{-1}\text{cm}^{-1}$) and 220 nm ($-1.5 \text{ M}^{-1}\text{cm}^{-1}$), the positive absorption band was at 195 nm ($+1.1 \text{ M}^{-1}\text{cm}^{-1}$).

The quantitative data (Figure 5.20 B), predicted that following exposure to 1% SDS the NYH, NYY and SSY peptides contained similar amounts of α -helix (22%, 20% and 23%) with the increases offset by a reduction in the β -sheet component.



B

Peptides+SDS	α -helix %	β -sheet %	Unordered %
AvBD1 NYH	22	24	54
AvBD1 NYY	22	26	53
AvBD1 SSY	23	22	55

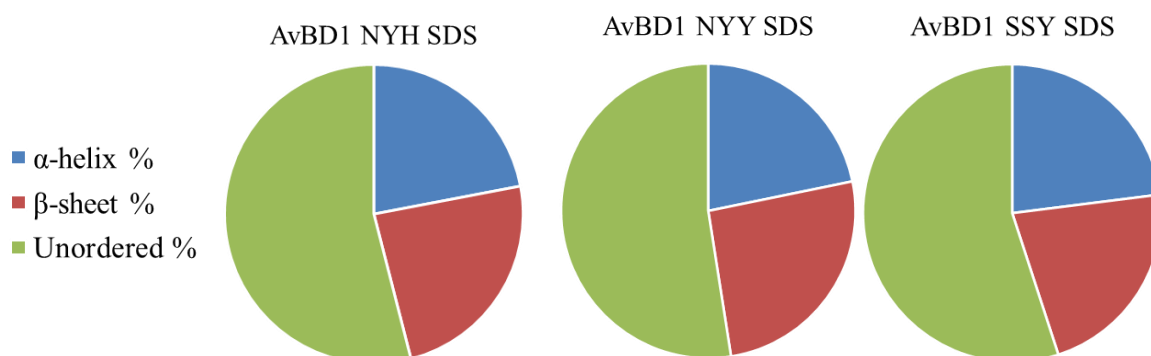


Figure 5.20 A: CD spectra of sAvBD1, NYH (Blue), NYY (Red) and SSY (Green).

B: Table and Pie charts show quantification of CD secondary structures (%) including α -helices (Blue), β -sheet (Red), and unordered (Green) following exposure of sAvBD1 to 1% SDS.

The paired CD spectra of each of the sAvBD1 peptides in NaP buffer and 1% SDS are shown in Figures 5.21-5.23. Figures 5.21 and 5.22 show the clear changes in the CD spectra of the NYH and SSY peptides following their exposure to 1% SDS with the α -helices characterised by negative bands at 208 and 220nm, and a positive band at around 193nm.

The NYY spectra were shallower and less supportive of a change in secondary structure in the 1% SDS environment, with a mixture of β -sheet and α -helix structure predicted (Figure 5.23A).

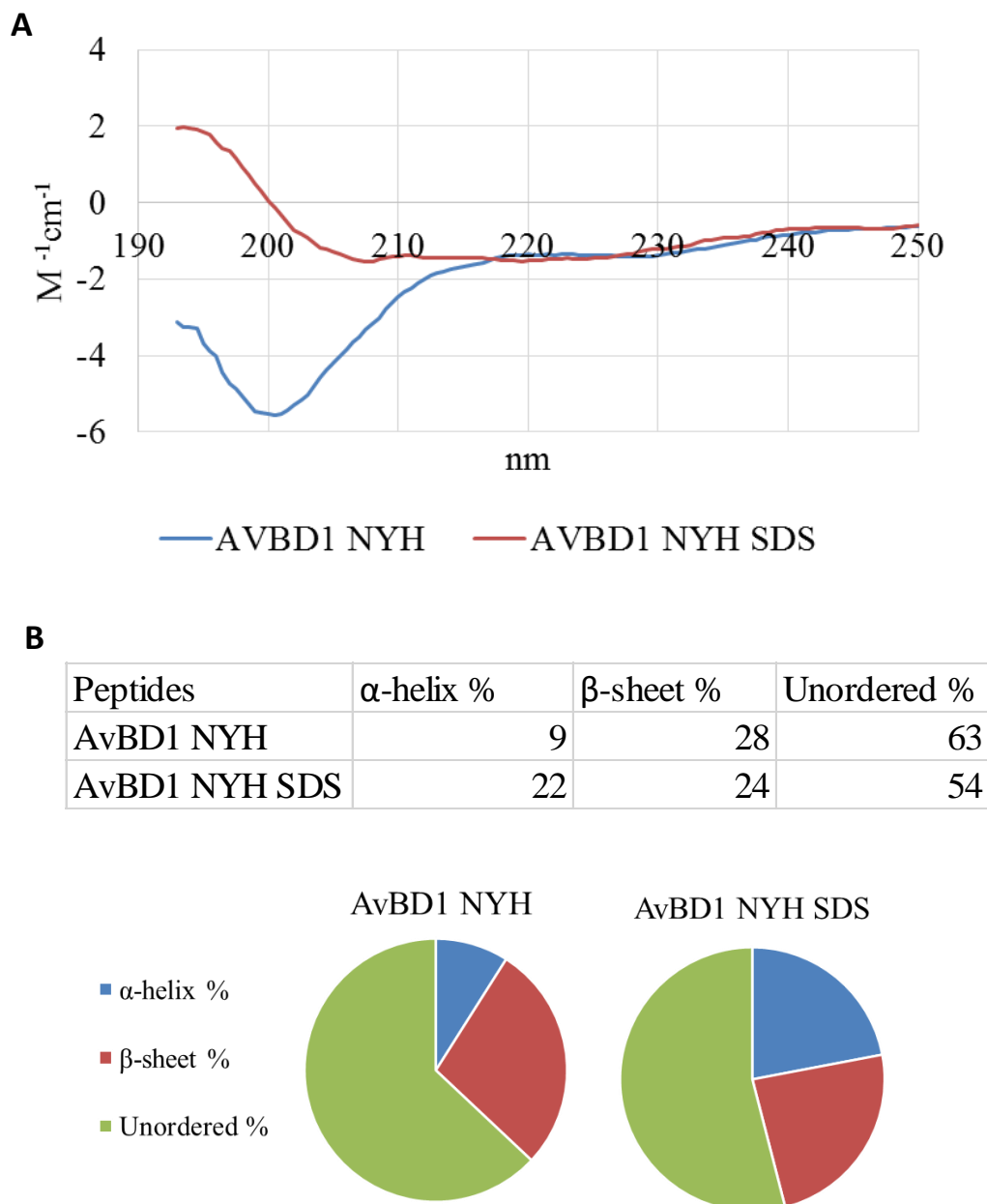
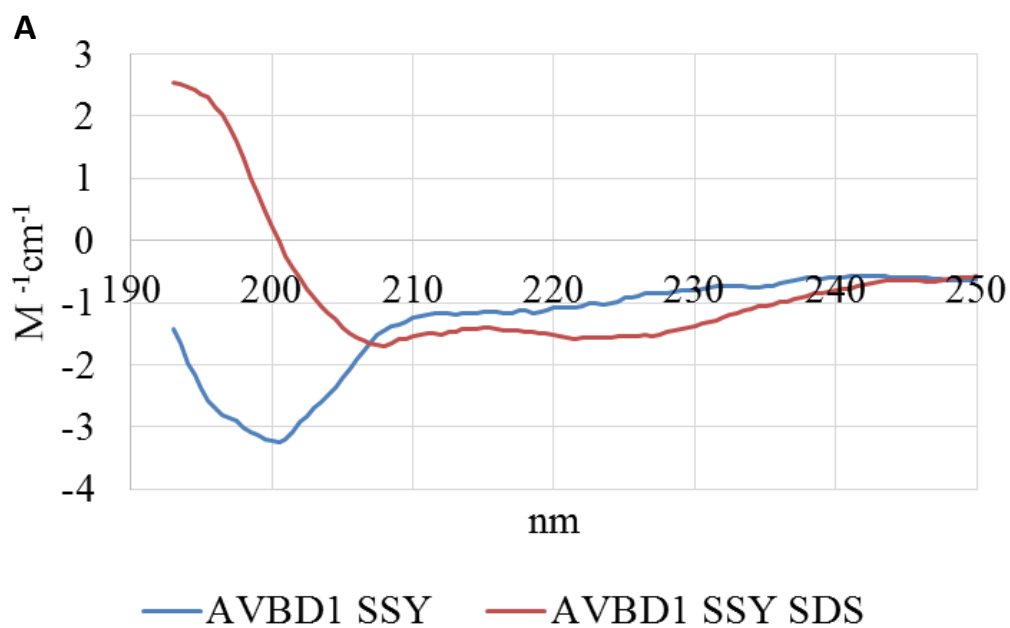


Figure 5.21 A: CD spectra of sAvBD1 NYH in NaP buffer (Blue) and 1% SDS micelle solution (Red).

B: Table and Pie charts show quantification of CD secondary structures (%) including α -helices (Blue), β -sheets (Red) and unordered (Green) following exposure of sAvBD1 NYH to NaP and 1% SDS micelle solution.



B

Peptides	α -helix %	β -sheet %	Unordered %
AvBD1 SSY	8	44	48
AvBD1 SSY SDS	23	22	55

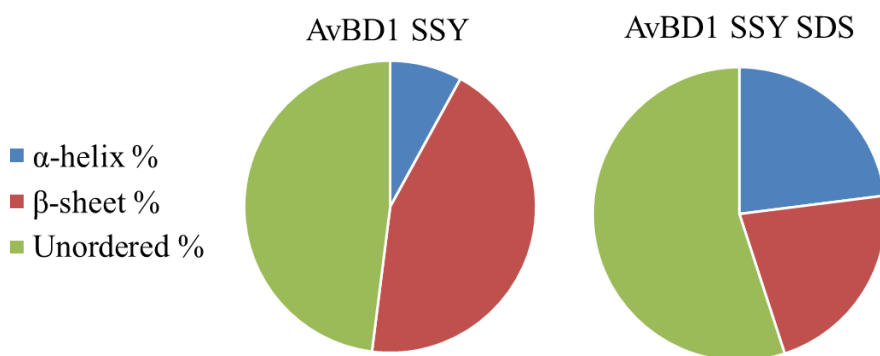
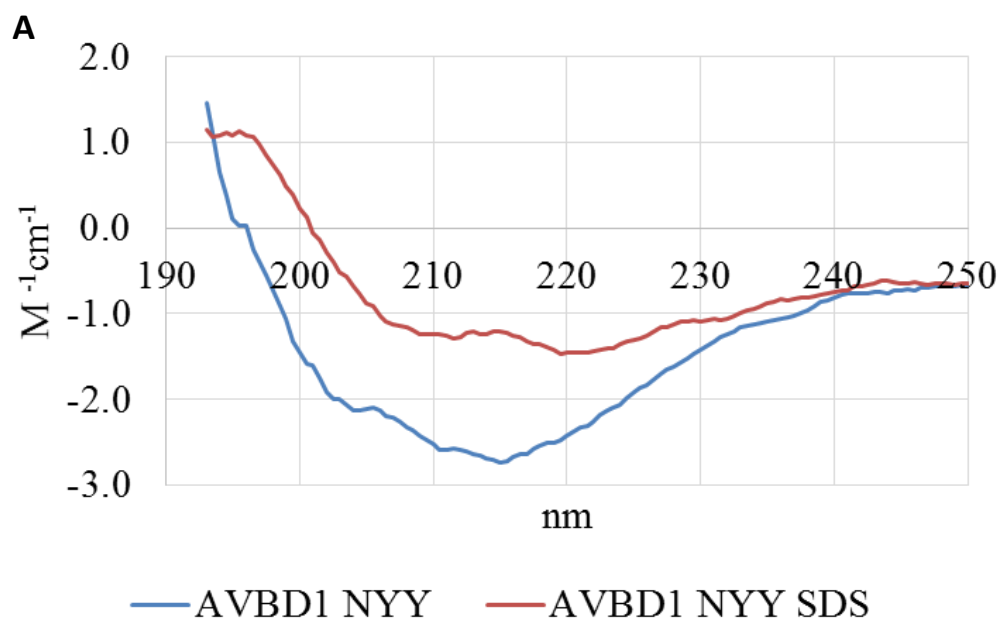


Figure 5.22 A: CD spectra of sAvBD1 SSY in NaP buffer (Blue) and 1% SDS micelle solution (Red).

B: Table and Pie charts show quantification of CD secondary structures (%) including α -helices (Blue), β -sheets (Red) and unordered (Green) following exposure of sAvBD1 SSY to NaP and 1% SDS micelle solution.



B

Peptides	α -helix %	β -sheet %	Unordered %
AvBD1 NYY	15	30	55
AvBD1 NYY SDS	22	26	53

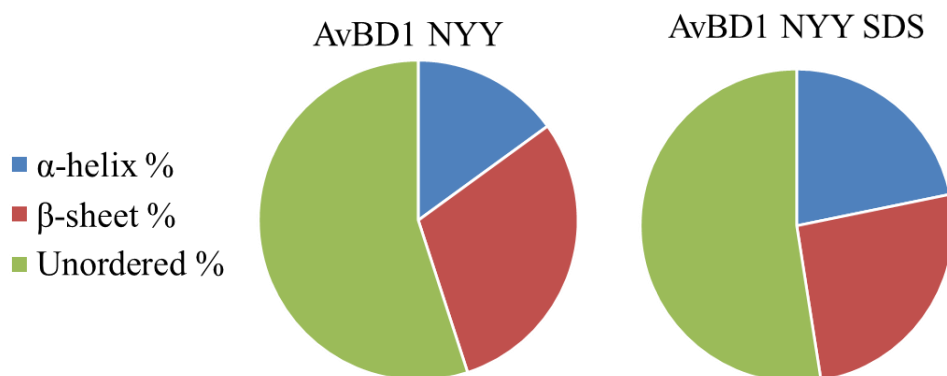


Figure 5.23 A: CD spectra of sAvBD1 NYY in NaP buffer (Blue) and 1% SDS micelle solution (Red).

B: Table and Pie charts show quantification of CD secondary structures (%) including α -helices (Blue), β -sheets (Red) and unordered (Green) following exposure of sAvBD1 NYY to NaP and 1% SDS micelle solution.

5.9. Leakage assay and sAvBD1 Peptides

The calcein entrapped liposome assay described previously was used to investigate and compare the abilities of the AvBD1 variants to disrupt bacterial membranes. The leakage assay data (Figure 5.24 A and B) showed that sAvBD1 NYH (blue line), SSY (green) and NYY (red) at concentrations of 1.5ug/ml induced $47.9\pm 2.9\%$, $26.5\pm 1.4\%$ and $21.7\pm 0.3\%$ calcein leakage, within 6 seconds of addition (Panel A). The control peptide was melittin (purple), which caused $46.4\pm 0.5\%$ leakage. In each case leakage plateaued within three minutes at $58.9\pm 1.6\%$, $38.6\pm 1.9\%$ and $32.7\pm 2.5\%$ (Panel B), which compared to $70.5\pm 1.9\%$ for melittin.

These data suggested that the sAvBD1 NYH peptide was significantly more potent ($P<0.0001$) in permeabilising membranes compared to the NYY and SSY peptides. In addition the sAvBD1 SSY variant was significantly more potent ($P<0.05$) than the NYY variant.

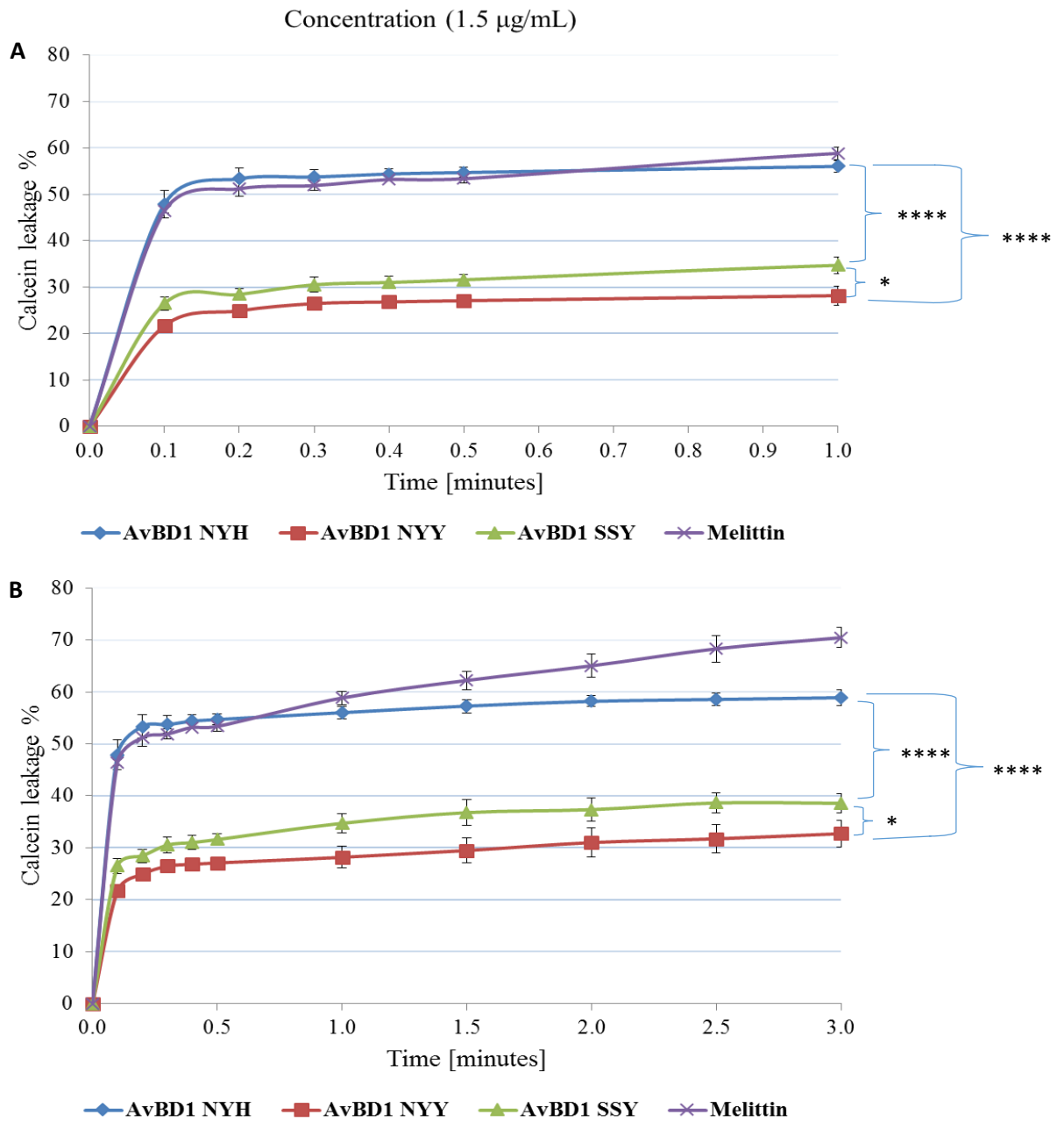


Figure 5.24 Calcein leakage recorded using entrapped liposomes incubated for up to 1 minute (A) and 3 minutes (B) at room temperature in 50 mM NaP buffer and 1.5 $\mu\text{g/ml}$ sAvBD1 NYH (blue), SSY (green), NYY (red) and melittin (purple). Experiments=3. Mean \pm SEM. * $P < 0.05$ and **** $P < 0.0001$. Data were analysed using one way ANOVA, followed by Dunnett's multiple comparison test.

Increasing the peptide concentrations to 2.5 $\mu\text{g/ml}$ caused increased leakage as shown in Figure 5.25 A and B. Although this experiment was performed only once due to limited peptide stocks, the AvBD1 peptide potency patterns were comparable to previous. Indeed, sAvBD1 NYH (blue), SSY (green) and NYY (red) induced 78.0%, 61.4% and 47.5% leakage within 6 seconds, (Panel A), which compared to 72.7% for melittin. Leakage was stable at 3 minutes (Panel B) and recorded as 89.8 % (melittin), 100% (NYH), 88.0 % (SSY) and 74.6 % (NYY) respectively.

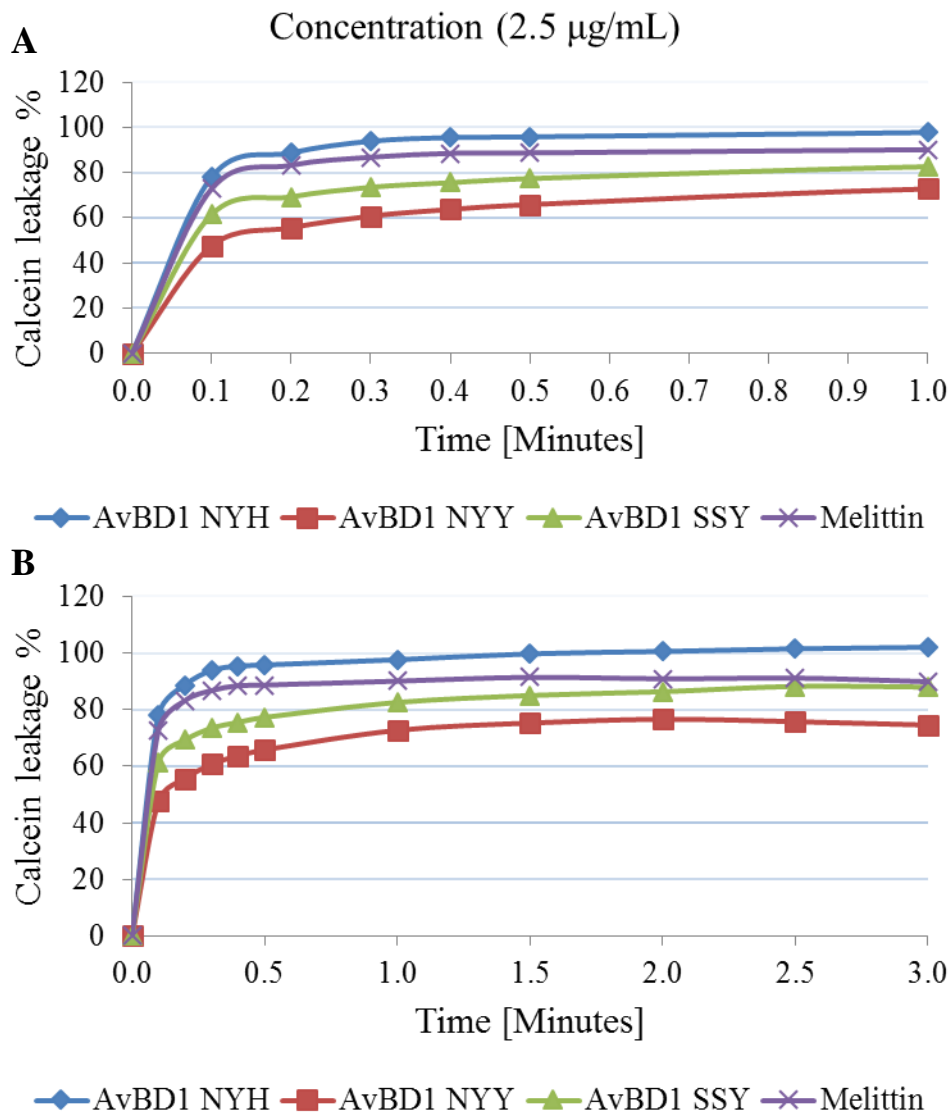


Figure 5.25 Calcein leakage recorded using entrapped liposomes incubated for up to 1 minute (A) and 3 minutes (B) at room temperature in 50 mM NaP buffer and 2.5 $\mu\text{g/ml}$ sAvBD1 NYH (blue) SSY (green) NYY (red) and melittin (purple). n=1.

5.10. AvBD1 modelling

The primary amino acid sequences of the AvBD1 variants differ in amino acids 10, 20 and 32, with NYH, SSY and NYY composed of asparagine (N)10, tyrosine (Y)20 and histidine(H)32; S10, S20 and Y32 and N10, Y20 and Y32, respectively.

Modelling the AvBD1 variant sequences using Raptor X on line software resulted in comparable backbone structures displaying β -sheet structures corresponding to the three disulphide bonds and a N-terminal α -helix (Figure 5.26 A-C). The predicted 3D structures all three variants were, as expected, also similar, with areas of positive charge and hydrophobicity, but the three amino acid ‘substitutions’ did appear to impact on the model structures (Figure 5.27 A-C).

Most marked was that the 3D model of AvBD1 NYH (Panel A) predicted that the W39 and K9 side chains, and R30 and R2 side chains formed ‘claw-like’ structures. The NYH model predicted externalisation and clustering of the positively charged side chains relating to K36, K9, R8, R37 and potentially K17, and K27, H32 and K3. Clustering and externalisation of the hydrophobic amino acids Y20 and W39, and four phenylalanine side chains F7, F12, F15 and F31 were also predicted.

Although the SSY model predicted a similar configuration to NYH, subtle changes were evident. For example the hydrophobicity of the Y20/W39 cluster was disrupted to the replacement of Y20 with a negatively charged serine residue; Only the R30 and R2 ‘claw’ structure was modelled in the SSY model but the claw-like structure modelled around W39 and K9 was lost presumably due to the impact of substituting the serine (S) for N10 and the presence of Y32 (replacing H32) disrupted the positively charged K27, H32 and K3 cluster.

The model relating to the NYY variant, the least antimicrobial of the three peptides, was particularly characterised by the loss of the two claw-like structures presumably related to the N10 and Y32 substitutions.

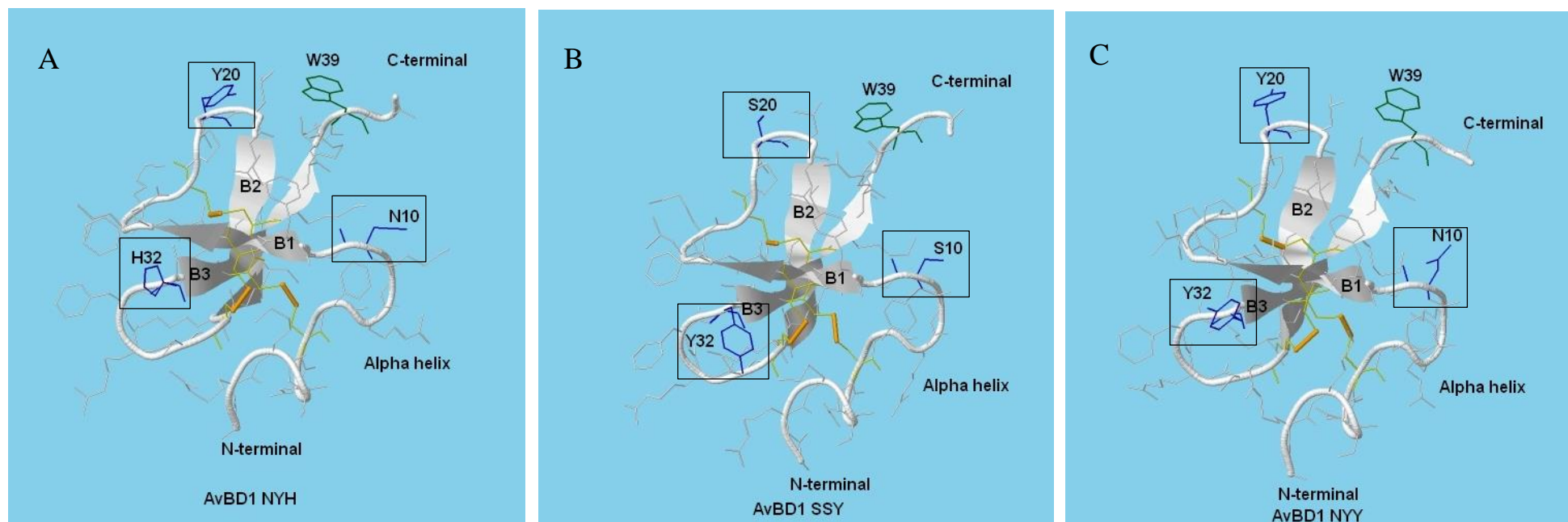


Figure 5.26 Predicted secondary structures (β -sheet and α -helix) of AvBD1 variants NYH (A), SSY (B) and NYY (C).

Disulphide bonds (orange). C-terminal tryptophan (green). Blue boxes show different amino acid side chains.

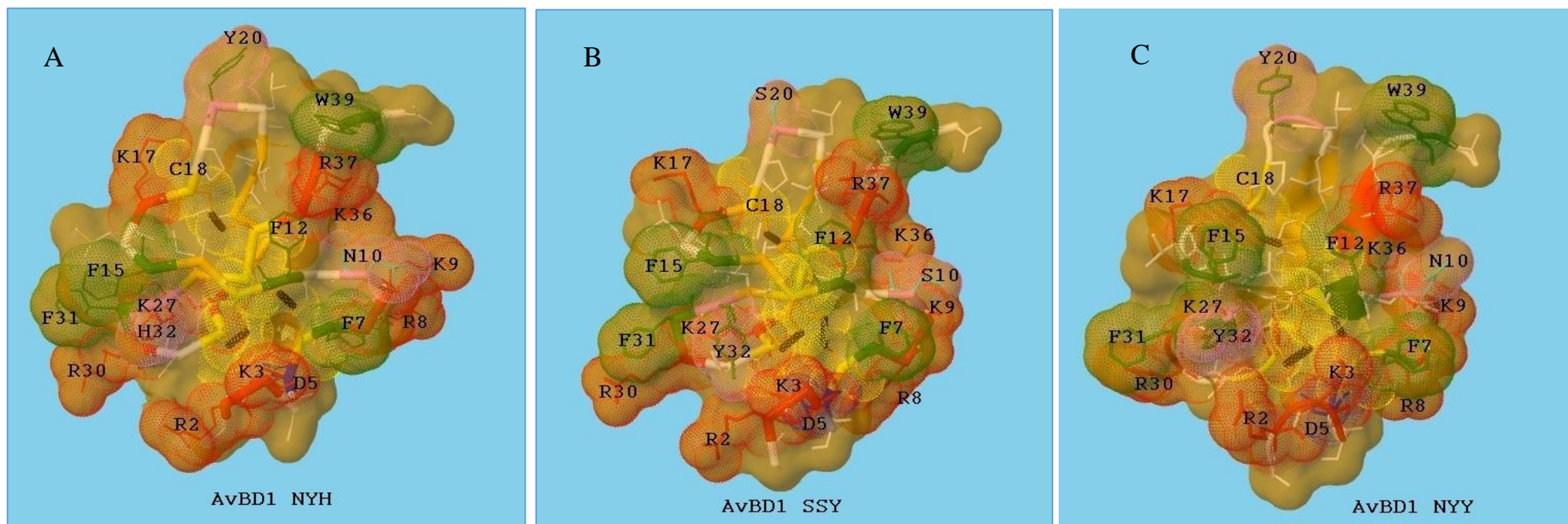


Figure 5.27 Simulated 3D structures of AvBD1 NYH (A), SSY (B) and NYY (C) variants.

Aromatic amino acids including tryptophan (W); phenylalanine (F) and tyrosine are highlighted in green; cationic residues including arginine (R), lysine (K) and histidine (H) in red; anionic residue aspartic acid (D) in purple; cysteines in yellow and disulphide bonds in orange.

5.11. Discussion

The earliest response to a microbial attack is determined by innate immune factors and genetic variants of these can increase or decrease susceptibility to infection and disease. The defensins are key innate elements in controlling microbial numbers thus SNPs resulting in non-synonymous amino acid changes are rare. Genome analyses of commercial chicken broiler lines linked to Aviagen Ltd identified SNP variants of the AvBD1 gene that encoded amino acid changes at positions 10, 20 and 32 of the AvBD1 mature peptide. The resulting peptides were identified as NYH, SSY and NYY AvBD1 variants. Bacterial killing data using synthetic linear peptides (Cadwell 2014, PhD), indicated that NYH >SSY> NYY (Figure 5.18). The aim of this chapter was to further understand this hierarchy by comparing the membrane interactive and disruptive activities of these three AvBD1 variants. To achieve this CD spectra and calcein leakage assays were performed.

The CD spectral data showed that all three peptides assumed an α -helix conformation when exposed to SDS (Figure 5.20). These data suggested that all the AvBD1 variants bound to anionic lipid membranes via similar mechanisms. It was acknowledged however that this α -helix mechanism was also consistent with the data recorded for the defensins AvBD6 and 9, and thus may have reflected the use of synthetic linear AvBD peptides generally. However, the leakage data supported NYH>SSY>NYY, which was consistent with the AMA data and indicated that the NYH variant was the most efficient permeabilising agent. Previous studies focussed on ostrich defensins have linked membrane leakage to the overall net charge of the peptides (Sugiarto and Yu, 2007b). However, in this scenario overall charge appears less important as the net charge of the NYH peptide was calculated as +7.8 at pH 7 compared to net charges of +7.7 for SSY and NYY. Still it is tempting to speculate that the increased leakage capacity of the NYH variant was influenced locally by the histidine residue at position 32, which modelling indicated created a very cationic cluster comprising R30, K27, H32, R2 and K3 (Figure 5.27A). The calcein leakage data supported the NYH peptide to be the most potent permeabilising agent thus the importance of the hydrophobic residues cannot be ignored since they are thought to have a significant impact on membrane insertion (Cuperus *et al.*, 2013). None-the-less, the low AMA and reduced leakage ability of the NYY variant with its two tyrosine bulky side chains did not support a role for these particular hydrophobic amino acids in membrane permeabilisation.

The modelling data showed that the basic structures of AvBD1 NYH, AvBD1 SSY and AvBD1 NYY, for example disulphide bond arrangement, β -sheet structures and N-terminal α -helix were similar (Figure 5.26). The differences, according to the proposed models, were in the distribution of the ‘substituted’ amino acids over the surface of the peptides. Interestingly, the AvBD1 NYH model predicted the side chain of K9 to protrude and form a ‘claw-like appearance’ with W39 (Figure 5.27 A). In the predicted SSY (Figure 5.27 B) and NYY (Figure 5.27 C) models this claw appeared to be ‘lost’ due to the impacts of the S10 and N10 side chains. Similar claw-like structures were shaped between R2 and R30 in the NYH and SSY models, but not in the NYY model. As the antimicrobial potency of the three peptides is NYH >SSY> NYY, these data predict a key role for the claw-like structures in AvBD antimicrobial activity. It has been suggested that the claw-like region plays a role in microbial membrane attachment (Soman *et al.*, 2010) and as described previously, was also predicted as part of the AvBD6, a potent antimicrobial agent, structure. The AvBD1 variants were characterised by four phenylalanine amino acids F7, F12, F15 and F31. It is worthy to note that the phenylalanine residues of the cathelicidin LL-37 molecule have been shown by NMR to play key roles in the binding of the peptide to anionic membranes (Wang, 2008). Although LL-37 is a linear peptide this information indicates the importance of the phenylalanine side-chains in attaching to bacterial membranes. The AvBD1 NYH, SSY and NYY models predict the four phenylalanine residues to be located on the exterior surface of the peptides, which strengthens their putative roles in microbial binding. However, the siting of H32 and K27 in the NYH (the most antimicrobial) model compared to Y32/K27 in SSY and NYY again provide support for localised charge effects in determining the activities and potencies of the peptides.

The prevalence of these non-synonymous SNPs in different bird lines could impact on gut health status since AvBD1 NYH peptides were synthesised by Line X (birds with less optimal gut performance), and SSY and NYY peptides by Lines Y and Z (birds with optimal gut performance), respectively (Butler, 2010). It is therefore easy to speculate that the AM potency of the NYH variant was linked to disruption of the gut microbiota of the Line X birds, for example through killing of *Lactobacillus* sp, leading to dysbacteriosis and reduced gut health (Cadwell 2014).

In vitro analyses indicated that the identified AvBD1 peptide non-synonymous amino acid changes did impact on the antimicrobial activity of the resultant peptides, and the data indicated that this occurred in part through effects on [bacterial] membrane

permeabilisation. *In silico* models suggested that this involved localised charge effects and the formation of claw-like structures.

5.12. Conclusions

The CD spectra indicated that the AvBD1 NYH, SSY and NYY peptide variants formed α -helix conformations in the presence of lipid micelles, modelling bacterial membranes, although it is acknowledged that linear peptides were used in all the experiments.

In the calcein leakage experiments AvBD1 NYH induced more leakage than SSY, which in turn was more potent than NYY.

Modelling simulations indicated that AvBD1 NYH contained two claw-like structures, SSY one claw-like structure and NYY no claw-like structures (NYY) suggesting roles for claw-like structures in the AvBD mechanism of action.

Chapter 6

Final Discussion

The European Union regulation 1831/2003/EC banning the use of antibiotic growth promoters in animal feed since 2006 was introduced to address problems of antimicrobial resistance. Its introduction has forced commercial livestock breeding companies to focus their research on the immune systems of animals with the objectives of selecting for and breeding disease resistant animals. In particular the innate system has been targeted as it is important in the early days of life with the premise being that a ‘robust’ innate immune system helps to protect young animals against infectious diseases. One facet of the innate immune system is the epithelial synthesis of host defence proteins, particularly antimicrobial peptides, which are <5kDa in size, show broad antimicrobial activity and are constitutively synthesised or induced in response to bacterial challenges. The focus of this thesis was avian β -defensins (AvBDs), particularly the expression, anti-microbial activities and mechanisms of action of AvBDs 6 and 9.

Birds raised in commercial poultry farm environments are continually exposed through bedding, feed and faeces to numerous microbes. Thus robust birds, ie those resisting disease and showing optimal feed to weight gain ratio, are particularly desired by the breeders. As the defensins are predicted to play a role in shaping the resistance of such birds to microbial diseases, analyses of their gene expression profiles and peptide anti-microbial activities are essential. However, for the data to be valuable such studies need to be performed using birds from commercial breeding lines and the rearing environments need to mimic commercial establishments rather than those of the laboratory. The resultant data will then inform breeders which, if any, of the defensin genes are the most desirable to select for.

To date the majority of chicken *in vivo* microbial challenge studies have focussed on the expression of AvBDs and pro-inflammatory cytokines in ‘laboratory raised’ birds following inoculation with a single bacterial or parasitic species (Zhao *et al.*, 2001; Hong *et al.*, 2012). *In vitro* experiments have similarly used specific cell lines and single bacterial challenges (Derache *et al.*, 2009a; Abdelsalam *et al.*, 2012). These approaches have produced informative data about disease pathology and mechanisms, from both the perspective of the microbe and the avian tissue examined. However, these data do not directly reflect what actually happens in the bird tissues *in vivo* during exposure of either newly hatched, young or adult chickens, raised in commercial environments, to multiple

microbial challenges. Chapter three addressed this by focussing on a line of Aviagen Ltd (Line X) birds raised in two different farm environments, low hygiene and high hygiene, and exploring AvBD6 and 9 as well as cytokine gene expression in an array of bird tissues. Despite the supposed genetic identity of the Line X birds the quantitative PCR data showed the AvBD6 and 9 expression were highly variable among individual birds. AvBD6 and 9 were selected for study due to SNPs within introns and non-coding regions, so the variation was perhaps not particularly surprising. For example, the AvBD9 gene contains a SNP in its 3'UTR (Table 3.1), which potentially can affect expression through mRNA stability, as shown for sheep β -defensin 1 (Monteleone *et al.*, 2011). Both genes also carry intronic SNPs (Table 3.1) and such SNPs can also affect expression. Indeed, a recent study reported the impact of intronic SNPs on human β -defensin 1 gene expression with individuals with a 5'UTR homozygous polymorphism showing increased salivary peptide concentrations (Polesello *et al.*, 2015). However, as the corresponding genomic DNA sequences of the birds were not available it was only possible to report trends and not link the expression data to actual SNPs. As a result it was also not possible to link the expression data to either environmental and/or genomic effects. It was also acknowledged that the numbers of birds used in the AvBD gene expression studies were low, thus reducing the statistical power of the analyses. Future studies involving SNP analyses will require significantly greater numbers of birds.

None-the-less, interesting trends in AvBD expression were observed. Increased baseline expression of AvBD6 in the lung and AvBD9 in both kidney and liver may relate to functions other than antimicrobial activity including wound healing, and immunomodulation. Indeed, such functions have been reported for mammalian defensins (Steinstraesser *et al.*, 2011; Semple and Dorin, 2012), and for duck Apl_AvBD2 (Soman *et al.*, 2009). Additionally, AvBD6 expression in the caecal tonsils compared to the caecum indicated a potential role for this secondary lymphoid tissue in the innate defences of the chicken gut and this requires further investigation. In support, AvBD6 expression was also increased in the caecal tonsils of chicks infected with *Salmonella enterica* serovar Typhimurium (Akbari *et al.*, 2008).

The line of birds examined in the study was characterised by its increased susceptibility to gut inflammation. However, overall the pro-inflammatory and anti-inflammatory cytokine gene responses in the different environments, although limited to IL-6 and TGF β 4, were supportive of physiological rather than pathological inflammatory responses. While it

cannot be excluded that other pro-inflammatory cytokines, e.g IL β 1 were involved in the responses, the fact that the guts of the birds were not scored for inflammation and hence damage when the tissues were collected makes it difficult to reach any definitive conclusions. Future studies focussed on Line X birds will also need to concentrate on the gut pathology and cytokine responses of individual birds.

It was noteworthy that chicken galectin-3 (CG3) expression was elevated in the gut compared to other tissues. Galectin-3 functions as an opsonin, facilitating microbial destruction through attachment to the lipopolysaccharide (LPS) of the bacteria cell membrane and phagocyte surface glycoproteins (Almkvist and Karlsson, 2004). It also has chemo-attractive properties, attracting macrophages and stimulating monocyte migration (Sano *et al.*, 2000). The levels of expression support potential roles for CG3 in the innate defences of the gut and warrant further investigations, including IHC to confirm protein synthesis and gut localisation. Such studies in birds with healthy versus inflamed guts will be particularly interesting.

The data revealed individual birds with 'high' levels of AvBD expression (Figure 3.16 A). Although it is tempting for breeders to select birds showing such high expression in the gut tissues and hence increased AMA, it could be argued that this may not always be beneficial. For example in the caecum, high AvBD peptide concentrations may actually cause disruption of the enteric commensal community leading to dysbacteriosis and gut problems including inflammation. As discussed earlier future studies, to be informative for breeders, will need to increase the bird numbers, and explore the gut pathology, defensin and cytokine responses of individual birds as well as the groups per se.

Mammalian defensins are secreted in the intestinal crypts at concentrations of up to 10 mg/ml and in epithelial cells at concentrations of 10-100 μ g/ml (Ganz, 2003). Measurement of the actual AvBD peptide concentrations in the tissues and blood were absent in this study due to the lack of appropriate samples, antibodies and synthetic peptides for ELISA development. It is acknowledged that future studies need to address this as mRNA levels can indicate, but do not always reflect, peptide concentrations.

It is assumed from their primary structures that the AvBD6 and 9 peptides are antimicrobial agents. To actually confirm this the peptides encoded by the Line X AvBD6 and 9 bird genes were synthesised *in vitro* using a BL21 hyper-expression system, and the AMAs of the recombinant peptides tested using radial immuno-diffusion and time kill colony

counting assays. The data reported in Chapter four indicated that both rAvBD6 and 9 have killing properties against both Gram positive and negative bacteria. The bacteria used in these studies were isolated from chickens raised on Aviagen farms, which strengthened the antimicrobial data as many clinical strains often show increased resistance to AMPs compared to laboratory passaged microbial strains (Derache *et al.*, 2009b). The assays showed that recombinant (r) AvBD6 was a more potent antimicrobial agent than rAvBD9, which probably related to charge, with AvBD6 being more cationic (+6.8) than AvBD9 (+3.8), and hydrophobicity. It was interesting that the presence of a pro-piece did not appear to affect the antimicrobial activity of rAvBD6 or 9 especially as the pro-piece of a mouse α -defensin, cryptdin-4, although 36 amino acids in size and anionic, has been reported to reduce the killing properties of the peptide (Figueredo *et al.*, 2009). Interestingly, the *in vivo* cleavage of the AvBD hexapeptide pro-piece has not been confirmed (Xiao *et al.*, 2004; van Dijk *et al.*, 2007), but if it is retained *in vivo* then its size and hydrophobicity could be argued as aiding killing by facilitating membrane perforation and disruption (Soman *et al.*, 2010; Tai *et al.*, 2014).

A previous study had suggested the importance of the 6C in AvBD2 activity (Derache *et al.*, 2012), thus Chapter four also explored the roles of the six conserved cysteines (6C) and the C-terminal tryptophan in AvBD9 antimicrobial activity. The AvBD9 6CA/G variant with no cysteines showed antimicrobial activity and in fact was more antimicrobial against *E. faecalis* than *E. coli* although this may have reflected its stability in the presence of proteases synthesised by the different bacteria. However, the AMA data relating to both AvBD9 analogues, 3CA and AvBD9 6CA/G, strongly supported the roles of the disulphide bonds in protecting against the proteolytic activities of enzymes secreted by bacteria and presumably those synthesised by eukaryote tissues. Essentially the folding produces a globular AvBD structure that is more resistant to proteolysis than is a linear one. Interestingly, some mammalian defensins have been reported to work efficiently both in the linear and folded forms. For example, HBD1 and HD6 are secreted into the gut lumen as folded peptides, but following linearisation in the reducing environment of the gut still retain their AMA killing properties (Schroeder *et al.*, 2011; Schroeder *et al.*, 2015). It is probable that the AvBDs show similar properties although further experiments are needed to explore this.

While the AvBD structures and mechanisms of action are not wholly relevant to poultry breeders, they are of scientific interest and may help explain the evolution of an array of

AvBD peptides in the avian tissues. Through work using mammalian peptides it is generally accepted that the defensin killing mechanism is via microbial membrane interaction and disruption (Ganz, 2003). To investigate this further in relation to the AvBDs 6 and 9, CD spectra and calcein leakage assays were adopted. These data, reported in Chapter five, predicted a predominantly β -sheet structure for rAvBD9 and this was supported by the reduced β -sheet structures of rAvBD9 3CA and 6CAG peptides. These data also suggested spontaneous folding of the 6C recombinant peptide; in support a recent study has shown that the mouse α -defensin cryptidin-4 expressed in BL21 (DE3) pLysS folds spontaneously and correctly (Tomisawa *et al.*, 2015). Interestingly, the β -sheet content of rAvBD9 W38G, which contained 6C, but lacked the C-terminally located tryptophan conserved in 10/14 AvBDs (Figure 4.12), was reduced and suggested a major impact of tryptophan on the *in vitro* folding of the peptide.

The actual mechanisms by which AvBD causes microbial killing are not known. The CD spectra and calcein leakage data described in Chapter five suggested it involves an initial binding step in which the N-terminal α -helix of the molecule lines up parallel to the membrane surface, followed by insertion of the peptide into the bi-layer and disruption of membrane permeability through pore formation. The calcein data relating to the linear sAvBD1 and sAvBD6 peptides were particularly supportive of membrane disruption. Modelling data also predicted the structure of AvBD6 to contain a hook-like foramen structure containing two tryptophans, which presumably facilitates peptide attachment to a target microbial membrane. A similar claw-like structure was predicted for AvBD1 NYH, which had potent AMA, suggesting important roles for such structures in microbial killing. Interestingly the linear sAvBD1 peptides were reported to be highly antimicrobial against *E. coli* (Kevin Cadwell, 2014, PhD thesis), suggesting they function as anti-microbial agents even in reducing conditions. These data were comparable to that of the mammalian HBD1 and HD6 peptides, following reduction by thioredoxin in the gut epithelium (Schroeder *et al.*, 2011; Schroeder *et al.*, 2015), and suggests key roles for the AvBD1 peptides in the innate defences of the gut.

In contrast AvBD9 was associated with AMA, but minor calcein leakage, suggesting its action was not directly through membrane destruction. Alternative killing mechanisms include inhibition of nucleic acid synthesis and/or cell division (Sugiarto and Yu, 2007b; Teng *et al.*, 2014). In relation to AvBD9 these require further investigation through the use of fluorescent and electron microscopy studies of dividing bacteria in the presence and

absence of peptide (Peng *et al.*, 2013; Teng *et al.*, 2014). It was interesting that the C-terminal tryptophan of AvBD9 was also important for its AMA. As tryptophans are known to facilitate peptide insertion into membranes (Wei *et al.*, 2010) it would be interesting, scientifically, to explore this idea further.

In selecting for chicken genes that focus on innate immunity care must be taken to fully investigate the targeted genes in all rearing conditions and to ensure that the genes selected encode peptides/proteins that enhance protection, and do not cause, for example, gut dysbacteriosis. Work presented in this thesis has shown the expression of two AvBD genes in a line of commercial birds raised in different rearing environments. Despite the genetic identity of the birds the AvBD expression patterns were very variable between individual birds. However, the small bird numbers and lack of individual bird genomic DNA sequences did not allow these data to be related specifically to either the external environment and/or specific SNPS. Future studies will address these parameters. It was demonstrated *in vitro* that the AvBDs 6 and 9 genes expressed by the Line X birds encode potent antimicrobial killing agents that presumably function in defending the epithelia through microbial killing. Their synthesis as globular structures helps reduce potential degradation by proteases although the *in vitro* AMA data did support the linear peptides as having killing properties. This may have immunological significance *in vivo* especially in relation to the reductive environment of the gut where it may permit fine control of the microbial numbers and communities. Gut microbiota studies will allow this to be explored further. Interestingly, the *in vitro* studies supported different mechanisms of action of the two defensins studied with AvBD6 causing membrane damage compared to AvBD9, which probably functions through disrupting intracellular systems. These data suggest that the AvBD peptides work in synergy in defending the epithelia and perhaps caution against poultry geneticists just selecting individual AvBD genes for breeding purposes.

References:

- Abdelsalam, M., Isobe, N. and Yoshimura, Y. (2012) 'Effects of lipopolysaccharide and interleukins on the expression of avian β -defensins in hen ovarian follicular tissue', *Poult Sci*, 91(11), pp. 2877-84.
- Akbari, M.R., Haghighi, H.R., Chambers, J.R., Brisbin, J., Read, L.R. and Sharif, S. (2008) 'Expression of antimicrobial peptides in cecal tonsils of chickens treated with probiotics and infected with *Salmonella enterica* serovar typhimurium', *Clin Vaccine Immunol*, 15(11), pp. 1689-93.
- Almkvist, J. and Karlsson, A. (2004) 'Galectins as inflammatory mediators', *Glycoconj J*, 19(7-9), pp. 575-81.
- Avery, S., Rothwell, L., Degen, W.D., Schijns, V.E., Young, J., Kaufman, J. and Kaiser, P. (2004) 'Characterization of the first nonmammalian T2 cytokine gene cluster: the cluster contains functional single-copy genes for IL-3, IL-4, IL-13, and GM-CSF, a gene for IL-5 that appears to be a pseudogene, and a gene encoding another cytokinelike transcript, KK34', *J Interferon Cytokine Res*, 24(10), pp. 600-10.
- Bals, R., Wang, X., Wu, Z., Freeman, T., Bafna, V., Zasloff, M. and Wilson, J.M. (1998) 'Human β -defensin 2 is a salt-sensitive peptide antibiotic expressed in human lung', *J Clin Invest*, 102(5), pp. 874-80.
- Barondes, S.H., Cooper, D.N., Gitt, M.A. and Leffler, H. (1994) 'Galectins. Structure and function of a large family of animal lectins', *J Biol Chem*, 269(33), pp. 20807-10.
- Bevins, C.L. and Salzman, N.H. (2011) 'The potter's wheel: the host's role in sculpting its microbiota', *Cell Mol Life Sci*, 68(22), pp. 3675-85.
- Bi, X., Wang, C., Dong, W., Zhu, W. and Shang, D. (2014) 'Antimicrobial properties and interaction of two Trp-substituted cationic antimicrobial peptides with a lipid bilayer', *J Antibiot (Tokyo)*, 67(5), pp. 361-8.
- Bi, X., Wang, C., Ma, L., Sun, Y. and Shang, D. (2013) 'Investigation of the role of tryptophan residues in cationic antimicrobial peptides to determine the mechanism of antimicrobial action', *J Appl Microbiol*, 115(3), pp. 663-72.

- Bonucci, A., Balducci, E., Pistolesi, S. and Pogni, R. (2013) 'The defensin-lipid interaction: insights on the binding states of the human antimicrobial peptide HNP-1 to model bacterial membranes', *Biochim Biophys Acta*, 1828(2), pp. 758-64.
- Bowdish, D.M., Davidson, D.J. and Hancock, R.E. (2006) 'Immunomodulatory properties of defensins and cathelicidins', *Curr Top Microbiol Immunol*, 306, pp. 27-66.
- Brisbin, J.T., Gong, J. and Sharif, S. (2008) 'Interactions between commensal bacteria and the gut-associated immune system of the chicken', *Animal health research reviews / Conference of Research Workers in Animal Diseases*, 9(1), pp. 101-10.
- Burt, D.W. and Jakowlew, S.B. (1992) 'Correction: a new interpretation of a chicken transforming growth factor- β -4 complementary DNA', *Mol Endocrinol*, 6(6), pp. 989-92.
- Butler, V. (2010) *The effects of genetics, age and rearing environment on AvBD gene expression and gut anti-microbial activities in three chicken lines*. Newcastle University [Online]:<https://theses.ncl.ac.uk/dspace/bitstream/10443/2240/1/Butler%20V.L.%2010.pdf>.
- Cadwell, K. (2014): *Investigations of the Gut Innate Defences of Commercial Broilers*. Newcastle University, UK, PhD thesis.
- Campopiano, D.J., Clarke, D.J., Polfer, N.C., Barran, P.E., Langley, R.J., Govan, J.R., Maxwell, A. and Dorin, J.R. (2004) 'Structure-activity relationships in defensin dimers: a novel link between β -defensin tertiary structure and antimicrobial activity', *J Biol Chem*, 279(47), pp. 48671-9.
- Casteleyn, C., Doom, M., Lambrechts, E., Van den Broeck, W., Simoens, P. and Cornillie, P. (2010) 'Locations of gut-associated lymphoid tissue in the 3-month-old chicken: a review', *Avian Pathol*, 39(3), pp. 143-50.
- Chandrababu, K.B., Ho, B. and Yang, D. (2009) 'Structure, dynamics, and activity of an all-cysteine mutated human β -defensin-3 peptide analogue', *Biochemistry*, 48(26), pp. 6052-61.
- Choi, K.D. and Lillehoj, H.S. (2000) 'Role of chicken IL-2 on gammadelta T-cells and Eimeria acervulina-induced changes in intestinal IL-2 mRNA expression and gammadelta T-cells', *Vet Immunol Immunopathol*, 73(3-4), pp. 309-21.

- Choi, K.D., Lillehoj, H.S. and Zalenga, D.S. (1999) 'Changes in local IFN-gamma and TGF- β 4 mRNA expression and intraepithelial lymphocytes following *Eimeria acervulina* infection', *Vet Immunol Immunopathol*, 71(3-4), pp. 263-75.
- Crhanova, M., Hradecka, H., Faldynova, M., Matulova, M., Havlickova, H., Sisak, F. and Rychlik, I. (2011) 'Immune response of chicken gut to natural colonization by gut microflora and to *Salmonella enterica* serovar enteritidis infection', *Infect Immun*, 79(7), pp. 2755-63.
- Cuperus, T., Coorens, M., van Dijk, A. and Haagsman, H.P. (2013) 'Avian host defense peptides', *Dev Comp Immunol*, 41(3), pp. 352-69.
- Das, S.C., Isobe, N. and Yoshimura, Y. (2011) 'Expression of Toll-like receptors and avian β -defensins and their changes in response to bacterial components in chicken sperm', *Poult Sci*, 90(2), pp. 417-25.
- Davison, F., Kaspers, B. and Schat, K.A. (2008) 'Avian Immunology', in Oxford: Elsevier Ltd, pp. 203-222.
- de Geus, E.D. and Vervelde, L. (2013) 'Regulation of macrophage and dendritic cell function by pathogens and through immunomodulation in the avian mucosa', *Dev Comp Immunol*, 41(3), pp. 341-51.
- Derache, C., Esnault, E., Bonsergent, C., Le Vern, Y., Quere, P. and Lalmanach, A.C. (2009a) 'Differential modulation of β -defensin gene expression by *Salmonella* Enteritidis in intestinal epithelial cells from resistant and susceptible chicken inbred lines', *Dev Comp Immunol*, 33(9), pp. 959-66.
- Derache, C., Labas, V., Aucagne, V., Meudal, H., Landon, C., Delmas, A.F., Magallon, T. and Lalmanach, A.C. (2009b) 'Primary structure and antibacterial activity of chicken bone marrow-derived β -defensins', *Antimicrob Agents Chemother*, 53(11), pp. 4647-55.
- Derache, C., Meudal, H., Aucagne, V., Mark, K.J., Cadene, M., Delmas, A.F., Lalmanach, A.C. and Landon, C. (2012) 'Initial insights into structure-activity relationships of avian defensins', *J Biol Chem*, 287(10), pp. 7746-55.
- Dhirapong, A., Lleo, A., Leung, P., Gershwin, M.E. and Liu, F.T. (2009) 'The immunological potential of galectin-1 and -3', *Autoimmun Rev*, 8(5), pp. 360-3.
- Dorin, J.R. and Barratt, C.L. (2014) 'Importance of β -defensins in sperm function', *Mol Hum Reprod*, 20(9), pp. 821-6.

- Figueredo, S.M., Weeks, C.S., Young, S.K. and Ouellette, A.J. (2009) 'Anionic Amino Acids near the Pro- α -defensin N Terminus Mediate Inhibition of Bactericidal Activity in Mouse Pro-cryptdin-4', *The Journal of Biological Chemistry*, 284(11), pp. 6826-6831.
- Ganz, T. (2003) 'Defensins: antimicrobial peptides of innate immunity', *Nat Rev Immunol*, 3(9), pp. 710-20.
- Ganz, T. (2004) 'Defensins: antimicrobial peptides of vertebrates', *C R Biol*, 327(6), pp. 539-49.
- Garcia, J.R., Krause, A., Schulz, S., Rodriguez-Jimenez, F.J., Kluver, E., Adermann, K., Forssmann, U., Frimpong-Boateng, A., Bals, R. and Forssmann, W.G. (2001) 'Human β -defensin 4: a novel inducible peptide with a specific salt-sensitive spectrum of antimicrobial activity', *Faseb j*, 15(10), pp. 1819-21.
- Gharaibeh, S. and Mahmoud, K. (2013) 'Decay of maternal antibodies in broiler chickens', *Poult Sci*, 92(9), pp. 2333-6.
- Goldman, M.J., Anderson, G.M., Stolzenberg, E.D., Kari, U.P., Zasloff, M. and Wilson, J.M. (1997) 'Human β -defensin-1 is a salt-sensitive antibiotic in lung that is inactivated in cystic fibrosis', *Cell*, 88(4), pp. 553-60.
- Gong, D., Wilson, P.W., Bain, M.M., McDade, K., Kalina, J., Herve-Grepinet, V., Nys, Y. and Dunn, I.C. (2010) 'Gallin; an antimicrobial peptide member of a new avian defensin family, the ovodefensins, has been subject to recent gene duplication', *BMC Immunol*, 11, p. 12.
- Hancock, R.E. and Scott, M.G. (2000) 'The role of antimicrobial peptides in animal defenses', *Proc Natl Acad Sci U S A*, 97(16), pp. 8856-61.
- Hasenstein, J.R. and Lamont, S.J. (2007) 'Chicken gallinacin gene cluster associated with Salmonella response in advanced intercross line', *Avian Dis*, 51(2), pp. 561-7.
- Hellgren, O. and Ekblom, R. (2010) 'Evolution of a cluster of innate immune genes (β -defensins) along the ancestral lines of chicken and zebra finch', *Immunome Res*, 6, p. 3.
- Herve, V., Meudal, H., Labas, V., Rehaut-Godbert, S., Gautron, J., Berges, M., Guyot, N., Delmas, A.F., Nys, Y. and Landon, C. (2014) 'Three-dimensional NMR structure of Hen Egg Gallin (Chicken Ovodefensin) reveals a new variation of the β -defensin fold', *J Biol Chem*, 289(10), pp. 7211-20.

- Higgs, R., Lynn, D.J., Cahalane, S., Alana, I., Hewage, C.M., James, T., Lloyd, A.T. and O'Farrelly, C. (2007) 'Modification of chicken avian β -defensin-8 at positively selected amino acid sites enhances specific antimicrobial activity', *Immunogenetics*, 59(7), pp. 573-80.
- Hong, Y.H., Lillehoj, H.S., Lee, S.H., Dalloul, R.A. and Lillehoj, E.P. (2006) 'Analysis of chicken cytokine and chemokine gene expression following *Eimeria acervulina* and *Eimeria tenella* infections', *Vet Immunol Immunopathol*, 114(3-4), pp. 209-23.
- Hong, Y.H., Song, W., Lee, S.H. and Lillehoj, H.S. (2012) 'Differential gene expression profiles of β -defensins in the crop, intestine, and spleen using a necrotic enteritis model in 2 commercial broiler chicken lines', *Poult Sci*, 91(5), pp. 1081-8.
- Howard, A., Townes, C., Milona, P., Nile, C.J., Michailidis, G. and Hall, J. (2010) 'Expression and functional analyses of liver expressed antimicrobial peptide-2 (LEAP-2) variant forms in human tissues', *Cell Immunol*, 261(2), pp. 128-33.
- Hu, W.N., Jiao, W.J., Ma, Z., Dong, N., Ma, Q.Q., Shao, C.X. and Shan, A.S. (2013) 'The influence of isoleucine and arginine on biological activity and peptide-membrane interactions of antimicrobial peptides from the bactericidal domain of AvBD4', *Protein Pept Lett*, 20(11), pp. 1189-99.
- Huyghebaert, G., Ducatelle, R. and Van Immerseel, F. (2011) 'An update on alternatives to antimicrobial growth promoters for broilers', *Vet J*, 187(2), pp. 182-8.
- Hyldgaard, M., Sutherland, D.S., Sundh, M., Mygind, T. and Meyer, R.L. (2012) 'Antimicrobial mechanism of monocaprylate', *Appl Environ Microbiol*, 78(8), pp. 2957-65.
- Ibrahim, H.R., Sugimoto, Y. and Aoki, T. (2000) 'Ovotransferrin antimicrobial peptide (OTAP-92) kills bacteria through a membrane damage mechanism', *Biochim Biophys Acta*, 1523(2-3), pp. 196-205.
- Jakowlew, S.B., Mathias, A. and Lillehoj, H.S. (1997) 'Transforming growth factor- β -isoforms in the developing chicken intestine and spleen: increase in transforming growth factor- β -4 with coccidia infection', *Vet Immunol Immunopathol*, 55(4), pp. 321-39.
- Jenssen, H., Hamill, P. and Hancock, R.E. (2006) 'Peptide antimicrobial agents', *Clin Microbiol Rev*, 19(3), pp. 491-511.

- Kaiser, M.G., Cheeseman, J.H., Kaiser, P. and Lamont, S.J. (2006) 'Cytokine expression in chicken peripheral blood mononuclear cells after *in vitro* exposure to Salmonella enterica serovar Enteritidis', *Poultry science*, 85(11), pp. 1907-11.
- Kaiser, P. and Mariani, P. (1999) 'Promoter sequence, exon:intron structure, and synteny of genetic location show that a chicken cytokine with T-cell proliferative activity is IL-2 and not IL15', *Immunogenetics*, 49(1), pp. 26-35.
- Kaiser, P., Poh, T.Y., Rothwell, L., Avery, S., Balu, S., Pathania, U.S., Hughes, S., Goodchild, M., Morrell, S., Watson, M., Bumstead, N., Kaufman, J. and Young, J.R. (2005) 'A genomic analysis of chicken cytokines and chemokines', *J Interferon Cytokine Res*, 25(8), pp. 467-84.
- Kaiser, P., Rothwell, L., Goodchild, M. and Bumstead, N. (2004) 'The chicken proinflammatory cytokines interleukin-1 β -and interleukin-6: differences in gene structure and genetic location compared with their mammalian orthologues', *Animal genetics*, 35(3), pp. 169-75.
- Kaltner, H., Kubler, D., Lopez-Merino, L., Lohr, M., Manning, J.C., Lensch, M., Seidler, J., Lehmann, W.D., Andre, S., Solis, D. and Gabius, H.J. (2011) 'Toward comprehensive analysis of the galectin network in chicken: unique diversity of galectin-3 and comparison of its localization profile in organs of adult animals to the other four members of this lectin family', *Anat Rec (Hoboken)*, 294(3), pp. 427-44.
- Kaltner, H., Solis, D., Andre, S., Lensch, M., Manning, J.C., Murnseer, M., Saiz, J.L. and Gabius, H.J. (2009) 'Unique chicken tandem-repeat-type galectin: implications of alternative splicing and a distinct expression profile compared to those of the three prototype proteins', *Biochemistry*, 48(20), pp. 4403-16.
- Kannan, L., Liyanage, R., Lay Jr., J. and Packialakshmi, B. (2013) 'Identification and Structural Characterization of Avian B-Defensin 2 Peptides from Pheasant and Quail', *Journal of Proteomics & Bioinformatics*, 6(2), p. 031.
- Kasai, K. and Hirabayashi, J. (1996) 'Galectins: a family of animal lectins that decipher glycocodes', *Journal of biochemistry*, 119(1), pp. 1-8.
- Kelly, S.M., Jess, T.J. and Price, N.C. (2005) 'How to study proteins by circular dichroism', *Biochim Biophys Acta*, 1751(2), pp. 119-39.

- Kim, S.J., Kim, J.S., Lee, Y.S., Sim, D.W., Lee, S.H., Bahk, Y.Y., Lee, K.H., Kim, E.H., Park, S.J., Lee, B.J. and Won, H.S. (2013) 'Structural characterization of de novo designed L5K5W model peptide isomers with potent antimicrobial and varied hemolytic activities', *Molecules*, 18(1), pp. 859-76.
- Kluver, E., Schulz-Maronde, S., Scheid, S., Meyer, B., Forssmann, W.G. and Adermann, K. (2005) 'Structure-activity relation of human β -defensin 3: influence of disulfide bonds and cysteine substitution on antimicrobial activity and cytotoxicity', *Biochemistry*, 44(28), pp. 9804-16.
- Kudryashova, E., Seveau, S., Lu, W. and Kudryashov, D.S. (2015) 'Retrocyclins neutralize bacterial toxins by potentiating their unfolding', *Biochem J*, 467(2), pp. 311-20.
- Lan, H., Chen, H., Chen, L.-C., Wang, B.-B., Sun, L., Ma, M.-Y., Fang, S.-G. and Wan, Q.-H. (2014) 'The first report of a Pelecaniformes defensin cluster: Characterization of [bgr]-defensin genes in the crested ibis based on BAC libraries', *Sci. Rep.*, 4, p. 6923.
- Landon, C., Thouzeau, C., Labbe, H., Bulet, P. and Vovelle, F. (2004) 'Solution structure of spheniscin, a β -defensin from the penguin stomach', *J Biol Chem*, 279(29), pp. 30433-9.
- Lehrer, R.I., Cole, A.M. and Selsted, M.E. (2012) 'theta-Defensins: cyclic peptides with endless potential', *J Biol Chem*, 287(32), pp. 27014-9.
- Lehrer, R.I. and Lu, W. (2012) ' α -Defensins in human innate immunity', *Immunol Rev*, 245(1), pp. 84-112.
- Lindberg, M. and Graslund, A. (2001) 'The position of the cell penetrating peptide penetratin in SDS micelles determined by NMR', *FEBS Lett*, 497(1), pp. 39-44.
- Linde, A., Wachter, B., Höner, O., Dib, L., Ross, C., Tamayo, A., Blecha, F. and Melgarejo, T. (2009) 'Natural History of Innate Host Defense Peptides', *Probiotics and Antimicrobial Proteins*, 1(2), pp. 97-112.
- Liu, F.T. (2005) 'Regulatory roles of galectins in the immune response', *Int Arch Allergy Immunol*, 136(4), pp. 385-400.
- Lowenthal, J.W., Bean, A.G. and Kogut, M.H. (2013) 'What's so special about chicken immunology? Preface', *Dev Comp Immunol*, 41(3), pp. 307-9.

- Lu, L., Li, S.M., Zhang, L., Liu, X.Q., Li, D.Y., Zhao, X.L. and Liu, Y.P. (2015) 'Expression of β -defensins in intestines of chickens injected with vitamin D3 and lipopolysaccharide', *Genet Mol Res*, 14(2), pp. 3330-7.
- Lu, S., Peng, K., Gao, Q., Xiang, M., Liu, H., Song, H., Yang, K., Huang, H. and Xiao, K. (2014) 'Molecular cloning, characterization and tissue distribution of two ostrich β -defensins: AvBD2 and AvBD7', *Gene*, 552(1), pp. 1-7.
- Lu, X., Shen, J., Jin, X., Ma, Y., Huang, Y., Mei, H., Chu, F. and Zhu, J. (2012) 'Bactericidal activity of *Musca domestica* cecropin (Mdc) on multidrug-resistant clinical isolate of *Escherichia coli*', *Appl Microbiol Biotechnol*, 95(4), pp. 939-45.
- Lynn, D.J., Higgs, R., Gaines, S., Tierney, J., James, T., Lloyd, A.T., Fares, M.A., Mulcahy, G. and O'Farrelly, C. (2004) 'Bioinformatic discovery and initial characterisation of nine novel antimicrobial peptide genes in the chicken', *Immunogenetics*, 56(3), pp. 170-7.
- Ma, D., Zhang, K., Zhang, M., Xin, S., Liu, X., Han, Z., Shao, Y. and Liu, S. (2012a) 'Identification, expression and activity analyses of five novel duck β -defensins', *PLoS One*, 7(10), p. e47743.
- Ma, D., Zhang, M., Zhang, K., Liu, X., Han, Z., Shao, Y. and Liu, S. (2013) 'Identification of three novel avian β -defensins from goose and their significance in the pathogenesis of *Salmonella*', *Mol Immunol*, 56(4), pp. 521-9.
- Ma, D., Zhou, C., Zhang, M., Han, Z., Shao, Y. and Liu, S. (2012b) 'Functional analysis and induction of four novel goose (*Anser cygnoides*) avian β -defensins in response to salmonella enteritidis infection', *Comp Immunol Microbiol Infect Dis*, 35(2), pp. 197-207.
- Ma, D.Y., Liu, S.W., Han, Z.X., Li, Y.J. and Shan, A.S. (2008) 'Expression and characterization of recombinant gallinacin-9 and gallinacin-8 in *Escherichia coli*', *Protein Expr Purif*, 58(2), pp. 284-91.
- Maemoto, A., Qu, X., Rosengren, K.J., Tanabe, H., Henschen-Edman, A., Craik, D.J. and Ouellette, A.J. (2004) 'Functional analysis of the α -defensin disulfide array in mouse cryptdin-4', *J Biol Chem*, 279(42), pp. 44188-96.
- Mann, K. (2007) 'The chicken egg white proteome', *Proteomics*, 7(19), pp. 3558-68.
- Mann, K. (2008) 'Proteomic analysis of the chicken egg vitelline membrane', *Proteomics*, 8(11), pp. 2322-32.

- Mann, K., Macek, B. and Olsen, J.V. (2006) 'Proteomic analysis of the acid-soluble organic matrix of the chicken calcified eggshell layer', *Proteomics*, 6(13), pp. 3801-10.
- Meade, K.G., Higgs, R., Lloyd, A.T., Giles, S. and O'Farrelly, C. (2009a) 'Differential antimicrobial peptide gene expression patterns during early chicken embryological development', *Dev Comp Immunol*, 33(4), pp. 516-24.
- Meade, K.G., Narciandi, F., Cahalane, S., Reiman, C., Allan, B. and O'Farrelly, C. (2009b) 'Comparative *in vivo* infection models yield insights on early host immune response to *Campylobacter* in chickens', *Immunogenetics*, 61(2), pp. 101-10.
- Milona, P., Townes, C.L., Bevan, R.M. and Hall, J. (2007) 'The chicken host peptides, gallinacins 4, 7, and 9 have antimicrobial activity against *Salmonella* serovars', *Biochem Biophys Res Commun*, 356(1), pp. 169-74.
- Min, W. and Lillehoj, H.S. (2002) 'Isolation and characterization of chicken interleukin-17 cDNA', *J Interferon Cytokine Res*, 22(11), pp. 1123-8.
- Min, W. and Lillehoj, H.S. (2004) 'Identification and characterization of chicken interleukin-16 cDNA', *Dev Comp Immunol*, 28(2), pp. 153-62.
- Monteleone, G., Calascibetta, D., Scaturro, M., Galluzzo, P., Palmeri, M., Riggio, V. and Portolano, B. (2011) 'Polymorphisms of β -defensin genes in Valle del Belice dairy sheep', *Mol Biol Rep*, 38(8), pp. 5405-12.
- Mukamoto, M. and Kodama, H. (2000) 'Regulation of early chicken thymocyte proliferation by transforming growth factor- β -from thymic stromal cells and thymocytes', *Vet Immunol Immunopathol*, 77(1-2), pp. 121-32.
- Nile, C.J., Townes, C.L., Michailidis, G., Hirst, B.H. and Hall, J. (2004) 'Identification of chicken lysozyme g2 and its expression in the intestine', *Cell Mol Life Sci*, 61(21), pp. 2760-6.
- Nizet, V. (2006) 'Antimicrobial peptide resistance mechanisms of human bacterial pathogens', *Curr Issues Mol Biol*, 8(1), pp. 11-26.
- Ouellette, A.J., Darmoul, D., Tran, D., Huttner, K.M., Yuan, J. and Selsted, M.E. (1999) 'Peptide localization and gene structure of cryptdin 4, a differentially expressed mouse paneth cell α -defensin', *Infect Immun*, 67(12), pp. 6643-51.

- Park, S.H., Kim, H.E., Kim, C.M., Yun, H.J., Choi, E.C. and Lee, B.J. (2002) 'Role of proline, cysteine and a disulphide bridge in the structure and activity of the anti-microbial peptide gaegurin 5', *Biochem J*, 368(Pt 1), pp. 171-82.
- Patil, A.A., Ouellette, A.J., Lu, W. and Zhang, G. (2013) 'Rattusin, an intestinal α -defensin-related peptide in rats with a unique cysteine spacing pattern and salt-insensitive antibacterial activities', *Antimicrob Agents Chemother*, 57(4), pp. 1823-31.
- Peng, J. and Xu, J. (2011) 'RaptorX: exploiting structure information for protein alignment by statistical inference', *Proteins*, 79 Suppl 10, pp. 161-71.
- Peng, K.S., Ruan, L.S., Tu, J., Qi, K.Z. and Jiang, L.H. (2013) 'Tissue distribution, expression, and antimicrobial activity of *Anas platyrhynchos* avian β -defensin 6', *Poult Sci*, 92(1), pp. 97-104.
- Pistolesi, S., Pogni, R. and Feix, J.B. (2007) 'Membrane insertion and bilayer perturbation by antimicrobial peptide CM15', *Biophys J*, 93(5), pp. 1651-60.
- Polesello, V., Zupin, L., Di Lenarda, R., Biasotto, M., Ottaviani, G., Gobbo, M., Cecco, L., Alberi, G., Pozzato, G., Crovella, S. and Segat, L. (2015) 'Impact of DEFB1 gene regulatory polymorphisms on hBD-1 salivary concentration', *Arch Oral Biol*, 60(7), pp. 1054-8.
- Ramasamy, K.T., Verma, P. and Reddy, M.R. (2012) 'Differential gene expression of antimicrobial peptides β -defensins in the gastrointestinal tract of *Salmonella* serovar Pullorum infected broiler chickens', *Vet Res Commun*, 36(1), pp. 57-62.
- Rothwell, L., Young, J.R., Zoorob, R., Whittaker, C.A., Hesketh, P., Archer, A., Smith, A.L. and Kaiser, P. (2004) 'Cloning and characterization of chicken IL-10 and its role in the immune response to *Eimeria maxima*', *J Immunol*, 173(4), pp. 2675-82.
- Ruiz, N., Kahne, D. and Silhavy, T.J. (2006) 'Advances in understanding bacterial outer-membrane biogenesis', *Nat Rev Microbiol*, 4(1), pp. 57-66.
- Sadeyen, J.R., Trotreau, J., Velge, P., Marly, J., Beaumont, C., Barrow, P.A., Bumstead, N. and Lalmanach, A.C. (2004) 'Salmonella carrier state in chicken: comparison of expression of immune response genes between susceptible and resistant animals', *Microbes Infect*, 6(14), pp. 1278-86.
- Salzman, N.H. (2010) 'Paneth cell defensins and the regulation of the microbiome: detente at mucosal surfaces', *Gut Microbes*, 1(6), pp. 401-6.

- Salzman, N.H. and Bevins, C.L. (2013) 'Dysbiosis--a consequence of Paneth cell dysfunction', *Semin Immunol*, 25(5), pp. 334-41.
- Salzman, N.H., Hung, K., Haribhai, D., Chu, H., Karlsson-Sjoberg, J., Amir, E., Tegatz, P., Barman, M., Hayward, M., Eastwood, D., Stoel, M., Zhou, Y., Sodergren, E., Weinstock, G.M., Bevins, C.L., Williams, C.B. and Bos, N.A. (2010) 'Enteric defensins are essential regulators of intestinal microbial ecology', *Nat Immunol*, 11(1), pp. 76-83.
- Sano, H., Hsu, D.K., Yu, L., Apgar, J.R., Kuwabara, I., Yamanaka, T., Hirashima, M. and Liu, F.T. (2000) 'Human galectin-3 is a novel chemoattractant for monocytes and macrophages', *J Immunol*, 165(4), pp. 2156-64.
- Schneider, K., Puehler, F., Baeuerle, D., Elvers, S., Staeheli, P., Kaspers, B. and Weining, K.C. (2000) 'cDNA cloning of biologically active chicken interleukin-18', *J Interferon Cytokine Res*, 20(10), pp. 879-83.
- Schroder, J.M. and Harder, J. (2006) 'Antimicrobial skin peptides and proteins', *Cell Mol Life Sci*, 63(4), pp. 469-86.
- Schroeder, B.O., Ehmann, D., Precht, J.C., Castillo, P.A., Kuchler, R., Berger, J., Schaller, M., Stange, E.F. and Wehkamp, J. (2015) 'Paneth cell α -defensin 6 (HD-6) is an antimicrobial peptide', *Mucosal Immunol*, 8(3), pp. 661-71.
- Schroeder, B.O., Wu, Z., Nuding, S., Groscurth, S., Marcinowski, M., Beisner, J., Buchner, J., Schaller, M., Stange, E.F. and Wehkamp, J. (2011) 'Reduction of disulphide bonds unmasks potent antimicrobial activity of human β -defensin 1', *Nature*, 469(7330), pp. 419-23.
- Selsted, M.E. and Ouellette, A.J. (2005) 'Mammalian defensins in the antimicrobial immune response', *Nat Immunol*, 6(6), pp. 551-557.
- Semple, C.A., Rolfe, M. and Dorin, J.R. (2003) 'Duplication and selection in the evolution of primate β -defensin genes', *Genome Biol*, 4(5), p. R31.
- Semple, F. and Dorin, J.R. (2012) ' β -Defensins: multifunctional modulators of infection, inflammation and more?', *J Innate Immun*, 4(4), pp. 337-48.
- Sergeant, M.J., Constantinidou, C., Cogan, T.A., Bedford, M.R., Penn, C.W. and Pallen, M.J. (2014) 'Extensive microbial and functional diversity within the chicken cecal microbiome', *PLoS One*, 9(3), p. e91941.

- Shimizu, M., Watanabe, Y., Isobe, N. and Yoshimura, Y. (2008) 'Expression of avian β -defensin 3, an antimicrobial peptide, by sperm in the male reproductive organs and oviduct in chickens: an immunohistochemical study', *Poult Sci*, 87(12), pp. 2653-9.
- Singh, P.K., Solanki, V., Sharma, S., Thakur, K.G., Krishnan, B. and Korpole, S. (2015) 'The intramolecular disulfide-stapled structure of laterosporulin, a class IId bacteriocin, conceals a human defensin-like structural module', *Febs j*, 282(2), pp. 203-14.
- Singh, P.K., Tack, B.F., McCray, P.B., Jr. and Welsh, M.J. (2000) 'Synergistic and additive killing by antimicrobial factors found in human airway surface liquid', *Am J Physiol Lung Cell Mol Physiol*, 279(5), pp. L799-805.
- Soman, S.S., Nair, S., Issac, A., Arathy, D.S., Niyas, K.P., Anoop, M. and Sreekumar, E. (2009) 'Immunomodulation by duck defensin, Apl_AvBD2: *in vitro* dendritic cell immunoreceptor (DCIR) mRNA suppression, and B- and T-lymphocyte chemotaxis', *Mol Immunol*, 46(15), pp. 3070-5.
- Soman, S.S., Sivakumar, K.C. and Sreekumar, E. (2010) 'Molecular dynamics simulation studies and *in vitro* site directed mutagenesis of avian β -defensin Apl_AvBD2', *BMC Bioinformatics*, 11 Suppl 1, p. S7.
- Sonoda, Y., Abdel Mageed, A.M., Isobe, N. and Yoshimura, Y. (2013) 'Induction of avian β -defensins by CpG oligodeoxynucleotides and proinflammatory cytokines in hen vaginal cells *in vitro*', *Reproduction*, 145(6), pp. 621-31.
- Sreerama, N. and Woody, R.W. (2000) 'Estimation of protein secondary structure from circular dichroism spectra: comparison of CONTIN, SELCON, and CDSSTR methods with an expanded reference set', *Anal Biochem*, 287(2), pp. 252-60.
- Steinstraesser, L., Kraneburg, U., Jacobsen, F. and Al-Benna, S. (2011) 'Host defense peptides and their antimicrobial-immunomodulatory duality', *Immunobiology*, 216(3), pp. 322-33.
- Subasinghage, A.P., O'Flynn, D., Conlon, J.M. and Hewage, C.M. (2011) 'Conformational and membrane interaction studies of the antimicrobial peptide alyteserin-1c and its analogue [E4K]alyteserin-1c', *Biochim Biophys Acta*, 1808(8), pp. 1975-84.
- Subedi, K., Isobe, N., Nishibori, M. and Yoshimura, Y. (2007) 'Changes in the expression of gallinacins, antimicrobial peptides, in ovarian follicles during follicular growth and in

response to lipopolysaccharide in laying hens (*Gallus domesticus*)', *Reproduction*, 133(1), pp. 127-33.

Sudheendra, U.S., Dhople, V., Datta, A., Kar, R.K., Shelburne, C.E., Bhunia, A. and Ramamoorthy, A. (2015) 'Membrane disruptive antimicrobial activities of human β -defensin-3 analogs', *Eur J Med Chem*, 91, pp. 91-9.

Sugiarto, H. and Yu, P.L. (2004) 'Avian antimicrobial peptides: the defense role of β -defensins', *Biochem Biophys Res Commun*, 323(3), pp. 721-7.

Sugiarto, H. and Yu, P.L. (2007a) 'Effects of cations on antimicrobial activity of ostricacins-1 and 2 on *E. coli* O157:H7 and *S. aureus* 1056MRSA', *Curr Microbiol*, 55(1), pp. 36-41.

Sugiarto, H. and Yu, P.L. (2007b) 'Mechanisms of action of ostrich β -defensins against *Escherichia coli*', *FEMS Microbiol Lett*, 270(2), pp. 195-200.

Sunkara, L.T., Zeng, X., Curtis, A.R. and Zhang, G. (2014) 'Cyclic AMP synergizes with butyrate in promoting β -defensin 9 expression in chickens', *Mol Immunol*, 57(2), pp. 171-80.

Sydora, B.C., MacFarlane, S.M., Lupicki, M., Dmytrash, A.L., Dieleman, L.A. and Fedorak, R.N. (2010) 'An imbalance in mucosal cytokine profile causes transient intestinal inflammation following an animal's first exposure to faecal bacteria and antigens', *Clin Exp Immunol*, 161(1), pp. 187-96.

Tai, K.P., Le, V.V., Selsted, M.E. and Ouellette, A.J. (2014) 'Hydrophobic determinants of α -defensin bactericidal activity', *Infect Immun*, 82(6), pp. 2195-202.

Taylor, K., Barran, P.E. and Dorin, J.R. (2008) 'Structure-activity relationships in β -defensin peptides', *Biopolymers*, 90(1), pp. 1-7.

Teng, D., Wang, X., Xi, D., Mao, R., Zhang, Y., Guan, Q., Zhang, J. and Wang, J. (2014) 'A dual mechanism involved in membrane and nucleic acid disruption of AvBD103b, a new avian defensin from the king penguin, against *Salmonella enteritidis* CVCC3377', *Appl Microbiol Biotechnol*, 98(19), pp. 8313-25.

Thouzeau, C., Le Maho, Y., Froget, G., Sabatier, L., Le Bohec, C., Hoffmann, J.A. and Bulet, P. (2003) 'Spheniscins, avian β -defensins in preserved stomach contents of the king penguin, *Aptenodytes patagonicus*', *J Biol Chem*, 278(51), pp. 51053-8.

- Tomisawa, S., Sato, Y., Kamiya, M., Kumaki, Y., Kikukawa, T., Kawano, K., Demura, M., Nakamura, K., Ayabe, T. and Aizawa, T. (2015) 'Efficient production of a correctly folded mouse α -defensin, cryptdin-4, by refolding during inclusion body solubilization', *Protein Expr Purif*, 112, pp. 21-8.
- Townes, C.L., Michailidis, G., Nile, C.J. and Hall, J. (2004) 'Induction of cationic chicken liver-expressed antimicrobial peptide 2 in response to *Salmonella enterica* infection', *Infect Immun*, 72(12), pp. 6987-93.
- Ulvatne, H., Haukland, H.H., Samuelsen, O., Kramer, M. and Vorland, L.H. (2002) 'Proteases in *Escherichia coli* and *Staphylococcus aureus* confer reduced susceptibility to lactoferricin B', *J Antimicrob Chemother*, 50(4), pp. 461-7.
- Van Crombruggen, K., Jacob, F., Zhang, N. and Bachert, C. (2013) 'Damage-associated molecular patterns and their receptors in upper airway pathologies', *Cell Mol Life Sci*, 70(22), pp. 4307-21.
- van Dijk, A., Veldhuizen, E.J. and Haagsman, H.P. (2008) 'Avian defensins', *Vet Immunol Immunopathol*, 124(1-2), pp. 1-18.
- van Dijk, A., Veldhuizen, E.J., Kalkhove, S.I., Tjeerdsma-van Bokhoven, J.L., Romijn, R.A. and Haagsman, H.P. (2007) 'The β -defensin gallinacin-6 is expressed in the chicken digestive tract and has antimicrobial activity against food-borne pathogens', *Antimicrob Agents Chemother*, 51(3), pp. 912-22.
- Varkey, J. and Nagaraj, R. (2005) 'Antibacterial activity of human neutrophil defensin HNP-1 analogs without cysteines', *Antimicrob Agents Chemother*, 49(11), pp. 4561-6.
- Varney, K.M., Bonvin, A.M., Pazgier, M., Malin, J., Yu, W., Ateh, E., Oashi, T., Lu, W., Huang, J., Diepeveen-de Buin, M., Bryant, J., Breukink, E., Mackerell, A.D., Jr. and de Leeuw, E.P. (2013) 'Turning defense into offense: defensin mimetics as novel antibiotics targeting lipid II', *PLoS Pathog*, 9(11), p. e1003732.
- Villaverde, A. and Carrio, M.M. (2003) 'Protein aggregation in recombinant bacteria: biological role of inclusion bodies', *Biotechnol Lett*, 25(17), pp. 1385-95.
- Wang, G. (2008) 'Structures of human host defense cathelicidin LL-37 and its smallest antimicrobial peptide KR-12 in lipid micelles', *J Biol Chem*, 283(47), pp. 32637-43.

- Wang, R., Ma, D., Lin, L., Zhou, C., Han, Z., Shao, Y., Liao, W. and Liu, S. (2010a) 'Identification and characterization of an avian β -defensin orthologue, avian β -defensin 9, from quails', *Appl Microbiol Biotechnol*, 87(4), pp. 1395-405.
- Wang, R., Ma, D., Lin, L., Zhou, C., Han, Z., Shao, Y., Liao, W. and Liu, S. (2010b) 'Identification and characterization of an avian β -defensin orthologue, avian β -defensin 9, from quails', *Applied microbiology and biotechnology*, 87(4), pp. 1395-405.
- Wanniarachchi, Y.A., Kaczmarek, P., Wan, A. and Nolan, E.M. (2011) 'Human defensin 5 disulfide array mutants: disulfide bond deletion attenuates antibacterial activity against *Staphylococcus aureus*', *Biochemistry*, 50(37), pp. 8005-17.
- Watanabe, Y., Isobe, N. and Yoshimura, Y. (2011) 'Detection of avian β -defensins mRNA and proteins in male reproductive organs in chicken', *The Journal of Poultry Science*, 48(4), pp. 275-280.
- Wei, G., Pazgier, M., de Leeuw, E., Rajabi, M., Li, J., Zou, G., Jung, G., Yuan, W., Lu, W.Y., Lehrer, R.I. and Lu, W. (2010) 'Trp-26 imparts functional versatility to human α -defensin HNP1', *J Biol Chem*, 285(21), pp. 16275-85.
- Whitmore, L. and Wallace, B.A. (2004) 'DICHROWEB, an online server for protein secondary structure analyses from circular dichroism spectroscopic data', *Nucleic Acids Res*, 32(Web Server issue), pp. W668-73.
- Whitmore, L. and Wallace, B.A. (2008) 'Protein secondary structure analyses from circular dichroism spectroscopy: methods and reference databases', *Biopolymers*, 89(5), pp. 392-400.
- Wigley, P. (2013) 'Immunity to bacterial infection in the chicken', *Dev Comp Immunol*, 41(3), pp. 413-7.
- Wigley, P. and Kaiser, P. (2003) 'Avian cytokines in health and disease', *Revista Brasileira de Ciênciã Avícola*, 5, pp. 1-14.
- Wilmes, M. (2012) *Antibiotic mechanisms of invertebrate and mammalian defensins*. Doctoral dissertation thesis. Universitäts-und Landesbibliothek Bonn [Online]. Available at: hss.ulb.uni-bonn.de/2013/3120/3120.pdf.
- Wilmes, M., Cammue, B.P., Sahl, H.G. and Thevissen, K. (2011) 'Antibiotic activities of host defense peptides: more to it than lipid bilayer perturbation', *Nat Prod Rep*, 28(8), pp. 1350-8.

- Woody, R.W. (2010) 'A significant role for high-energy transitions in the ultraviolet circular dichroism spectra of polypeptides and proteins', *Chirality*, 22 Suppl 1, pp. E22-9.
- Wu, J., Wang, C., He, H., Hu, G., Yang, H., Gao, Y. and Zhong, J. (2011) 'Molecular analysis and recombinant expression of bovine neutrophil β -defensin 12 and its antimicrobial activity', *Mol Biol Rep*, 38(1), pp. 429-36.
- Wu, Z., Prahl, A., Powell, R., Ericksen, B., Lubkowski, J. and Lu, W. (2003) 'From pro defensins to defensins: synthesis and characterization of human neutrophil pro α -defensin-1 and its mature domain', *J Pept Res*, 62(2), pp. 53-62.
- Xiao, Y., Hughes, A.L., Ando, J., Matsuda, Y., Cheng, J.F., Skinner-Noble, D. and Zhang, G. (2004) 'A genome-wide screen identifies a single β -defensin gene cluster in the chicken: implications for the origin and evolution of mammalian defensins', *BMC Genomics*, 5(1), p. 56.
- Yacoub, H.A., Galal, A., Fathi, M.M., El Fiky, S.A. and Ramadan, H.A.I. (2011) 'Association Between Candidate Genes of Innate Immunity, Gallinacin Genes and Resistance to Marek's Disease in Chicken', *International Journal of Poultry Science*, 10(8), pp. 656-661.
- Yeaman, M.R. and Yount, N.Y. (2003) 'Mechanisms of antimicrobial peptide action and resistance', *Pharmacol Rev*, 55(1), pp. 27-55.
- Zhang, L., Liu, R., Ma, L., Wang, Y., Pan, B., Cai, J. and Wang, M. (2012) 'Eimeria tenella: expression profiling of toll-like receptors and associated cytokines in the cecum of infected day-old and three-week old SPF chickens', *Exp Parasitol*, 130(4), pp. 442-8.
- Zhao, C., Nguyen, T., Liu, L., Sacco, R.E., Brogden, K.A. and Lehrer, R.I. (2001) 'Gallinacin-3, an inducible epithelial β -defensin in the chicken', *Infect Immun*, 69(4), pp. 2684-91.
- Zhao, L., Ericksen, B., Wu, X., Zhan, C., Yuan, W., Li, X., Pazgier, M. and Lu, W. (2012) 'Invariant gly residue is important for α -defensin folding, dimerization, and function: a case study of the human neutrophil α -defensin HNP1', *J Biol Chem*, 287(23), pp. 18900-12.
- Zhu, S. and Gao, B. (2013) 'Evolutionary origin of β -defensins', *Dev Comp Immunol*, 39(1-2), pp. 79-84.

Zou, G., de Leeuw, E., Li, C., Pazgier, M., Li, C., Zeng, P., Lu, W.Y., Lubkowski, J. and Lu, W. (2007) 'Toward understanding the cationicity of defensins. Arg and Lys versus their noncoded analogs', *J Biol Chem*, 282(27), pp. 19653-65.